University of Alberta

Identification and Characterization of Genes Involved in the Regulation of Filamentous Growth of the Dimorphic Yeast *Yarrowia lipolytica*

by

Cleofe Antonio Rodríguez Hurtado 

A thesis submitted to the Faculty of Graduate Studies and Research in partial fulfilment of the requirements for the degree of Doctor of Philosophy

Department of Cell Biology

Edmonton, Alberta

Fall 2002

University of Alberta

Library Release Form

Name of Author: Cleofe Antonio Rodríguez Hurtado

Title of Thesis: Identification and Characterization of Genes Involved in the Regulation of Filamentous Growth of the Dimorphic Yeast *Yarrowia lipolytica*

Degree: Doctor of Philosophy

Year this Degree Granted: 2002

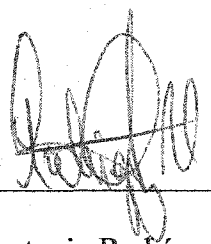

Cleofe Antonio Rodríguez Hurtado
#208 - 10745 79 Ave.
Edmonton, AB
T6E 1S4

Date: August 26, 2002

University of Alberta

Faculty of Graduate Studies and Research

The undersigned certify that they have read, and recommend to the Faculty of Graduate Studies and Research for acceptance, a thesis entitled **Identification and Characterization of Genes Involved in the Regulation of Filamentous Growth of the Dimorphic Yeast *Yarrowia lipolytica*** submitted by Cleofe Antonio Rodriguez Hurtado in partial fulfilment of the requirements for the degree of Doctor of Philosophy.

Richard A. Rachubinski, Ph.D.

David Y. Thomas, Ph.D.

Frank E. Nargang, Ph.D.

Manijeh Pasdar, Ph.D.

Tom C. Hobman, Ph.D.

June 11, 2002

Date

For

Andrea Hurtado Carneiro

and

Cleofe Rodríguez Marroquín

ABSTRACT

Most fungal species have the ability to alternate between a unicellular yeast form and a filamentous form (dimorphism). Fungal dimorphism has received increasing attention because of its implication in pathogenesis and its potential as a simple experimental model of eukaryotic cell differentiation. To date, only a few species have been systematically investigated with an aim to understanding the molecular aspects of dimorphism. Studies have concentrated mainly on *Candida albicans*, the most common human fungal pathogen, and *Saccharomyces cerevisiae*, the most extensively studied fungus at the genetic, biochemical and physiological levels. In order to overcome some of the difficulties and shortcomings presented by these organisms, we have chosen to study dimorphic transition in *Yarrowia lipolytica*, because it can reproduce sexually, is amenable to genetic and molecular biological analysis, and its response to the induction of mycelial growth is highly reproducible.

This thesis describes the isolation and initial characterization of *MHY1*, *YlRAC1*, *YlBEM1* and *YlBMH1*, four genes involved in the induction of hyphal growth in *Y. lipolytica*. These genes were isolated by their ability to restore hyphal growth to mutant *Y. lipolytica* strains obtained by chemical mutagenesis. We found that the transcript levels of these genes are increased during the yeast-to-hypha transition. *MHY1* encodes a C_2H_2-type zinc finger protein, Mhy1p, which can bind putative *cis*-acting DNA stress response elements and appears to be concentrated in the nuclei of actively growing cells found at the hyphal tip, suggesting that Mhy1p may act as a transcription factor. The protein products of *YlRAC1* and *YlBEM1*, in turn, appear to be involved in some aspects of cell

polarization. *YlBMH1* encodes a member of the 14-3-3 family of proteins whose exact function in the induction of filamentous growth is still unknown.

The identification of the *YlCDC42*, *YlSEC31* and *YlBMH2* genes is also described in this work. *YlSEC31* encodes a putative component of COPII secretory vesicles and was isolated by its ability to enhance hyphal growth when overexpressed in wild-type *Y. lipolytica* cells. The roles of *YlCDC42* and *YlBMH2* in the induction of filamentous growth in *Y. lipolytica* remain undetermined.

ACKNOWLEDGEMENTS

Foremost, I would like to thank my supervisor, Rick Rachubinski, for giving me the opportunity to work in a first-class laboratory and for his unconditional support and friendship. He is a role model of humanity, personal integrity, scientific excellence and professionalism. Working with him has been a constant learning experience and has greatly contributed for my growth as both a person and a scientist.

My sincere appreciation to the members of my Ph.D. Supervisory Committee and Candidacy Examining Committee, John Aitchison, Tom Hobman, Frank Nargang, Manijeh Pasdar and Rick Wozniak, for their invaluable guidance and for their understanding and support during the difficult times.

I would also like to thank my former and current colleagues in the Rachubinski lab (Vladimir Titorenko, Roger Bascom, Juan Carlos Torres, Melchior Evers, Chris Winrow, Sandra Marcus, Pam Lagali, Altaf Kassam, Rachel Szilard, Jennifer Smith, Trevor Brown, Gareth Lambkin, Chris Tam, Franco Joseph, Oleh Petriv and Sarah Keen) for their friendship and important suggestions. A special thanks to Chris Winrow, Rachel Szilard and Vladimir Titorenko for their invaluable ideas and technical guidance during my first months in the lab.

My deepest appreciation to Rachel Oates, Eileen Reklow, Gareth Lambkin, Rick Poirier, Hanna Kroliczak, Cecilia Acat, Elena Savidov and Dwayne Weber for their friendship and excellent technical assistance, and to the office staff of the Department of Cell Biology (Robert Venketraman, James Kendall, Colleen Langard, Melanie Grams, Veronica Clough and Claire Lavergne) for their friendship and for making everything a lot

easier in the day-to-day.

Finally, I would like to thank the Department of Cell Biology, the Alberta Heritage Foundation for Medical Research, the Faculty of Graduate Studies and Research, and the Faculty of Medicine and Dentistry for the financial support provided throughout my studies.

TABLE OF CONTENTS

LIST OF TABLES

LIST OF FIGURES

List of Symbols and Abbreviations

A	Ampere
ADP	adenosine diphosphate
ARE	AP-1 response element
ATP	adenosine triphosphate
ATPase	adenosine triphosphatase
bp	base pair
c	centi ($\times 10^{-2}$)
°C	degrees Celsius
cAMP	cyclic adenosine monophosphate
CDK	cyclin-dependent protein kinase
cDNA	complementary deoxyribonucleic acid
Ci	Curie
cpm	counts per minute
D	dalton
DNA	deoxyribonucleic acid
DNase	deoxyribonuclease
dATP	deoxyadenosine triphosphate
dCTP	deoxycytidine triphosphate
dGTP	deoxyguanosine triphosphate
dTTP	deoxythymidine triphosphate
dNTP	deoxyribonucleoside triphosphate
EMSA	electrophoretic mobility shift analysis
F	farad
FRE	filamentation response element
g	gram
g	gravitational force
GAP	guanosine triphosphatase-activating protein
GDP	guanosine diphosphate
GEF	guanosine diphosphate/guanosine triphosphate exchange factor
GFP	green fluorescent protein
GPI	glycosylphosphoinositol
GTP	guanosine triphosphate
GTPase	guanosine triphosphatase
h	hour
IgG	immunoglobulin G
J	Joule
k	kilo ($\times 10^{3}$)
L	liter
m	meter *or* milli ($\times 10^{-3}$)
M	moles per liter
MAP	mitogen-activated protein
MAPK	mitogen-activated protein kinase
MAPKK	mitogen-activated protein kinase kinase

MAPKKK	mitogen-activated protein kinase kinase kinase
MAPs	microtubule-associated proteins
min	minute
mRNA	messenger RNA
MTOC	microtubule-organizing center
μ	micro ($\times 10^{-6}$)
n	nano ($\times 10^{-9}$)
ORF	open reading frame
p	pico ($\times 10^{-12}$)
PAK	p21-activated protein kinase
PCR	polymerase chain reaction
PKA	protein kinase A
Ω	ohm
pH	$-\log[H^+]$
RNA	ribonucleic acid
RNase	ribonuclease
r.p.m.	revolutions per minute
RT	reverse transcriptase
RT-PCR	reverse transcription-polymerase chain reaction
SPB	spindle pole body
STRE	stress response element
U	units of enzyme activity
UV	ultraviolet
v	volume
V	volt
w	weight

CHAPTER 1

INTRODUCTION

1.1 Medical importance of fungi

Fungal disease is an important medical problem of increasing concern, and the prediction is that both the frequency of life-threatening infections and the number of potentially invasive species will continue to grow in the coming years. As most fungal pathogens are opportunistic and the vast majority of fungal infections are not life-threatening, their medical importance is primarily related to the rising number of immunocompromised individuals affected by diseases such as AIDS and diabetes, cancer chemotherapy, immunosuppressive therapy for organ transplants, and the use of broad-spectrum antibiotics and glucocorticosteroids. Other factors contributing to this scenario include modern aggressive medical procedures, such as the implantation of prosthetic devices, extensive surgery, parenteral nutrition, and dialysis (Beck-Sague and Jarvis, 1993; Georgopapadakou and Tkacz, 1995; Pfaller *et al.*, 1998a; 1998b).

Although the effectiveness of the host immune system is a critical determinant in the onset and progress of fungal diseases, the virulence of the microorganism plays a significant role in this process. Virulence factors are extremely diverse, and they are generally defined as those features that allow an etiological agent to recognize and invade host tissues, evade specific aspects of the host defense, and proliferate in the host organism. Thus, they include attributes as different as the production of surface adhesion factors, ability to respond to physical contact (thigmotropism), secretion of toxins and lytic enzymes (such as proteases and hydrolases), antigenic variability, ability to grow at 37°C and physiological pH, and morphological variability (Calderone, 1993; Cutler, 1991; Hogan *et al.*, 1996; Mitchell, 1998; Odds, 1994).

1.2 Fungal dimorphism and pathogenicity

Although most of the 70,000 fungal species identified thus far (O'Donnell *et al.*, 1994) are polymorphic (*i.e.*, exhibit a variety of shapes and forms), the term "dimorphism" is used in a broad sense to define the ability that fungi possess to alternate their pattern of growth between a spherical or ellipsoidal form and a filamentous form in response to environmental cues. Filamentous growth, in turn, may occur in several degrees, and ranges from a state where the cells are elongated, but still ellipsoidal, and remain attached to each other after division (pseudohyphal growth), to a condition where the cells that form the filaments are highly elongated, cylindrical, and partially separated by perpendicular septa (hyphal growth).

Fungal dimorphism has been a subject of great interest because it is a feature common to most fungal pathogens that contributes to several aspects of their virulence (Banuett, 1995; Hogan *et al.*, 1996; Lo *et al.*, 1997; Mitchell, 1998; Odds, 1988; San-Blas and San-Blas, 1984; Shepherd, 1988). For example, in *Candida albicans*, the most common human fungal pathogen, filamentous cells exhibit increased invasiveness and adhere more easily to epithelial and endothelial tissues than do spherical blastospores (Cutler, 1991; Kimura and Pearsall, 1980; Lo *et al.*, 1997), nonfilamentous mutant strains are less virulent than filamentous wild-type strains (Lo *et al.*, 1997), and yeast cells ingested by macrophages produce filaments to lyse them and escape from within (Cutler, 1991; Odds, 1988). In a similar way, haploid yeast cells of *Ustilago maydis* are not pathogenic, whereas the dikaryotic hyphal form can infect plants (Banuett, 1995). In other pathogenic species, such as *Blastomyces dermatitidis*, *Coccidioides immitis*, *Cryptococcus*

neoformans, *Histoplasma capsulatum*, and *Paracoccidioides brasiliensis*, however, the yeast form is required for survival and propagation in infected organisms, whereas filamentous cells are rarely observed in infected tissues (Alspaugh *et al.*, 1998; Brummer *et al.*, 1993; Hogan *et al.*, 1996; Maresca and Kobayashi, 1989). Thus, although it is intuitively assumed that filamentous cells are better suited to penetrate host tissues, and yeast cells are more suited for dissemination of the fungus in the host organism (Odds, 1988), it appears that the existence of different morphologies may in fact contribute to pathogenesis through the expression of specific sets of virulence factors during the various stages of the infection process.

1.3 Fungal model systems for the study of dimorphism

As the most extensively studied fungus at the genetic, biochemical, and physiological levels, *Saccharomyces cerevisiae* is a natural model system for the investigation of fungal dimorphism. Accordingly, most of the current knowledge on the molecular mechanisms governing filamentous growth is based on studies performed in this species, and important analogies have been demonstrated in other fungi.

However, regardless of the implications of fungal dimorphism for pathogenesis and its great potential as a simple experimental model of eukaryotic cell differentiation, only a few fungal species have been systematically investigated with regard to the physiological and molecular events that regulate this phenomenon. These include *C. albicans*, *H. capsulatum*, *B. dermatitidis*, *P. brasiliensis*, *C. neoformans*, *C. immitis*, *U. maydis*, *Sporothrix schenkii*, *Wangiella dermatitidis*, and several *Mucor* species. Studies in these

organisms have revealed that the dimorphic transition is a multifactorial process, that the morphological responses to individual environments are usually not homogeneous (mixed morphologies are extremely common in fungal cultures), and that different species may respond in opposite ways to the same signals. Together, these observations serve to illustrate the complexity of the interactions of a fungus with its environment and to support the assertion that further studies in a larger number of systems are necessary to achieve a better understanding of this phenomenon.

Due to the substantial differences frequently observed among various fungal species, particular emphasis will be given in this introduction to the ascomycetous yeasts *C. albicans*, because of its medical importance, and *S. cerevisiae*, because of its industrial applications and the availability of a large number of tools for its study.

1.4 Environmental factors that regulate fungal dimorphism

The complexity of the mechanisms that regulate fungal dimorphism is best illustrated for *C. albicans*, for which an enormous diversity of environmental factors that influence yeast and hyphal growth have been described (Ernst, 2000; Gow, 1994c; Odds, 1988; San-Blas and San-Blas, 1984; Shepherd *et al.*, 1985). In this organism, hyphal development is generally favoured by high temperatures (37-40°C), pH around neutrality, and relatively poor culture media (although some reports exist indicating that none of these factors is essential), but it is also induced by proline, *N*-acetylglucosamine (GlcNAc), exogenous cAMP and its precursors, serum of different sources, and microaerophilic conditions (Dabrova *et al.*, 1976; Gow, 1994c; Land *et al.*, 1975; Niimi *et al.*, 1980; Odds,

1988; Sabie and Gadd, 1992; Sonneborn *et al.*, 1999). Yeast growth, in turn, has been described to be favoured by low temperatures, pH below 6.5, enriched media, high glucose concentrations, presence of easily utilizable nitrogen sources (such as ammonium salts), high cell density, high osmolarity, and calmodulin inhibitors (Alex *et al.*, 1998; Buffo *et al.*, 1984; Ernst, 2000; Gow, 1994c; Sabie and Gadd, 1989). This situation is in clear contrast to other dimorphic fungal systems, in which a single environmental parameter is critical for dimorphism, and medium composition appears to be irrelevant. Thus, for example, anaerobic atmospheres containing at least 30% CO_2 are essential for yeast growth in *Mucor rouxii* (San-Blas and San-Blas, 1984), and temperature is a critical factor for morphogenesis in *H. capsulatum*, *P. brasiliensis* and *S. schenkii*, in which, contrary to what is observed in *C. albicans*, mycelial development occurs at 22-25°C, and yeast growth is induced by increasing incubation temperatures to 37°C (Maresca and Kobayashi, 1989).

In *S. cerevisiae,* filamentous growth of haploid cells can be observed only after long periods of incubation on rich solid medium (Roberts and Fink, 1994), but it is strongly induced by fusel alcohols, such as 1-butanol, isobutanol, isoamyl alcohol, and *tert*-amyl alcohol, in both solid and liquid media (Lorenz *et al.*, 2000a). Pseudohyphal growth, in turn, is easily induced in diploid cells by nitrogen limitation (Gimeno *et al.*1992; Kron *et al.*, 1994), fusel alcohols (Lorenz *et al.*, 2000a), and poorly used carbon sources, such as amylopectin (Lambrechts *et al.*, 1996), and is enhanced by the presence of ethanol in low-nitrogen media (Lorenz *et al.*, 2000a).

1.5 Cell biological aspects of morphogenesis in ascomycetous yeasts

In general, the major processes of cell growth in yeast, hyphal and pseudohyphal cells are similar, and cell shape is ultimately determined by the relative extent and timing of localized cell wall synthesis through the cell cycle.

1.5.1 Yeast growth

In ellipsoidal yeast cells, growth is initially directed to a small region of the cell surface, which then enlarges to form a bud. This process starts with the selection of the site of growth, which in haploid cells of *S. cerevisiae* corresponds to a position adjacent to the previous mother-daughter cell junction, while in diploid *S. cerevisiae* yeast cells and in *C. albicans* blastospores may be located at the same position or at the opposite cell pole (Chaffin, 1984; Chant and Pringle, 1991). Subsequently, several proteins are relocated to the potential budding site, and cytoskeletal elements become polarized towards that site (Chant and Pringle, 1991). New cell surface material is then continuously delivered to the budding site through the secretory apparatus (Schekman, 1985), and the bud first appears at the end of the G_1 phase, after the landmark Start in the cell cycle (Byers, 1981). Growth remains polarized to the bud tip through the S phase, when DNA replication takes place in the mother cell (Lew and Reed, 1993). At the end of the G_2 phase, the nucleus migrates to the budding neck of the emerging daughter cell, the nuclear envelope, with one of the duplicated spindle pole bodies (SPB) preceding, extends into the growing bud cell, and mitosis occurs at the budding neck (Byers, 1981). At this point, the deposition of cell wall material has gradually become more diffuse over the surface of the emerging bud (Lew and

Reed, 1993) and, after mitosis, the two daughter nuclei migrate to the centers of the respective cells, and the cell growth machinery is directed to the mother-bud neck for the formation of a septum (Lew and Reed, 1993). The fluctuation of polarity between a first phase of polarized growth at the distal end, a second phase of more diffuse growth, and a third phase of polarized growth at the proximal end gives the bud its characteristic ellipsoidal shape. After cytokinesis, the daughter cell undergoes a new phase of isotropic growth in G_1 before reaching the critical size for progression to S phase at Start (Fig. 1-1A).

1.5.2 Pseudohyphal growth

The cellular events that lead to pseudohyphal growth are essentially identical to those observed in yeast growth. During this type of growth, however, more elongated ellipsoidal cells are produced as a consequence of a significant extension of the G_2/M phase, which results in longer periods of increased cell polarization and a drastic reduction of the period of isotropic deposition of new cell material at the surface of the daughter cell (Kron *et al.*, 1994) (Fig. 1-1B).

1.5.3 Hyphal growth

In *C. albicans*, hyphal formation starts with the random selection of a site of growth (Chaffin, 1984). Subsequently, as in ellipsoidal growth, the cytoskeleton becomes polarized, and new cell surface material is continuously delivered to this site. This state of polarization, however, remains constant, and a small tubular structure soon becomes

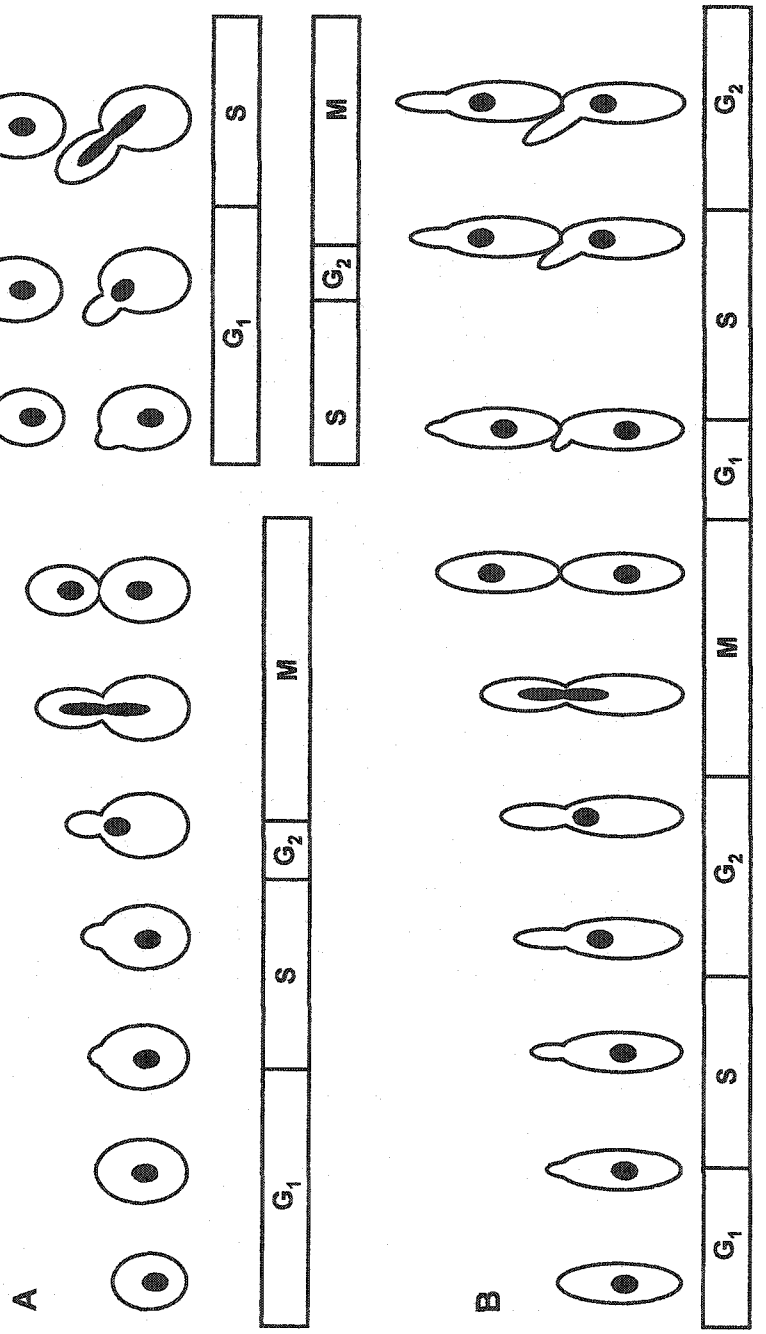

Figure 1-1. The cell cycle during yeast (A) and pseudohyphal (B) growth in *S. cerevisiae*
Adapted from Kron *et al.* (1994).

apparent. The germ tube then continues to grow apically, the parent nucleus migrates to the parent-hypha junction as it does in blastospores, and the nucleus divides (Soll *et al.*, 1978). After mitosis, the cytoplasm from the parent yeast cell migrates into the growing germ tube, leaving behind a vacuolated mother cell with a single nucleus, and a perpendicular septum is formed in the vicinity of the mother-daughter junction (Gow and Gooday, 1984). Polarized growth and nuclear division then continue in the apical cell, and a new perpendicular septum is formed between the two daughter nuclei as the cytoplasm from the hyphal parent cell migrates to the apical cell, leaving behind an extensively vacuolated cell. Thus, only the apical cell remains metabolically active, and a series of extensively vacuolated, uninucleate cells are left behind (Gow and Gooday, 1984; Gow *et al.*, 1986). The cytoplasmic space of the mother yeast cell and of the intercalary compartments can remain inactive for prolonged periods, possibly arrested in G_1 (Gow, 1994a), and is regenerated at the expense of the vacuolar space prior to the formation of a second germ tube, a hyphal branch, or a lateral blastospore (Gow and Gooday, 1984) (Fig. 1-2).

1.6. The cell wall and morphogenesis in ascomycetous yeasts

The cell wall is the major determinant of overall shape in fungi and the primary interface between the fungus and its environment. It accounts for up to 30% of the dry weight of *S. cerevisiae* yeast cells and is primarily composed of β-glucan, chitin, and mannoproteins (Cid *et al.*, 1995; Klis, 1994; Valentin *et al.*, 1987). The first two components are unique and essential to fungi, and consequently have attracted much

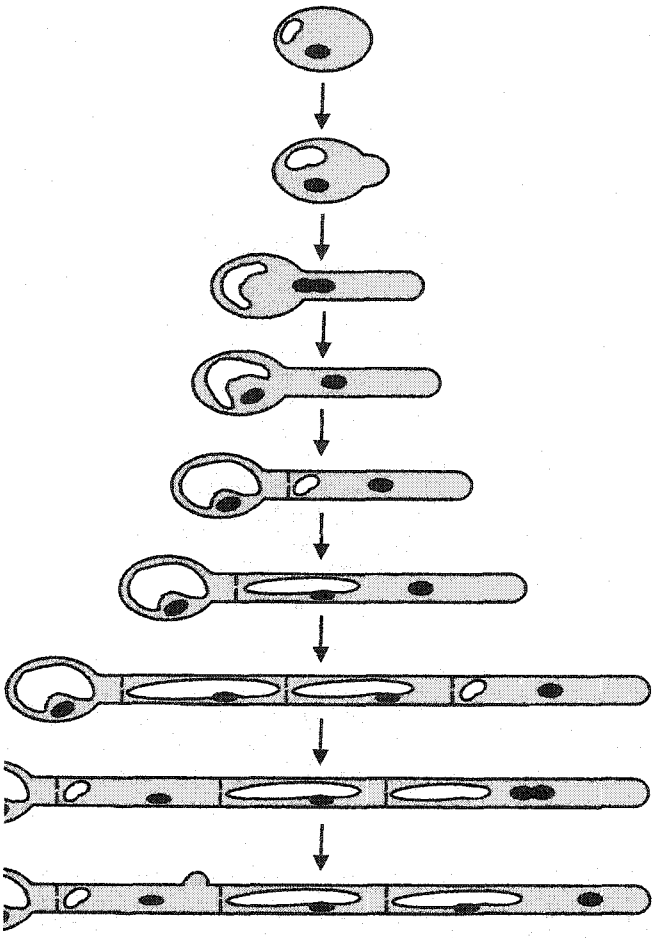

Figure 1-2. Hyphal growth and vacuolation in *C. albicans*
Adapted from Gow (1994c).

attention because of their potential as targets for antifungal agents (Georgopapadakou and Tkacz, 1995). Similarly, a group of mannoprotein adhesins has been suggested as virulence factors (Calderone, 1993), and an integrin-like protein, Int1p, has been shown to play an important role in adhesion, morphogenesis and virulence in *C. albicans* (Gale *et al.*, 1998).

1.6.1 Cell wall structure

Under the electron microscope, the fungal cell wall appears as a bilayered structure consisting of a fibrillar outer layer and an amorphous inner layer (Horisberger and Vonlanthen, 1977; Klis, 1994; Kopecka *et al.*,1974).

The fibrillar external layer is rich in mannoproteins, large molecules containing about 95% carbohydrate (mainly mannose) covalently complexed with proteins, is very sensitive to proteolytic attack, and can be removed without affecting cell shape (Horisberger and Vonlanthen, 1977). Most mannoproteins are integral components of the cell wall (structural mannoproteins) and are responsible for the surface properties of the fungal cell, such as hydrophobicity, flocculence, and pathogenicity, as well as for the permeability of the cell wall to macromolecules (de Nobel and Barnett, 1991; Tokunaga *et al.*, 1990). A second group of mannoproteins is composed of hydrolytic enzymes located in the cell wall or in the periplasmic space (Cid *et al.*, 1995).

The inner layer of the fungal cell wall is responsible for its mechanical strength and exhibits an inner fibrillar zone, close to the membrane and rich in proteins, and a more amorphous outer zone, facing the mannan-rich area and rich in β-(1,6)-glucan (Horisberger

and Vonlanthen, 1977; Klis, 1994; Kopecka *et al.*,1974). β-glucan is the major component of the cell wall and is composed primarily of large linear β-(1,3)-glucan polymers, with occasional side chains having β-(1,6) linkages. A minor structural component is also found in yeast cell walls and consists of a highly branched β-(1,6)-glucan with occasional β-(1,3) linkages and β-(1,6)-linked side chains (Manners *et al.*, 1973a; 1973b).

The third major component of the fungal cell wall, chitin, is a linear homopolymer of β-(1,4)-*N*-acetylglucosamine. It accounts for less than 1% of the dry weight of yeast cells, where it is primarily localized in the septal region and bud scars of mother cells but can also be detected within the inner part of the glucan-rich portion of the lateral walls (Roncero *et al.*, 1988). In hyphal cells of *C. albicans*, however, the chitin content is two- to three-fold higher than in blastospores, whereas only small quantitative differences are observed in the glucan and mannoprotein components of the cell wall (Shepherd *et al.*, 1985; Sullivan *et al.*, 1983).

A schematic diagram of the *S. cerevisiae* cell wall is presented in Figure 1-3.

1.6.2 Cell wall synthesis

The molecular mechanisms of cell wall synthesis are identical in ellipsoidal and hyphal cells, but there are significant quantitative differences in the enzymatic activities and modes of surface expansion between these forms. For example, in *S. cerevisiae* yeast cells and *C. albicans* blastospores, apical growth accounts for 70% of surface expansion during the first two-thirds of bud development, and general surface growth occurs throughout the last third of the budding cycle. In *C. albicans* hyphal cells, in turn, apical

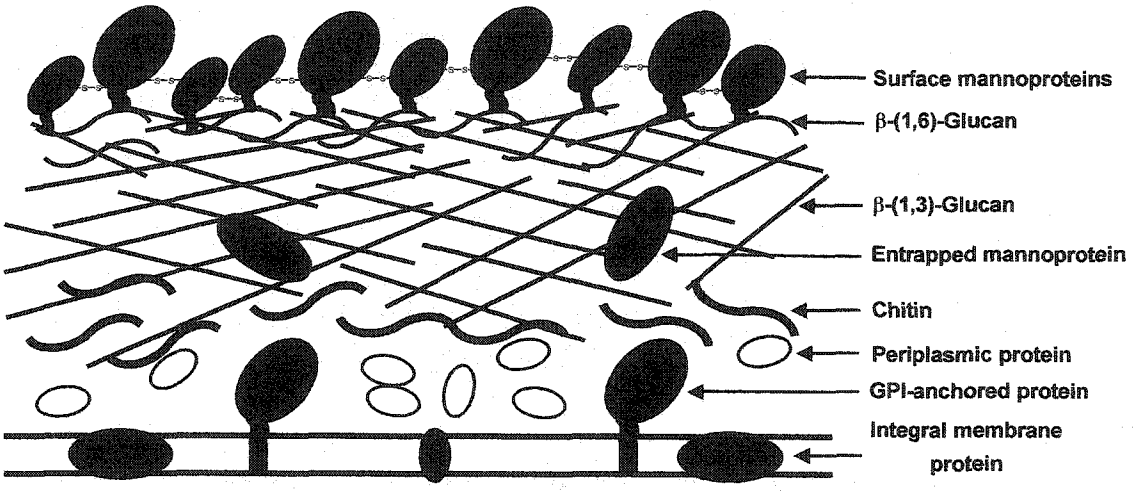

Figure 1-3. Schematic diagram of the cell wall of *S. cerevisiae*
Adapted from Georgopapadakou and Tkacz (1995).

growth is continuous, and less than 10% of growth corresponds to general surface expansion (Odds, 1988). In addition, both chitin synthase and β-(1,3)-glucan synthase activities are much greater in hyphae than in *C. albicans* blastospores (Frost *et al.*, 1994; Ram *et al.*, 1983).

Biosynthesis of cell wall components occurs in the cytosol, the plasma membrane, and the cell wall. The structural polymers are initially synthesized in the cytosol and plasma membrane as plastic microfibrils, but they are gradually cross-linked, thickened and rigidified in the cell wall itself to create the rigid lateral fungal wall, as they are displaced laterally by the insertion of new material (Gooday, 1994; Gow, 1994a; Wessels, 1986).

Chitin is synthesized on the cytosolic surface of the plasma membrane, extruded to the cell surface, and crystallized outside the cell through the extensive formation of hydrogen bonds. In yeast cells, chitin is intensely synthesized at two points: before budding, when a ring is formed at the site of bud emergence, and at the end of mitosis, when a primary chitin septum is placed within the chitin ring on the side of the mother cell (Cabib *et al.*, 1974). In hyphal cells, chitin synthesis occurs continuously at the growing tip and is a major factor in cell morphogenesis (Odds, 1988). There are three chitin synthases in *S. cerevisiae* and *C. albicans* (encoded by the genes *CHS1-CHS3* and *CaCHS1-CaCHS3*, respectively), which are under both spatial and temporal control (Cid *et al.*, 1995; Georgopapadakou and Tkacz, 1995; Stratford, 1994). In *S. cerevisiae*, for example, chitin synthase I has a role in repair during cell separation, chitin synthase II is involved in the synthesis of the primary septum disk, and chitin synthase III is responsible

for the synthesis of the chitin ring at the bud base and at the lateral walls of yeast cells and spores (Stratford, 1994).

Like chitin, β-glucan is vectorially synthesized at the cell membrane by transmembrane synthases that recruit sugar precursors from the cytosol and deposit polymerized chains at the sites of growth. In *S. cerevisiae*, β-(1,3)-glucan is produced by two synthases composed of two subunits: the first subunit, encoded by the genes *FKS1* and *GSC2* (*FKS2*), is membrane-bound and contains the catalytic center of the enzyme, whereas the second subunit is encoded by *RHO1* and activates Fks1p and Gsc2p in the presence of GTP (Cabib and Kang, 1987; Mazur and Baginsky, 1996). β-(1,6)-glucan, in turn, is produced by other two synthases, whose catalytic subunits are encoded by the genes *KRE6* and *SKN1* (Roemer *et al.*, 1993). As cell wall synthesis proceeds, β-(1,6)-glucan is matured at the subapical region of the wall, distal to the growing tip, through the addition of side chains in a reaction catalyzed by the protein product of *KRE1* (Roemer and Bussey, 1995), and β-(1,3)-glucan is cross-linked with β-(1,6)-glucan and chitin by Gas1p and Bgl2p (Popolo *et al.*, 1997). In *C. albicans*, the homologs of *KRE1*, *KRE6*, *SKN1*, *BGL2*, and three genes encoding subunits of the β-(1,3)-glucan synthase (*CaFKS1*, *CaFKS2* and *CaFKS3*) have been identified (Boone *et al.*, 1991; Mio *et al.*, 1997a; 1997b).

Cell wall mannoproteins follow the secretory pathway. There, sugar chains are attached to the protein moieties by *O*-glycosylation or *N*-glycosylation, or through the addition of a glycosylphosphoinositol (GPI) anchor at their carboxyl-terminal end (Cid *et al.*, 1995; de Sampaio *et al.*, 1999). More than 30 mannosyl transferases have been shown to be involved in the glycosylation of cell wall mannoproteins in *S. cerevisiae* (Cid *et al.*,

1995; Herscovics and Orlean, 1993). Upon their arrival at the periplasmic space or the glucan matrix, the resulting molecules are cross-linked to the cell wall through a series of reactions that in *S. cerevisiae* are mediated by Gas1p and Bgl2p (Popolo and Vai, 1999), whereas in *C. albicans* these events involve Phr1p and Phr2p, two GPI-anchored cell surface proteins that are required for cell morphogenesis and virulence in this organism (Fonzi, 1999).

1.7 Polarization of cell growth in ascomycetous yeasts

1.7.1 The cytoskeleton

The cytoskeleton has a major role in the process of cell polarization and tip growth. It is a complex structure composed primarily of microtubules and actin microfilaments, and comprises more than 60 proteins that are collectively responsible for the movement of organelles and the localization of exocytic vesicles to the cell apex during cell growth (Gow, 1994b; Harold, 1990; Heath, 1994; Madden *et al.*, 1992).

1.7.1.1 Microtubules

Microtubules are helical structures composed of 13 protofilaments laterally connected to form a cylinder. Each protofilament consists of dimers of α- and β-tubulin, two closely related proteins of approximately 55 kDa that in *S. cerevisiae* are encoded by the genes *TUB1*, *TUB2* and *TUB3* (Schatz *et al.*, 1986; Thomas *et al.*, 1985). Microtubules also contain γ-tubulin, a component of the microtubule-organizing centers (MTOCs), that in *S. cerevisiae* is encoded by the *TUB4* gene and appears to be involved

in microtubule nucleation (Marschall *et al.*, 1996). The *C. albicans* homologs of *TUB1*, *TUB2* and *TUB4* have been identified (Daly *et al.*, 1997; Smith *et al.*, 1988).

In fungi, the vast majority of microtubules is organized into bundles that are oriented parallel to the long axis of both hyphal and yeast cells, performing their functions through their interactions with a large number of proteins that are collectively known as microtubule-associated proteins (MAPs) (Heath, 1994). Organizational MAPs regulate the polymerization, spatial organization and stability of microtubules, whereas functional MAPs are involved primarily in organelle motility, mitotic spindle formation, chromosome separation, nuclear migration and nuclear distribution (Hackney, 1996; Heath, 1994). The best known functional MAPs are mechanochemical translocators that glide along microtubules to move vesicles and cellular organelles throughout the cell, and belong to two superfamilies: dyneins and kinesins. Dyneins are molecular motors that show a preference for movement towards the minus-end of microtubules and are composed of two identical chains of 500 kDa, three intermediate chains of 70 kDa, and four light chains of ~55 kDa (Vallee, 1991). Kinesins, in turn, have members that move in opposite directions and consist of a motor domain of approximately 350 amino acids, with binding sites for ATP and microtubules, and a globular tail that determines functional specificity (Goldstein, 1991). The involvement of microtubules in fungal morphogenesis is controversial, but it is clear that they play an important role in the transport of some organelles to the daughter cell and in nuclear positioning along hyphae (Gow, 1994c; Yamashita and May, 1998).

1.7.1.2 Actin microfilaments

The fungal actin cytoskeleton is composed of actin microfilaments and cortical patches. Actin microfilaments are long cables of F-actin composed of G-actin monomers of ~42 kDa that in *S. cerevisiae* and *C. albicans* are encoded by the gene *ACT1* (Losberger and Ernst, 1989; Novick and Botstein, 1984), whereas the cortical patches are discrete cytoskeletal bodies composed of more than 30 proteins that, like the actin cables, reside at the cell cortex in a polarized distribution that correlates with directed growth (Adams and Pringle, 1984; Amberg, 1998; Chant and Pringle, 1995; Lew and Reed, 1995; Pruyne and Bretscher, 2000b).

There is abundant evidence that actin plays a vital role in the polarization of cell growth and morphogenesis. For example, it has been shown that actin granules cluster at the site of initial cell evagination in both yeast and hyphal cells, remain primarily located at the apex in hyphae, but gradually become distributed throughout the budding outgrowths (Akashi *et al.*, 1994; Amberg, 1998; Anderson and Soll, 1986). During apical growth, more than 40 cytoskeletal and regulatory proteins accumulate at the site of growth, forming a tight actin cap that overlaps a cluster of cortical patches, and actin cables from throughout the cell converge on this area (Chant and Pringle, 1995; Lew and Reed, 1995; Pruyne and Bretscher, 2000b). During isotropic bud growth, cap components and cortical patches redistribute over the surface of the bud, and actin cables extend from the mother cell into a network in the bud. After nuclear division, all three structures reorient to the mother-bud junction (Pruyne and Bretscher, 2000b).

The fungal actin cytoskeleton guides cell surface expansion by directing the

delivery of internal membranes and other factors to the sites of growth, using a transport system that is based on the interaction of actin cables with myosin (Bretscher *et al.*, 1994; Finger and Novick, 1998). In *S. cerevisiae*, polarized growth at the cell surface depends upon delivery of secretory vesicles along actin cables by Myo2p, a motor protein that forms 400-kDa dimers that interact with secretory vesicles through their carboxyl-terminal tails and possess two globular head domains that interact with F-actin to produce ATP-powered mutual sliding (Heath, 1994; Pruyne *et al.*, 1998; Pruyne and Bretscher, 2000b).

The actin cytoskeleton has also been shown to play an important role in fungal septation and cytokinesis, through the formation of a contractile ring composed of many cytoskeletal proteins, including actin and myosin, at the division plane (Tolliday *et al.*, 2001; Yamashita and May, 1998).

1.7.2 Selection of sites of polarized growth in *S. cerevisiae*

In *S. cerevisiae*, the establishment of cell polarity is guided by pre-existing cortical proteins, which include Bud3p and Axl2p in haploid yeast cells, and Bud8p and Bud9p in diploid cells (Chant *et al.*, 1995; Kang *et al.*, 2001; Pruyne and Bretscher, 2000a; Roemer *et al.*, 1996a; Taheri *et al.*, 2000). These cellular landmarks, which are remnants of previous budding events, are thought to recruit Bud5p, a GDP/GTP exchange factor (GEF) that, along with the GTPase-activating protein (GAP) Bud2p, regulates the activity of the small GTPase, Rsr1p (Park *et al.*, 1993; Kang *et al.*, 2001). During early G_1 phase, activated Rsr1p binds to the molecular scaffold protein Bem1p and the GEF Cdc24p, thereby triggering the recruitment and activation of the small GTPase, Cdc42p, and

defining the site of bud emergence (Park *et al.*, 1999; Zheng *et al.*, 1995).

Cdc42p is the key element in the polarization of the actin cytoskeleton. In its absence, cortical patches and actin cables are still formed, but they are completely disorganized, and cells are unable to form buds (Adams *et al.*, 1990). The GTPase activity of Cdc42p is necessary for signaling to the actin cytoskeleton and is positively regulated by the GEFs, Cdc24p, Zds1p and Zds2p, and negatively regulated by the GAPs, Bem3p, Rga1p and Rga2p (Bi and Pringle, 1996; Stevenson *et al.*, 1995; Zheng *et al.*, 1995; Ziman *et al.*, 1991). In its active GTP-bound state, Cdc42p signals to the actin cytoskeleton through its several effectors, including the p21-activated kinases (PAKs) Ste20p and Cla4p (Cvrckova *et al.*, 1995; Eby *et al.*, 1998) (Fig. 1-4B). These PAKs in turn mediate cytoskeletal organization through the phosphorylation of Myo3p and Myo5p, two myosins that are normally found at cortical patches (Geli and Riezman, 1996; Wu *et al.*, 1997). Two other proteins, Gic1p and Gic2p, have been found to bind GTP-Cdc42p, but the mechanisms by which they mediate cytoskeletal polarization are still unknown (Brown *et al.*, 1997; Chen *et al.*, 1997) (Fig. 1-4A).

1.7.3 Maintenance of cell polarity in *S. cerevisiae*

During early vegetative bud growth and pseudohyphal growth, the Cdc42p-Cdc24p complex dissociates from Rsr1p and the bud-site selection scaffold but continues to guide cytoskeletal polarity through its interaction with a protein complex known as the polarisome (Pruyne and Bretscher, 2000a). This apical scaffold, which comprises Bni1p, Bud6p, Pea2p, Spa2p and Sph1p, shows a cap-like distribution in the growing bud and is

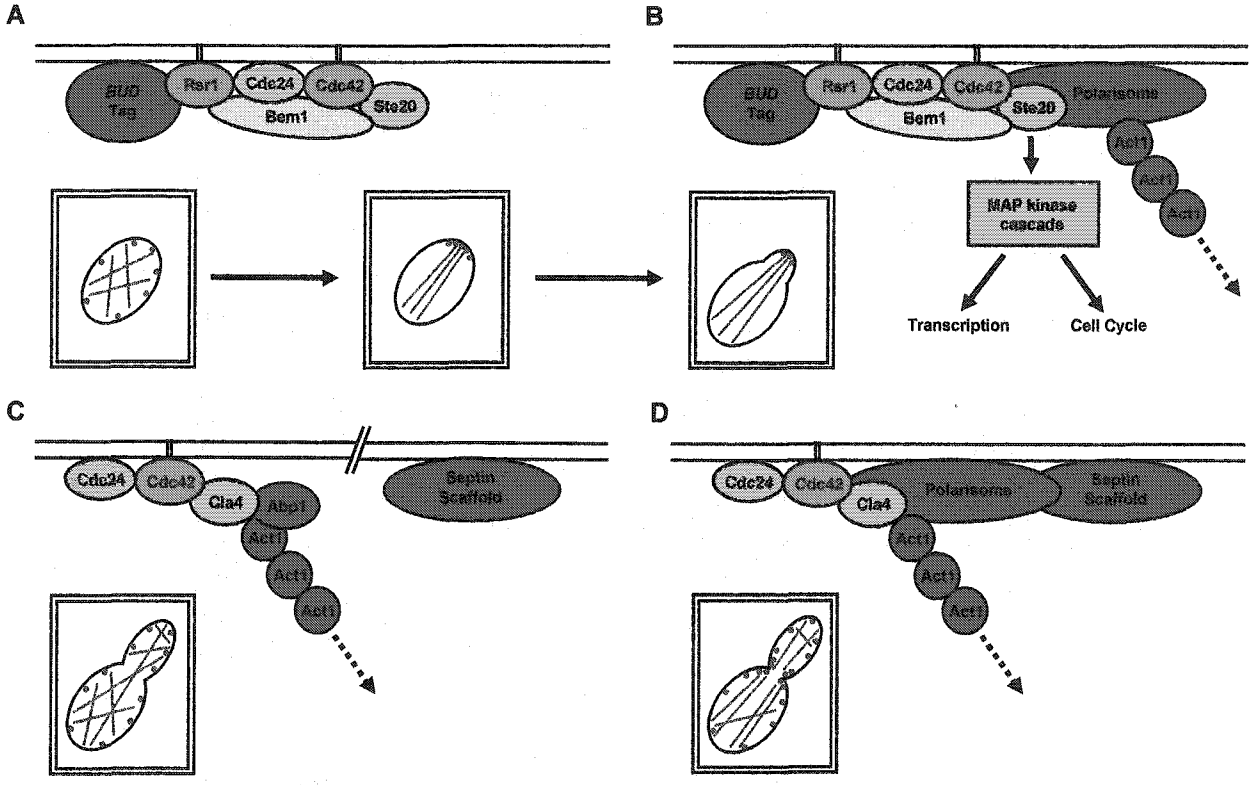

Figure 1-4. Establishment, maintenance and changes of cell polarity in *S. cerevisiae*
(A) Bud-site selection; (B) bud emergence; (C) isotropic bud growth;
(D) post-cytokinesis. Adapted from Pruyne and Bretscher (2000a).

thought to link RhoGTPase signaling to actin filament assembly (Evangelista *et al.*, 1997; Kohno *et al.*, 1996; Pruyne and Bretscher, 2000a; Sheu *et al.*, 1998) (Fig. 1-4B). Pea2p, Spa2p and Sph1p appear to provide a docking site for Bud6p and Bni1p (Amberg *et al.*, 1997; Pruyne and Bretscher, 2000a; Roemer *et al.*, 1998; Sheu *et al.*, 1998). Bud6p is an actin-interacting protein (Amberg *et al.*, 1997), whereas Bni1p binds profilin (Pfy1p), a protein that stimulates actin polymerization (Imamura *et al.*, 1997; Mockrin and Korn, 1980), Tef1p/Tef2p, a translation elongation factor that plays a role in the formation of actin bundles (Umikawa *et al.*, 1998), and activated Rho GTPases, such as Cdc42p, Rho1p, Rho3p and Rho4p (Kohno *et al.*, 1996; Evangelista *et al.*, 1997).

1.7.4 Apical-isotropic switch in *S. cerevisiae*

Polarity changes reflect variations in the distribution of activated Cdc42p, which is regulated by the cyclin-dependent protein kinase (CDK) Cdc28p and the PAKs Cla4p and Ste20p (Pruyne and Bretscher, 2000a).

During the G_1/S transition, Cdc28p forms a complex with the G_1 cyclins Cln1p and Cln2p, promoting cytoskeleton polarization and early apical bud growth through the phosphorylation of Ste20p and subsequent formation of the Cdc42p-Ste20p complex (Lew and Reed, 1993; Oda *et al.*, 1999). At G_2/M, however, the mitotic cyclins Clb1p and Clb2p replace the G_1 cyclins in the Cdc28p-cyclin complex to promote the phosphorylation of Cla4p and the subsequent formation of the Cdc42p-Cla4p complex (Benton *et al.*, 1997; Lew and Reed, 1993; Tjandra *et al.*, 1998) (Fig. 1-4C).

The molecular mechanisms by which the Cdc42p-Cla4p complex regulates polarity

switches are not completely clear, but the observation that Ste20p binds directly to Bem1p, whereas Cla4p does not, suggests that the Cdc42p-Ste20p complex has a higher affinity for apical scaffolds than does Cdc42p-Cla4p (Leeuw *et al.*, 1995; 1998; Pruyne and Bretscher, 2000a). In addition, the Cdc42p-Cla4p complex appears to promote the apical-isotropic switch through the activation of Hsl7p via the Nim1-related kinases Gin4p, Hsl1p and Kcc4p (McMillan *et al.*, 1999; Pruyne and Bretscher, 2000a). Hsl7p is a protein of unknown function that facilitates the phosphorylation of Swe1p by the protein kinase Hsl1p, thus promoting recognition of Swe1p by the ubiquitination complex and its subsequent degradation. Swe1p, in turn, is a protein tyrosine kinase that inhibits Cdc28p and, consequently, degradation of Swe1p at G_2/M results in higher concentrations of Cdc42p-Cla4p (McMillan *et al.*, 1999). Furthermore, Hsl7p is thought to compete with Cdc42p for binding to Ste20p, thus providing additional Cdc42p for association with Cla4p to promote cytoskeleton disorganization during isotropic growth (Fujita *et al.*, 1998). Finally, a Rho guanine-nucleotide-dissociation factor, Rdi1p, has been found to bind GDP-Cdc42p in the cytosol, and a potential a role in the redistribution of Cdc42p during the changes of polarity states has been proposed (Koch *et al.*, 1997).

During *S. cerevisiae* pseudohyphal growth, the mitogen-activated protein kinase (MAPK) Kss1p both cooperates with Swe1p to inactivate the Cdc28p-Clb1p and Cdc28p-Clb2p complexes, and stimulates the production of Cln1p via the transcription factor Tec1p (Section 1.8.1). As a result, the Cdc42p-Ste20p complex remains active for longer periods of time, the G_2 phase is extended, and the cells become elongated due to a delay in the apical-isotropic switch (Ahn *et al.*, 1999; Edgington *et al.*, 1999; Madhani *et al.*,

1999) (Fig. 1-5).

1.7.5 Cytokinesis and septation in *S. cerevisiae*

Prior to bud emergence, the Cdc42p-Cla4p complex mediates the formation of a 10-nm ring at the site of growth. This ring is composed of the septins Cdc3p, Cdc10p, Cdc11p, Cdc12p and Shs1p, and remains immobilized as a collar of filaments surrounding the mother-bud neck throughout bud growth (Cvrckova *et al.*, 1995; Holly and Blumer, 1999) (Fig. 1-4D). At the moment of cytokinesis and cell separation, these proteins play a role in the repolarization of the cortical patches and actin cables towards the mother-bud neck, function as anchors for plasma membrane enzymes that synthesize a chitin ring around this neck (De Marini *et al.*, 1997; Longtine *et al.*, 1996), and form a template for a contractile double ring which contains F-actin, the myosin Myo1p, and other proteins that promote cytokinesis (Field *et al.*, 1999). After cytokinesis, this double ring is split, and the old septin complex serves as a landmark for the establishment of a new budding site (Roemer *et al.*, 1996b).

1.8 Signal transduction pathways regulating dimorphism in *S. cerevisiae*

Pseudohyphal growth in *S. cerevisiae* requires the cooperation of two different signaling pathways: a MAP kinase cascade and a cAMP-dependent pathway.

1.8.1 The MAP kinase cascade

In *S. cerevisiae*, most signals that activate pseudohyphal growth appear to converge

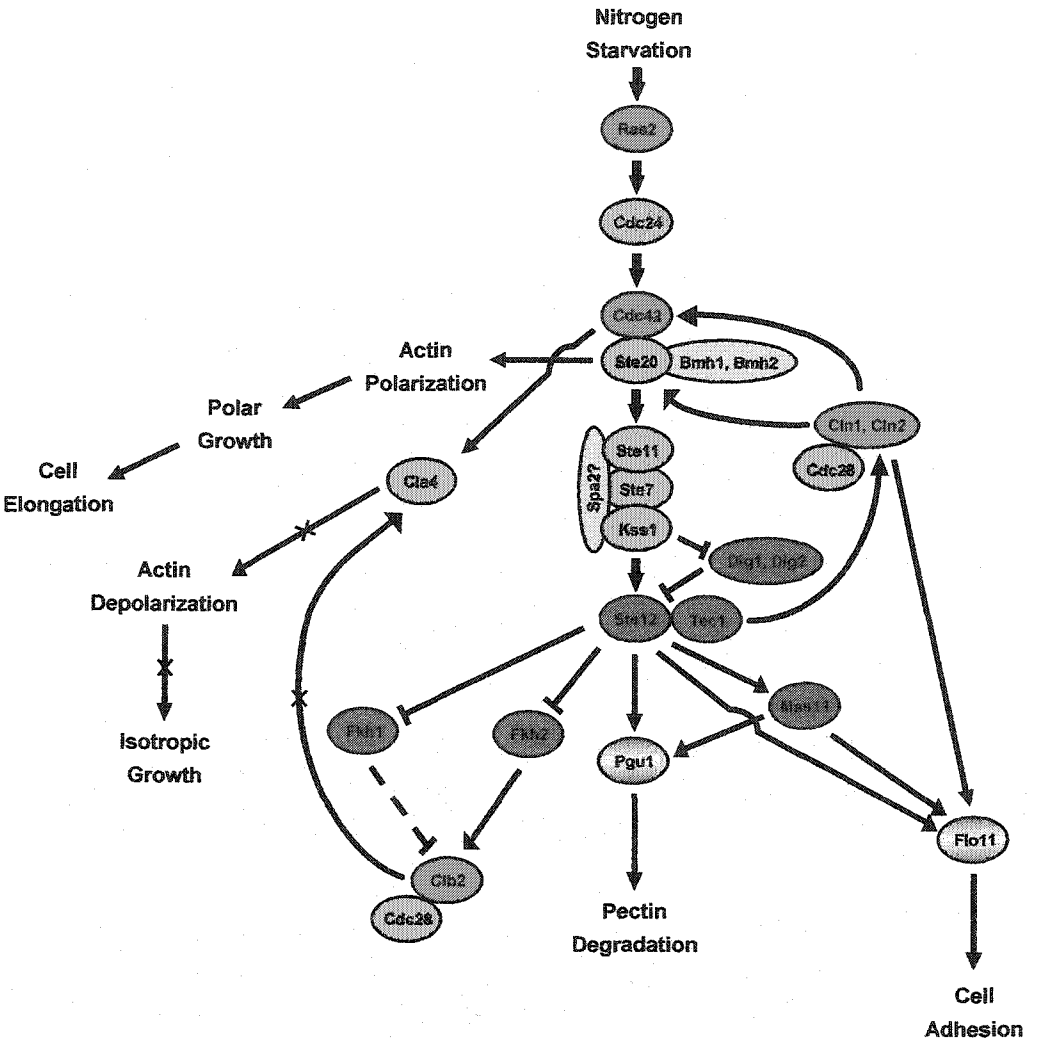

Figure 1-5. Regulation of pseudohyphal growth in *S. cerevisiae* by the MAP kinase cascade

in the activation of the small GTPase, Ras2p (Kron and Gow, 1995; Madhani and Fink, 1998).

For activation of the MAP kinase pathway (Fig. 1-5), Ras2p promotes activation of Cdc24p through a still unknown mechanism, resulting in displacement of the negative regulator Hsl7p and consequent formation of the Cdc42p-Ste20p complex (Fujita *et al.*, 1999; Leberer *et al.*, 1997a; Mösch *et al.*, 1996). The activated protein kinase Ste20p then activates a MAP kinase cascade formed by Ste11p, Ste7p and Kss1p (Cook *et al.*, 1996; Liu *et al.*, 1993; Madhani *et al.*, 1997).

In its unphosphorylated state, Kss1p interacts with the transcription factor Ste12p and potentiates transcriptional repression by its interaction with the negative regulators Dig1p and Dig2p. After its phosphorylation by Ste7p, Kss1p is able to phosphorylate Ste12p, Dig1p and Dig2p, thus promoting dissociation of Ste12p from its down-regulators (Cook *et al.*, 1996; Bardwell *et al.*, 1998). Released Ste12p is then able to cooperate with another transcription factor, Tec1p, thereby mediating transcriptional activation of genes containing regulatory elements known as FREs (Filamentation Response Elements). These elements consist of two adjacent sites, which contain the sequences TGAAACA and CATTCT/C and are cooperatively bound by Ste12p and Tec1p, respectively (Madhani and Fink, 1997). Recently, it has been shown that mutations in the karyopherin Kap121p result in mislocalization of Ste12p and subsequent defects in the dimorphic transition (Leslie *et al.*, 2002).

Recent studies have also identified dozens of genes that are regulated by the MAP kinase pathway (Madhani and Fink, 1997; Madhani *et al.*, 1999; Rupp *et al.*, 1999). These

include *FLO11*, a gene encoding a GPI-anchored flocculin that is necessary for cell-cell adhesion after cytokinesis (Lo and Dranginis, 1998), *TEC1* itself, and *PGU1*, a gene encoding a secreted polygalacturonase that is believed to play a role in the invasion of plant tissues by *S. cerevisiae* (Madhani *et al.*, 1999). In addition, it is known that transcription of *CLN1* is activated by the MAP kinase signaling cascade (Ahn *et al.*, 1999; Madhani *et al.*, 1999), whereas *CLB2* expression seems to be regulated by this pathway via the putative cell-cycle transcriptional regulators Fkh1p and Fkh2p (Hollenhorst *et al.*, 2000).

Other proteins involved in the regulation of the MAP kinase cascade include Ste50p, Bmh1p, Bmh2p, and possibly Spa2p. Ste50p is a protein of unknown function that appears to modulate Ste11p activity (Wu *et al.*, 1999), whereas the 14-3-3 proteins Bmh1p and Bmh2p are known to associate with Ste20p and are required for FRE-driven gene expression (Roberts *et al.*, 1997). Spa2p, in turn, has been shown to interact with many of the components of the MAP kinase cascade, and it is consequently thought to function as a scaffold during filamentous growth (Roemer *et al.*, 1998).

1.8.2 The cAMP-dependent pathway

Following its activation by nutrient signals (Section 1.8.4), Ras2p interacts with the adenylate cyclase Cyr1p, thereby stimulating the production of cAMP and activating the cAMP-dependent protein kinases Tpk1p, Tpk2p and Tpk3p through repression of their regulatory subunit, Bcy1p (Robertson and Fink, 1998; Pan and Heitman, 1999). During pseudohyphal growth, Tpk2p interacts with Sfl1p, a transcriptional repressor of *FLO11*

whose absence stimulates pseudohyphal growth (Robertson and Fink, 1998), and positively regulates the transcription factor Flo8p, which in turn regulates *FLO11* expression (Pan and Heitman, 1999). Tpk1p and Tpk3p, in turn, appear to repress pseudohyphal growth, possibly by a feedback loop that down-regulates cAMP accumulation (Mbonyi *et al.*, 1990; Nikawa *et al.*, 1987; Pan and Heitman, 1999; Rupp *et al.*, 1999). Intracellular cAMP concentrations and pseudohyphal growth are also regulated by the phosphodiesterases Pde1p and Pde2p (Ma *et al.*, 1999) (Fig. 1-6).

1.8.3 Upstream signals

In *S. cerevisiae*, pseudohyphal growth is activated by nitrogen limitation, poor carbon sources, and possibly by some stress conditions (Gancedo, 2001; Gimeno *et al.*, 1992; Lambrechts *et al.*, 1996; Lorenz *et al.*, 2000a).

Nitrogen starvation is sensed by the ammonium permease Mep2p to produce a signal that activates both Ras2p and the heterotrimeric G protein α subunit Gpa2p (Gagiano *et al.*, 1999b; Lorenz and Heitman, 1998b). Gpa2p is also activated by the G protein-coupled receptor Gpr1p, an integral membrane protein that has been shown to sense both sugar and nitrogen levels and which requires the phosphatidylinositol-specific phospholipase C, Plc1p, for its interaction with Gpa2p through its soluble carboxyl-terminal tail (Ansari *et al.*, 1999; Lorenz *et al.*, 2000b). Activated Gpa2p stimulates cAMP production by Cyr1p and, consequently, induces pseudohyphal growth via the cAMP-dependent pathway (Kübler *et al.*, 1997; Nakafuku *et al.*, 1988) (Fig. 1-7).

The glutamine $tRNA_{CUG}$ molecule has also been proposed to play a role in signaling

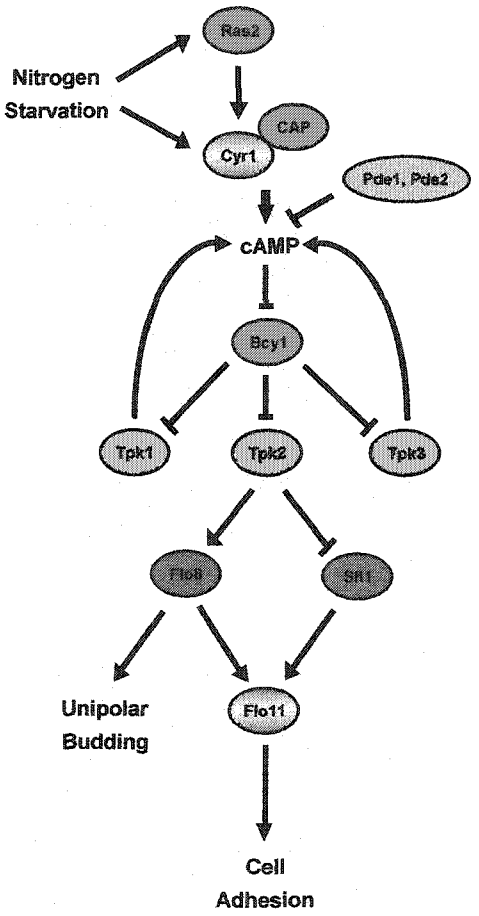

Figure 1-6. Regulation of pseudohyphal growth in *S. cerevisiae* by the cAMP-dependent pathway

nitrogen starvation and inducing pseudohyphal growth, possibly through the cAMP-dependent pathway (Murray *et al.*, 1998). In addition, both glucose and amino acid levels are also sensed by a still unknown mechanism to induce dimorphism through Grr1p, a complex assembly protein that is required for ubiquitin-mediated degradation of the G_1 cyclins Cln1p and Cln2p (Kishi and Yamao, 1998; Loeb *et al.*, 1999). Furthermore, intracellular acidification may also play a role in the induction of pseudohyphal growth through inhibition of Ira1p and Ira2p, two GAPs that regulate Ras2p activity in conjunction with the GEFs Cdc25p and Sdc25p (Colombo *et al.*, 1998; Palecek *et al.*, 2000) (Fig. 1-7).

1.8.4 Other genes regulating pseudohyphal growth in *S. cerevisiae*

Several other genes that regulate pseudohyphal growth in *S. cerevisiae* have been identified and do not appear to be components of the MAP kinase cascade or the cAMP-dependent pathway. These include *ACE2*, *ASH1*, *GLN3*, *MKS1*, *MSN1*, *PHD1*, *SWI5*, *SOK2* and *URE2* (Edskes *et al.*, 1999; Gagiano *et al.*, 1999a; 1999b; Gimeno and Fink, 1994; Matsuura and Anraku, 1993; Pan and Heitman, 2000). *MKS1* encodes a protein of unknown function that represses Ure2p, a negative regulator of nitrogen catabolism that inhibits the transcriptional activator Gln3p (Edskes *et al.*, 1999). In addition, Mks1p has been suggested to be a negative regulator of gene transcription downstream of the cAMP-dependent pathway (Matsuura and Anraku, 1993). *SOK2*, in turn, encodes a transcription factor that negatively regulates pseudohyphal growth through repression of the genes encoding the transcription factors Ash1p, Phd1p and Swi5p, independently of the MAP

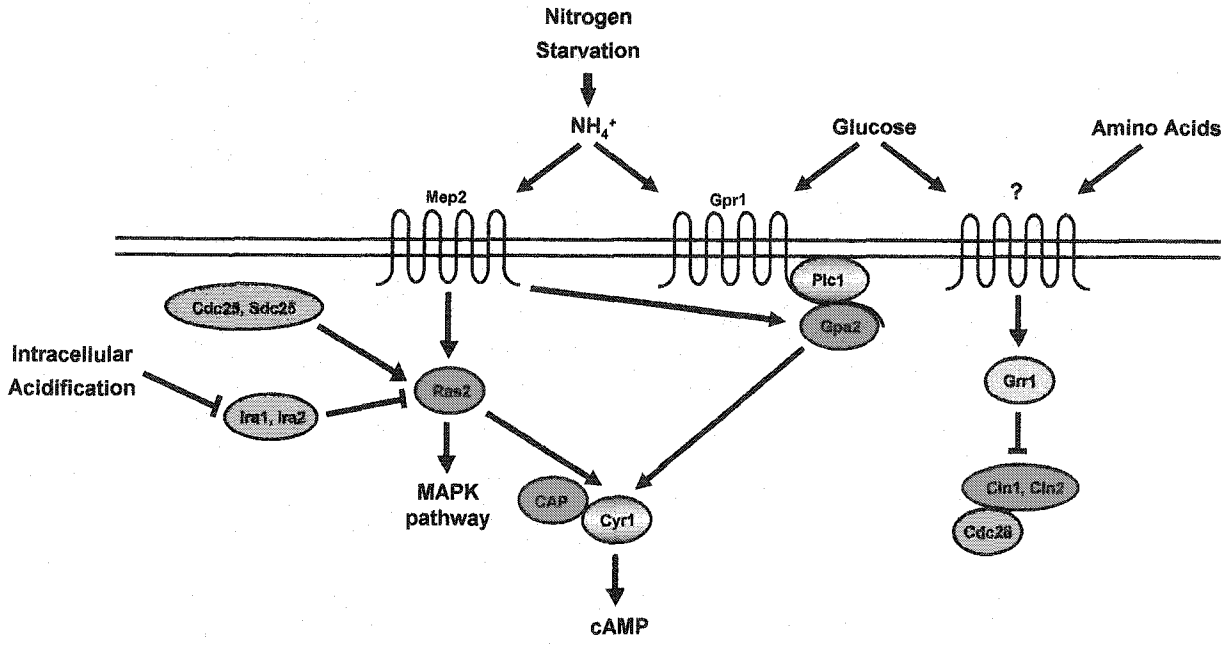

Figure 1-7. Upstream signals and the induction of pseudohyphal growth by the MAP kinase and cAMP-dependent pathways in *S. cerevisiae*

kinase and cAMP/PKA pathways (Chandarlapaty and Errede, 1998). In the absence of Sok2p, Phd1p induces transcription of *FLO11*, whereas Swi5p mediates pseudohyphal growth through transcriptional activation of *FLO11* via the GATA family transcription factor Ash1p. When *SWI5* is deleted, however, pseudohyphal growth occurs due to an increase in mother-daughter cell adhesion, which is caused by repression of the genes encoding the endochitinase Cts1p and the endoglucanase Egt2p (Pan and Heitman, 2000). Finally, Ace2p is a putative transcription factor that positively regulates the production of Cts1p (Doolin *et al.*, 2001), and *MSN1* encodes a transcription factor that operates downstream of Ras2p and induces *FLO11* transcription both independently and through activation of *MSS11* (Gagiano *et al.*, 1999a; 1999b) (Fig. 1-8).

Furthermore, mutations in the genes *RIM1* (*RIM101*), *RIM8*, *RIM9* and *RIM13* have been shown to prevent the invasive growth of haploid strains, thereby suggesting that the RIM pathway is also involved in the regulation of pseudohyphal growth in *S. cerevisiae* (Li and Mitchell, 1999; Treton *et al.*, 2000).

More recently, it has been demonstrated that the TOR signaling cascade controls filamentous growth in *S. cerevisiae* independent of the MAP kinase, cAMP, and Sok2p pathways (Cutler *et al.*, 2001). The protein kinases Tor1p and Tor2p are believed to act as regulators of translational initiation and progression through G_1 (Barbet *et al.*, 1996; Di Como and Arndt, 1996), and Tor2p has been shown to promote both organization of the actin cytoskeleton and activation of cell wall synthesis genes during G_1 via the the small GTPase, Rho1p, and protein kinase C (Pkc1p) (Gustin *et al.*, 1998; Helliwell *et al.*, 1998). The exact mechanisms by which the TOR pathway regulates dimorphism are still unclear,

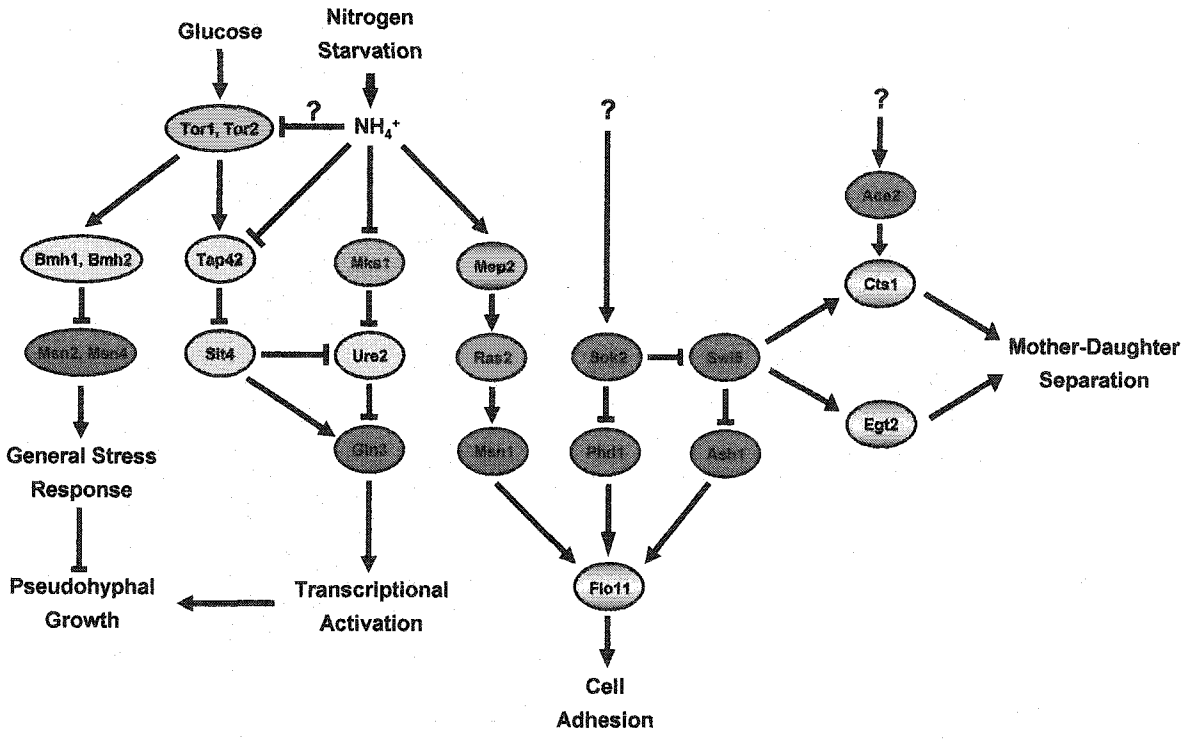

Figure 1-8. Other pathways regulating pseudohyphal growth in *S. cerevisiae*

but it has been shown that, in the presence of rich nitrogen sources, Tor1p and Tor2p inhibit the phosphatase Sit4p through its regulatory subunit Tap42p, and thereby Tor1p and Tor2p contribute to maintaining the association of the phosphorylated transcription factor Gln3p with its cytoplasmic anchor Ure2p. Under nitrogen limiting conditions, however, Gln3p is dephosphorylated by Sit4p, thus promoting its prompt accumulation in the nucleus (Beck and Hall, 1999; Cutler *et al.*, 2001) (Fig. 1-8). Interestingly, TOR has also been demonstrated to promote Tap42p-independent association of the transcription factors Msn2p and Msn4p (Section 1.10.1) with the cytoplasmic anchor Bmh2p in the absence of carbon source starvation (Beck and Hall, 1999; Görner *et al.*, 2002) (Fig. 1-8).

Dozens of other genes potentially involved in the regulation of pseudohyphal growth in *S. cerevisiae* have recently been identified through a genetic screening of repressors of *FLO11* (Palecek *et al.*, 2000) and by microarray hybridization experiments to identify MAP kinase-regulated genes (Madhani *et al.*, 1999).

1.8.5 Cross-talk between signaling pathways

There is much evidence of interaction between the MAP kinase and cAMP-dependent signaling pathways in the regulation of pseudohyphal growth. First, Mep2p and Ras2p play a dual role, activating both pathways (Gagiano *et al.*, 1999b; Kübler *et al.*, 1997; Lorenz and Heitman, 1998b; Mösch *et al.*, 1999). Second, cAMP inhibits the expression of FRE-driven reporter genes (Lorenz and Heitman, 1997), and high levels of cAMP or protein kinase A (PKA) activity enhance filamentous growth (Pan and Heitman,

1999). Third, Ste12p has several putative PKA phosphorylation sites, and it has been observed that signaling by the MAP kinase cascade can be induced by PKA at a level downstream of Ste20p (Lorenz and Heitman, 1998a; Mösch *et al.*, 1999). Fourth, these two pathways converge with the Sok2p-mediated pathway to regulate the large, complex promoter of the *FLO11* gene (Lo and Dranginis, 1998; Pan and Heitman, 1999; Rupp *et al.*, 1999) (Fig. 1-9). Finally, it has recently been shown that the protein kinase Yak1p regulates pseudohyphal growth through modulation of both the Ras-dependent MAP kinase and cAMP/PKA pathways, but the exact mechanisms by which Yak1p affects Ras2p-regulated signal transduction remain unclear (Zhang *et al.*, 2001).

Also, some components of the MAP kinase cascade are shared with other regulatory pathways. For example, pheromones activate the Ste20p-Ste11p-Ste7p cascade, and high osmolarity induces activation of Ste11p (Posas *et al.*, 1998). However, inappropriate cross-talk between these pathways seems to be prevented by formation of specific protein complexes that eventually activate MAP kinases of different affinities. Thus, Kss1p is responsible for pseudohyphal growth, the pheromone response activates Fus3p, and Hog1p responds to osmotic stress (Posas *et al.*, 1998).

1.9 Signal transduction pathways regulating dimorphism in *C. albicans*

1.9.1 The MAP kinase cascade

A MAP kinase cascade similar to that of *S. cerevisiae* is involved in the regulation of dimorphism in *C. albicans*. Components of this cascade include *Ca*Ras1p, *Ca*Cdc42p, *Ca*Bmh1p, Hst7p (homolog of *Sc*Ste7p), the MAP kinase Cek1p, and the PAKs *Ca*Cla4p

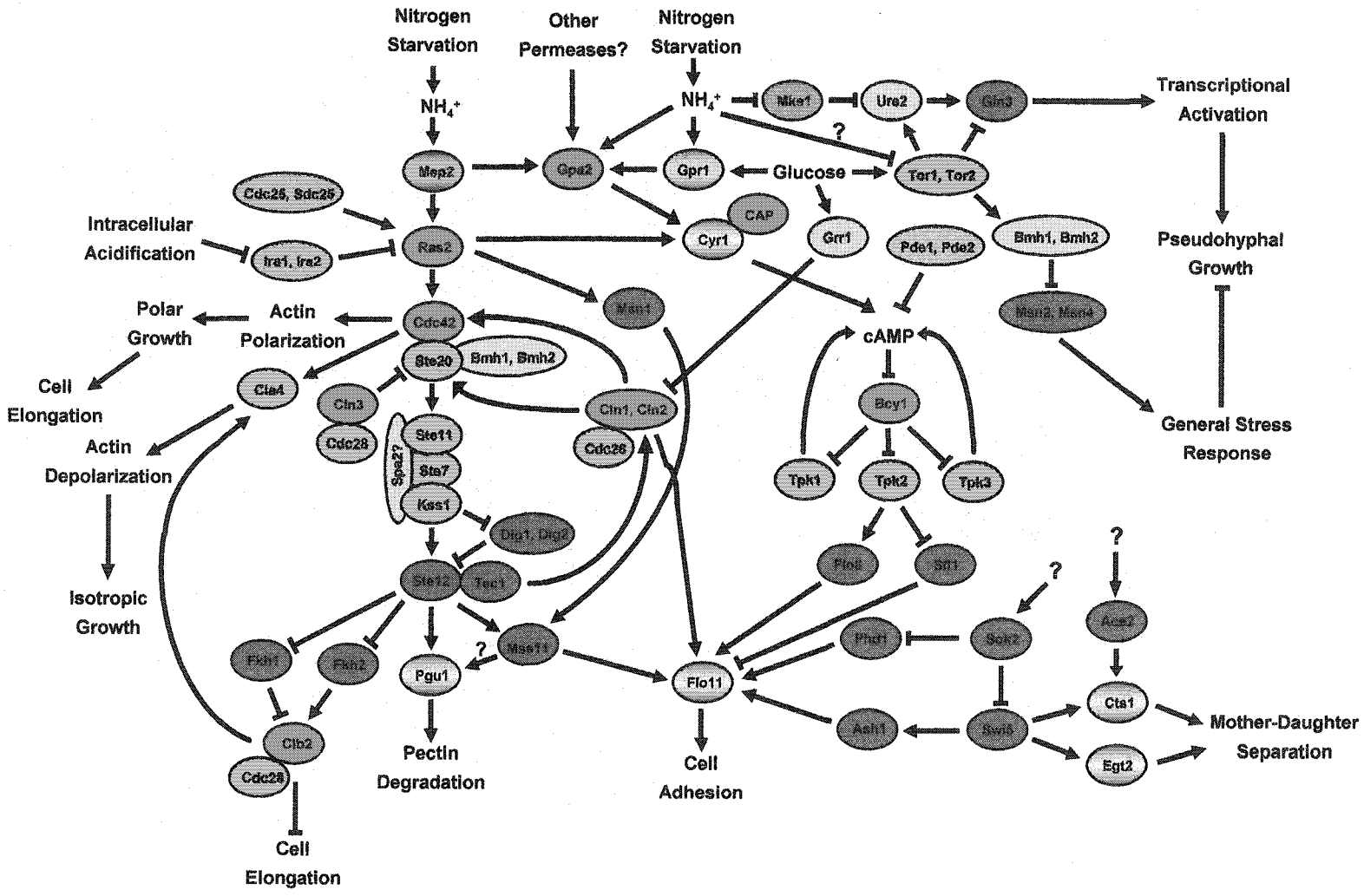

Figure 1-9. Cross-talk between signaling pathways in *S. cerevisiae*

and Cst20p (homolog of *Sc*Ste20p) (Cognetti *et al.*, 2002; Csank *et al.*, 1998; Feng *et al.*, 1999; Leberer *et al.*, 1996, 1997b; Ushinsky *et al.*, 2002). The *C. albicans* homolog of Ste11p has not yet been identified.

As in *S. cerevisiae*, this cascade appears to activate the transcription factor Cph1p (homolog of *Sc*Ste12p), and possibly also *Ca*Tec1p (Liu *et al.*, 1994; Schweizer *et al.*, 2000). An additional component of this signaling pathway is Cpp1p, a putative MAP kinase phosphatase that suppresses hyphal formation through its probable substrate, Cek1p (Schroppel *et al.*, 2000) (Fig. 1-10).

1.9.2 The cAMP-dependent pathway

The cAMP-dependent pathway also plays a crucial role in the induction of filamentous growth in *C. albicans*. In this organism, there are only two PKA catalytic subunits, *Ca*Tpk1p and *Ca*Tpk2p. However, unlike the three *S. cerevisiae* PKA isoforms, both *C. albicans* catalytic subunits are positive regulators of hyphal growth, and they appear to play specific roles under different environmental conditions (Bockmuhl *et al.*, 2001). The activity of *Ca*Tpk1p and *Ca*Tpk2p appears to be induced by an increase in the cytoplasmic concentration of cAMP, which in turn is regulated by the adenylate cyclase *Ca*Cyr1p and the Cyr1p-associated protein Cap1p (Bahn and Sundstrom, 2001; Mallet *et al.*, 2000). A gene encoding the putative regulatory subunit of PKA, *Ca*Bcy1p, has been identified through genome sequencing of *C. albicans* (Whiteway, 2000).

Like *Sc*Ras2p, *Ca*Ras1p is an important regulator of filamentous growth in *C. albicans* and is believed to act upstream of the cAMP-dependent pathway, mediating the

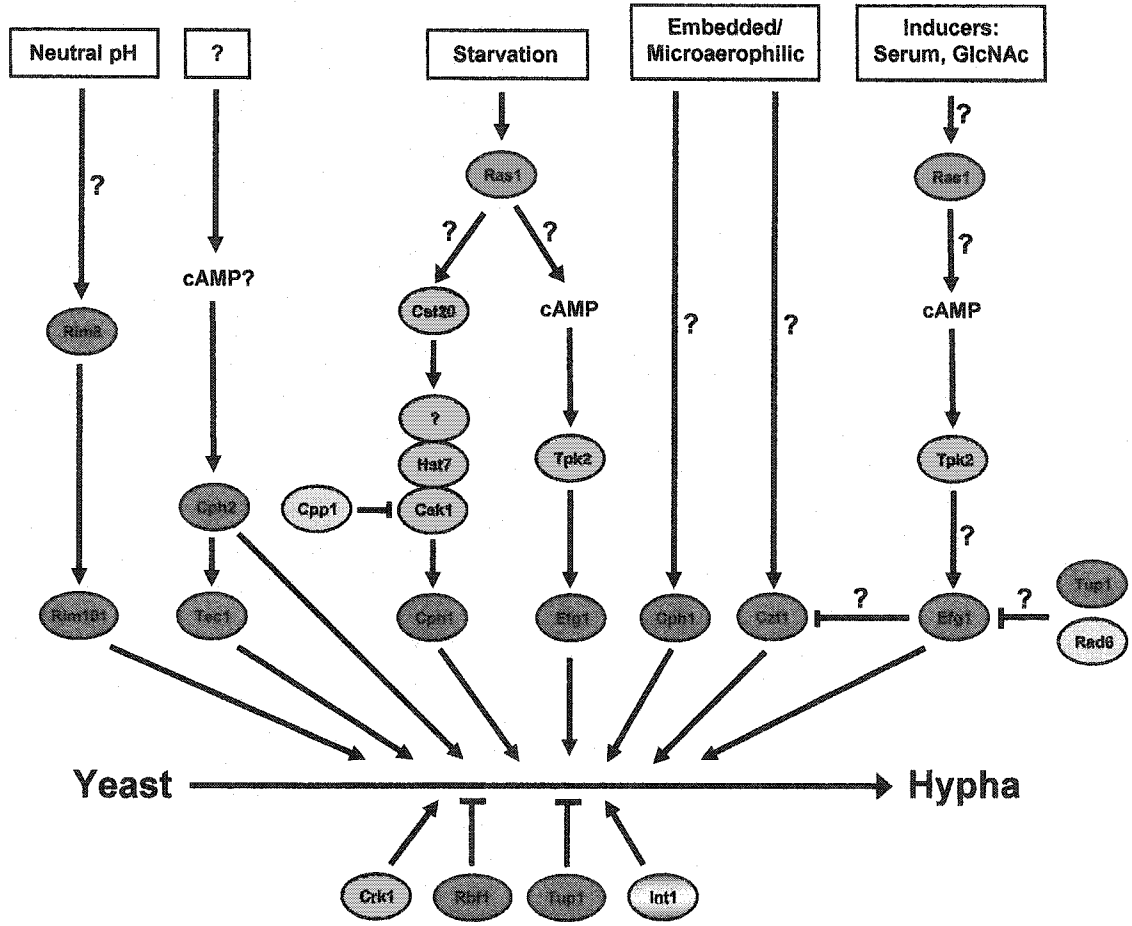

Figure 1-10. Regulation of hyphal growth in *C. albicans*
Modified from Ernst (2000).

filamentous response to starvation, serum and GlcNAc (Feng *et al.*, 1999). In addition, genes encoding the *C. albicans* homologs of Gpa2p and Gpr1p have also been identified, but it is not yet known whether they are involved in the activation of the cAMP pathway (Liu, 2001).

Several targets for the cAMP-dependent pathway potentially exist. These include the transcription factor Efg1p, a bHLH protein similar to Phd1p and Sok2p of *S. cerevisiae*, which plays an important role in the regulation of hyphal morphogenesis in *C. albicans* (Leng *et al.*, 2001; Stoldt *et al.*, 1997) (Fig. 1-10). Efg1p has a potential phosphorylation site for PKA, the mutation of which affects hyphal growth, suggesting that Efg1p is a central downstream component of the cAMP-dependent pathway (Bockmuhl and Ernst, 2001).

1.9.3 Other signaling pathways

The existence of additional regulatory pathways (other than the MAP kinase-Cph1p cascade and the Efg1p-transmitted cAMP pathway) is suggested by the fact that *cph1/cph1 efg1/efg1 tup1/tup1* triple mutants of *C. albicans* are still able to undergo environmentally induced hyphal growth (Braun and Johnson, 2000). *CaTUP1* encodes a putative transcription factor that is believed to repress genes required for the induction of hyphal growth in *C. albicans* (Braun and Johnson, 1997). *Ca*Tup1p itself seems to represent a third regulatory pathway and requires the formation of complexes with other transcription factors, such as *Ca*Mig1p, *Ca*Nrg1p and *Ca*Rfg1p, in order to be targeted to specific subsets of genes involved in the regulation of metabolism, stress response and

morphogenesis in *C. albicans* (Khalaf and Zitomer, 2001; Murad *et al.*, 2001) (Fig. 1-10).

Other transcription factors involved in the regulation of hyphal morphogenesis in *C. albicans* include Czf1p, *Ca*Tec1p and *Ca*Rim101p (Brown *et al.*, 1999; Davis *et al.*, 2000; Schweizer *et al.*, 2000). Czf1p is a novel transcription factor that, like Efg1p, promotes hyphal growth in response to physical/microaerophilic conditions (Brown *et al.*, 1999), whereas *Ca*Tec1p is a member of the TEA/ATTS family of transcription factors that regulates hyphal morphogenesis in *C. albicans*, likely downstream of Efg1p and independently of Cph1p (the homolog of *S. cerevisiae* Ste12p) (Liu, 2001; Schweizer *et al.*, 2000). *Ca*Rim101p, in turn, is a zinc finger protein whose production depends on *Ca*Rim8p and *Ca*Rim20p to induce hyphal growth in response to alkaline conditions. This transcription factor regulates morphogenesis in *C. albicans* through the induction of several genes, including *PHR1*, *PRA1* and *RIM101* itself (Davis *et al.*, 2000). *Ca*Pra1p is a putative vesicular transport protein (Yang *et al.*, 1998), whereas Phr1p is required for proper cross-linking of cell wall glucans (Section 1.6.2) (Fonzi, 1999). Interestingly, *PHR2*, the gene encoding the other Phr protein identified in *C. albicans*, appears to be activated by a different pH-response pathway, that is independent of *Ca*Rim101p (Davis *et al.*, 2001) (Fig. 1-10).

The growing number of proteins believed to regulate hyphal morphogenesis in *C. albicans* through alternative pathways also includes Cph2p, Crk1p and Rbf1p (Chen *et al.*, 2000; Ishii *et al.*, 1997; Lane *et al.*, 2001). Cph2p, a bHLH transcription factor that induces hyphal growth partly through regulatory elements found upstream of *Ca*Tec1p, appears to function independently of the Cph1p-mediated MAP kinase pathway and the

Efg1p-transmitted cAMP pathway (Lane *et al.*, 2001). However, Cph2p contains several potential phosphorylation sites for casein kinase II, protein kinase C, and PKA, and a partial role for Cph2p downstream of the cAMP-dependent pathway cannot be completely ruled out (Lane *et al.*, 2001). Crk1p (Cdc2-related protein kinase), in turn, has been found to induce filamentation in *C. albicans* through a route independent of Cph1p and Efg1p. However, when expressed in *S. cerevisiae*, Crk1p activity requires Flo8p, but not Ste12p or Phd1p, indicating that it may also be a downstream effector of the *C. albicans* cAMP-dependent pathway (Chen *et al.*, 2000). Finally, Rbf1p is another putative transcription factor that seems to function as a repressor of hyphal growth, but not of pseudohyphal growth (Ishii *et al.*, 1997; Ernst 2000) (Fig. 1-10).

1.9.4 Other genes involved in filamentous growth in *C. albicans*

As in *S. cerevisiae*, dozens of other genes involved in the regulation of hyphal morphogenesis in *C. albicans* have been identified through genetic screens, differential display, and microarray hybridization experiments. The products of these genes include important virulence factors such as Hwp1p, Int1p, Rbt1p and Rbt4p (Braun *et al.*, 2000; Gale *et al.*, 1998; Staab *et al.*, 1999).

1.10 Stress response and dimorphism in *S. cerevisiae*

It has been observed that nitrogen starvation, thermal stress, osmotic stress, and compounds that affect the lipid bilayer organization of the cell membrane are able to induce pseudohyphal growth in *S. cerevisiae*, likely through the coordinated action of the

MAP kinase cascade and the cAMP-dependent pathway (Zaragoza and Gancedo, 2000).

Although the molecular mechanisms by which these stress conditions induce pseudohyphal growth are not yet clear, it is known that most stress response pathways share several components with the signal transduction pathways that regulate dimorphism in *S. cerevisiae*.

1.10.1 The general stress response pathway

General stress response in *S. cerevisiae* is mediated by Msn2p and Msn4p, two transcription factors that are known to bind to sequences containing the pentanucleotide CCCCT or AGGGG (termed Stress Response Elements or STREs) in the upstream regulatory regions of genes, thereby inducing the expression of genes involved in the response to adverse environmental conditions, such as nutrient starvation, thermal stress, high osmolarity, oxidative stress, low pH, or the presence of ethanol or sorbitol (Görner *et al.*, 1998; Martinez-Pastor *et al.*, 1996; Treger *et al.*, 1998).

Nuclear localization of Msn2p and Msn4p, and consequently the transcription of genes containing STREs, is negatively regulated by the cAMP-dependent pathway (Görner *et al.*, 1998), likely through the induction of nuclear export of Msn2p and Msn4p by Msn5p, a known modulator of the activity of these factors (Estruch, 2000; Görner *et al.*, 2002).

There is ample genetic evidence supporting a negative role for Msn2p and Msn4p in the induction of pseudohyphal growth in *S. cerevisiae*. For example, overexpression of *MSN5* restores filamentation to cells lacking *MEP1* and *MEP2* (Lorenz and Heitman,

1998a), mutants defective in Gpr1p and/or Gpa2p (Section 1.8.3) show increased expression of STRE-controlled genes (Colombo *et al.*, 1998; Kraakman *et al.*, 1999), and deletion of *MSN2* and *MSN4* restores cell polarity and pseudohyphal growth to strains lacking *RAS2* (Ho and Bretscher, 2001; Stanhill *et al.*, 1999) (Fig. 1-11).

1.10.2 The high osmolarity glycerol (HOG) response pathway

When *S. cerevisiae* cells are exposed to high osmolarity environments, a MAP kinase pathway is activated to produce and accumulate glycerol and thus counteract cell dehydration and protect cellular structures (Albertyn *et al.*, 1994; Brewster *et al.*, 1993).

Hyperosmolarity is detected by two transmembrane osmosensors, Sho1p and Sln1p, which activate the same MAP kinase, Hog1p (Maeda *et al.*, 1994; 1995). To activate Hog1p, Sho1p transmits a signal to the MAPKK, Pbs2p, via the MAPKKK, Ste11p (Posas and Saito, 1997), whereas Sln1p uses a two-component phosphorelay system consisting of Ssk1p and Ypd1p coupled to the MAPKKKs, Ssk2p and Ssk22p, to activate Pbs2p (Posas and Saito, 1998) (Fig. 1-11).

Hog1p has been demonstrated to have some inhibitory effect on the Ste12p-mediated MAP kinase signaling pathway (Madhani and Fink, 1997), and phosphorylated Hog1p is believed to induce a high osmolarity response through activation of the transcription factors Hot1p, Msn1p, Msn2p and Msn4p (Estruch, 2000). In agreement with these observations, mutant strains lacking *HOG1* have been shown to be consistently more filamentous than wild-type strains (Madhani and Fink, 1997). Interesting, however,

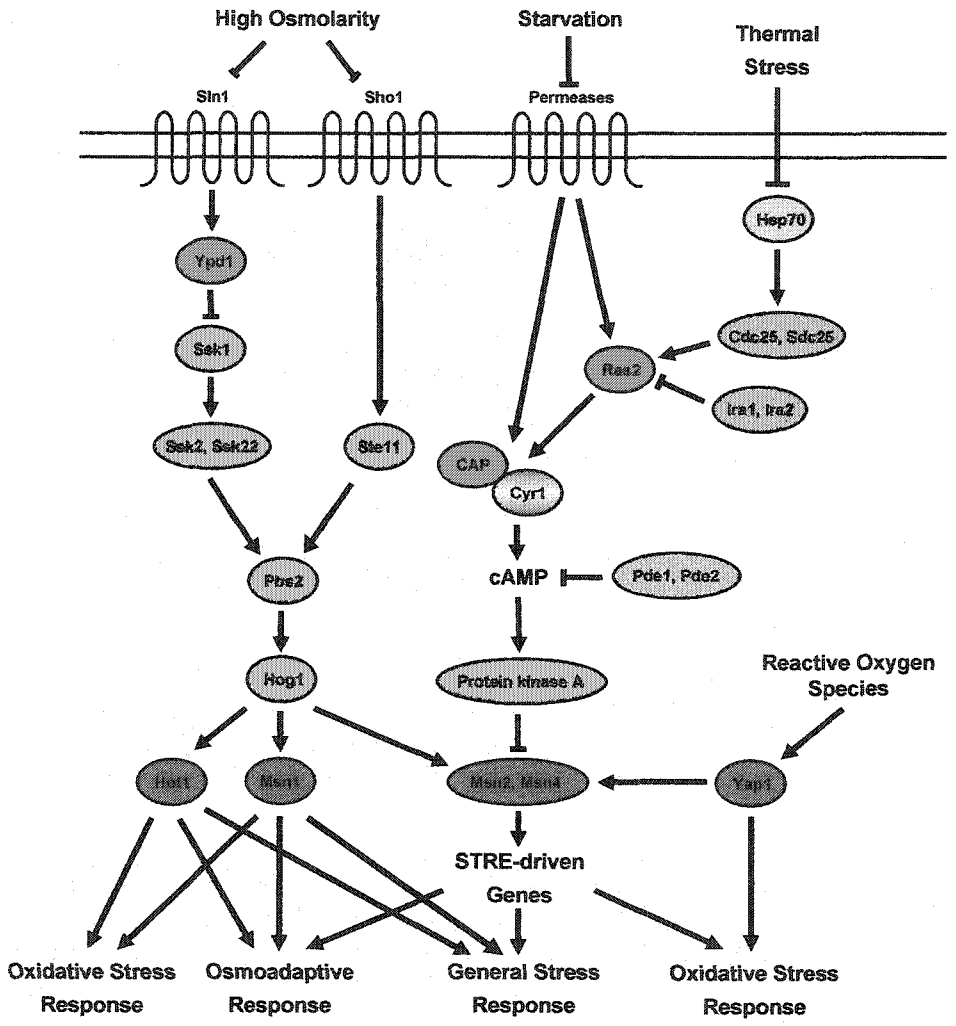

Figure 1-11. Major stress response pathways of *S. cerevisiae*

is the fact that the osmosensor Sho1p is required for normal pseudohyphal growth, as well as for the hyperfilamentous phenotype of *hog1* strains (O'Rourke and Herskowitz, 1998). Accordingly, it has been hypothesized that, since Sho1p activates Ste11p in response to osmotic stress, this transmembrane protein may act as a detector of osmolarity signals that induce morphogenesis through the MAP kinase cascade (Gancedo, 2001) (Fig. 1-11).

1.10.3 Oxidative stress response

Several transcription factors have been shown to be involved in the regulation of gene expression under oxidative stress conditions (Estruch, 2000). The best characterized of them is Yap1p, a *b-ZIP* protein that activates the transcription of a subset of genes encoding defenses against reactive oxygen species (ROS) through its interaction with *cis*-acting AP-1 response elements (ARE; TGACTCA) (Estruch, 2000; Harshman *et al.*, 1988). In addition, Yap1p has been demonstrated to be required for transcriptional activation of STRE-containing genes and, consequently, is believed to function upstream of Msn2p and Msn4p (Gounalaki and Thireos, 1994; Ruis and Schüller, 1995) (Fig. 1-11).

A potential role for Yap1p in the repression of filamentous growth in *S. cerevisiae* is suggested by the observation that deletion of *YAP1* restores pseudohyphal growth to strains lacking *RAS2* (Stanhill *et al.*, 1999), and it has been postulated that some gene(s) activated by the transcription factors Msn2p, Msn4p and Yap1p may have a negative effect on the induction of the dimorphic transition in *S. cerevisiae* (Gancedo, 2001).

1.11 *Y. lipolytica* as a model organism for the study of fungal dimorphism

1.11.1 General characteristics of *Y. lipolytica*

The ascomycetous yeast *Y. lipolytica* is a nonpathogenic, strictly aerobic organism with a genome that, at an estimated size of 21-22 megabases, is almost twice those of *S. cerevisiae* and *Schizosaccharomyces pombe* (Casaregola *et al.*, 2000). *Y. lipolytica* is heterothallic, and virtually all natural isolates are haploid, thereby suggesting that the haploid state is the most stable (Barth and Gaillardin, 1996). The mating types are determined by the genes *MATA* and *MATB*, and both mating frequencies and sporulation rates of natural isolates have been found to be extremely low (Bassel *et al.*, 1971; Casaregola *et al.*, 2000; Kurischko *et al.*, 1992). These defects, however, have been partially alleviated by inbreeding programs, and a transformation system was developed in the 1980s, thus making this organism more amenable to genetic and molecular biological analyses (Barth and Weber, 1984, 1986; Davidow *et al.*, 1985).

Y. lipolytica is a dimorphic fungus that is able to alternate between a unicellular yeast form and distinct filamentous forms (hyphae and pseudohyphae). Yeast cells measure approximately 3 μm × 5 μm, pseudohyphal cells may reach 5 μm × 11 μm, and mycelium consists of septate hyphae 3 to 5 μm in width and up to several millimeters in length. Mycelial filaments are divided in segments of 50 to 70 μm, each containing a single nucleus (van der Walt and von Arx, 1980). A central pore is normally found in the hyphal septa, with endoplasmic reticulum extending through it from one cell to the next (Kreger-van Rij and Veenhuis, 1973). Interestingly, budding in *Y. lipolytica* follows a bipolar pattern, as opposed to the axial pattern of *C. albicans* diploid cells and *S.*

cerevisiae haploid cells, and germ tube emission occurs on the pole opposite that of the previous bud scar (Herrero *et al.*, 1999).

Y. lipolytica has been of interest since the 1940s due to its many potential uses in biotechnology. This organism secretes large amounts of several enzymes, such as lipases and proteases (Ogrydziak and Schraf, 1982; Peters and Nelson, 1948; Tobe *et al.*, 1976; Yamada and Ogrydziak, 1983), and has the ability to utilize hydrocarbons as a substrate for the production of single-cell protein and metabolites such as citric acid, isocitric acid, 2-ketoglutaric acid, and γ-decalactone (peach flavor) (Bassel *et al.*, 1971; Gaillardin and Heslot, 1988). More recently, *Y. lipolytica* has also received attention because of its potential use as an expression system for heterologous proteins (Buckholz and Gleeson, 1991), and it has been used as a model system to study the secretion of extracellular enzymes (Beckerich *et al.*, 1998; Ogrydziak *et al.*, 1982), the lysine catabolic pathway (Beckerich *et al.*, 1984), peroxisome biogenesis (Nuttley *et al.*, 1993; Titorenko *et al.*, 2000), and fungal dimorphism (Barth and Gaillardin, 1996).

1.11.2 Environmental factors that regulate dimorphism in *Y. lipolytica*

Early studies on dimorphism in *Y. lipolytica* were done to determine the nutritional factors that could induce mycelial development during the industrial production of lipases. These studies revealed that mycelial growth was inhibited by a deficiency of magnesium sulfate and ferric chloride or by the addition of cysteine and reduced glutathione (Ota *et al.*, 1984). No correlation between filamentous growth and the production of lipase has been found at this time (Novotny *et al.*, 1994).

The yeast-to-hypha transition in *Y. lipolytica* is normally induced in minimal medium containing GlcNAc as the sole carbon source (Rodriguez and Dominguez, 1984), but this procedure has been observed to be strain-dependent (Barth and Gaillardin, 1996). Recently, it has been shown that both horse and bovine calf serum are stronger inducers of filamentous growth than GlcNAc (Dominguez *et al.*, 2000; Kim *et al.*, 2000). This is not entirely surprising, since *Y. lipolytica* can normally be found in dairy products (van der Walt and von Arx, 1980). Interestingly, serum-specific mutants, which form hyphae in GlcNAc-containing medium but not in serum medium, have been isolated, suggesting that these inducers may promote hyphal growth through different regulatory pathways (Kim *et al.*, 2000).

Bovine serum albumin has also been demonstrated to be able to induce the yeast-to-hypha transition, although to a lesser extent than serum or GlcNAc, and it was suggested that nitrogen starvation is not an inducer of dimorphism in *Y. lipolytica* (Perez-Campo and Dominguez, 2001). Accordingly, it has recently been shown that, in contrast to *S. cerevisiae*, filament formation is inhibited by nitrogen starvation in *Y. lipolytica*, and the presence of organic sources of nitrogen is critical for the yeast-to-hypha transition in this organism (Szabo, 1999; Szabo and Štofaníková, 2002).

The role of pH and temperature in the induction of filamentous growth of *Y. lipolytica* has also been controversial. Thus, while some authors argue that pH does not play a relevant role in the morphogenetic switch (Perez-Campo and Dominguez, 2001), others have observed that pH control is sufficient to induce filamentous growth in minimal medium containing glucose as the sole carbon source, and that this induction is more

effective in citrate-buffered medium than it is in medium buffered with phosphate (Novotny *et al.*, 1994). However, more recent studies suggest that, in *Y. lipolytica*, pH indirectly affects the formation of hyphae by modulating the availability and/or utilization of transportable sources of nitrogen (Szabo and Štofaníková, 2002). In a similar way, Perez-Campo and Dominguez (2001) argue that *Y. lipolytica* does not require any change in temperature for the induction of hyphal growth, but Guevara-Olvera *et al.* (1993) reported that the yeast-to-hypha transition can be enhanced by submitting cells to a heat shock during inoculation in medium containing GlcNAc as the sole carbon source.

Inhibitors of mitochondrial respiration have also been described to suppress strongly the development of hyphae (Szabo, 1999), and both osmotic and oxidative stresses were demonstrated to inhibit hyphal growth induced by GlcNAc, but not by serum (Kim *et al.*, 2000; Perez-Campo and Dominguez, 2001).

1.11.3 Physiological and structural changes during morphogenesis in *Y. lipolytica*

Although no ultrastructural differences have been found between the cell walls of hyphal and yeast cells of *Y. lipolytica*, chemical analyses have demonstrated that there are significant differences in their chitin and protein contents. Thus, yeast cell walls appear to contain 7% of aminosugars and 15% of protein, whereas hyphal cell walls are composed approximately of 14% of aminosugars and 6% of protein (Vega and Dominguez, 1986). Remarkably, *Y. lipolytica* yeast cells appear to have high chitin content (6-8%, as compared to less than 1% in *S. cerevisiae*) (Vega and Dominguez, 1986). The qualitative protein content of the cell wall also seems to vary between both

forms (Dominguez *et al.*, 2000; Vega and Dominguez, 1986), and a cell wall protein specific to the mycelial form, Ywp1p, has been identified (Ramon *et al.*, 1996).

An increase in both the polyamine cell pools and ornithine decarboxylase (ODC) activity during the yeast-to-hypha transition (Guevara-Olvera *et al.*, 1993), as well as differences in the DNA methylation patterns of these two forms (Reyna-Lopez *et al.*, 1997), have also been described.

1.11.4 Genes involved in the regulation of morphogenesis of *Y. lipolytica*

In order to identify genes involved in the regulation of the dimorphic transition of *Y. lipolytica,* three approaches have been adopted: PCR amplification of conserved regions of genes whose homologs are known to regulate morphogenesis in other fungal species (Dominguez *et al.*, 2000), functional complementation of mutants unable to undergo the yeast-to-hypha transition (Torres-Guzman and Dominguez, 1997), and transposon-tagged insertional mutagenesis (Richard *et al.*, 2001). In addition, phenotypic analysis of mutations in genes whose products are involved in peroxisome biogenesis, and in the synthesis and/or secretion of extracellular proteases, has revealed that several of these genes are also involved in the regulation of hyphal growth in *Y. lipolytica* (Enderlin and Ogrydziak, 1994; Gonzalez-Lopez *et al.*, 2002; Lopez *et al.*, 1994; Titorenko *et al.*, 1997). Table 1-1 lists the genes involved in the regulation of morphogenesis of *Y. lipolytica* identified to date and the key features of their protein products.

Interestingly, the *Y. lipolytica* genes *YlRIM9*, *YlRIM13*, *YlRIM20* and *YlRIM101* have been shown not to be required for hyphal formation, indicating that, in contrast to the

situation in *C. albicans* and *S. cerevisiae*, the Rim pathway is not essential for the dimorphic transition in *Y. lipolytica* (Gonzalez-Lopez *et al.*, 2002; Treton *et al.*, 2000). In a similar way, the *Y. lipolytica* homolog of *STE7* has been demonstrated to be required for mating but not for hyphal growth (Dominguez *et al.*, 2000).

Table 1-1 *Y. lipolytica* Genes Involved in the Regulation of the Dimorphic Transition

Gene	Features	Reference
YlBUD6	Encodes a putative actin-interacting protein; *Sc*Bud6p is a component of the apical scaffold and is required for cell polarization; disruption results in severe morphological defects and inability to form hyphae	Amberg *et al.*, 1997; Richard *et al.*, 2001; Sheu *et al.*, 1998
YlCDC25	Encodes a putative GEF; *Sc*Cdc25p is a GEF for *Sc*Ras2p, which is a critical regulator of pseudohyphal growth; null mutants are unable to form hyphae	Colombo *et al.*, 1998; Mösch *et al.*, 1996; Richard *et al.*, 2001
YlCLA4	Encodes a putative PAK whose homologs in *S. cerevisiae* and *C. albicans* are known regulators of cell polarity and morphogenesis; null mutants are unable to form hyphae	Leberer *et al.*, 1997b; Pruyne and Bretscher, 2000a; Szabo, 2001
YlGPI7	Encodes a protein of unknown biochemical function, which may be involved in the addition of GPI anchors to cell surface proteins; *Sc*Gpi7p is associated with either the ER, the vacuole, or the plasma membrane, but not with the Golgi; *Sc*Gpi7p is thought to play a role in bud site selection; null mutants are unable to form hyphae	Benachour *et al.*, 1999; Ni and Snyder, 2001; Richard *et al.*, 2001
GPR1	Encodes a protein of unknown biochemical function, which appears to be a regulator of the glyoxylate pathway; *trans*-dominant *GPR1*mutants are unable to form hyphae and show enlarged mitochondria, reduced ER, and large vacuoles	Tzschoppe *et al.*, 1999
HOY1	Encodes a putative transcription factor; null mutants are unable to form hyphae	Torres-Guzman and Dominguez, 1997
YlMED4	Encodes a putative transcription factor; *Sc*Med4p is involved in chromatin organization and is a component of the RNA polymerase II complex; disruption results in reduced hyphal growth	Gonzalez-Lopez *et al.*, 2002; Lorch *et al.*, 2000

YlNUP85	Encodes a putative nucleoporin; *Sc*Nup85p is involved in nuclear export of mRNA; disruption results in reduced hyphal growth	Gonzalez-Lopez *et al.*, 2002; Goldstein *et al.*, 1996
YlOPT1	Encodes a putative member of the oligopeptide transporter (OPT) family of secondary active membrane transporters; *Sc*Opt1p is involved in extracellular amino acid sensing; disruption results in reduced hyphal growth	Gonzalez-Lopez *et al.*, 2002; Hauser *et al.*, 2000
YlPEX2	Encodes an integral membrane protein of peroxisomes; disruption affects the export of plasma membrane and cell wall-associated proteins specific for the hyphal form; null mutants are unable to form hyphae	Eitzen *et al.*, 1996; Titorenko *et al.*, 1997
YlPEX5	Encodes the peroxisomal targeting signal-1 (PTS1) import receptor; cytosolic and/or peroxisome-associated; disruption affects the export of plasma membrane and cell wall-associated proteins specific for the hyphal form; null mutants are unable to form hyphae	Szilard *et al.*, 1995; Titorenko *et al.*, 1997
YlPEX6	Encodes a cytosolic and peripheral peroxisomal membrane protein; belongs to the AAA family of ATPases; disruption affects the export of plasma membrane and cell wall-associated proteins specific for the hyphal form; null mutants are unable to form hyphae	Nuttley *et al.*, 1994; Titorenko *et al.*, 1997
YlPEX8	Encodes a peripheral peroxisomal membrane protein; part of the import docking complex of peroxisomes; null mutants are unable to form hyphae	Smith *et al.*, 1997; Titorenko *et al.*, 1997
YlPEX9	Encodes a peroxisomal integral membrane protein; null mutants are unable to form hyphae	Eitzen *et al.*, 1995; Titorenko *et al.*, 1997
YlPEX16	Encodes a peripheral peroxisomal membrane protein; involved in peroxisome proliferation; null mutants are unable to form hyphae	Eitzen *et al.*, 1997; Titorenko *et al.*, 1997
YlPHD1	Encodes a putative transcription factor; *Sc*Phd1p is related to transcriptional regulators of fungal development, including *Aspergillus nidulans* StuAp and *Neurospora crassa* Asm-1p1; *Sc*Phd1p regulates pseudohyphal growth partly via transcriptional activation of *FLO11*; overexpression of *YlPHD1* in *Ylras2Δ* mutant cells restores only pseudohyphal growth; null mutants are unable to form hyphae	Gimeno and Fink, 1994; Pan and Heitman, 2000; Richard *et al.*, 2001
YlPPH21	Encodes a putative protein phosphatase; *Sc*Pph21p is involved in organization of the actin cytoskeleton, cell cycle control, and cell wall synthesis; null mutants are unable to form hyphae and pseudohyphae but retain the ability to invade agar	Lin and Arndt, 1995; Richard *et al.*, 2001

YlRAS2	Encodes a small GTPase; *Sc*Ras2p and *Ca*Ras1p are important regulators of filamentous growth, acting upstream of both the MAP kinase and the cAMP-dependent pathways; null mutants are unable to form hyphae and pseudohyphae	Feng *et al.*, 1999; Mösch *et al.*, 1996; Richard *et al.*, 2001
YlSEC14	Encodes a phosphatidylinositol/phosphatidylcholine transfer protein (PI/PC-TP); *Yl*Sec14p is associated with the Golgi apparatus; null mutant strains are unable to form hyphae	Lopez *et al.*, 1994
YlSIN3	Encodes a putative transcription factor; *Sc*Sin3p is involved in transcriptional repression through localized histone deacetylation; null mutant strains are unable to form hyphae	Gonzalez-Lopez *et al.*, 2002; Pazin and Kadonaga, 1997
YlSNF5	Encodes a putative transcription factor; *Sc*Snf5p is a transcriptional regulator that affects expression of a broad spectrum of genes; null mutants are unable to form hyphae	Laurent *et al.*, 1990 Richard *et al.*, 2001
YlSRP54	Encodes a putative component of the secretory signal recognition particle; null mutants are unable to form hyphae	Lee and Ogrydziak, 1997; Titorenko *et al.*, 1997
YlSSY5	Encodes a putative secondary active membrane transporter; *Sc*Ssy5p is involved in extracellular amino acid sensing; disruption results in reduced hyphal growth	Forsberg and Ljungdahl, 2001; Gonzalez-Lopez *et al.*, 2002
YlTUP1	Encodes a putative transcription factor; like in *C. albicans,* disruption results in constitutive hyphal growth	Braun and Johnson, 2000; Dominguez *et al.*, 2000
YlVPS28	Encodes a protein of unknown biochemical function; *Sc*Vps28p appears to be involved in vacuole organization and biogenesis; disruption results in reduced hyphal growth	Gonzalez-Lopez *et al.*, 2002; Rieder *et al.*, 1996
XPR6	Encodes a dibasic processing endoprotease with significant homology to *S. cerevisiae* Kex2p; null mutant strains form large cell aggregates and are unable to undergo the dimorphic transition.	Enderlin and Ogrydziak, 1994; Szabo, 1999

1.12 Purpose of this work

Despite the development of specific molecular and genetic tools for *C. albicans* in the last few years, a better understanding of the yeast-to-hypha transition in this organism has largely been hampered by its diploid nature and its lack of a known sexual cycle. To

circumvent these difficulties, *S. cerevisiae* has been used as a model of dimorphic transition, and results with this yeast have been extrapolated to other organisms, particularly *C. albicans*. Although significant advances in our understanding of the dimorphic transition have been made using *S. cerevisiae*, the inability of this yeast to form true hyphae, and the hypothesis that true hyphal formation and pseudohyphal growth occur at least in part by separate pathways, limit this approach. In the last few years, *Y. lipolytica* has received increasing attention as an alternative model system for the study of the dimorphic transition because it can reproduce sexually, it is amenable to genetic and molecular biological analyses, it can alternate between a unicellular yeast form and distinct filamentous forms (hyphae and pseudohyphae), and its response to the induction of mycelial growth is highly reproducible. The purpose of this work was to identify and characterize genes involved in the regulation of the yeast-to-hypha transition of *Y. lipolytica,* thereby contributing to an understanding of the mechanisms by which environmental conditions induce changes in the pattern of cell growth, a phenomenon with strong implications for the development of virulence by fungal pathogens and for the elucidation of the molecular mechanisms controlling differentiation in higher eukaryotes.

CHAPTER 2

MATERIALS AND METHODS

2.1 Materials

2.1.1 Chemicals and reagents

1-methyl-3-nitro-1-nitrosoguanidine	Sigma
2-mercaptoethanol	BDH
2,5-diphenyloxazole (PPO)	Sigma
4-[2-hydroxyethyl]-1-piperazineethanesulphonic acid (HEPES)	Roche
4,6-diamidino-2-phenylindole (DAPI)	Sigma
5-bromo-4-chloro-3-indolyl-β-D-galactoside (X-gal)	Vector Biosystems
acetone	Fisher
acrylamide	Invitrogen
acrylamide solution, ExplorER	J.T. Baker
acrylamide solution, Long Ranger	J.T. Baker
agar	Difco
agarose, electrophoresis grade	Invitrogen
albumin, bovine serum (BSA)	Roche
ammonium phosphate, monobasic ($NH_4H_2PO_4$)	Sigma
ammonium persulfate [$(NH_4)_2S_2O_8$]	BDH
ammonium sulfate [$(NH_4)_2SO_4$]	BDH
ampicillin	Sigma
antipain	Roche
aprotinin	Roche
benzamidine hydrochloride	Sigma
Bio-Rad protein assay dye reagent	Bio-Rad
boric acid	Caledon
bromophenol blue	BDH
cDNA Spin Columns	Amersham
citric acid	Sigma
complete supplement mixture (CSM)	BIO 101
complete supplement mixture minus leucine (CSM-leu)	BIO 101
Coomassie Brilliant Blue R-250	ICN
D-(+)-glucose	Sigma
diethyl pyrocarbonate (DEPC)	Sigma
dimethyl formamide (DMF)	ICN
dimethyl sulphoxide (DMSO)	Caledon
dithiothreitol (DTT)	ICN
ethanol	Commercial Alcohols
ethylenediaminetetraacetic acid (EDTA)	Sigma
Fluorescent Brightener 28	Sigma
formamide	BDH
formaldehyde, 37% (v/v)	BDH
glycerol	BDH

histidine	Sigma
hydrochloric acid	Fisher
hydrogen peroxide solution, 30% (w/v)	Sigma
isopropanol	Fisher
isopropyl β-D-thiogalactopyranoside (IPTG)	Vector Biosystems
leucine	Sigma
leupeptin	Roche
L-glutamic acid, monopotassium salt	Sigma
lithium acetate	Sigma
lysine	Sigma
maltose	BDH
magnesium acetate	BDH
magnesium chloride	BDH
methanol	Fisher
N-acetylglucosamine	Sigma
N,N'-methylene bisacrylamide	Invitrogen
N-propyl gallate	Calbiochem
N,N,N',N'-tetramethylethylenediamine (TEMED)	Invitrogen
Oregon Green 488 phalloidin	Molecular Probes
Pefabloc SC	Roche
pepstatin A	Sigma
peptone	Difco
phenol, buffer-saturated	Invitrogen
phenylmethylsulphonylfluoride (PMSF)	Roche
poly(dI-dC) · poly(dI-dC)	Amersham
poly *L*-lysine (1 mg/mL)	Sigma
Ponceau S	Sigma
potassium chloride	BDH
potassium phosphate, monobasic (KH_2PO_4)	Merck
potassium phosphate, dibasic (K_2HPO_4)	Merck
RNasin	Promega
salmon sperm DNA, sonicated	Sigma
Sephadex G50	Amersham
sodium acetate	BDH
sodium chloride	Merck
sodium citrate	BDH
sodium dodecyl sulfate (SDS)	Sigma
sodium hydroxide	BDH
sodium phosphate, dibasic (Na_2HPO_4)	BDH
sorbitol	BDH
tris[hydroxymethyl]aminomethane (Tris)	Roche
Triton X-100	Sigma
tryptone	Difco

Tween 20 (polyoxyethylenesorbitan monolaureate)	Sigma
Tween 40 (polyoxyethylenesorbitan monopalmitate)	Sigma
uracil	Sigma
urea	ICN
xylene cyanol	Sigma
yeast extract	Difco
yeast nitrogen base without amino acids (YNB)	Difco
yeast nitrogen base without amino acids and ammonium sulfate	Difco

2.1.2 Enzymes

2.1.2.1 DNA modifying enzymes

calf intestinal alkaline phosphatase (CIP)	NEB
Klenow fragment of DNA polymerase I, *Escherichia coli*	NEB
restriction endonucleases	NEB, Roche, Promega
T4 DNA ligase	NEB
T4 DNA polymerase	NEB
T4 polynucleotide kinase	NEB
Taq DNA polymerase	Invitrogen

2.1.2.2 Other enzymes

RNaseA, bovine pancreas	Sigma
SUPERSCRIPT II RNase H^- reverse transcriptase	Invitrogen
Zymolyase 100T	ICN

2.1.3 Molecular size standards

1 kb DNA ladder	NEB
100 bp DNA ladder	NEB
prestained protein marker, broad range (6-175 kDa)	NEB

2.1.4 Multicomponent systems

BigDye Terminator Cycle Sequencing Ready Reaction Kit	ABI
Expand High Fidelity PCR System	Roche
Oligotex mRNA Midi Kit	Qiagen
pGEM-T Vector System	Promega

QIAprep MiniPrep Kit	Qiagen
QIAquick Gel Extraction Kit	Qiagen
Ready-To-Go PCR Beads	Amersham
Sequenase Version 1.0 / 2.0 DNA Sequencing Kit	USB
TNT T7-Coupled Reticulocyte Lysate System	Promega
ZAP Express cDNA Synthesis Kit	Stratagene
ZAP Express cDNA Gigapack III Gold Cloning Kit	Stratagene

2.1.5 Radiochemicals and detection kits

α-[^{32}P]dATP, Redivue (3,000 Ci/mmol, 10 μCi/μL)	Amersham
L-[^{35}S]methionine (1,175 Ci/mmol, 10 μCi/μL)	Amersham
ECL Detection Kit for Immunoblotting	Amersham
ECL Direct Nucleic Acid Labelling and Detection System	Amersham
Hybond-N+ (nitrocellulose)	Amersham
Trans-Blot Transfer Medium (nitrocellulose)	Bio-Rad
X-ray film (BioMaxMR, X-Omat AR and X-Omat XK-1)	Kodak

2.1.6 Antibodies

mouse monoclonal anti-HA (12CA5)	BAbCo
anti-mouse IgG (from goat), rhodamine (TRITC)-conjugated	Sigma

2.1.7 Plasmid vectors

2.1.7.1 *E. coli* vectors

pBluescript SKII (+)	Stratagene
pGEM-5Zf	Promega
pGEM-7Zf	Promega
pGEM-T	Promega

2.1.7.2 *E. coli*/*Y. lipolytica* shuttle vectors

pINA445	Dr. Claude Gaillardin, Institut National Agronomique Paris-Grignon, Thiverval-Grignon, France (*ARS68*, *LEU2*)

2.1.8 Oligonucleotides

The oligonucleotides used in this study were synthesized on an Oligo 1000M DNA Synthesizer (Beckman) and are described in Table 2-1.

Table 2-1 Oligonucleotides

Name	Sequence	Application
STRE-Sense	5'-gatcTGA*CCCCT*TGTTGTGCTGA*CCCCT*TGTTGTG-3'	Mhy1p, DNA-binding assays
STRE-Anti	5'-gatcCACAACA*AGGGGT*CAGCACAACA*AGGGGT*C AG-3'	Mhy1p, DNA-binding assays
STREMut-Sense	5'-gatcTGA*CCCCA*TGTTGTGCTGA*CCCCA*TGTTGTG-3'	Mhy1p, DNA-binding assays
STREMut-Anti	5'-gatcCACAACA*TGGGGT*CAGCACAACA*TGGGGT*C AG-3'	Mhy1p, DNA-binding assays
MHY1-ApaF	5'-CGCCCAGCATATGCGTACGCATCCTCGGGCCCAG AGGTAGAGCGCC-3'	Tagging of Mhy1p
MHY1-ApaR	5'-CCAATGCATCTAGACTGGACATACGTGAATCTAC ACTGCCAAACCAG-3'	Tagging of Mhy1p
HA-ApaF	5'-TTAGGGCCCCGCTAGCCATGTACCCATACGACGT CCCAGACTAC-3'	HA-tagging of Mhy1p
HA-ApaR	5'-TTAGGGCCCTCTTCTATTCACCCTTACCCATGGCA GCGTAGTCT-3'	HA-tagging of Mhy1p
GFP-ApaF	5'-TTAGGGCCCTGAGTAAAGGAGAAGAACTTTTCAC TGGAG-3'	GFP-tagging of Mhy1p and *Yl*Bem1p
GFP-ApaR	5'-TTAGGGCCCTTATTTGTATAGTTCATCCATGCCA TGTGT-3'	GFP-tagging of Mhy1p and *Yl*Bem1p
RAC1-KO1	5'-CTCTCCTGATCTGCATCTGATCTG-3'	Confirmation of disruption of *YlRAC1*
RAC1-KO2	5'-TAGCTGAAGACTCAATCTGGAGGG-3'	Confirmation of disruption of *YlRAC1*
T3	5'-CCAAGCTCGAAATTAACCCTCACTAA -3'	Amplification from cDNA library

T7	5'-GTAATACGACTCACTATAGGGCGAAT-3'	Amplification from cDNA library
CDC42U	5'-CCTAGCCCGTGCACAGACCCTCAA-3'	Amplification of *YlCDC42* from genomic DNA library
CDC42M	5'-TCCGAGTGTGTAGGGCTCGTCTCC-3'	Amplification of *YlCDC42* from genomic DNA library
RAC1-PR1	5'-TTAGGGCCCAATCTAAGATAGACACACGCTCAC CACCCA-3'	Mutation of STREs in the *YlRAC1* promoter
RAC1-PR2	5'-CTGGTCGACCATTTTGGAACCGGTAGCGAGAGT GGATGTAGG-3'	Mutation of STREs in the *YlRAC1* promoter
RAC1-NT1	5'-ATGGTCGACCAGAGTATAAAATGTGTCGTCACT GGCGACGGG-3'	Mutation of STREs in the *YlRAC1* promoter
RAC1-NT2	5'-GGCCCGCGGTATCCCAAAGTCCGAGGTTTATCG GTTTGT-3'	Mutation of STREs in the *YlRAC1* promoter
RAC1-SE1	5'- ACTAGTGAGTCGATGGGCAACAAACCACAG-3'	Mutation of STREs in the *YlRAC1* promoter
RAC1-SE2	5'-AGAATTCAGAGAGCTTAGTGCACGGCTGGCT TG-3'	Mutation of STREs in the *YlRAC1* promoter
RAC1-EH1	5'-TGAATTCTTGTTGTGCTGAGTTTGTCTTTTTTTCA TCAA-3'	Mutation of STREs in the *YlRAC1* promoter
RAC1-EH2	5'-AAAGCTTGTGGTTTGGGTGGTGAGCGTGTGTCTA TC-3'	Mutation of STREs in the *YlRAC1* promoter
RAC1-HB1	5'-CAAGCTTTCTTTTGCACACCACCCCACGACCGAA AC-3'	Mutation of STREs in the *YlRAC1* promoter
RAC1-HB2	5'-CAGATCTTGTAGTGAGTGACGCAAAAACTGAGA CCG-3'	Mutation of STREs in the *YlRAC1* promoter
RAC1-BS1	5'-AAGATCTGCACAAGTCTCAATCAAGACACTCGC AAG-3'	Mutation of STREs in the *YlRAC1* promoter
RAC1-BS2	5'-GGTCGACCATTTTGGAACCGGTAGCGAGAGTGG ATGTA-3'	Mutation of STREs in the *YlRAC1* promoter
BEM1TAG-5F	5'-GCGGTACCTCGTCAACGCAGAGCTGGAGGACGG CTC-3'	Tagging of *Yl*Bem1p
BEM1TAG-5R	5'-CCGGGCCCGACTAGCGTACAAAACTAGCTTGTTC TTTCCGTAC-3'	Tagging of *Yl*Bem1p

BEM1TAG-3F	5'-CCGGGCCCGGTAAGAGTGGCCTTTGGGAGTGCTG GAGTCAAAT-3'	Tagging of *Yl*Bem1p
BEM1TAG-3R	5'-CGGATCCAATCTCTCGGGCTCATGCATTAATCATG CA-3'	Tagging of *Yl*Bem1p
BEM1F	5'-GTGGACACAGAGGTCATTC-3'	Semi-quantitative RT-PCR
BEM1R	5'-CTGGACCTCTCGTTGTAGC-3'	Semi-quantitative RT-PCR
BMH1F	5'-GGTCAACTACATGAAGGACG-3'	Semi-quantitative RT-PCR
BMH1R	5'-AATGACGGTAGAGTCTCGG-3'	Semi-quantitative RT-PCR
BMH2F	5'-CGTTACGAAGACATGGTGG-3'	Semi-quantitative RT-PCR
BMH2R	5'-CAATGTCAGCAATGGCATCG-3'	Semi-quantitative RT-PCR
HIS1F	5'-TCAAGTTTGTCGGAGGCTC-3'	Semi-quantitative RT-PCR
HIS1R	5'-CCAGAATGTCACTAGCACC-3'	Semi-quantitative RT-PCR
pINA445-PrC	5'-AGCCACTATCGACTACGCGATCATGG -3'	Amplification of *YlBMH2* from genomic DNA library
pINA445-PrD	5'-TGATGCCGGCCACGATGCGTCCGGCG-3'	Amplification of *YlBMH2* from genomic DNA library
BMH2U	5'-CGACATTCTCAACGTGCTTGAGAAGC-3'	Amplification of *YlBMH2* from genomic DNA library
BMH2D	5'-GCTTCTCAAGCACGTTGAGAATGTCG-3'	Amplification of *YlBMH2* from genomic DNA library
5'BMH2F	5'-CCTGAGCAGATTCTGGACCCTCTAAG-3'	Amplification of *YlBMH2* from genomic DNA library
5'BMH2R	5'-ACGGGAGATAAACCGCATGCGGCAT-3'	Amplification of *YlBMH2* from genomic DNA library
3'BMH2F	5'-ATGCCGCATGCGGTTTATCTCCCGT-3'	Amplification of *YlBMH2* from genomic DNA library
3'BMH2R	5'-CCGGATCCAGTCCTGAATCAGTCCTGCCAAG-3'	Amplification of *YlBMH2* from genomic DNA library

2.1.9 Standard buffers and solutions

The compositions of some commonly used buffered solutions are detailed in Table 2-2.

Table 2-2 Buffered solutions

Solution	Composition	Reference
20 × Borate buffer	0.4 M boric acid, 4 mM EDTA, pH 8.3	Ausubel *et al.*, 1989
Breakage buffer	2% (v/v) Triton X-100, 1% SDS, 100 mM NaCl, 10 mM Tris-HCl, pH 8.0, 1 mM EDTA	Ausubel *et al.*, 1989
5 × KGB	0.5 M potassium glutamate, 125 mM Tris-acetate, pH 7.6, 50 mM magnesium acetate, 250 μg BSA/mL, 2.5 mM 2-mercaptoethanol	Hanish and McClelland, 1988
LTE buffer	100 mM lithium acetate, 10 mM Tris-HCl, pH 7.5, 1 mM EDTA	Ausubel *et al.*, 1989
1 × PBS	137 mM NaCl, 2.7 mM KCl, 8 mM Na_2HPO_4, 1.5 mM K_2HPO_4, pH 7.3	Pringle *et al.*, 1991
RNA buffer	0.5 M NaCl, 0.2 M Tris-HCl, pH 7.5, 0.01 M EDTA	Ausubel *et al.*, 1989
SM buffer	100 mM NaCl, 8 mM $MgSO_4$, 50 mM Tris-HCl, pH 7.5, 0.01% gelatin	Ausubel *et al.*, 1989
20 × SSC	3 M NaCl, 0.3 M sodium citrate, pH 7.0	Maniatis *et al.*, 1982
10 × STE	1 M NaCl, 200 mM Tris-HCl, pH 7.5, 100 mM EDTA	Ausubel *et al.*, 1989
10 × TBE	0.89 M Tris-borate, 0.89 M boric acid, 0.02 M EDTA	Maniatis *et al.*, 1982
TBST	20 mM Tris-HCl, pH 7.5, 150mM NaCl, 0.05% (w/v) Tween 20	Huynh *et al.*, 1988
TE	10 mM Tris-HCl (pH 7.0-8.0, as needed), 1 mM EDTA	Maniatis *et al.*, 1982

2.2 Microbiological techniques

2.2.1 Bacterial strains and culture conditions

The *E. coli* strains and culture media used in this study are described in Tables 2-3 and 2-4, respectively. Bacteria were grown at 37°C, unless otherwise indicated.

Table 2-3 *E. coli* Strains

Strain	Genotype	Source
DH5α	F⁻ ϕ80d*lacZ*ΔM15 Δ(*lacZ*YA-*arg*F)U169 *deo*R *rec*A1 *end*A1 *hsd*R17(r_K^-, m_K^+) *pho*A *sup*E44 λ⁻ *thi*-1 *gyr*A96 *rel*A1	Invitrogen
XL1-Blue MRF'	Δ(*mcr*A)183 Δ(*mcr*CB-*hsd*SMR-*mrr*)173 *end*A1 *sup*E44 *thi*-1 *rec*A1 *gyr*A96 *rel*A1 *lac*[F' *pro*AB *lacI*^{q}ZΔM15 *Tn10*(Tet^r)]	Stratagene

Table 2-4 Bacterial Culture Media

Medium	Composition	Reference
LB[a, b]	1% tryptone, 0.5% yeast extract, 1% NaCl	Maniatis *et al.*, 1982
NZY[c]	1% NZ amine, 0.5% yeast extract, 0.5% NaCl, 8 mM $MgSO_4$	Maniatis *et al.*, 1982
SOC	2% tryptone, 0.5% yeast extract, 10 mM NaCl, 2.5 mM KCl, 10 mM $MgCl_2$, 10 mM $MgSO_4$, 0.36 % glucose	Maniatis *et al.*, 1982

[a] Ampicillin (100 μg/mL) or tetracycline (15 μg/mL) was added for plasmid selection when necessary.
[b] For solid media, agar was added to 1.5%.
[c] For top agar, agarose was added to 0.7%.

2.2.2 *Y. lipolytica* strains and culture conditions

The *Y. lipolytica* strains and culture media used in this study are described in Tables 2-5 and 2-6, respectively. Yeasts were grown at 30°C, unless otherwise indicated.

Table 2-5 *Y. lipolytica* Strains

Strain	Genotype
E122[a]	*MATA, ura3-302, leu2-270, lys8-11*
22301-3[a]	*MATB, ura3-302, leu2-270, his1*
E122//22301-3	*MATA/MATB, ura3-302/ura3-302, leu2-270/leu2-270, lys8-11/+, +/his1*
CHY545	*MATA, ura3-302, leu2-270, lys8-11, fil1*
CHY1220	*MATA, ura3-302, leu2-270, lys8-11, fil2*
CHY33169	*MATA, ura3-302, leu2-270, lys8-11, fil3*
CHY3350	*MATA, ura3-302, leu2-270, lys8-11, fil4*
mhy1KO9	*MATA, ura3-302, leu2-270, lys8-11, mhy1::URA3*
mhy1KO9-B4	*MATB, ura3-302, leu2-270, his1, mhy1::URA3*
E122//mhy1KO9-B4	*MATA/MATB, ura3-302/ura3-302, leu2-270/leu2-270, lys8-11/+, +/his1, +/mhy1::URA3*
22301-3//mhy1KO9	*MATA/MATB, ura3-302/ura3-302, leu2-270/leu2-270, +/lys8-11, his1/+, +/mhy1::URA3*
mhy1KO9//mhy1KO9-B4	*MATA/MATB, ura3-302/ura3-302, leu2-270/leu2-270, lys8-11/+, +/his1, mhy1::URA3/mhy1::URA3*
rac1KO30	*MATA, ura3-302, leu2-270, lys8-11, rac1::URA3*
rac1KO30-B36	*MATB, ura3-302, leu2-270, his1, rac1::URA3*
E122//rac1KO30-B36	*MATA/MATB, ura3-302/ura3-302, leu2-270/leu2-270, lys8-11/+, +/his1, +/rac1::URA3*
22301-3//rac1KO30	*MATA/MATB, ura3-302/ura3-302, leu2-270/leu2-270, +/ lys8-11, his1/+, +/rac1::URA3*
rac1KO30//rac1KO30-B36	*MATA/MATB, ura3-302/ura3-302, leu2-270/leu2-270, lys8-11/+, +/his1, rac1::URA3/rac1::URA3*
bem1KO157	*MATA, ura3-302, leu2-270, lys8-11, bem1::URA3*

[a] Dr. Claude Gaillardin, Institut National Agronomique Paris-Grignon, Thiverval-Grignon, France

Table 2-6 Culture Media for *Y. lipolytica*

Medium	Composition[a]	Reference
CSM[b]	0.17% YNB without amino acids and ammonium sulfate, 0.5% $NH_4H_2PO_4$, 0.15% KH_2PO_4, 1.5% sodium citrate	Barth and Weber, 1986
PSM	0.5% yeast extract, 0.5% $(NH_4)_2SO_4$, 0.2% KH_2PO_4, 2% glucose	Gaillardin *et al.*, 1973
YEPD	1% yeast extract, 2% peptone, 2% glucose	Rose *et al.*, 1988
YM	0.3% yeast extract, 0.5% peptone, 0.3% malt extract	Gaillardin *et al.*, 1973
YNA[c]	0.67% YNB without amino acids, 2% sodium acetate	Brade, 1992
YNBD[c]	0.67% YNB without amino acids, 2% glucose	Rose *et al.*, 1988
YNBGlc[d]	1.34% YNB without amino acids, 1% glucose	Guevara-Olvera *et al.*, 1993
YNBGlcNAc[d]	1.34% YNB without amino acids, 1% *N*-acetylglucosamine, 50 mM citric acid, pH 6.0	Guevara-Olvera *et al.*, 1993

[a] For solid media, agar was added to 2%.
[b] Sodium citrate was added after adjusting the pH to 6.5 and autoclaving.
[c] Supplemented with leucine, uracil, lysine and histidine, each at 50 μg/mL, as required.
[d] Supplemented with 2 × complete supplement mixture or 2 × complete supplement mixture minus leucine, as required.

2.2.3 Mating and sporulation of *Y. lipolytica*

Yeast strains were mated and sporulated as described by Barth and Gaillardin (1996). For mating, haploid strains of opposite mating types were grown overnight on YEPD agar at 30°C, mixed on PSM agar (Table 2-6), incubated for 24 h at 30°C, transferred to YM agar (Table 2-6), and incubated for another 4 days at 30°C. Diploids were then selected by transferring portions of this growth onto YNA agar supplemented with the required amino acids and an additional incubation at 30°C until single colonies

were obtained.

For sporulation, diploid strains were grown on YNA agar for 3 days at 30°C, transferred to CSM agar (Table 2-6), and incubated for 4 to 7 days at room temperature. A loop of cells was transferred to a culture tube containing a suspension of 5 mg of Zymolyase 100T in 5 mL of 50 mM sodium citrate buffer, pH 5.0, and incubated for 4 h at 30°C with gentle agitation. Serial dilutions were prepared, spread on YEPD plates, and incubated at 30°C for 2 to 3 days. Isolated colonies were selected by their appearance, and their auxotrophic characteristics were determined after transfer to YNA agar plates (Table 2-6) supplemented with different combinations of amino acids (leucine, uracil, lysine and histidine). Mating types were determined by the ability of strains to mate with A- or B-mating type haploid strains.

2.2.4 Mycelial induction of *Y. lipolytica*

Mycelial growth was induced as described by Guevara-Olvera *et al.* (1993). A loop of cells was inoculated into 10 mL of YEPD (Table 2-6) or YNBD medium (Table 2-6) containing 1% YEPD, and incubated at 28°C until the culture had reached an OD_{600} (optical density at a wavelength of 600 nm) of 1.0-1.5. Cells were harvested by centrifugation at 2,000 × *g*, used to inoculate 50 mL of YNBGlc medium (Table 2-6), and incubated for 12 h at 28°C (initial and final OD_{600} of approximately 0.1 and 1.5, respectively). Cells were harvested by centrifugation as before, washed with sterile distilled water, kept on ice for 15 min in YNB medium without a carbon source, and inoculated at an OD_{600} of 0.20-0.25 into 200 mL of YNBGlcNAc (Table 2-6) (for

induction of the yeast-to-hypha transition) or YNBGlc medium (for growth as the yeast form) prewarmed to 28°C. The induction of mycelial growth was then allowed to proceed at 28°C in a rotary shaker operating at 100 r.p.m.

2.2.5 Assessment of invasive growth of *Y. lipolytica*

Cells were incubated for 5 days at 28°C on YNBD or YNA agar (Table 2-6), and plates were washed with running water to remove cells from the agar surface. Photographs were taken with a Polaroid FCR-10 camera system(Fotodyne) before and after washes.

2.2.6 Measurement of sensitivity to stress in *Y. lipolytica*

Sensitivity to stress was measured in *Y. lipolytica* essentially as described by Martinez-Pastor *et al.* (1996).

2.2.6.1 Carbon source starvation

Cells from a single colony were inoculated into 10 mL of YEPD medium (Table 2-6), incubated overnight at 28°C, added to 40 mL of fresh YEPD medium, and incubated in a rotary shaker at 28°C until the culture had reached an OD_{600} of approximately 1.0. Cells were harvested by centrifugation at 2,000 × *g* for 5 min, washed twice with sterile distilled water, resuspended in 3 mL of YNB medium without a carbon source (Table 2-6), and incubated at 28°C for 5 h. Samples were taken after 1, 3 and 5 h, diluted in YEPD, inoculated in duplicate onto YEPD agar plates, and incubated at 30°C for 2 days.

2.2.6.2 Thermotolerance

Cells were inoculated into 10 mL of YEPD medium (Table 2-6), incubated overnight at 28°C, added to 40 mL of fresh YEPD medium, and allowed to grow in a rotary shaker at 28°C until an OD_{600} of approximately 1.0 was reached. Cells were then diluted into fresh YEPD medium to an OD_{600} of approximately 0.15, and 1 mL aliquots were transferred to haemolysis tubes prewarmed to 35°C. Samples were taken every 30 min during incubation at 35°C with occasional mixing, diluted in YEPD, spread in duplicate onto YEPD agar plates, and incubated at 30°C for 2 days.

2.2.6.1 Osmotic stress

10 mL of YEPD medium (Table 2-6) was inoculated with a single colony, incubated overnight at 28°C, and added to 40 mL of fresh YEPD medium. Cells were allowed to grow in a rotary shaker at 28°C until the culture had reached an OD_{600} of approximately 1.0. Cells were subsequently diluted to an OD_{600} of approximately 0.25 in YEPD medium containing NaCl at a final concentration of 0.4 M, and incubated in a rotary shaker at 28°C for 2 h. Samples were taken every 30 min, diluted in YEPD, inoculated in duplicate onto YEPD agar plates, and incubated at 30°C for 2 days.

2.2.6.1 Oxidative stress

Cells from a single colony were inoculated into 10 mL of YEPD medium (Table 2-6), incubated overnight at 28°C, added to 40 mL of fresh YEPD medium, and incubated in a rotary shaker at 28°C until an OD_{600} of approximately 1.0 was reached. Hydrogen

peroxide was added to a final concentration of 0.8 mM, and the cells were maintained at 28°C for a further 2 h. Samples were taken every 30 min, diluted in YEPD, spread in duplicate onto YEPD agar plates, and incubated at 30°C for 2 days.

2.2.7 Chemical mutagenesis of *Y. lipolytica*

Mutagenesis of *Y. lipolytica E122* cells with 1-methyl-3-nitro-1-nitrosoguanidine (MNNG) was performed by Rachel K. Szilard using the method of Gleeson and Sudbery (1988). Mutant strains were selected by their inability to form wild-type rough-surfaced colonies after 3 days of incubation at 28°C on YEPD agar plates.

2.3 Introduction of DNA into microorganisms

2.3.1 Chemical transformation of *E. coli*

Plasmid DNA was generally amplified in Subcloning Efficiency, chemically competent *E. coli* DH5α cells (Invitrogen), as recommended by the manufacturer. Accordingly, 1 to 2 μL of a ligation reaction (Section 2.5.10) or 0.5 to 1.0 μL (0.25-0.5 μg) of plasmid DNA was added to 25 μL of cells, incubated on ice for 30 min, submitted to a 20 sec heat shock at 37°C, and returned to ice for 2 min. One mL of LB medium (Table 2.4) was then added, and the cells were incubated in a rotary shaker for 45 to 60 min at 37°C, spread onto LB-ampicillin plates (Table 2-4), and incubated overnight at 37°C. When necessary, 50 μL of 2% X-gal in DMF and 30 μL of 100 mM IPTG were added to agar plates to allow for blue/white selection of colonies carrying recombinant plasmids.

2.3.2 Electroporation of *E. coli*

For high efficiency transformation, *E. coli* DH5α cells were prepared as recommended by Bio-Rad. Briefly, 5 mL of LB medium was inoculated with a bacterial colony, incubated overnight at 37°C, added to 500 mL of fresh LB medium, and cells were grown at 37°C until the culture reached an OD_{600} (optical density at a wavelength of 600 nm) of 0.5. Cells were then harvested by centrifugation at 4,000 × *g* for 15 min at 4°C, washed twice with 500 mL of ice-cold water, once with 10 mL of ice-cold 10% (v/v) glycerol, and resuspended in 1.5 mL of 10% (v/v) glycerol. Cells were either used immediately, or frozen as 50 μL aliquots by immersion in a dry ice/ethanol bath and stored at −80°C. For transformation, 25 μL of cells was mixed with 1 to 2 μL of a plasmid-containing solution, placed between the bosses of an ice-cold Biometra microelectroporation chamber (width ~0.15 cm), and submitted to an electrical pulse of 395 V (amplified to ~2.4 kV) at a capacitance of 2 μF and a resistance of 4 kΩ using a Biometra Cell-Porator connected to a Biometra Voltage Booster. Cells were then immediately transferred to a culture tube containing 1 mL of SOC medium (Table 2-4), incubated in a rotary shaker at 37°C for 45 to 60 min, and plated as described in Section 2.3.1.

2.3.3 Electroporation of *Y. lipolytica*

For transformation of *Y. lipolytica*, electrocompetent cells were prepared as recommended by Ausubel *et al.* (1989). A 10 mL overnight culture of yeast cells in YEPD medium (Table 2-6) was added to 50 mL of fresh YEPD and incubated in a rotary shaker

at 30°C until an OD_{600} of approximately 1.0 was reached. Cells were then harvested by centrifugation at 2,000 × *g*, resuspended in 50 mL of LTE solution (Table 2-2), and incubated for 30 min at room temperature with gentle agitation. DTT was added to a final concentration of 20 mM, and the incubation was continued for a further 15 min. Cells were harvested by centrifugation at 2,000 × *g*, washed once with 50 mL each of room-temperature water, ice-cold water, and ice-cold 1 M sorbitol, and finally resuspended in approximately 300 μL of 1 M sorbitol. For transformation, 20 μL of cells was mixed with 1 to 2 μL of DNA, placed between the bosses of an ice-cold Biometra microelectroporation chamber (width ~0.15 cm), and submitted to an electrical pulse of 250 V (amplified to ~1.6 kV) at a capacitance of 2 μF and a resistance of 4 kΩ using a Biometra Cell-Porator connected to a Biometra Voltage Booster. Cells were immediately mixed with 100 μL of ice-cold 1 M sorbitol, plated onto YNA agar supplemented with appropriate amino acids (Table 2-6), and incubated at 30°C for 3 to 6 days.

2.4 Nucleic acid isolation from microorganisms

2.4.1 Plasmid DNA isolation from *E. coli*

Isolated bacterial colonies were inoculated into 3 mL of LB-ampicillin medium (Table 2-4), and incubated overnight at 37°C. Plasmid DNA was isolated by either the alkaline lysis method (Maniatis *et al.*, 1982) or with the use of the QIAprep Miniprep Kit (Qiagen).

For the alkaline lysis method, cells collected by microcentrifugation at 16,000 ×

g for 2 min were resuspended in 100 μL of Solution I (50 mM glucose, 25 mM Tris-HCl, pH 8.0, 10 mM EDTA) and mixed with 200 μL of Solution II (0.2 M NaOH, 1% SDS). After a 5 min incubation on ice, 150 μL of Solution III (3 M potassium acetate, pH 4.8-5.5) was added, and incubation on ice was continued for another10 min. The precipitate was then pelleted by a 10 min microcentrifugation at 16,000 × *g* at 4°C, and the supernatant was transferred to a new microcentrifuge tube and submitted to consecutive extractions with equal volumes of phenol/chloroform/isoamyl alcohol (25:24:1) and chloroform/isoamyl alcohol (24:1). The nucleic acid in the aqueous phase was precipitated by the addition of two volumes of absolute ethanol and microcentrifugation for 10 min at 16,000 × *g*, washed once with 1 mL of 70% (v/v) ethanol, and dried in a rotary vacuum desiccator. The dried pellet was dissolved in 50 μL of TE, pH 8.0 (Table 2-2) containing 20 μg RNaseA/mL.

Plasmid DNA isolation with the QIAprep Miniprep Kit involves a modified alkaline lysis procedure to disrupt the cells, followed by purification of the DNA on a silica-gel membrane in a high-salt environment, and was carried out as recommended by the manufacturer.

2.4.2 Plasmid DNA isolation from *Y. lipolytica*

Yeast plasmid DNA was isolated by the method of Ausubel *et al.* (1989). Accordingly, cells were inoculated into 10 mL of selective YNA medium (Table 2-6), incubated for 2 days at 30°C, harvested by centrifugation for 5 min at 2,000 × *g*, and

washed twice with sterile water. Subsequently, cells were resuspended in 200 μL of Breakage Buffer (Table 2-2), transferred to a microfuge tube, and glass beads (425-600 μm) (Sigma) were added until they reached the meniscus. Following the addition of 200 μL of phenol/chloroform/isoamyl alcohol (25:24:1), the mixture was vortexed for 3 min at 4°C to disrupt the cells. 200 μL of TE buffer, pH 8.0, (Table 2-2) was then added, and the organic and aqueous phases were separated by centrifugation at 16,000 × *g* for 5 min at 4°C. The aqueous phase was extracted twice against an equal volume of phenol/chloroform/ isoamyl alcohol (25:24:1) and once against chloroform/isoamyl alcohol (24:1). Nucleic acid was precipitated by the addition of 2.5 volumes of absolute ethanol and centrifugation at 16,000 × *g* for 30 min at 4°C. The pellet was washed once with 1 mL of 70% (v/v) ethanol, dried in a rotary vacuum desiccator, and dissolved in 20 μL of water. The material thus obtained was subsequently introduced into *E. coli* DH5α cells by electroporation (Section 2.3.2), and the amplified plasmid DNA was isolated as described in Section 2.4.1.

2.4.3 Chromosomal DNA isolation from *Y. lipolytica*

For isolation of yeast genomic DNA, the same procedure as for yeast plasmid DNA isolation (Section 2.4.2) was followed, except that yeast cells were grown overnight in YEPD medium, precipitated nucleic acids were collected by centrifugation at room temperature for 5 min, and the final nucleic acid pellet was dissolved in 100 μL of TE buffer, pH 8.0, (Table 2-2) containing 20 μg RNaseA/mL.

2.4.4 Total RNA isolation from *Y. lipolytica*

Total RNA was isolated from *Y. lipolytica* cells by the method of Ausubel *et al.* (1989). Cells were harvested by centrifugation for 5 min at 2,000 × *g*, washed twice with 50 mL of sterile water, transferred to a microcentrifuge tube, washed once with 1 mL of ice-cold RNA buffer (Table 2-2), and resuspended in 300 µL of RNA buffer. Glass beads (425-600 µm) (Sigma) were added until they reached the meniscus, 300 µL of phenol/chloroform/isoamyl alcohol (25:24:1; equilibrated with RNA buffer) was added, and the mixture was vortexed for 2 min at 4°C to disrupt the cells. Following a 1 min centrifugation at room temperature, the top 200-250 µL were collected and extracted against an equal volume of phenol/chloroform/isoamyl alcohol (25:24:1) until the aqueous phase was nearly limpid. Residual phenol was then extracted with chloroform/isoamyl alcohol (24:1), and RNA was precipitated by the addition of 3 volumes of ice-cold absolute ethanol, followed by incubation at −20°C for 30 to 60 min and centrifugation at 16,000 × *g* for 2 min at 4°C. The RNA pellet was resuspended in 1 mL of 70% (v/v) ethanol, incubated on ice for 10 min, collected by centrifugation at 16,000 × g for 2 min at room temperature, dried in a rotary vacuum desiccator, and dissolved in 50 µL of DEPC-treated water.

2.4.5 Isolation of Poly A^+ mRNA from *Y. lipolytica*

Poly A^+ mRNA was purified from total RNA (isolated as described in Section 2.4.4) using the Oligotex mRNA Midi Kit (Qiagen) as recommended by the manufacturer.

This method consists primarily in the hybridization of the polyadenylated tails of mRNA molecules to oligo-dT sequences that are coupled to a solid phase matrix, and a subsequent reduction of the concentration of salt to destabilize the dT:A hybrids, thus releasing the poly A^+ mRNA.

2.5 Standard DNA manipulations

Unless otherwise noted, reactions were carried out in 1.5 mL microcentrifuge tubes. Microcentrifugation was performed in an Eppendorf microcentrifuge at 16,000 × *g*, and all procedures were performed essentially as described by Ausubel *et al.* (1989).

2.5.1 Polymerase chain reaction

The polymerase chain reaction (PCR) was used to amplify specific DNA sequences or to introduce modifications in the amplified DNA sequence. Primer design, reaction components and cycling conditions were performed as established for standard procedures (Innis and Gelfand, 1990; Saiki, 1990). Typically, a reaction contained 0.1 to 1.0 µg of template DNA (100-200 ng of plasmid DNA or 0.5-1.0 µg of *Y. lipolytica* genomic DNA), 25 pmol of each primer, 50 µM of each dNTP (dATP, dCTP, dGTP and dTTP), and 5 U of *Taq* DNA polymerase in 50 µL of the supplied reaction buffer. Reactions were carried out in 0.6 mL microcentrifuge tubes in a Robocycler 40 with a Hot Top attachment (Stratagene). Alternatively, Ready-to-Go PCR beads (Amersham-Pharmacia) were used as recommended by the manufacturer.

For high-fidelity amplification of DNA fragments, the Expand High Fidelity PCR

System (Roche) was used according to the instructions of the manufacturer.

2.5.2 Restriction endonuclease digestion

In general, 1 to 2 μg of plasmid DNA or 10 μg of genomic DNA was subjected to restriction endonuclease digestion following the recommendations of the enzyme's manufacturer.

2.5.3 Dephosphorylation of 5' ends

In order to prevent self-ligation of plasmid vectors, phosphate groups were removed from the 5'-ends of DNA by treatment with calf intestinal alkaline phosphatase (CIP) according to the manufacturer's instructions.

2.5.4 Phosphorylation of 5' ends

Phosphorylation of the 5'-termini of DNA molecules was occasionally carried out to enable their ligation to other DNA fragments or to plasmid vectors. A typical 30 μL reaction contained 10-20 μg of DNA, 3 μL of 10 × PNK buffer (700 mM Tris-HCl, pH 7.6, 100 mM $MgCl_2$, 50 mM DTT), 1 mM ATP, and 10 U of T4 polynucleotide kinase. The reaction was performed at 37°C for 1 h and terminated by heating at 65°C for 20 to 30 min.

2.5.5 Creation of blunt-ended DNA fragments

DNA fragments with 5' overhangs were made blunt using the Klenow fragment of

E. coli DNA polymerase I. A typical 25 μL reaction contained 2-3 μg of DNA, 5 U of enzyme, and 25 μM of each dNTP. The reaction was performed at 30°C for 15 min and terminated by immediately subjecting it to agarose gel electrophoresis (Section 2.5.8).

To make blunt 3' overhangs, 25 μL reactions contained 2-3 μg of DNA, 10 U of T4 DNA polymerase, and 25 μM of each dNTP. The reactions were allowed to proceed at 11°C for 20 min and terminated by phenol/chloroform extraction (Section 2.5.6) or by heating at 75°C for 15 min.

2.5.6 Phenol/chloroform extraction

Modifying enzymes and contaminating proteins were removed from nucleic acid-containing solutions by extraction with phenol/chloroform as described by Ausubel *et al.* (1989). In general, DNA solutions were brought to 200 μL by the addition of water, an equal volume of phenol/chloroform/isoamyl alcohol (25:24:1) was added, and the sample was vortexed vigorously for 10 sec. Subsequently, the sample was subjected to microcentrifugation at 16,000 × *g* for 2 min at room temperature, and the aqueous phase was transferred to a new microcentrifuge tube. This procedure was then repeated with an equal volume of chloroform/isoamyl alcohol (24:1), and DNA was concentrated by precipitation with ethanol, as described in Section 2.5.7.

2.5.7 Ethanol precipitation of DNA

Typically, 0.1 volume of 3 M sodium acetate, pH 5.2, and 2.5 volumes of absolute

ethanol at −20°C were added to a DNA-containing solution, and the sample was gently mixed by inversion and incubated at −20°C for 30 to 60 min. Precipitated DNA was collected by centrifugation at 16,000 × *g* for 20 min at 4°C, rinsed with 1 mL of 70% ethanol, dried in a rotary vacuum desiccator, and dissolved in an appropriate amount of buffer or water, as required.

2.5.8 Agarose gel electrophoresis of DNA fragments

Following PCR (Section 2.5.1) or treatment with modifying enzymes (Section 2.5.2), 0.2 volume of 6 × DNA sample dye (40% sucrose, 0.25% bromophenol blue, 0.25% xylene cyanol) (Maniatis *et al.*, 1982) was added to the reaction mixture, and DNA fragments were separated by electrophoresis in agarose gels (1% or 2% agarose, as required) in 1 × TBE containing 0.5 μg of ethidium bromide/mL. Gels were submitted to electrophoresis at 10 V/cm in 1 × TBE containing 0.5 μg of ethidium bromide/mL, and DNA fragments were subsequently visualized on an ultraviolet transilluminator (Photodyne, Model 3-3006).

2.5.9 Purification of DNA fragments

Gel fragments containing DNA of interest were excised with a razor blade, and DNA was purified using the QIAquick Gel Extraction Kit (Qiagen), as recommended by the manufacturer. This method consists in the dissolution of the agarose gel in the presence of chaotropic salts, followed by adsorption and purification of DNA on a silica-gel membrane at pH ≤7.5, and elution of DNA with a small volume (30-50 μL) of 10 mM

Tris-HCl, pH 8.5.

2.5.10 Ligation of DNA fragments

DNA fragments obtained by restriction enzyme digestion (Section 2.5.2) were purified as described in Sections 2.5.8 and 2.5.9 and ligated to plasmid vectors using 1 U of T4 DNA ligase in the buffer supplied by the manufacturer. Ligation reactions were performed in a total volume of 10 μL, and the molar ratio of plasmid to insert was generally between 1:3 and 1:5, with a maximum total DNA concentration of 25 ng/μL. Following a 4 to 12 h incubation at 4°C, ligation products were transformed into chemically competent *E. coli* cells (Section 2.3.1) for amplification.

DNA fragments obtained by PCR (Section 2.5.1) were processed in a similar way, except that these products were cloned using the pGEM-T Vector System (Promega) according to the manufacturer's instructions.

2.5.11 Annealing of oligonucleotides

Complementary single-stranded oligonucleotides were annealed in reactions containing 10 pmol of each oligonucleotide, 10 μL of 5 × annealing buffer (250 mM Tris-HCl, pH 8.0, 50 mM $MgCl_2$) and water to a final volume of 50 μL. Reactions were incubated for 4 min at 90°C in a heating block and subsequently allowed to cool gradually to room temperature.

2.6 DNA and RNA analysis

2.6.1 DNA sequencing

2.6.1.1 Sequenase Kits

Sequenase DNA Sequencing Kits (Versions 1.0 and 2.0) (USB) were used according to the instructions of the manufacturer, except that 2 pmol of primer were employed. These kits are based on the method of Sanger *et al.* (1977), and involve radioactive labeling of DNA using a genetic variant of the bacteriophage T7 DNA polymerase lacking 3'→5' exonuclease activity. Reaction products were separated on 5% ExplorER (J.T. Baker) or 5% Long Ranger (J.T. Baker) denaturing acrylamide gels in 0.6 × TBE or 1 × TBE buffer (Table 2-2), respectively. Gels were dried at 80°C for 45 min and exposed to BioMax or X-Omat AR film at room temperature for signal detection.

2.6.1.2 Automated sequencing

Dideoxynucleotide sequencing using fluorescently labeled DNA was performed using the BigDye Terminator Cycle Sequencing Ready Reaction Kit (PE Applied Biosystems) as recommended by the manufacturer. This procedure is also based on the method of Sanger et *al.* (1977) and consists in the random incorporation of fluorescent dideoxy terminators during the elongation of DNA sequences with a modified version of *Taq* DNA polymerase. Reaction products were separated by capillary electrophoresis, and fluorescence was detected and recorded by an ABI 310 Genetic Analizer (PE Applied Biosystems).

2.6.2 Southern blot analysis

DNA was transferred to nitrocellulose membranes by the method of Ausubel *et al.* (1989), with a few modifications. Approximately 10 μg of yeast genomic DNA (Section 2.4.3) was digested overnight with the appropriate restriction enzyme(s), and fragments were separated by agarose gel electrophoresis (Section 2.5.8). DNA was subsequently nicked by placing the gel on an ultraviolet transilluminator (Photodyne, Model 3-3006) for 5 min, denatured in 1.5 M NaCl, 0.5 M NaOH for 30 min, and neutralized in 3 M NaCl, 1.5 M Tris-HCl, pH 8.0, for 30 min. DNA was transferred overnight to nitrocellulose by capillary action in 5 × SSC (Table 2-2) and cross-linked to the nitrocellulose by exposure to 120,000 μJ of ultraviolet light (λ = 254 nm)/cm^2 of membrane with a UV Stratalinker 1800 apparatus (Stratagene). Immobilized DNA was used as a target for hybridization as described in Section 2.6.4.

2.6.3 Northern blot analysis

RNA was prepared and transferred to nitrocellulose by the method of Ausubel *et al.* (1989), with some modifications. Samples containing approximately 10 μg of total yeast RNA (Section 2.4.4), 18% (v/v) formamide, 18% (v/v) formaldehyde, and 2 × borate buffer (Table 2-2) in 20 μL were incubated at 65°C for 5 min to denature RNA and immediately cooled on ice. Following the addition of 4 μL of 6 × DNA sample dye (Section 2.5.8), RNA was separated by gel electrophoresis in 1 × borate buffer (Table 2-2) containing 3.3% (v/v) formaldehyde as denaturant, stained for 15 min in 0.5 μg of

ethidium bromide/mL, visualized on an ultraviolet transilluminator (Photodyne, Model 3-3006), and washed for 30 min in water. RNA was then partially hydrolyzed by incubation in 0.05 N NaOH for 20 min, and following rinsing of the gel with water and equilibrating the gel in 20 × SSC for 45 min, the RNA was transferred overnight to nitrocellulose by capillary action in 20 × SSC. RNA was cross-linked to nitrocellulose by exposure to 120,000 μJ of ultraviolet light ($\lambda = 254$ nm)/cm^2 of membrane with a UV Stratalinker 1800 apparatus (Stratagene) and used as a target for hybridization as described in Section 2.6.4.

2.6.4 Labeling of DNA probes and hybridization

In order to identify or quantify specific DNA or RNA molecules immobilized on nitrocellulose membranes by Southern or northern blotting (Sections 2.6.2 and 2.6.3), DNA probes were labeled and hybridized using the Enhanced Chemiluminescence (ECL) Direct Nucleic Acid Labeling and Detection System (Amersham/Pharmacia) according to the instructions of the manufacturer. This method consists primarily in the direct labeling of DNA with horseradish peroxidase, followed by hybridization of the labeled probe with immobilized DNA or RNA, and eventual detection (on an X-ray film) of the blue light produced by a sequence of reactions that results finally in the oxidation of luminol.

2.6.5 Semi-quantitative RT-PCR analysis

The relative amounts of low-abundance mRNA molecules were determined through the sequencial use of reverse transcriptase and the PCR (RT-PCR) as described by Wang *et al.* (1989), with some modifications. Prior to amplification, 4 μg of total RNA

was digested in a 20 μL reaction with RNase-free DNase I (Invitrogen) for 15 min at room temperature, and the enzyme was inactivated by the addition of 0.8 μL of 25 mM EDTA followed by incubation at 65°C for 10 min.

For reverse transcription, 7 μL of the previous reaction (approximately 1 μg of RNA) was mixed with 1 μL (400-450 ng/μL) of random hexamers (Invitrogen) and 4 μL of water, heated at 70°C for 10 min, and immediately chilled on ice. The sample was then submitted to reverse transcription with SuperScript II reverse transcriptase (Invitrogen) in a 20 μL reaction containing 10 mM DTT, 500 μM dNTPs, 1 U RNasin/μL (Promega), and 1 × First Strand Buffer (supplied by the enzyme's manufacturer). The reaction was conducted in 0.6 mL microcentrifuge tubes in a Robocycler 40 with a Hot Top attachment (Stratagene) for 10 min at 25°C, 30 min at 42°C, 15 min at 99°C, and storage at 4°C. A negative control without reverse transcriptase was included in all experiments, to assure that the digestion by DNase had been total.

The material thus obtained was brought to 40 μL by the addition of cDNA dilution mix (30 mM $MgCl_2$, 3 mM dNTPs, 1 × Invitrogen PCR buffer), and several tubes containing 20 μL of cDNA at different concentrations in cDNA dilution mix were prepared from this sample. Subsequently, 50 μL polymerase chain reactions containing 10 pmol of primers/μL, 1 × Invitrogen PCR buffer, and 0.1 U *Taq* DNA polymerase (Invitrogen)/μL were performed for 5 cycles of 60 sec at 96°C, 60 sec at 52°C, and 60 sec at 72°C in a Robocycler 40 with a Hot Top attachment (Stratagene). Finally, a second round of PCR was carried out for 30 cycles after the addition of 50 μL of a mixture

containing 10 pmol of endogenous internal standard primers/μL, 10 mM $MgCl_2$, 1 × Invitrogen PCR buffer and 0.1 U *Taq* DNA polymerase (Invitrogen)/μL.

Aliquots from each reaction were submitted to electrophoresis on 2% agarose gels (Section 2.5.8). Results were documented with the VersaDoc Imaging System (Bio-Rad) and analyzed with the quantitation software Quantity One (Bio-Rad). This information was used to establish a linear correlation between the amount of cDNA used and the level of product obtained, and the expression levels of the analyzed genes were determined using the data provided by the reactions in which amplification was exponential.

2.7 Analysis of proteins

2.7.1 Preparation of yeast whole cell lysates

Yeast lysates were prepared by disruption with glass beads, as adapted from Needleman and Tzagoloff (1975). Cells were harvested by centrifugation at 2,000 × *g* for 5 min, washed three times with water, and resuspended in an equal volume of ice-cold Disruption Buffer (20 mM Tris-HCl, pH 7.5, 0.1 mM EDTA, pH 7.5, 10 mM KCl, 10% (w/v) glycerol) containing protease inhibitors (1 μg/mL each of leupeptin, antipain, pepstatin and aprotinin, 0.5 mM benzamidine hydrochloride, 0.5 mg Pefabloc SC/mL). Glass beads (425-600 μm) (Sigma) were added until they reached the meniscus of the suspension, and cells were disrupted by vortexing for 5 min at 4°C. The mixture was submitted to centrifugation at 16,000 × *g* for 2 min at 4°C, and the supernatant was transferred to a new tube. The crude lysate thus obtained was clarified by centrifugation

at 16,000 × *g* for 20 min at 4°C, and the protein concentration was determined as described in Section 2.7.2.

2.7.2 Determination of protein concentration

The protein concentration of a sample was determined by the method of Bradford (1976). An aliquot of the protein sample was brought to a volume of 100 μL with water, mixed with 1 mL of Bio-Rad Protein Dye, and incubated at room temperature for 10 min. The absorbance of the sample was measured at 595 nm using a Beckman DU640 spectrophotometer, and protein concentration was determined by comparing the absorbance of the sample to the absorbance values of BSA protein standards of known concentrations (10, 20, 50, 100, 150, 200 and 250 μg/mL).

2.7.3 Electrophoretic separation of proteins

Proteins were separated by sodium dodecyl sulfate-polyacrylamide gel electrophoresis (SDS-PAGE) as described by Ausubel *et al.* (1989). Protein samples were mixed with concentrated sample buffer (to a final concentration of 2% SDS, 10% sucrose, 10 mM DTT, 0.001% bromophenol blue, 62.5 mM Tris-HCl, pH 6.8), denatured by boiling for 5 min, and separated by electrophoresis on discontinuous slab gels. Stacking gels consisted of 3% acrylamide (30:0.8 acrylamide:*N,N'*-methylene-bis-acrylamide), 60 mM Tris-HCl, pH 6.8, 0.1% SDS, 0.1% (v/v) TEMED, and 0.1% ammonium persulfate. Resolving gels consisted of 10% acrylamide (30:0.8 acrylamide:*N,N'*-methylene-bis-acrylamide), 370 mM Tris-HCl, pH 8.8, 0.1% SDS, 0.1 % (v/v) TEMED, and 0.042%

ammonium persulfate. Eletrophoresis was conducted in SDS-PAGE running buffer (50 mM Tris-HCl, pH 8.8, 0.4 M glycine, 0.1% SDS) at 50-200 V using a Bio-Rad Mini Protean II vertical gel system.

2.7.4 Detection of proteins

2.7.4.1 Staining of SDS-polyacrylamide gels with Coomassie Brilliant Blue

Proteins were visualized by staining gels with 0.1% Coomassie Brilliant Blue R-250 in 10% (v/v) acetic acid, 35% (v/v) methanol for 1 h with gentle agitation. Unbound dye was removed by multiple washes in 10% (v/v) acetic acid, 35% (v/v) methanol. Stained gels were dried for 1 h at 80°C on a Bio-Rad gel dryer Model 583.

2.7.4.2 Fluorography

Proteins labeled with *L*-[^{35}S]methionine were processed for fluorography as described by Bonner and Laskey (1974). After electrophoresis, gels were submitted to staining with Coomassie Blue, as described in Section 2.7.3.1, and subsequently dehydrated by two washes of 30 min in DMSO. Gels were then incubated for 3 h in DMSO-PPO (22.2% 2,5-diphenyloxazole in DMSO), rehydrated by two washes in water for 20 min, dried at 60°C for 2 h, and exposed to X-Omat AR film (Kodak).

2.8 Electrophoretic Mobility Shift Analysis (EMSA)

2.8.1 Coupled transcription/translation

In vitro synthesis of proteins was carried out in 25 μL reactions containing 0.5 μg

of plasmid DNA as template and the TNT T7-coupled reticulocyte lysate system (Promega) as recommended by the manufacturer. Parallel reactions containing 10 μCi of *L*-[^{35}S]methionine (1175 Ci/mol, 10 mCi/mL) were also done for assessment of the translation products.

2.8.2 Radioactive labeling of DNA probes

Twenty pmols of double-stranded oligonucleotides obtained as described in Section 2.5.11 were mixed with 5 μL of 5 × KGB buffer (Table 2-2), 10 μL of [α-^{32}P]dATP (3000 Ci/mmol, 10 μCi/μL), 0.5 mM each of dCTP, dGTP and dTTP, 1 μL (5 U) of the Klenow fragment of *E. coli* DNA polymerase I, water to a final volume of 25 μL, and incubated for 30 min at room temperature.

Radiolabeled DNA probes were purified from unincorporated radionucleotides by centrifugation through Sephadex G50, as described by Maniatis *et al.* (1982). Accordingly, a 1 mL syringe (BDH) was plugged with silanized glass wool (Sigma), filled with Sephadex G50 prepared in TE buffer, pH 8.0, placed into a 15 mL Falcon tube containing a microcentrifuge tube at the bottom, and subjected to centrifugation at 180 × *g* for 4 min. Excess buffer was discarded, additional Sephadex G50 was added, and the centrifugation step was repeated. The column was then washed twice with 100 μL of TE buffer, pH 8.0, and the microcentrifuge tube at the bottom of the Falcon tube was replaced with a fresh tube. The radiolabeling reaction was then brought to 100 μL by the addition of 75 μL of TE buffer, pH 8.0, added to the top of the Sephadex column, and submitted

to centrifugation at 180 × *g* for 4 min. The radiolabeled DNA probe was then collected from the microcentrifuge tube, and radionucleotide incorporation was measured by liquid scintillation counting in an LKB RackBeta 1209 scintillation counter.

2.8.3 Binding reactions with *in vitro* translated proteins

Binding was performed in 15 μL reactions containing 6 mM Hepes, pH 7.9, 120 mM NaCl, 0.4 mM $MgCl_2$, 0.1 mM EDTA, 7% (v/v) glycerol, 4 μg BSA, 4 μg salmon sperm DNA, and 4 μg poly (dI-dC)•poly (dI-dC) nonspecific competitor DNA. Water and unprogrammed lysate were added as appropriate to maintain constant total reaction volume and lysate concentration. *In vitro* translated protein (2 μL of a synthesis reaction) was incubated with unlabeled competitor at room temperature for 5 min, 1 × 10^6 cpm of radiolabeled probe (Section 2.8.2) was then added, and the reaction was continued for an additional 15 min at 25°C. Binding reactions were terminated by the addition of 1 to 2 μg of loading gel (30% (v/v) glycerol, 0.5% xylene cyanol, 0.5% bromophenol blue), and the reactions were then submitted to electrophoresis at 4°C on prerun 3.5% polyacrylamide gels (30:1 acrylamide:*N,N'*-methylene bisacrylamide weight ratio) in 22 mM Tris, 22 mM boric acid, 1 mM EDTA as running buffer. Gels were dried at 60°C for 2 h, and submitted to autoradiography on X-Omat AR film (Kodak) .

2.8.4 Binding reactions with yeast extracts

For EMSA using yeast extracts, the procedure in Section 2.8.3 was followed,

except that 60 μg of yeast whole cell lysate (Section 2.7.1) was used.

2.9 Microscopy

2.9.1 Immunofluorescence microscopy

Indirect immunofluorescence microscopy of yeast cells was carried out as described by Pringle *et al.* (1991). Cells were fixed by the addition of formaldehyde directly to the culture medium to a concentration of 3.7%, followed by a 45 min incubation at room temperature. Cells were then collected by centrifugation at 2,000 × *g* for 5 min, washed with solution B (1.2 M sorbitol, 100 mM potassium phosphate, pH 7.5), resuspended to a concentration of approximately 100 μg/mL in solution B containing 20 μg Zymolyase 100T /mL and 28 mM 2-mercaptoethanol, and incubated for 30 min at 30°C with gentle rotation. Spheroplasts thus obtained were spotted onto glass slides precoated with poly *L*-lysine, washed several times with solution B until individual spheroplasts were visibly separated, and allowed to dry at room temperature. Spheroplasts were permeabilized by immersion in −20°C methanol for 6 min and −20°C acetone for 30 sec, and were allowed to dry in air. Slides were subsequently placed into a dark humid box, and the spheroplasts were covered with 100 μL of blocking solution (1% skim milk in TBST (Table 2-2)) and incubated for 1 h at room temperature. Next, the spheroplasts were incubated for 1 h with the primary antibody diluted in blocking solution, washed ten times with 50 μL of blocking solution, and incubated with rhodamine-conjugated secondary antibody as for the primary antibody. Lastly, the spheroplasts were washed ten times with

blocking solution, three times with TBST, and covered with 10 μL of mounting medium (4% n-propyl gallate, 75% (w/v) glycerol in PBS buffer (Table 2-2)). Coverslips were placed over the slides, and the edges were sealed with nail polish. Cells were viewed on an Olympus BX50 microscope equipped for fluorescence, and images were recorded with a SPOT Camera digital imaging system (Model SP400, Diagnostic Instruments) and analysed with SPOT software 1.2.1 (Diagnostic Instruments).

2.9.2 Staining of yeast actin with fluorochrome-conjugated phalloidin

Staining of yeast actin was performed as described by Adams and Pringle (1991). Cells were fixed by the addition of formaldehyde directly to the culture medium to a concentration of 3.7%, followed by a 1 h incubation at room temperature. Cells were then collected by centrifugation at 2,000 × *g* for 5 min, washed three times with PBS buffer (Table 2-2), and resuspended in 100 μL of PBS. Staining of actin was then carried out by the addition of Oregon Green 488 phalloidin (Molecular Probes) to a concentration of 1.3 μM, and incubation of the cells for 1 h in the dark. Cells were washed five times with PBS, resuspended in a drop of mounting medium, and viewed on an Olympus BX50 microscope equipped for fluorescence. Images were recorded with a SPOT Camera digital imaging system and analysed with the SPOT software 1.2.1.

2.9.3 Staining of yeast bud scars and other cell wall chitin with calcofluor

Staining of yeast chitin was carried out as described by Pringle (1991). Cells were fixed as described in Section 2.9.2, collected by centrifugation at 2,000 × *g* for 5 min,

washed once with water, and resuspended in 0.1 mg Fluorescent Brightener 28 (Sigma)/mL. After a 5 min incubation at room temperature, cells were washed five times with water, mounted on slides, and observed on an Olympus BX50 microscope equipped for fluorescence. Images were recorded with a SPOT Camera digital imaging system and analysed with the SPOT software 1.2.1.

2.9.4 Staining of yeast nuclei with 4,6-diamidino-2-phenylindole (DAPI)

For visualization of yeast nuclei, 4,6-diamidino-2-phenylindole (DAPI) was added to either the cell suspension or to the mounting medium (Section 2.9.1) at a final concentration of 1 μg/mL. Cells were viewed using UV excitatory illumination on an Olympus BX50 microscope equipped for fluorescence. Images were recorded with a SPOT Camera digital imaging system and analysed with the SPOT software 1.2.1.

2.10 Construction of a *Y. lipolytica* cDNA library

Poly A^+ RNA was isolated from *Y. lipolytica* cells as described in Section 2.4.5 and used for cDNA synthesis using the ZAP Express cDNA synthesis kit (Stratagene) as recommended by the manufacturer. The cDNA thus obtained (4 μg) was subsequently ligated into the ZAP Express vector (Stratagene), packaged with the Gigapack III Gold cloning kit (Stratagene), and amplified in *E. coli* XL1-Blue MRF' cells (Stratagene) following the instructions of the manufacturer.

2.11 Isolation and sequencing of *Y. lipolytica* genes

2.11.1 Isolation and sequencing of *MHY1*, *YlRAC1*, *YlBEM1* and *YlBMH1*

The *Y. lipolytica* genes *MHY1*, *YlRAC1*, *YlBEM1* and *YlBMH1* were isolated by functional complementation of mutant strains (Section 2.2.7) using a *Y. lipolytica* genomic DNA library contained in the replicative *E. coli* shuttle vector, pINA445 (Nuttley *et al.*, 1993). Plasmid DNA was introduced into yeast cells by electroporation (Section 2.3.3), and Leu^+ transformants were screened on YNA-agar plates (Table 2-6) for their ability to give rise to rough-surfaced colonies on YEPD agar plates (Table 2-6) after 3 days of incubation at 30°C. Complementing plasmids were recovered as described in Section 2.4.2, transformed into *E. coli* for amplification (Section 2.3.2), and the smallest fragments capable of restoring hyphal growth were determined. Restriction fragments prepared from the genomic inserts of these constructs were subcloned into the vectors pGEM-5Zf(+)(Promega), pGEM-7Zf(+) (Promega), or pBluescript II SK(+) (Stratagene) for dideoxynucleotide sequencing of both strands (Section 2.6.1).

2.11.2 Isolation and sequencing of *YlSEC31*

The *Y. lipolytica* gene *YlSEC31* was isolated by its ability to enhance filamentous growth upon introduction into *Y. lipolytica E122* cells (Table 2-5). Plasmid DNA from a *Y. lipolytica* genomic DNA library (Nuttley *et al.*, 1993) was introduced into yeast cells as described in Section 2.3.3, and Leu^+ colonies were screened on YNA-agar plates (Table 2-6) for their enhanced rough aspect after 3 days of incubation on YEPD agar plates (Table

2-6) at 30°C. Plasmid DNA from one of these transformants was recovered as described in Section 2.4.2, transformed into *E. coli* for amplification (Section 2.3.2), and the smallest fragment capable of enhancing hyphal growth was determined. Restriction fragments prepared from the genomic insert of this construct were subcloned into the vector pGEM-7Zf(+) (Promega) for dideoxynucleotide sequencing of both strands (Section 2.6.1).

2.11.3 Isolation and sequencing of *YlCDC42* and *YlBMH2*

The *Y. lipolytica* genes *YlCDC42* and *YlBMH2* were amplified by PCR (Section 2.5.1) using both a *Y. lipolytica* DNA genomic library contained in the replicative *E. coli* shuttle vector, pINA445 (Nuttley *et al.*, 1993), and a *Y. lipolytica* cDNA library constructed in the ZAP Express vector (Section 2.10) as templates. Oligonucleotides (Table 2-1) used in PCR were based on partial sequences obtained from GenBank (National Center for Biotechnology Information, Bethesda, MD, USA).

2.12 Plasmid constructs

2.12.1 pMHY1

To construct the *Y.lipolytica* plasmid pMHY1, a 3.5-kbp *Bgl*II-*Hin*dIII fragment capable of complementing the mutant strain *CHY545* (Table 2-5, Section 2.11.1) and including the entire *Y. lipolytica MHY1* gene was cloned into the *Bam*HI/*Hin*dIII sites of pINA445.

2.12.2 pRAC1

Plasmid pRAC1 was obtained by cloning a 2.2-kbp *Cla*I-*Stu*I fragment capable of complementing the mutant strain *CHY1220* (Table 2-5, Section 2.11.1) and containing the entire *Y. lipolytica RAC1* gene into the *Cla*I/*Sma*I sites of pINA445.

2.12.3 pSEC31

To obtain the *Y.lipolytica* plasmid pSEC31, a 6.2-kbp *Bam*HI-*Sph*I fragment capable of enhancing filamentous growth when introduced into the wild-type strain *E122* (Table 2-5, Section 2.11.2) and comprising the entire *Y. lipolytica SEC31* gene was cloned into the *Bam*HI-*Sph*I sites of pINA445.

2.12.4 pBEM1

Plasmid pBEM1 was obtained by cloning a 4.7-kbp *Bam*HI-*Bam*HI fragment capable of restoring filamentous growth to *Y.lipolytica CHY33169* cells (Table 2-5, Section 2.11.1) and containing the entire *Y. lipolytica BEM1* gene into the *Bam*HI site of pINA445.

2.12.5 pBMH1

The *Y. lipolytica* plasmid pBMH1 was obtained by cloning a 5.0-kbp *Bam*HI-*Bam*HI fragment capable of restoring filamentous growth into the *CHY3350* strain (Table 2-5, Section 2.11.1) and including the entire *Y. lipolytica BMH1* gene into the *Bam*HI site of pINA445.

2.12.6 pBMH2

To obtain the *Y. lipolytica* plasmid pBMH2, a 3.7-kbp *Bam*HI-*Bam*HI fragment containing the entire *Y. lipolytica BMH2* gene was amplified by high-fidelity PCR using a *Y. lipolytica* genomic DNA library as template (Section 2.11.3) and then cloned into the *Bam*HI site of pINA445.

2.13 Construction of null mutant strains of *Y. lipolytica*

2.13.1 Integrative disruption of *MHY1*

The 0.8-kbp *Nco*I-*Nde*I fragment of pMHY1 (Section 2.12.1) was replaced by a 1.6-kbp *Nco*I-*Nde*I fragment containing the *Y. lipolytica URA3* gene. This construct was digested with *Hpa*I to liberate a 3.3-kbp fragment containing the entire *URA3* gene flanked by 1.3-kbp and 0.4-kbp of the 5' and 3' regions of the *MHY1* gene, respectively. This linear fragment was used to transform the wild-type *Y. lipolytica* strain *E122* (Table 2-5) to uracil prototrophy. Ura^+ transformants that displayed a smooth phenotype were further characterized by Southern blot analysis (Section 2.6.2).

2.13.2 Integrative disruption of *YlRAC1*

To dirsrupt the *Y. lipolytica RAC1* gene, the 1.0-kbp *Apa*I-*Nde*I fragment of pRAC1 (Section 2.12.2) was initially replaced by a 1.6-kbp *Apa*I-*Nde*I fragment containing the *Y. lipolytica URA3* gene. Subsequently, this construct was digested with the restriction enzymes *Dra*I and *Xba*I to liberate a 2.4-kbp fragment containing the entire *URA3* gene flanked by 0.5-kbp and 0.3-kbp of the 5' and 3' regions of the *YlRAC1* gene, respectively.

This linear fragment was used to transform the wild-type *Y. lipolytica* strain *E122* (Table 2-5) to uracil prototrophy. Ura^+ strains that were unable to form rough-surfaced colonies were further characterized by Southern blot and PCR analyses (Sections 2.5.1 and 2.6.2).

2.13.3 Integrative disruption of *YlBEM1*

A 2.7-kbp fragment of pBEM1 (Section 2.12.4), corresponding to nucleotides −3 to +2700 of *YlBEM1*, was replaced by a 1.6-kbp fragment containing the *Y. lipolytica URA3* gene. This construct was digested with the restriction enzymes *Bam*HI and *Cla*I to liberate a 3.2-kbp fragment containing the entire *YlURA3* gene flanked by 0.6-kbp and 1.0-kbp of the 5' and 3' regions of *YlBEM1*, respectively, and this linear fragment was used to transform the wild-type *Y. lipolytica* strain *E122* (Table 2-5) to uracil prototrophy. Ura^+ strains of smooth phenotype were further characterized by Southern blot analysis (Section 2.6.2).

2.14 Epitope tagging of proteins

2.14.1 HA-tagging of *Yl*Mhy1p

An *Apa*I site was introduced before the stop codon of the *MHY1* gene by replacement of the 0.8-kbp *Nde*I-*Xba*I fragment of pMHY1 (Section 2.12.1) with a 0.8-kbp *Nde*I-*Xba*I fragment obtained by PCR (Section 2.5.1) using the oligonucleotides MHY1-ApaF and MHY1-ApaR (Table 2-1), generating the plasmid pMHY1-ApaI. A fragment with *Apa*I termini, encoding the peptide PLAMYPYDVPDYAAMYPYDVPDYAAM GKGE, which contains two repeats of the influenza virus hemagglutinin (HA) epitope

(underlined residues) (Kolodziej and Young, 1991), was generated by PCR using the oligonucleotides HA-ApaF and HA-ApaR (Table 2-1), and ligated into the unique *Apa*I site of pMHY1-ApaI to obtain the plasmid pMHY1-HA encoding a Mhy1p tagged at its carboxyl terminus with two repeats of the HA epitope (Mhy1p-HA). The integrity of the final construct was confirmed by DNA sequencing (Section 2.6.1), and pMHY1-HA was used to transform the mutant strain *mhy1KO9* (Table 2-5) to leucine prototrophy (Section 2.3.3).

2.14.2 GFP-tagging of *Yl*Mhy1p

A fragment with *Apa*I termini encoding the green fluorescent protein (GFP) from the jellyfish *Aequorea victoria* was generated by PCR (Section 2.5.1) using the oligonucleotides GFP-ApaF and GFP-ApaR (Table 2-1) and ligated into the *Apa*I site of pMHY1-ApaI (Section 2.14.1) to obtain the plasmid pMHY1-GFP, encoding *Yl*Mhy1p tagged at its carboxyl terminus with GFP (*Yl*Mhy1p-GFP). The integrity of the final construct was confirmed by DNA sequencing (Section 2.6.1), and pMHY1-GFP was used to transform the mutant strain *mhy1KO9* (Table 2-5) to leucine prototrophy (Section 2.3.3).

2.14.3 GFP-tagging of *Yl*Bem1p

An *Apa*I site was introduced before the stop codon of the *YlBEM1* gene by replacement of the 2.2-kbp *Kpn*I-*Bam*HI fragment of pBEM1 (Section 2.12.4) with a 2.2-kbp *Kpn*I-*Bam*HI fragment obtained by ligation of a 0.8-kbp *Kpn*I-*Apa*I fragment amplified by PCR (Section 2.5.1) using the oligonucleotides BEM1TAG-5F and BEM1TAG-5R

(Table 2-1) and a 1.4-kbp *Apa*I-*Bam*HI fragment obtained by PCR using the oligonucleotides BEM1TAG-3F and BEM1TAG-3R (Table 2-1). A fragment with *Apa*I termini encoding GFP was then ligated into the newly introduced *Apa*I site of pBEM1 to obtain the plasmid pBEM1-GFP, carrying *Yl*Bem1p tagged at its carboxyl terminus with GFP (*Yl*Bem1p-GFP). The integrity of the final construct was confirmed by DNA sequencing (Section 2.6.1), and pBEM1-GFP was used to transform the mutant strain *bem1KO157* (Table 2-5) to leucine prototrophy (Section 2.3.3).

2.15 Computer-aided analyses of DNA and protein sequences

DNA sequences were analysed using the Clone Manager software, version 3.11 (Scientific and Educational Software). Protein sequences were analysed and compared to other sequences with the PC-GENE software package (IntelliGenetics), or using the BLAST algorithms (Altschul *et al.*, 1990, 1997) via the network service (http://www.ncbi.nlm.nih.gov) of the National Center for Biotechnology Information (Bethesda, MD, USA). Protein sequences were aligned using the ClustalW 1.8 algorithm of the BCM Search Launcher (Smith *et al.*, 1996) via the network service (http://dot.imgen.bcm.tmc.edu:9331/multi-align/multi-align.html) of the Human Genome Sequencing Center of the Baylor College of Medicine (Houston, TX, USA).

CHAPTER 3

ISOLATION AND CHARACTERIZATION OF *MHY1*, A GENE CODING FOR A ZINC FINGER PROTEIN THAT PROMOTES DIMORPHIC TRANSITION IN *Y. lipolytica*

A version of this chapter has previously been published as "*MHY1* Encodes a C_2H_2-type Zinc Finger Protein That Promotes Dimorphic Transition in the Yeast *Yarrowia lipolytica*" (Cleofe A.R. Hurtado and Richard A. Rachubinski. *J. Bacteriol.*, May 1999, Vol. 181, No. 10, p. 3051-3057). Reproduced with permission.

3.1 Overview

A genetic screen was carried out to isolate mutants of the dimorphic yeast *Y. lipolytica* that fail to undergo the yeast-to-hypha transition. The *Y. lipolytica* mutant strain *CHY545* was selected by its inability to form rough-surfaced colonies when grown on agar plates, and the gene *MHY1* was subsequently isolated by its ability to restore hyphal growth when introduced into *CHY545* cells. Deletion of *MHY1* is viable and has no effect on mating, but does result in a complete inability of cells to form both hyphae and pseudohyphae. *MHY1* encodes a C_2H_2-type zinc finger protein, Mhy1p, which can bind putative *cis*-acting DNA stress response elements, suggesting that Mhy1p may act as a transcription factor. Interestingly, Mhy1p tagged with a hemagglutinin epitope was concentrated in the nuclei of actively growing cells found at the hyphal tip, and transcription of *MHY1* is dramatically increased during the yeast-to-hypha transition in *Y. lipolytica*.

3.2 Isolation and characterization of the *MHY1* gene

The *Y. lipolytica* mutant strain *CHY545* (Table 2-5) was initially isolated by its inability to form wild-type rough-surfaced colonies on YEPD-agar plates after 3 days of incubation at 28°C. Further analysis revealed that strain *CHY545* was able to grow only in the budding form on both rich and minimal media and that this attribute was stably maintained through multiple generations (Fig. 3-1, panel C).

The *MHY1* gene was isolated from a *Y. lipolytica* genomic DNA library contained in the replicative *E. coli* shuttle vector pINA445 (Nuttley *et al.*, 1993) by its ability to

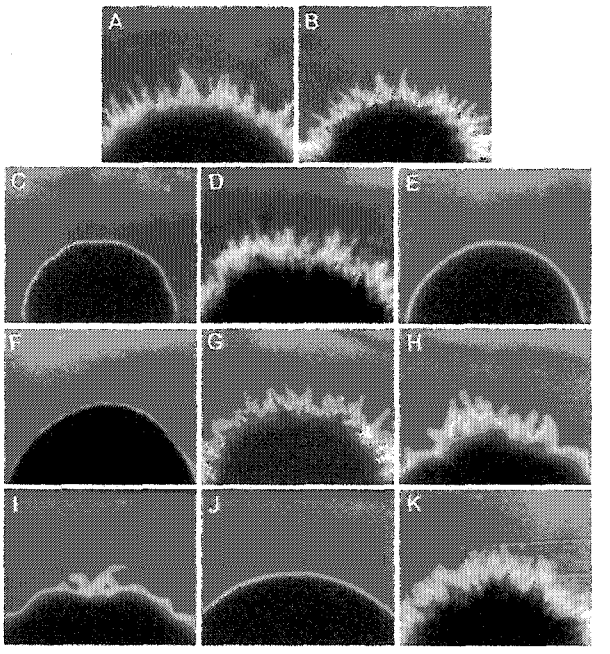

Figure 3-1. Colony morphology of various *Y. lipolytica* strains. (A and B) Wild-type strains *E122* and *22301-3*; (C) original mutant strain *CHY545*; (D) disruptant strain *mhy1KO9* transformed with plasmid pMHY1; (E and F) *MHY1* disruptant strains *mhy1KO9* and *mhy1KO9-B4*; (G) *MHY1//MHY1* diploid strain *E122//22301-3*; (H and I) *MHY1//mhy1* diploid strains *22301-3//mhy1KO9* and *E122//mhy1KO9-B4*; (J) *mhy1//mhy1* diploid strain *mhy1KO9//mhy1KO9-B4*; (K) *mhy1//mhy1* diploid strain *mhy1KO9//mhy1KO9-B4* carrying plasmid pMHY1. The colonies were photographed at ×100 magnification after 3 days of incubation at 28°C on YNA agar plates.

restore filamentous growth to *CHY545* cells. Of approximately 40,000 transformants screened, 4 showed an enhanced filamentous phenotype (Fig. 3-1, panel D). Restriction enzyme analysis demonstrated that all complementing plasmids shared a 3.5-kbp *Bgl*II-*Hin*dIII fragment capable of inducing hyphal growth upon introduction into the *CHY545* strain. Sequencing of this fragment revealed that the largest open reading frame (ORF), the *MHY1* gene, contained 855 bp coding for a 285-amino acid protein, Mhy1p, with a predicted molecular weight of 32,636 Da (Fig. 3-2A).

A putative TATA box, TATAATA, is found between nucleotides -119 and -113 from the A nucleotide of the potential initiating codon of the *MHY1* gene. Initial analysis has shown that transcription of the *MHY1* gene preferentially starts at position -74 from the A nucleotide of the first ATG codon, within a CCAAA sequence, a common structural feature of *Y. lipolytica* genes (Barth and Gaillardin, 1996). A nucleotides are also observed at positions -1 and -3 from the A nucleotide of the first ATG, a feature often observed in genes that are highly expressed in *Y. lipolytica* (Barth and Gaillardin, 1996). The upstream regulatory region of the *MHY1* gene contains consensus sequences for the binding of several transcription factors implicated in the regulation of fungal development and in the response of cells to specific environmental conditions, including multiple copies of the putative STRE, AGGGG (Kobayashi and McEntee, 1993), and multiple copies of a putative stationary phase response element (SPRE), AAAGG, commonly found upstream of stationary phase-responsive genes (Wang *et al.*, 1997) (Fig. 3-3). Interestingly, removal of the fragment upstream of the *Ssp*I site at position -722 of the *MHY1* gene results in impaired ability to induce hyphal growth.

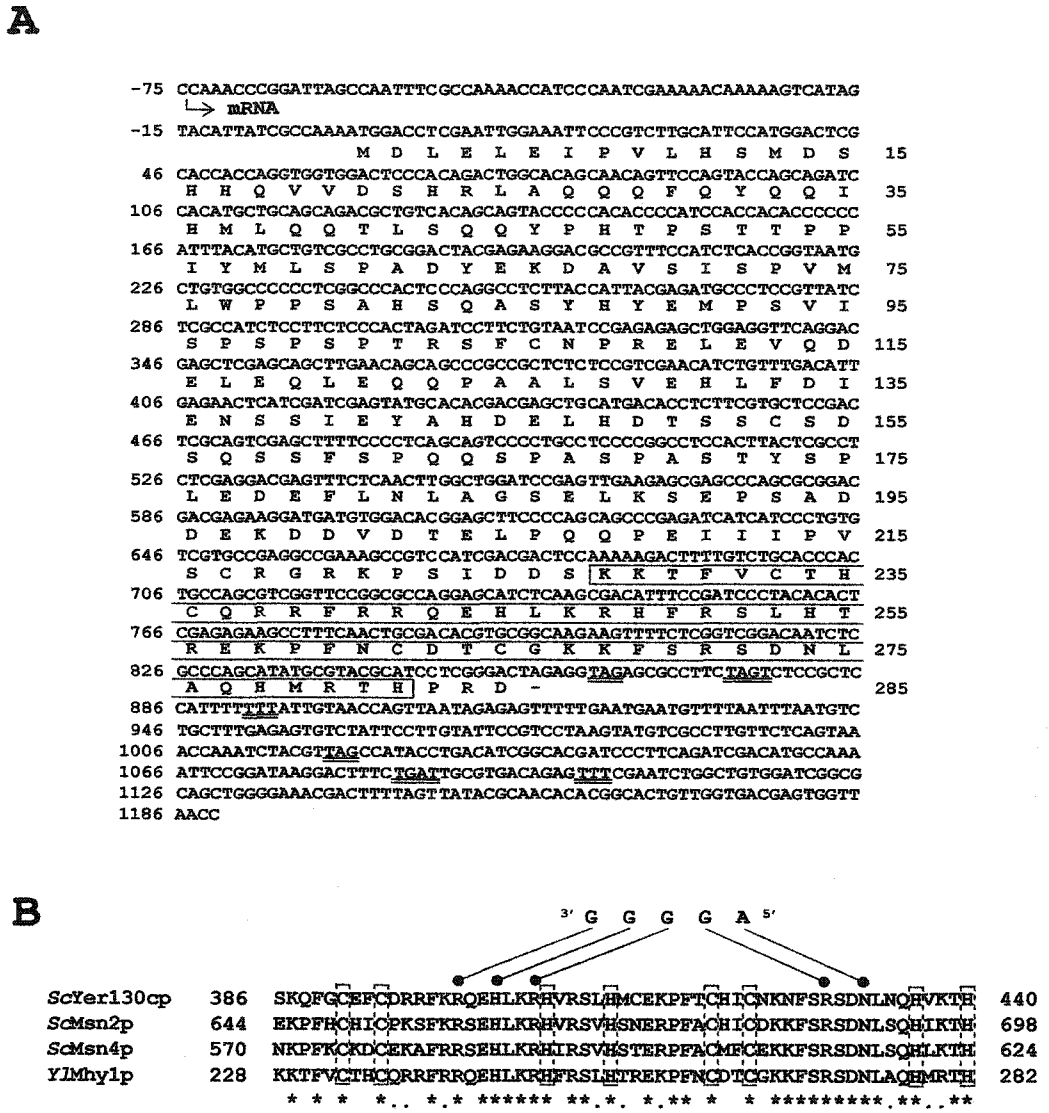

Figure 3-2. Characteristics of the *MHY1* gene and its encoded protein, Mhy1p. (A) Nucleotide sequence of the *MHY1* gene and deduced amino acid sequence of Mhy1p. Putative transcription termination signals are doubly underlined. The transcriptional start site of the *MHY1* gene is indicated. The segment of Mhy1p containing the two C_2H_2-type zinc-finger motifs is boxed. (B) Amino acid sequence alignment of the two zinc finger domains of Mhy1p and of those of *S. cerevisiae* Msn2p, Msn4p and Yer130cp. Identical (stars) and conserved (dots) amino acids are indicated. Cys and His residues capable of binding zinc ions are boxed. The STRE sequence 5'-AGGGG-3' and the amino acids that bind it are indicated.

Figure 3-3. Upstream regulatory region of the *MHY1* gene. A putative TATA box is boxed. The transcriptional start site of the *MHY1* gene is indicated by an arrow. Putative consensus sequences for the binding of transcription factors implicated in the regulation of fungal development and in the response to specific environmental conditions are indicated.

Mhy1p contains a glutamine-rich tract (52% of all residues between amino acids 27 and 45) at its amino terminus and two putative C_2H_2-type zinc finger motifs at its carboxyl terminus (Fig. 3-2A and 3-2B). Similar structural elements are found in transcription factors like the *S. cerevisiae* calcineurin-responsive zinc finger protein, Crz1p (Matheos *et al.*, 1997; Stathopoulos and Cyert, 1997), and *Drosophila melanogaster* Sp1, which is required for the development of the antennal, intercalary and mandibular segments of the head (Wimmer *et al.*, 1993). Moreover, the region in Mhy1p connecting these motifs (amino acids 46 to 175) is considerably rich in serine/proline (33%) and acidic residues (28%), a structural composition that has been implicated in protein-protein interactions (Frankel and Kim, 1991). Three putative PEST regions, commonly found in rapidly degraded proteins (Chevaillier, 1993; Rechsteiner and Rogers, 1996), are predicted at residues 49–65, 89–102, and 149–188 of Mhy1p.

3.3 Mhy1p binds *in vitro* to putative STRE elements

A search using the BLAST Network Service of the National Center for Biotechnology Information identified a number of *S. cerevisiae* transcription factors with homology to Mhy1p within the zinc finger motifs. Further analysis revealed that the two C_2H_2-type zinc fingers of Mhy1p displayed the same arrangement and main structural features as those found in the stress-responsive transcription factors Msn2p and Msn4p, and in the putative protein encoded by the ORF YER130C (Fig. 3-2B). Predictions based on computer-assisted molecular modeling of Msn2p and Msn4p (Martinez-Pastor *et al.*, 1996), combined with the presence of residues in Mhy1p (Arg242, His245, Arg248,

Arg271, and Asn273) identical to those shown to be responsible for specific DNA-binding by Msn2p and Msn4p, suggested that Mhy1p could also recognize and bind the AGGGG pentanucleotide of putative STREs. Specific binding of Mhy1p to the AGGGG pentanucleotide was demonstrated by EMSA. *In vitro* synthesized Mhy1p bound to a radiolabeled double-stranded probe derived from the upstream region of the *YlRAC1* gene (Fig. 3-4, lane 2), whose transcription is increased during the dimorphic transition in *Y. lipolytica* and which contains three copies of the AGGGG pentanucleotide (Chapter 4). This binding was efficiently competed by increasing amounts of unlabeled probe (Fig. 3-4, lanes 3 to 6). Mhy1p failed to bind to a probe containing mutations in the two AGGGG motifs (*T*GGGG) (Fig. 3-4, lane 7), thereby demonstrating the specificity of the interaction of Mhy1p and the putative STREs.

Gel retardation experiments performed with whole extracts from *E122* and *mhy1KO9* cells (Section 3.4 and Table 2-5) grown in YNBGlc or YNBGlcNAc medium showed that there was considerable AGGGG-binding activity in lysates of cells grown under conditions that induce mycelial growth, but little of this activity in lysates of mutant cells lacking functional *MHY1* or of wild-type cells incubated in medium containing glucose as the sole carbon source (Fig. 3-5).

3.4 Disruption of the *MHY1* gene does not affect viability and mating of *Y. lipolytica*

The 0.8-kbp *Nco*I-*Nde*I fragment of pMHY1 was replaced by a 1.6-kbp *Nco*I-*Nde*I fragment containing the *Y. lipolytica URA3* gene (Fig. 3-6A). This construct was digested with *Hpa*I to liberate a 3.3-kbp fragment containing the entire *YlURA3* gene flanked by 1.3

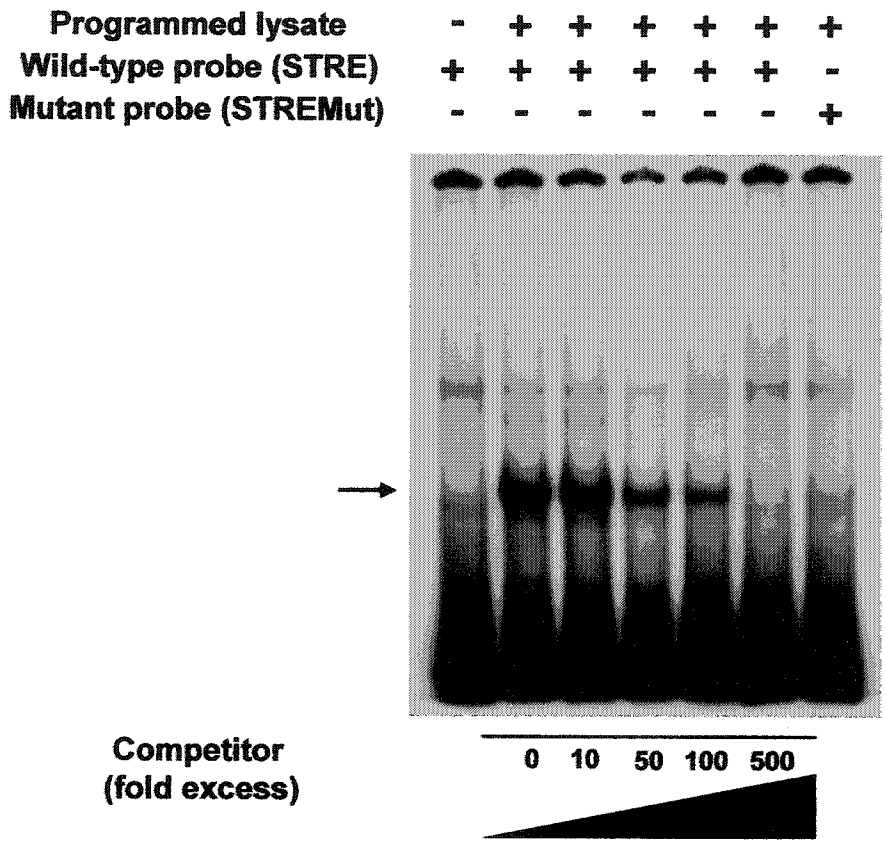

Figure 3-4. Mhy1p binds specifically *in vitro* to the putative STRE pentanucleotide AGGGG. Mhy1p was translated *in vitro*, incubated with a radiolabeled probe derived from the upstream region of the *YlRAC1* gene and which contains two copies of the AGGGG pentanucleotide, and analyzed by EMSA. The specificity of the DNA-protein interaction was determined by competition analysis with unlabeled probe and by EMSA with a mutant probe containing single base mutations (AGGGG to *T*GGGG) in the two putative STREs of the wild-type probe. Lane 1, wild-type probe incubated with unprogrammed lysate. Lane 2, wild-type probe incubated with *in vitro* translated Mhy1p. Lanes 3-6, wild-type probe incubated with *in vitro* translated Mhy1p and 10- 50-, 100-, and 500-fold molar excesses of unlabeled wild-type oligonucleotide, respectively. Lane 7, mutant probe incubated with *in vitro* translated Mhy1p. The arrow indicates the MHY1p/DNA complex.

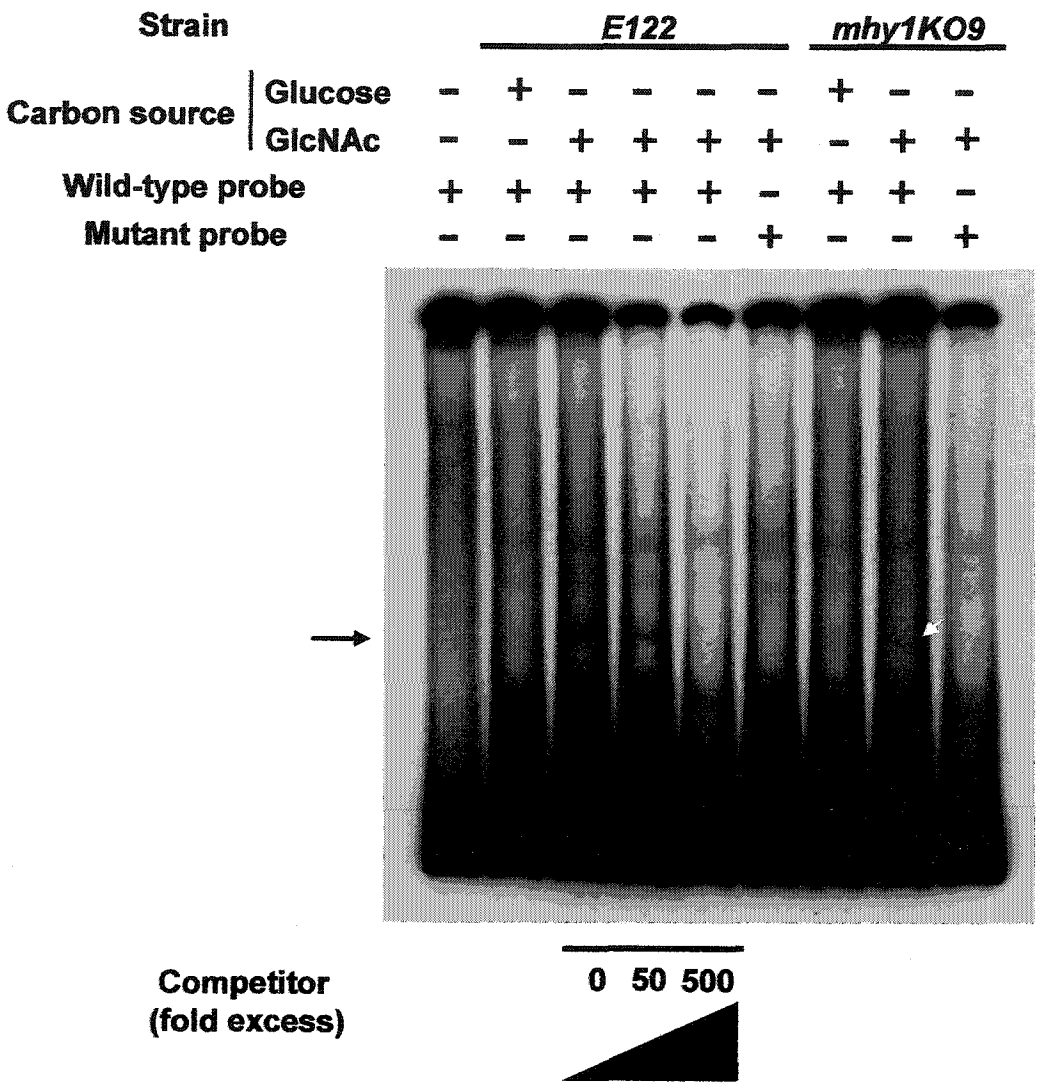

Figure 3-5. Specific binding of *Y. lipolytica* proteins to oligonucleotides containing putative STREs. Whole cell extracts (60 μg of protein) of wild-type strain *E122* and mutant strain *mhy1KO9* incubated at 28°C for 10 h in YNBGlc (yeast growth) or YNBGlcNAc (induction of filamentous growth) were incubated with ^{32}P-labeled wild-type (STRE) and mutant (STREMut) probes (Table 2-1) and submitted to gel electrophoresis. Lane 1, no protein added. Lane 2, protein from *E122* cells grown in YNBGlc. Lanes 3-6, protein from *E122* cells grown in YNBGlcNAc. Lane 7, protein from *mhy1KO9* cells grown in YNBGlc. Lanes 8-9, protein from *mhy1KO9* cells grown in YNBGlcNAc. Lanes 2, 7 and 8, wild-type probe incubated with yeast whole cell lysate. Lanes 3-5, wild-type probe incubated with yeast whole cell lysate and 50- and 500-fold molar excesses of unlabeled wild-type oligonucleotide, respectively. Lanes 6 and 9, mutant probe incubated with yeast whole cell lysate. Arrows indicate specific protein/DNA complexes.

kbp and 0.4 kbp of the 5' and 3' regions of the *MHY1* gene, respectively. This linear fragment was used to transform the wild-type *Y. lipolytica* strain *E122* (Table 2-5) to uracil prototrophy. Of 246 Ura^+ transformants obtained, 2 showed a fully smooth phenotype after 3 days on YEPD-agar plates. One of these transformants, *mhy1KO9* (Fig. 3-1 and Table 2-5), was confirmed by Southern blot analysis to have had its *MHY1* gene correctly replaced by the *YlURA3* gene (Fig. 3-6B).

Mating is a phenomenon that involves dramatic changes in cell morphology in response to environmental conditions and has been found to be intimately connected to dimorphism (Madhani and Fink, 1998). We therefore investigated whether disruption of the *MHY1* gene had any effect on the mating ability of *Y. lipolytica.* The B mating type strain *mhy1K09-B4* (Table 2-5), with its *MHY1* gene deleted, was obtained by crossing strain *mhy1KO9* with the isogenic wild-type strain *22301-3* (Table 2-5), followed by sporulation of the resultant diploid and selection for the inability to undergo dimorphic transition. The *mhy1::URA3* genotype of the *mhy1K09-B4* strain was confirmed by cosegregation of the Fil^- and Ura^+ phenotypes. *MHY1//mhy1* (Fig. 3-1, panels H and I) and *mhy1//mhy1* (Fig. 3-1, panel J) diploid strains were readily obtained by mating any combination of the mutant haploid strains *mhy1KO9* and *mhy1KO-B4*, and the wild-type strains *E122* and *22301-3*, indicating that no defect in mating ability was associated with the loss of *MHY1*.

3.5 Filamentation is affected by gene dosage of *MHY1*

Since transformation of *mhy1* mutant strains with the pINA445-based

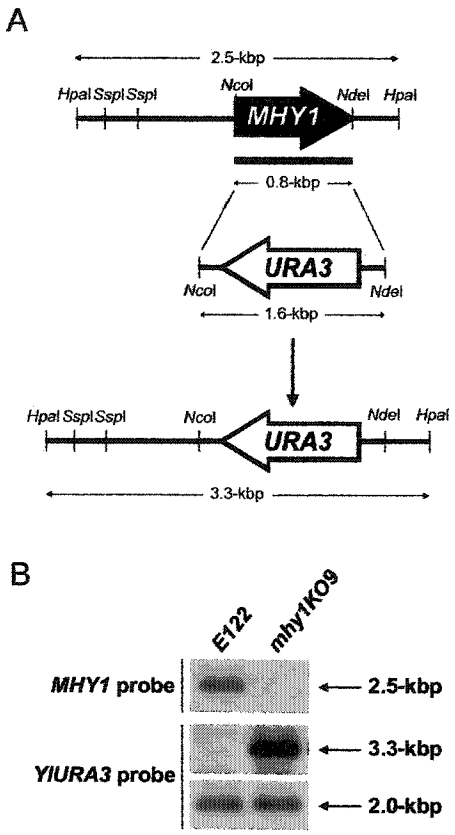

Figure 3-6. Integrative disruption of the *MHY1* gene. (A) Diagram illustrating the targeted gene replacement strategy for the *MHY1* gene. The ORFs and directionality of the *MHY1* and *YlURA3* genes are indicated by the wide arrows. (B) Southern blot analysis of *Hpa*I-digested genomic DNA from *Y. lipolytica* wild-type strain *E122* and mutant strain *mhy1KO9*, confirming the replacement of the *MHY1* gene segment by the *YlURA3*-containing linear molecule.

autonomously replicating plasmid pMHY1, which is believed to be present in two to five copies per cell (Fournier *et al.*, 1993), resulted in an enhanced filamentous phenotype (Fig. 3-1, panel D), crossings of the mutant strains *mhy1KO9* and *mhy1KO9-B4* were performed with the wild-type strains *E122* and *22301-3* to determine the effects of gene dosage on the filamentous growth of diploid strains. Diploid strains containing a single copy of *MHY1* (Fig. 3-1, panels H and I) gave rise to colonies with significantly reduced filamentation compared to wild-type haploid strains (Fig. 3-1, panels A and B), while transformation of an *mhy1//mhy1* diploid strain (Fig. 3-1, panel J) with the plasmid pMHY1 resulted in an enhanced filamentous phenotype (Fig. 3-1, panel K). Colonies formed by *MHY1//mhy1* diploid strains (Fig. 3-1, panels H and I) showed a substantial increase in the proportion of yeast-like cells when compared to colonies of the *MHY1//MHY1* strain (Fig. 3-1, panel G).

3.6 Transcription of the *MHY1* gene is increased during dimorphic transition

The yeast-to-hypha transition in exponentially growing *E122* cells was induced by a 15-min carbon source starvation period at 4°C, followed by transfer to YNBGlcNAc medium. Under these conditions, more than 90% of cells gave rise to germ tubes after 10 h of incubation at 28°C (Fig. 3-7, upper panels). In contrast, cells transferred to fresh glucose-containing (YNBGlc) medium grew almost exclusively as the budding form (Fig. 3-7, bottom panels), as previously described (Guevara-Olvera *et al.*, 1993). Northern blot analysis (Fig. 3-7) carried out with total RNA extracted from cells harvested following 3 and 10 h of incubation showed that *MHY1* mRNA levels dramatically increased during the

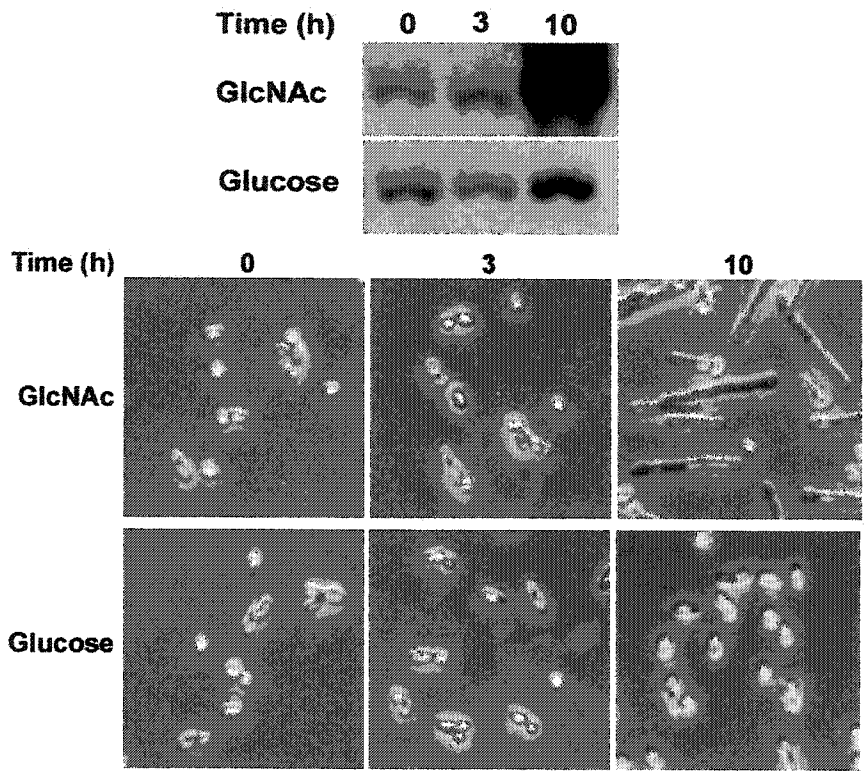

Figure 3-7. *MHY1* mRNA levels are increased during the dimorphic transition. Total RNA was isolated from *Y. lipolytica E122* cells incubated at 28°C in YNBGlcNAc (induction of filamentous growth) or YNBGlc (control culture, yeast-like cells) for the times indicated and subjected to northern blot analysis. 10 μg of RNA from each time point was separated on a formaldehyde agarose gel and transferred to nitrocellulose. Blots were hybridized with a probe specific for the *MHY1* gene (0.8-kbp *Nco*I-*Nde*I fragment, see Fig. 4). Equal loading of RNA was ensured by ethidium bromide staining (data not shown). Cell morphology at t = 0, 3 and10 h is shown.

dimorphic transition, but remained essentially constant during the first hours of incubation in YNBGlcNAc or YNBGlc. A smaller increase in the levels of *MHY1* mRNA (approximately 2-fold) was observed after 10 h of incubation in YNBGlc (Fig. 3-7), probably due to the few germ tubes (less than 1%) present.

3.7 Mhy1p is localized to the nucleus during the dimorphic transition and is concentrated in actively growing hyphal cells

To determine whether the subcellular localization of Mhy1p is consistent with its probable function as a transcription factor, indirect *in situ* immunofluorescence of a carboxyl-terminal HA-tagged version of Mhy1p was carried out in cells cultivated in YNBGlcNAc. Mhy1p-HA was undetectable in the nuclei of cells growing as the yeast form (Fig. 3-8A), but was readily detected in the nuclei of cells undergoing dimorphic transition (Fig. 3-8B, C, and D). Strikingly, Mhy1p-HA was found to be concentrated in actively growing hyphal cells. Thus, while Mhy1p-HA was detected in the nuclei of cells emitting germ tubes (Fig. 3-8B), once the transition step was completed, Mhy1p-HA was concentrated in the filamentous cells located at the growing hyphal tip, with no, or a barely detectable, signal being detected in the other cells of the filamentous chain (Fig. 3-8C and D).

Interestingly, a carboxyl-terminal GFP-tagged version of Mhy1p was unable to induce hyphal growth in *mhy1KO9* mutant cells and fluorescence microscopy revealed that the Mhy1p-GFP fusion protein was dispersed throughout the cell in the *E122* and *mhy1KO9* strains (Fig. 3-9).

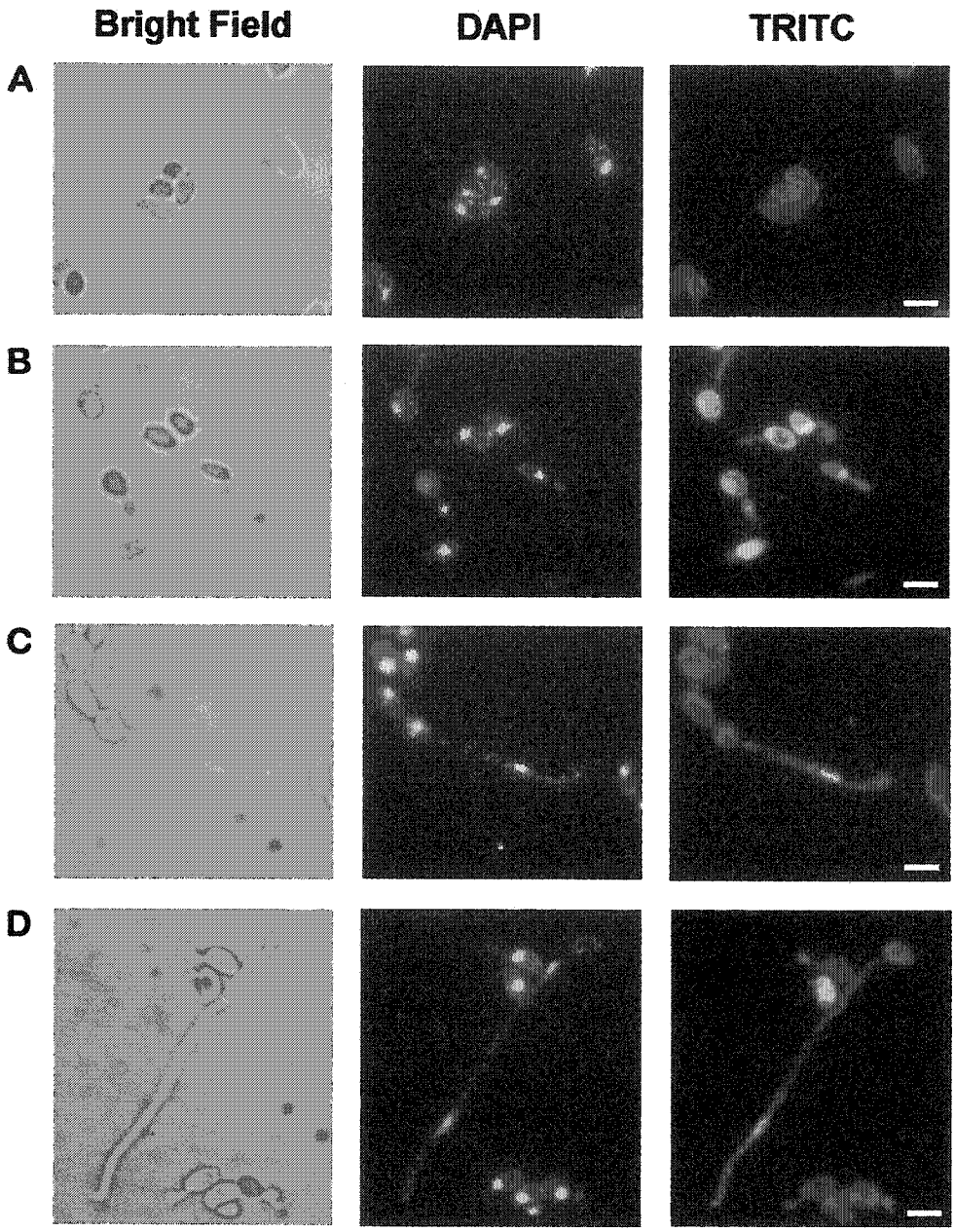

Figure 3-8. Nuclear localization of Mhy1p during filamentous growth of *Y. lipolytica*. Indirect immunofluorescence of HA-tagged Mhy1p was carried out on yeast-like cells (A) and at different stages of filamentation (B, C and D), as described in Materials and Methods (Section 2.9.1). (Left panels) cells visualized by bright field microscopy. (Middle panels) DAPI staining of nuclei. (Right panels) rhodamine (TRITC) staining observed with an anti-HA monoclonal antibody. Bars, 5 μm.

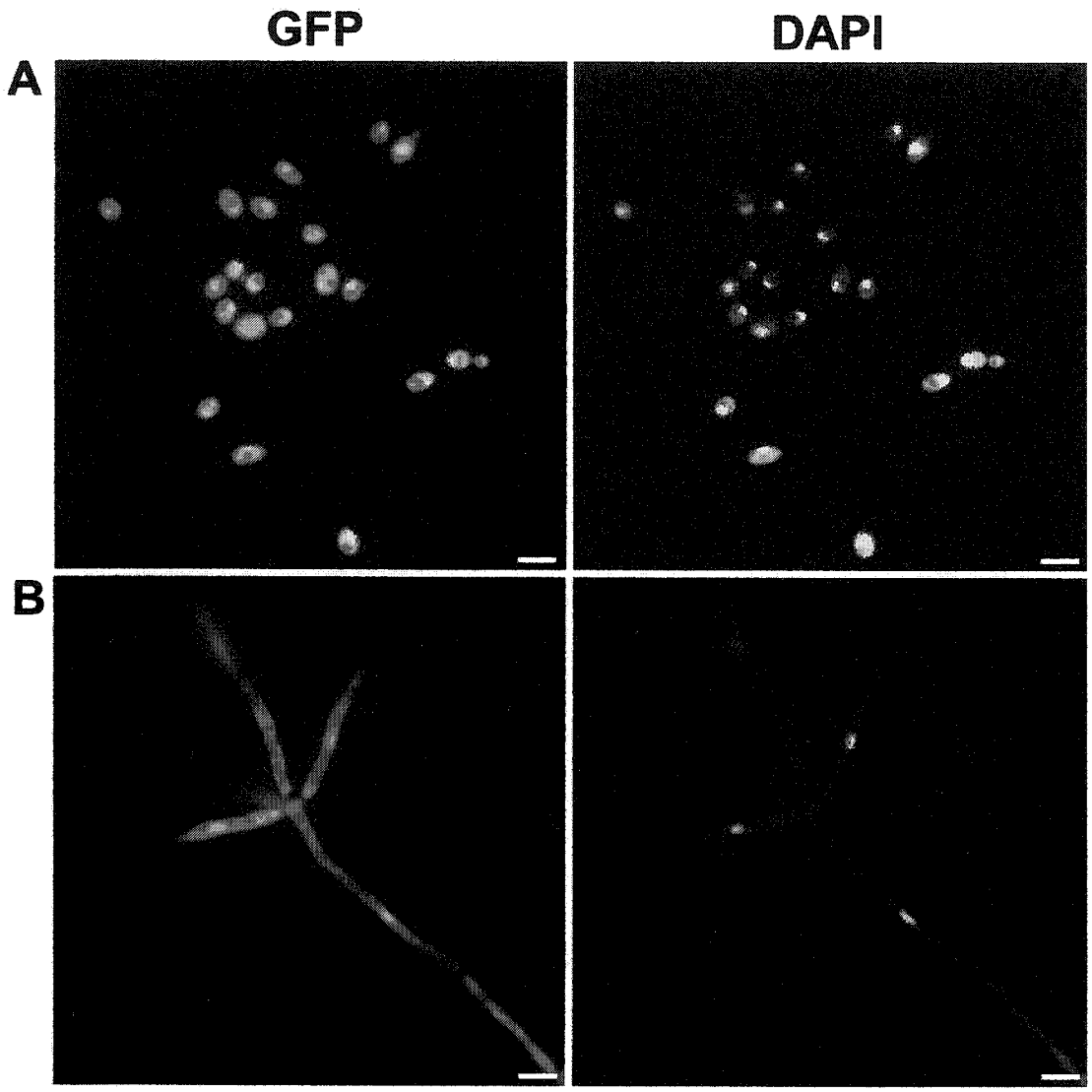

Figure 3-9. Localization of GFP-tagged Mhy1p in yeast *mhy1KO9* (A) and hyphal *E122* (B) cells. (Left panels) GFP-tagged Mhy1p visualized by fluorescence microscopy. (Right panels) DAPI staining of nuclei. Bars, 5 μm.

3.8 Transcription of *MHY1* during the stress response

To investigate possible links between the dimorphic transition program and the stress response in *Y. lipolytica* via *MHY1*, northern blotting of total RNA prepared from *E122* cells exposed to several stress conditions was carried out with a *MHY1* fragment as a probe (Fig. 3-10). Surprisingly, *MHY1* mRNA levels were found to decrease to barely detectable levels after 2 h of exposure to osmotic stress (0.4 M NaCl) and were undetectable after 1 h of carbon source starvation or 2 h of exposure to oxidative stress (0.8 mM H_2O_2). In contrast, transcription of *MHY1* remained essentially constant even after 2 h of exposure to thermal stress at 35°C. Interestingly, the viability of *E122* cells and *mhy1KO9* cells was essentially the same for both strains following exposure to a particular type of stress.

3.9 Discussion

This chapter describes the identification of a novel gene, *MHY1*, and the initial characterization of its product, Mhy1p, involved in the yeast-to-hypha transition of the dimorphic yeast *Y. lipolytica*. Although the exact role of Mhy1p in the dimorphic transition remains undetermined, several features of Mhy1p suggest that it may function as a transcription factor. The most striking of these is the presence near its carboxyl terminus of two C_2H_2-type zinc fingers, which are strongly homologous to zinc fingers found in the proteins encoded by the *S. cerevisiae* genes *MSN2*, *MSN4* and the ORF of unknown function, YER130C. Like Msn2p and Msn4p, Mhy1p specifically recognizes, and binds to, sequences containing the AGGGG pentanucleotide, strongly suggestive

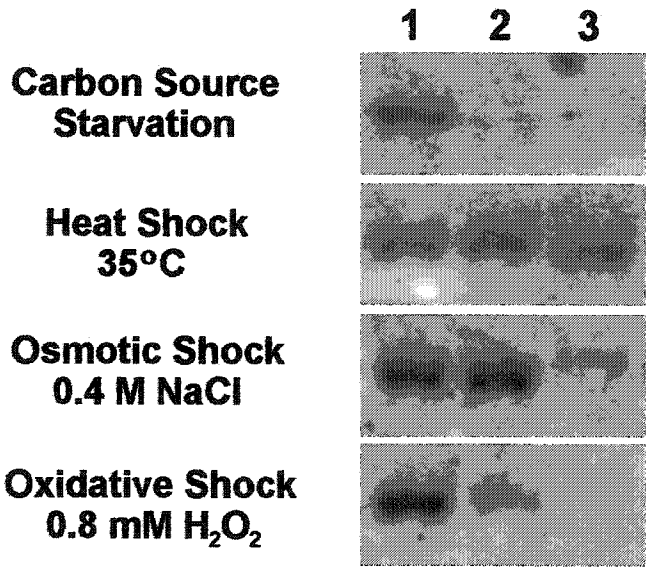

Figure 3-10. *MHY1* mRNA levels during the stress response. Total RNA was isolated from *E122* cells exposed to several stress conditions. For carbon source starvation, cultures were sampled at 0, 1 and 5 h (lanes 1, 2 and 3, respectively). For heat shock, osmotic and oxidative stresses, cultures were sampled at 0, 30 and 120 min (lanes 1, 2 and 3, respectively). 10 μg of RNA from each time point was separated on a formaldehyde agarose gel and transferred to nitrocellulose. Blots were hybridized with a probe specific for the *MHY1* gene (0.8-kbp *Nco*I-*Nde*I fragment, see Fig. 4). Equal loading of RNA was ensured by ethidium bromide staining (data not shown).

of a role for Mhy1p in the transcriptional regulation of genes containing this sequence in their promoter regions.

Database analysis revealed that most promoters of *Y. lipolytica* genes contain AGGGG sequences, but they are particularly abundant in the genes *HOY1* (6 copies) and *ICL1* (5 copies). *HOY1* has been shown to be directly involved in the yeast-to-hypha transition (Torres-Guzman and Dominguez, 1997), while *ICL1* encodes one of the two main enzymes of the glyoxylate pathway, a strongly regulated anaplerotic cycle that in *Y. lipolytica* is under control of *GPR1*, a gene also implicated in the dimorphic transition (Tzschoppe *et al.*, 1999).

MHY1 expression is dramatically increased during the yeast-to-hypha transition. Surprisingly, *MHY1* mRNA levels were significantly decreased under conditions that otherwise would activate Msn2p/Msn4p-mediated expression of stress-responsive genes in *S. cerevisiae*, *i.e.* carbon-source starvation, osmotic and oxidative shock. However, transcription of *MHY1* was unaffected by thermal stress. It has been suggested that heat shock, and not starvation, may act synergistically with *N*-acetylglucosamine to achieve full induction of mycelial growth (Guevara-Olvera *et al.*, 1993). Our results are in agreement with this hypothesis.

How might Mhy1p function in the yeast-to-hypha transition? One model is that under conditions promoting the dimorphic transition, Mhy1p would translocate from the cytosol to the nucleus. There, Mhy1p would act as a transcription factor controlling the expression of genes whose products are necessary both to redirect cell growth towards filamentation and to maintain this pattern. Once a cell had achieved its maximum

extension, it would divide, with Mhy1p being equally distributed to the nuclei of both mother and daughter cells. Mhy1p would then be rapidly degraded in the mother cell, but would continue to promote filamentous growth at the growing tip of the daughter cell. Interestingly, Mhy1p contains three potential PEST sequences, which have been implicated in rapid protein degradation and are often found in regulatory nuclear factors with specific and transient functions during cell growth (Chevaillier, 1993).

CHAPTER 4

ISOLATION OF *YlRAC1* AND DEMONSTRATION OF ITS INVOLVEMENT IN THE DIMORPHIC TRANSITION OF *Y. lipolytica*

A version of this chapter has previously been published as "A Rac Homolog Is Required for Induction of Hyphal Growth in the Dimorphic Yeast *Yarrowia lipolytica*" (Cleofe A.R. Hurtado, Jean-Marie Beckerich, Claude Gaillardin and Richard A. Rachubinski. *J. Bacteriol.*, May 2000, Vol. 182, No. 9, p. 2376-2386). Reproduced with permission.

4.1 Overview

The *Y. lipolytica* mutant strain *CHY1220* was selected by its inability to undergo the yeast-to-hypha transition, and the *YlRAC1* gene was subsequently isolated by its ability to restore hyphal growth when introduced into *CHY1220* cells. *YlRAC1*, a gene encoding a 192-amino acid protein, is essential for hyphal growth in the dimorphic yeast *Y. lipolytica* and characterizes the first Rac homolog described in fungi. *YlRAC1* is not an essential gene, and its deletion does not affect mating ability nor impair actin polarization in *Y. lipolytica*. However, strains lacking functional *YlRAC1* display alterations in cell morphology, thus suggesting that its function may be related to some aspects of the polarization of cell growth. Northern blot hybridization revealed that transcription of *YlRAC1* increases steadily during the yeast-to-hypha transition, and Southern blot analysis of genomic DNA suggests the presence of several related superfamily members in *Y. lipolytica*. Interestingly, strains lacking functional *YlRAC1* are still able to grow as the pseudohyphal form and to invade agar, thus pointing to a function for *YlRAC1* downstream of *MHY1*, a previously isolated gene that encodes a C_2H_2-type zinc finger protein with the ability to bind putative STREs (pentanucleotide CCCCT or AGGGG), and whose activity is essential for both hyphal and pseudohyphal growth in *Y. lipolytica* (Chapter 3).

4.2 Isolation of the *Y. lipolytica* mutant strain *CHY1220*

The *Y. lipolytica* mutant strain *CHY1220* (Fig. 4-1, panel B) was initially isolated by its inability to form wild-type rough-surfaced colonies on YEPD-agar plates after 3 days of incubation at 28°C (Fig. 4-1, panel A). Further analysis revealed that, like *rac1Δ* strains,

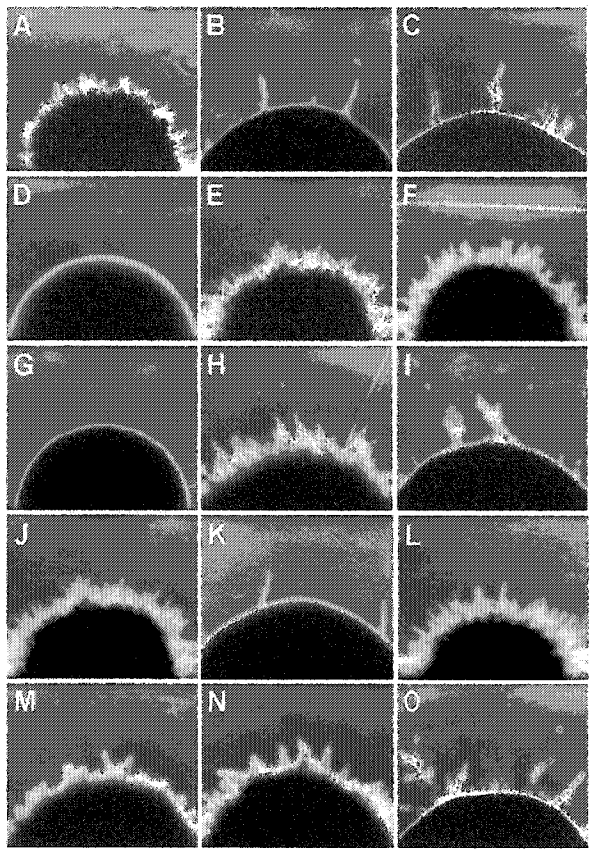

Figure 4-1. Colony morphology of various *Y. lipolytica* strains. (A) Wild-type strain *E122*; (B) mutant strain *CHY1220*; (C) *RAC1* disruptant strain *rac1KO30*; (D) *MHY1* disruptant strain *mhy1KO9*; (E) strain *CHY1220* transformed with plasmid pRAC1; (F) strain *rac1KO30* transformed with plasmid pRAC1; (G) strain *mhy1KO9* transformed with plasmid pRAC1; (H) strain *CHY1220* transformed with plasmid pMHY1; (I) strain *rac1KO30* transformed with plasmid pMHY1; (J) wild-type strain *22301-3*; (K) *RAC1* disruptant strain *rac1KO30-B36*; (L) *RAC1//RAC1* diploid strain *E122//22301-3*; (M and N) *RAC1//rac1* diploid strains *22301-3//rac1KO30* and *E122//rac1KO30-B36*; (O) *rac1//rac1* diploid strain *rac1KO30//rac1KO30-B36*. Colonies were photographed at ×100 magnification after 3 days of incubation at 28°C on YNA agar plates.

CHY1220 was able to form colonies having a small number of peripheral extensions after prolonged periods of incubation on both rich and minimal medium and that these extensions consisted of chains of elongated cells following a pseudohyphal pattern (Fig. 4-1, panels B, C, K, and O).

4.3 Isolation and characterization of the *YlRAC1* gene

The *YlRAC1* gene was isolated from a *Y. lipolytica* genomic DNA library contained in the replicative *E. coli* shuttle vector pINA445 (Nuttley *et al.*, 1993) by its ability to restore hyphal growth to *CHY1220* cells. Of approximately 70,000 transformants screened, 5 showed a restored filamentous phenotype (Fig. 4-1, panel E). Restriction enzyme analysis demonstrated that all complementing plasmids shared a 2.2-kbp *Spe*I-*Cla*I fragment capable of inducing hyphal growth in *CHY1220* cells. Sequencing of this fragment revealed an ORF of 576 bp interrupted by two introns, which are found at codons 12 and 36 (nucleotides +36 to +205 and +278 to +328 from the A residue of the potential initiating codon, respectively). The putative 5'-splice donor sequences of both introns (GTAAGTPu) diverge at the third and fourth positions from the GTGAGTPu and GTATGT consensus motifs found in *Y. lipolytica* (Lopez *et al.*, 1994; Strick *et al.*, 1992) and *S. cerevisiae* (Teem *et al.*, 1984), respectively. As in the *Y. lipolytica* genes *SEC14* (Lopez *et al.*, 1994) and *PYK1* (Strick *et al.*, 1992), a 3'-splice acceptor CAG sequence is found one nucleotide downstream of the consensus TACTAAC box (Teem *et al.*, 1984) or its abbreviated form CTAAC (Fig. 4-2).

No obvious TATA box or CT/CA-rich region, which is believed to play a role in

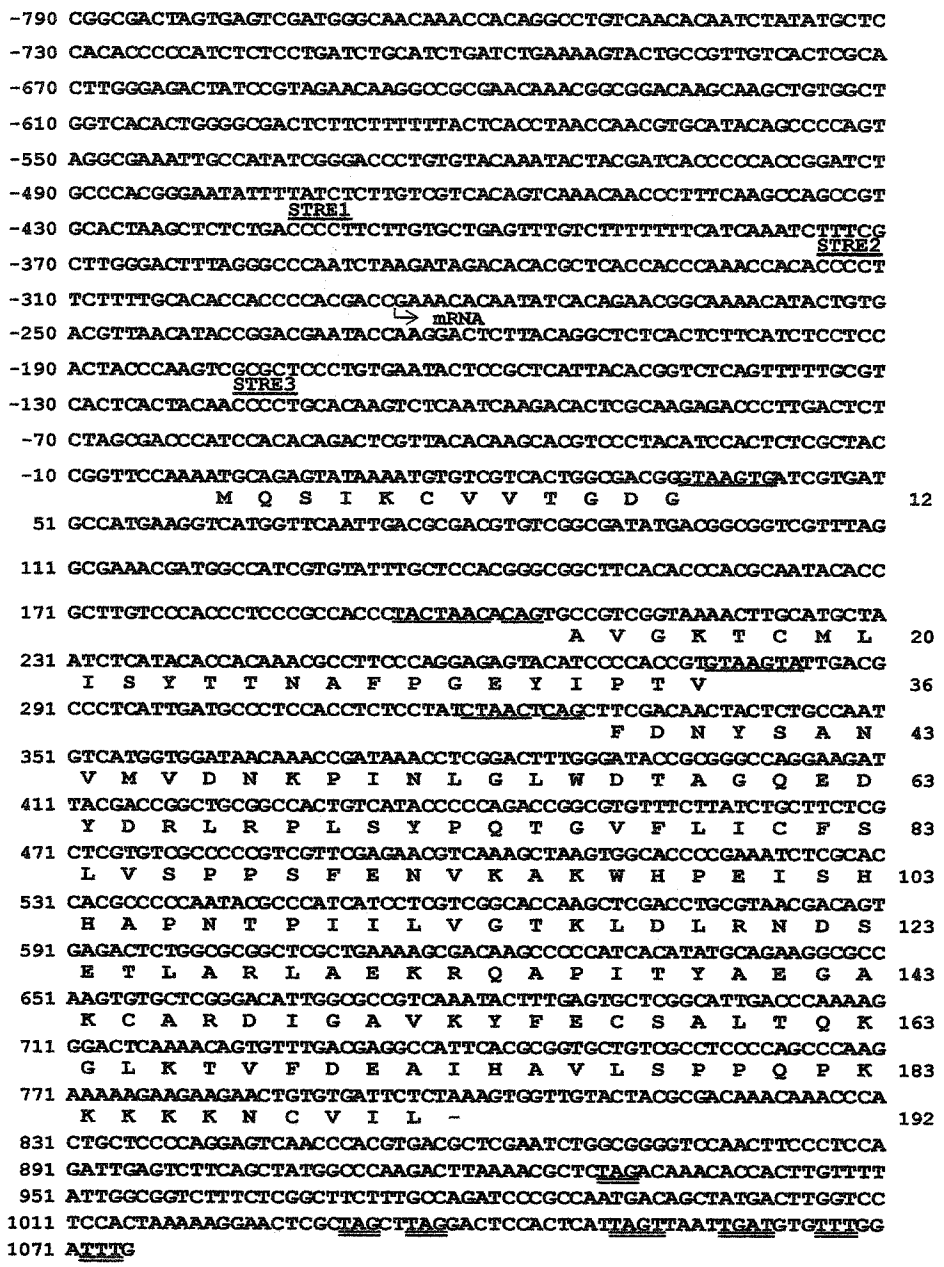

Figure 4-2. Nucleotide sequence of the *YlRAC1* gene and deduced amino acid sequence of *Yl*Rac1p. The transcriptional start site of the *YlRAC1* gene is indicated by an arrow. Putative STREs are indicated. Consensus sequences for intron splicing are underlined. Putative transcription termination signals are doubly underlined.

transcriptional regulation in *Y. lipolytica* (Nuttley *et al.*, 1994; Xuan *et al.*, 1990), is seen in the putative promoter of *YlRAC1*. However, analysis of cDNA showed that transcription of the *YlRAC1* gene preferentially starts at position -286 relative to the A nucleotide of the first ATG codon and that polyadenylation occurs following the G nucleotide at position +1075. Other features of *YlRAC1* include the presence of conserved A nucleotides at positions -1 and -3 relative to the A nucleotide of the initiating ATG and three putative STREs (pentanucleotide CCCCT) (Kobayashi and McEntee, 1993) in its upstream region (Fig. 4-2).

The deduced protein product of *YlRAC1*, *Yl*Rac1p, is 192 amino acids in length and has a predicted molecular weight of 21,173 Da (Fig. 4-2). Comparison of the predicted amino acid sequence of *Yl*Rac1p with the sequences of Rac proteins from different sources suggests that its closest homologue is human Rac1 (Fig. 4-3). In addition, *Yl*Rac1p has a relatively high pI (8.47), which is an attribute that distinguishes Rac proteins from Rho and Ras proteins (whose pIs are in the range of 5.0 to 6.5) (Delmer *et al.*, 1995).

Consensus elements GXXXXGK (GDGAVGK, residues 10 to 16) and DXXG (DTAG, residues 57 to 60) (Fig. 4-3), which are involved in interactions with the phosphate portion of the GTP molecule, are found in *Yl*Rac1p at positions conserved among GTP-binding proteins (Chen *et al.*, 1993; Dever *et al.*, 1987; Johnson and Pringle, 1990; Mirbod *et al.*, 1997). Conserved motifs are also present at the regions implicated in interaction with the GTPase-activating protein (GAP) (TVFDNY, residues 35 to 40) (Sekine *et al.*, 1989), and membrane association prior to biological activity (CVIL, residues 189 to 192) (Hancock *et al.*, 1989; Ziman *et al.*, 1993) (Fig. 4-3). Notably,

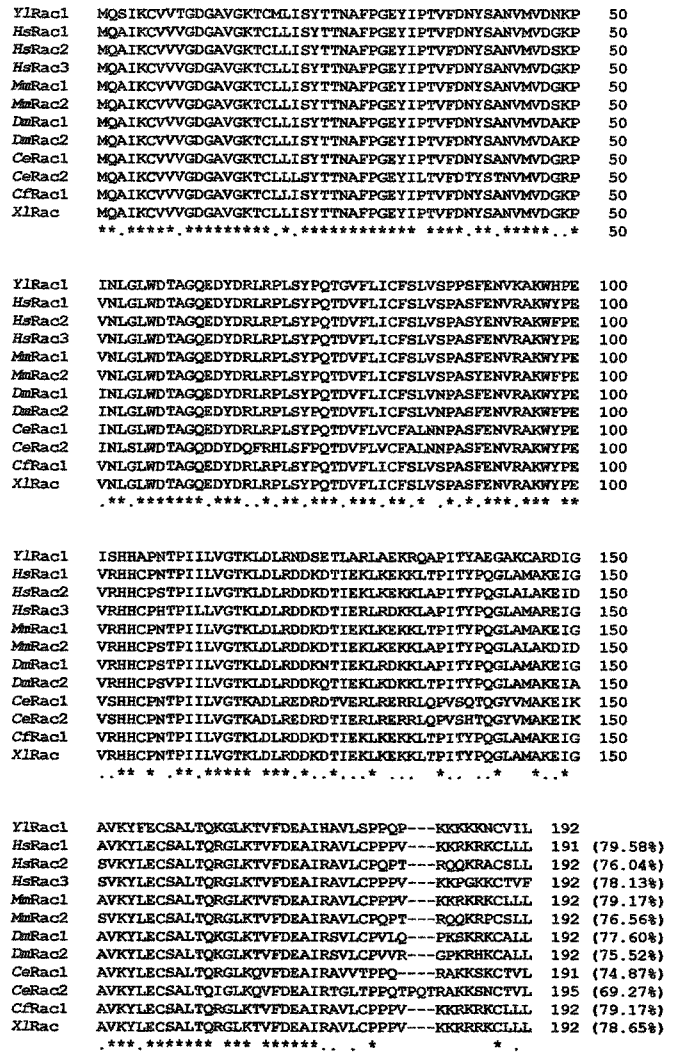

Figure 4-3. Amino acid sequence alignment of Rac1p of *Y. lipolytica* (*Yl*Rac1p) and Rac proteins from *Homo sapiens* (*Hs*Rac1, *Hs*Rac2 and *Hs*Rac3), *Mus musculus* (*Mm*Rac1 and *Mm*Rac2), *Drosophila melanogaster* (*Dm*Rac1 and *Dm*Rac2), *Caenorhabditis elegans* (*Ce*Rac1 and *Ce*Rac2), *Canis familiaris* (*Cf*Rac1), and *Xenopus laevis* (*Xl*Rac). GenBank accession numbers: M29870 (*Hs*Rac1), CAB45265 (*Hs*Rac2), AAC51667 (*Hs*Rac3), CAA40545 (*Mm*Rac1), Q05144 (*Mm*Rac2), AAA62870 (*Dm*Rac1), P48554 (*Dm*Rac2), AAA28141 (*Ce*Rac1), AAB40386 (*Ce*Rac2), P15154 (*Cf*Rac1) and AAD50299 (*Xl*Rac).

*Yl*Rac1p also contains the conserved motif TKXD (TKLD, residues 115 to 118), which is responsible for nucleotide specificity in Rac proteins and is involved in the determination of the unusually high intrinsic rate of GTP hydrolysis that distinguishes Rac from other Rho family members (Delmer *et al.*, 1995).

4.4 Isolation and characterization of the *YlCDC42* gene

Since no *RAC* gene had previously been reported for fungi and since the *CDC42* gene, which encodes a protein that belongs to the Rac subfamily of Rho GTPases (Garcia-Ranea and Valencia, 1998), is involved in the regulation of filamentous growth in *S. cerevisiae* and *C. albicans* (Mirbod *et al.*, 1997; Mösch *et al.*, 1996; Ushinsky *et al.*, 2002), the *CDC42* gene of *Y. lipolytica* (*YlCDC42*) was isolated to provide further evidence that the first fungal *RAC* gene had been identified.

The sequence of a partial *YlCDC42* clone, previously obtained by probing a *Y. lipolytica* genomic DNA library with an oligonucleotide derived from a highly conserved sequence in the Rab family of proteins (Pertuiset *et al.*, 1995), was combined with the sequence of a *YlCDC42* cDNA obtained by PCR of a *Y. lipolytica* cDNA library with oligonucleotides T3, T7, CDC42U and CDC42M (Table 2-1) to obtain the sequence of the *YlCDC42* gene. The *YlCDC42* gene contains an ORF of 573 bp, which is interrupted by two introns, as is the *YlRAC1* gene (Fig 4-4). The introns are found between codons 16 and 17 and at codon 45 (nucleotides +49 to +157 and +244 to +327 relative to the A nucleotide of the potential initiating codon, respectively). The putative 5'-splice donor sequences of both introns are identical to the consensus motif GTGAGTPu found in other

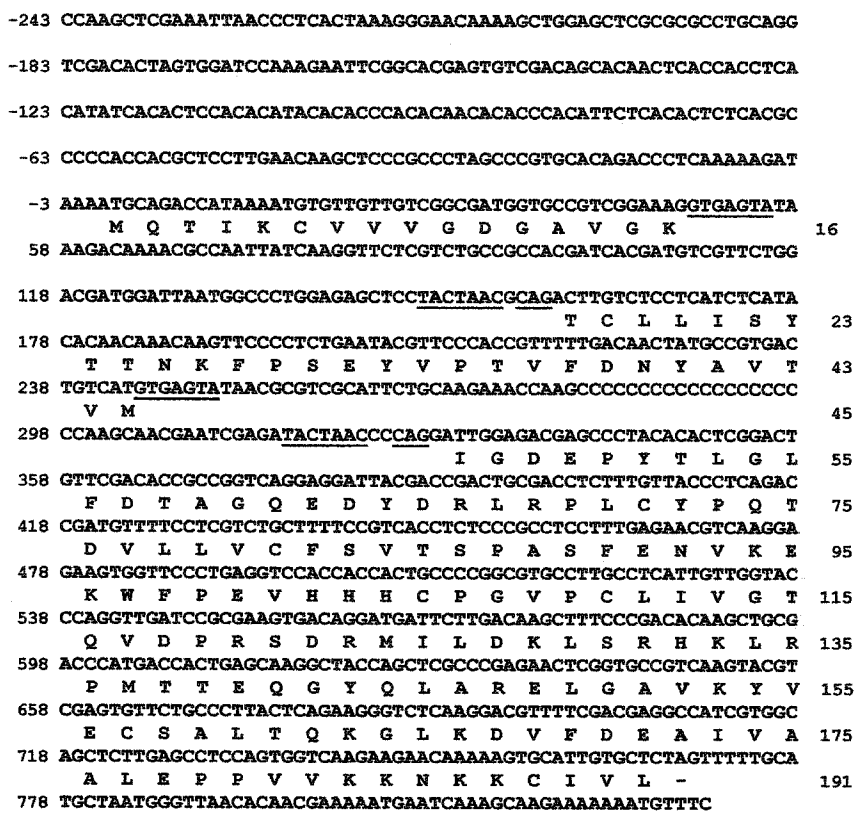

Figure 4-4. Nucleotide sequence of the *YlCDC42* gene and deduced amino acid sequence of *Yl*Cdc42p. Consensus sequences for intron splicing are underlined.

Y. lipolytica genes (Lopez *et al.*, 1994; Strick *et al.*, 1992), and a 3'-splice acceptor CAG sequence is found two nucleotides downstream of the consensus TACTAAC box (Teem *et al.*, 1984) (Fig. 4-4).

The deduced protein of *YlCDC42*, *Yl*Cdc42p, is 191 amino acids long and has a predicted molecular weight of 21,336 Da (Fig. 4-4) and an estimated pI of 6.09, which is characteristic of Cdc42 proteins (Delmer *et al.*, 1995). In addition, *Yl*Cdc42p contains all motifs required for the biological function of small GTPases of the Rho family (GDGAVGK, residues 10 to 16; TVFDNY, residues 35 to 40; DTAG, residues 57 to 60; and CIVL, residues 188 to 191) (Fig. 4-4 and Fig. 4-5). Comparison of *Yl*Cdc42p with Cdc42 proteins form a number of different organisms suggests that its closest relative is *Schizosaccharomyces pombe* Cdc42 (Fig. 4-5). Importantly, *Yl*Cdc42p contains the signature sequence of Cdc42 proteins, the motif TQXD (TQVD, residues 115 to 118) (Johnson, 1999), in the region responsible for nucleotide specificity.

4.5 Strains with the *YlRAC1* gene disrupted are viable and unaffected in mating ability

A 1.0-kbp *Apa*I-*Nde*I fragment of *YlRAC1* was replaced by a 1.6-kbp *Apa*I-*Nde*I fragment containing the *Y. lipolytica URA3* gene (Fig. 4-6A). This construct was digested with *Dra*I and *Xba*I to liberate a 2.4-kbp fragment containing the entire *YlURA3* gene flanked by 0.5 kbp and 0.3 kbp of the 5' and 3' regions of the *YlRAC1* gene, respectively. This linear fragment was used to transform the wild-type *Y. lipolytica* strain *E122* to uracil prototrophy.

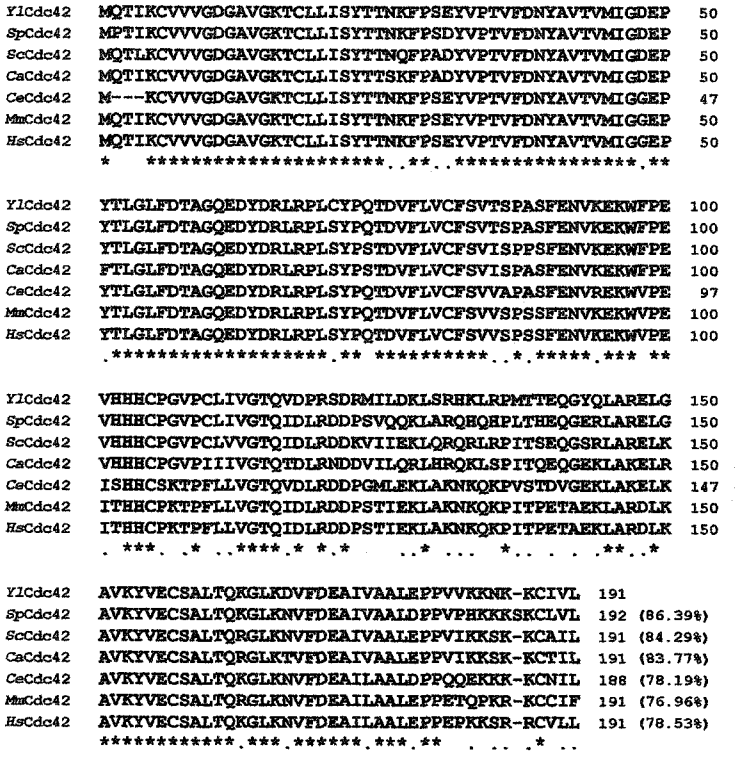

Figure 4-5. Amino acid sequence alignment of Cdc42p of *Y. lipolytica* (*Yl*Cdc42p) and its homologs in *S. pombe* (*Sp*Cdc42p), *S. cerevisiae* (*Sc*Cdc42p), *C. albicans* (*Ca*Cdc42p), *C. elegans* (*Ce*Cdc42p), *M. musculus* (*Mm*Cdc42p) and *H. sapiens* (*Hs*Cdc42p). GenBank accession numbers: AAA16472 (*Sp*Cdc42), P19073 (*Sc*Cdc42), 014426 (*Ca*Cdc42), Q05062 (*Ce*Cdc42), AAB40051 (*Mm*Cdc42), and NP_001782 (*Hs*Cdc42).

Of 303 Ura$^+$ transformants obtained, 3 showed a smooth phenotype after 3 days on YEPD agar plates. Two of these transformants were confirmed by Southern blot analysis and PCR to have had the *YlRAC1* gene correctly replaced by the *YlURA3* gene (Fig. 4-6), and one of them, *rac1KO30* (Table 2-5 and Fig. 4-1, panel C), was selected for further analysis.

Because mating has been found to be intimately connected to dimorphism and, like dimorphism, is a phenomenon that involves dramatic changes in cell morphology in response to environmental conditions (Madhani and Fink, 1998), we investigated whether disruption of the *YlRAC1* gene had any effect on the mating ability of *Y. lipolytica.* Crossing of the A mating type strain *rac1KO30* (*rac1Δ*) with the B mating type wild-type strain *22301-3* was readily attained (Fig. 4-1, panel M), indicating that no mating defect was associated with disruption of *YlRAC1* in these strains. To determine whether the lack of effect on mating by disruption of the *YlRAC1* gene was confined to A mating type cells, a B mating type strain, *rac1KO30-B36* (Table 2-5 and Fig. 4-1, panel K), with its *YlRAC1* gene deleted, was obtained by sporulation of the diploid strain *22301-3//rac1KO30* (Table 2-5 and Fig. 4-1, panel M) and selection of haploids for their inability to form hyphal cells. The *rac1::URA3* genotype of the *rac1KO30-B36* strain was confirmed by cosegregation of the Ura$^+$ and Fil$^-$ phenotypes, and this strain was found to be able to mate to both wild-type *E122* and *rac1KO30* strains (Fig. 4-1, panels N and O), demonstrating that *YlRAC1* is not essential for mating. One copy of the *YlRAC1* gene was sufficient to support dimorphic transition in diploid strains of *Y. lipolytica*, although a slight reduction in the proportion of hyphal cells could be observed in these strains (Fig. 4-1, panels M and N).

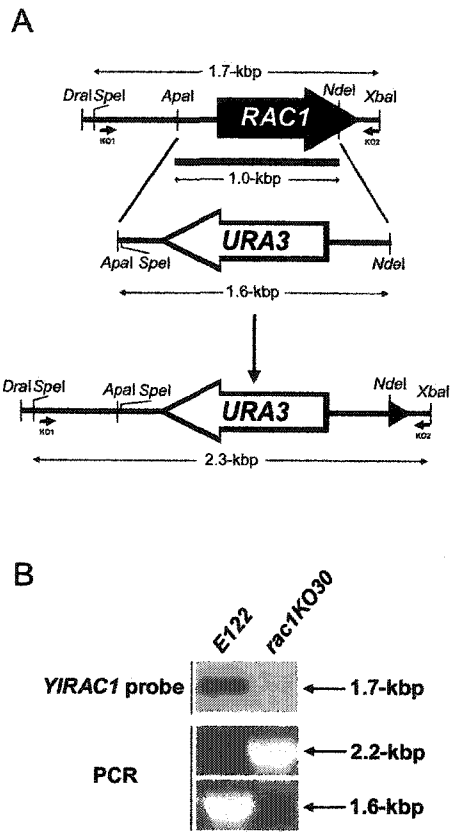

Figure 4-6. Integrative disruption of the *YlRAC1* gene. (A) Diagram illustrating the replacement of a 1.0-kbp *Apa*I-*Nde*I fragment of *YlRAC1* by a 1.6-kbp *Apa*I-*Nde*I fragment containing the *Y. lipolytica URA3* gene. (B) Southern blot analysis of *Spe*I-*Hpa*I-digested genomic DNA, and PCR analysis of total genomic DNA, from wild-type strain *E122* and strain *rac1KO30*, confirming the correct replacement of the *YlRAC1* gene with the *YlURA3*-containing linear molecule in strain *rac1KO30*. Primers Rac1-KO1 and Rac1-KO2 (Table 2-1) are indicated by black arrows in panel A.

4.6 Disruption of the *YlRAC1* gene affects cell morphology but does not impair actin polarization or cell invasiveness

Since the organization of the actin cytoskeleton is directly involved in the determination of cell shape and because Rac proteins play a fundamental role in this process (Hall, 1994, 1998; Ridley, 1995; Tapon and Hall, 1997), disruption of *YlRAC1* was anticipated to result in morphological defects in *Y. lipolytica* cells. Indeed, exponentially growing *rac1Δ* mutant cells were found to be round in shape, clearly contrasting with the typically ovoid cells observed for wild-type strains (Fig. 4-7, top panels). Continued incubation in rich medium yielded wild-type cultures composed of yeast cells, pseudohyphae, and a few germ tubes, while *rac1Δ* cultures contained only a small proportion of pseudohyphal cells and no germ tubes (Fig. 4-7, middle panels). In general, pseudohyphal *rac1Δ* cells were found to be shorter than their wild-type counterparts (Fig. 4-7, middle panels). As stationary phase was reached, hyphal growth became predominant in wild-type cultures, while only a limited number of chains composed of pseudohyphal cells were seen in the *rac1Δ* cultures (Fig. 4-7, bottom panels). Germ tubes arising from pseudohyphal cells were sometimes seen in the wild-type strain (Fig. 4-7, bottom right panel, inset). Interestingly, invasive pseudohyphal growth was found to be substantially induced in the *rac1Δ* strain by incubation on minimal medium containing glucose as the sole carbon source (YNBD agar), whereas this effect was not observed in *rac1Δ* cells grown on minimal medium containing acetate as the sole carbon source (YNA agar) or in *mhy1Δ* cells incubated under either condition (Fig. 4-8).

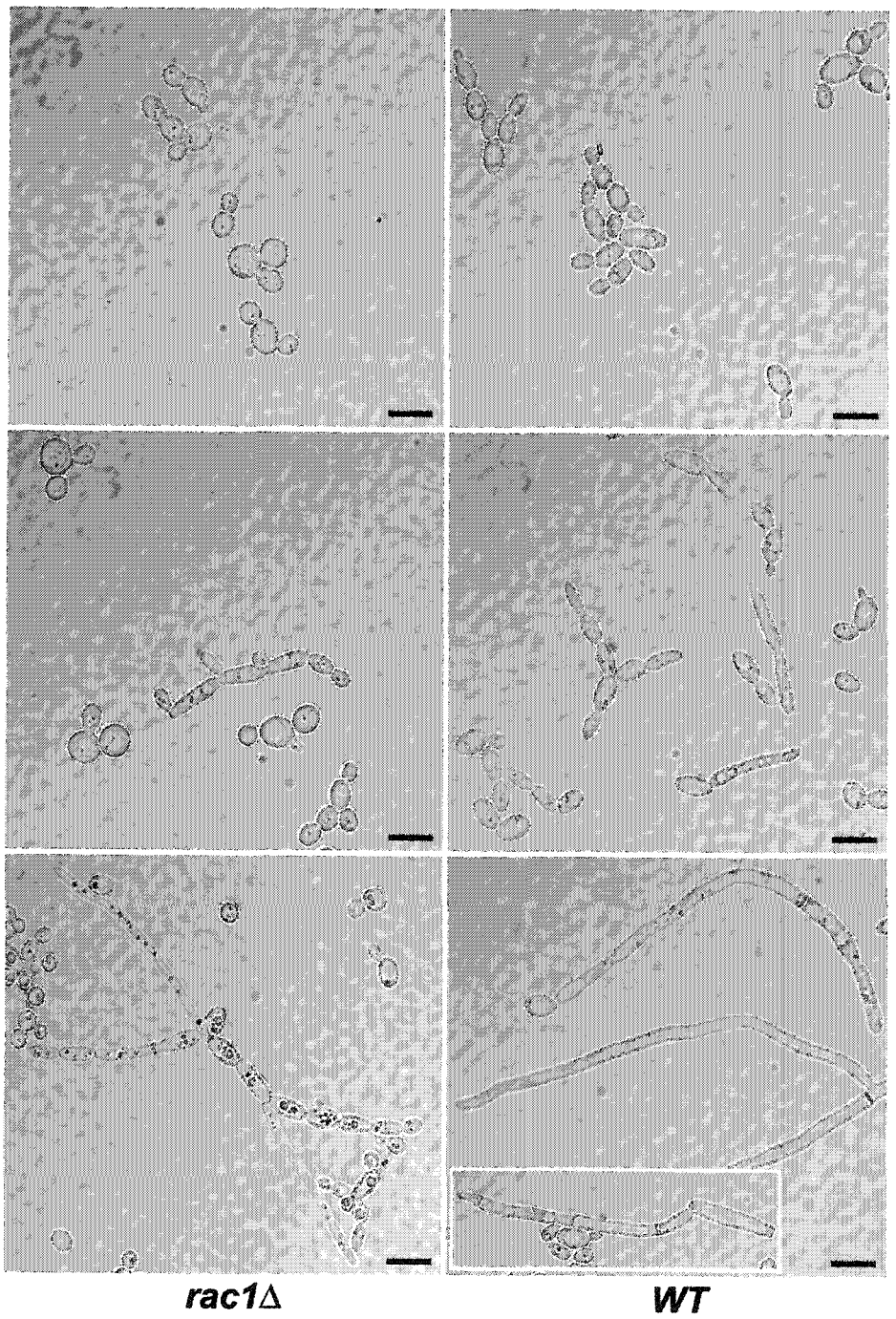

Figure 4-7. Disruption of *YlRAC1* affects cell morphology and impairs hyphal growth, but not pseudohyphal growth, in *Y. lipolytica*. Strains were grown in YEPD. Top panels, exponential growth phase (optical density at 600nm [OD_{600}] = 1). Middle panels, late exponential growth phase (OD_{600} = 4). Bottom panels and inset, stationary phase (OD_{600} = 10). *WT*, wild-type strain *E122*. *rac1Δ*, strain *rac1KO30*. Bars, 5 μm.

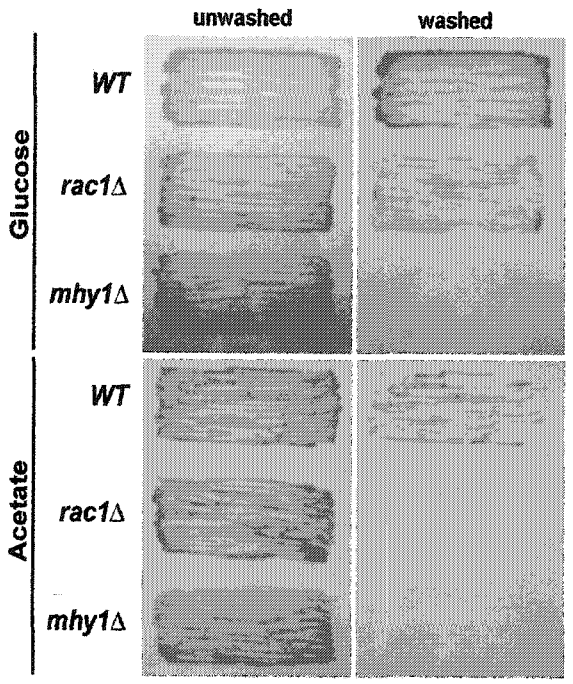

Figure 4-8. Invasive filamentous growth by different *Y. lipolytica* strains. Following 5 days of incubation at 28°C on minimal agar medium containing glucose or acetate as the sole carbon source, plates were washed with running water to remove cells from the agar surface. Pictures were taken before and after washes. *WT*, wild-type strain *E122*. *rac1Δ*, strain *rac1KO30*. *mhy1Δ*, strain *mhy1KO9*.

As described for a number of fungi (Adams and Pringle, 1984; Akashi *et al.*, 1994; Alfa and Hyams, 1990; Heath, 1987; Kwon *et al.*, 1991; Marks and Hyams, 1985; Roberson, 1992; Yokoyama *et al.*, 1990), actin rich zones at the sites of growth (apices of germ tubes, hyphae, pseudohyphae and yeast cells), combined with a background of diffuse actin staining with punctate actin patches, were observed for wild-type cells of *Y. lipolytica* (Fig. 4-9, panels A to G). Interestingly, despite alterations in cell morphology, *rac1Δ* mutant cells appeared to retain the ability to concentrate actin granules at the apices of pseudohyphal cells and emerging buds (Fig. 4-9, panels H and I).

4.7 Transcription of the *YlRAC1* gene is increased during the yeast-to-hypha transition

The dimorphic switch was induced in exponentially growing *Y. lipolytica E122* cells by a 15-min carbon source starvation period at 4°C, followed by transfer to pre-warmed (28°C) YNBGlcNAc medium. Under these conditions, more than 80% of the cell population gave rise to germ tubes after 10 h of incubation, while cells transferred to fresh YNBGlc medium grew almost exclusively as the budding form, as described previously (Guevara-Olvera *et al.*, 1993). Northern blot analysis performed with total RNA extracted from cells harvested after 0, 1, 3 and 10 h of incubation in YNBGlcNAc showed that *YlRAC1* mRNA levels increased steadily during the yeast-to-hypha transition, but they remained virtually constant during the incubation in YNBGlc (Fig. 4-10).

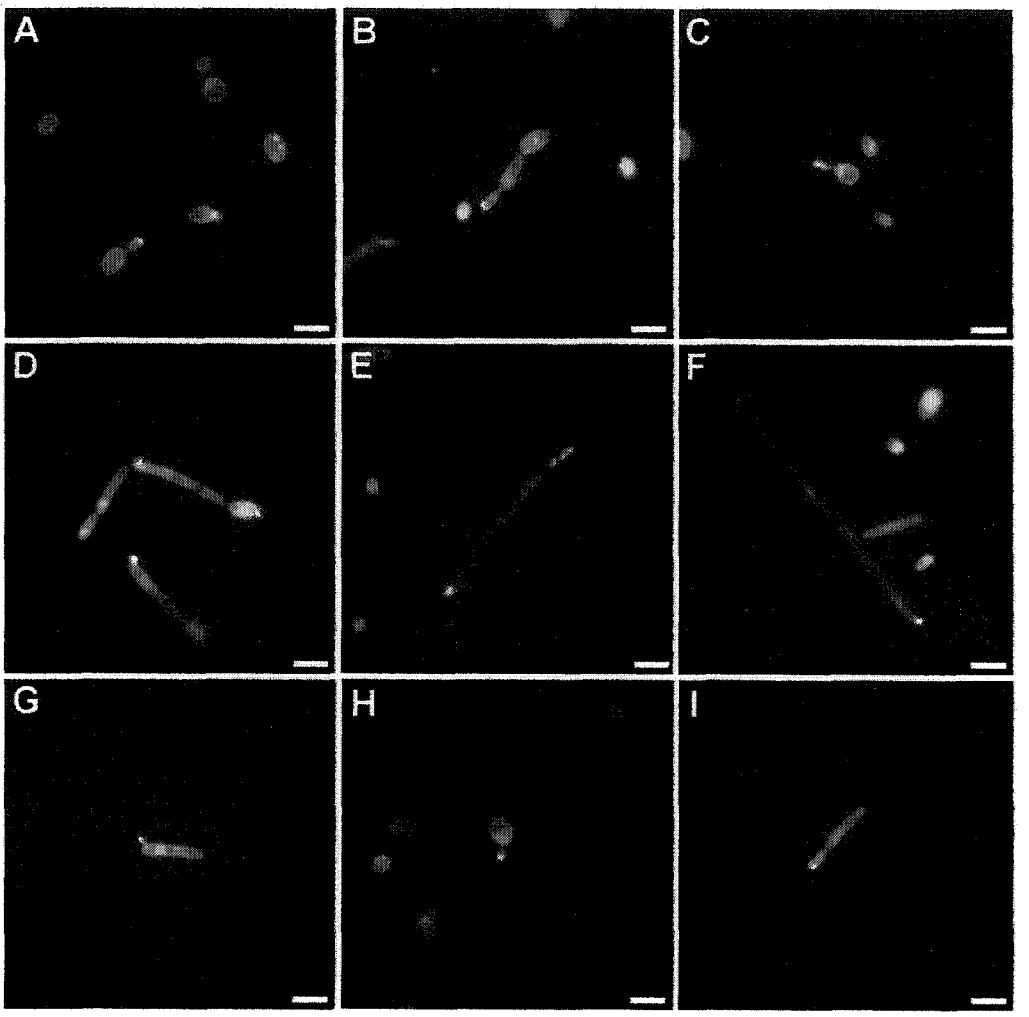

Figure 4-9. Actin localization during different stages of development of wild-type and *rac1Δ* cells. Actin was detected by staining cells with Oregon Green 488 phalloidin followed by fluorescence microscopy. (A to G) Wild-type strain *E122*. (H and I) *rac1Δ* strain *rac1KO30*. (A and H) Yeast-like cells; (B, G, and I) pseudohyphal growth; (C) early germ tube formation; (D) late germ tube formation; (E and F) hyphal growth. Bars, 5 μm.

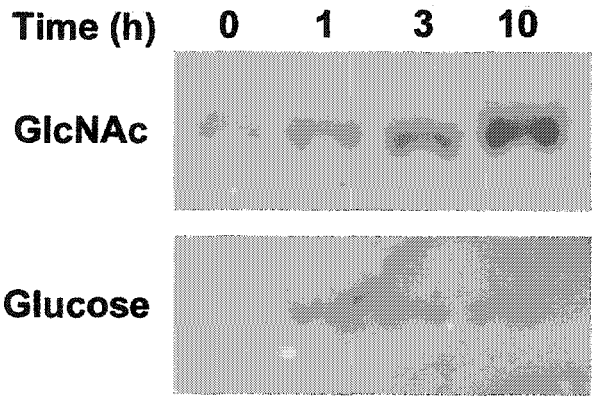

Figure 4-10. *YlRAC1* mRNA levels are increased during the dimorphic transition. Total RNA was isolated from *E122* cells incubated at 28°C in YNBGlcNAc (induction of filamentous growth) or YNBGlc (control culture, yeast-like cells) for the times indicated and subjected to Northern blot analysis. 10 μg of RNA from each time point was separated on a formaldehyde agarose gel and transferred to nitrocellulose. Blots were hybridized with a probe specific for the *YlRAC1* gene (1.0-kbp *Apa*I-*Nde*I fragment [see Fig. 4-6]). Equal loading of RNA was ensured by ethidium bromide staining.

4.8 Putative STREs in the *YlRAC1* gene are not necessary for the induction of hyphal growth

The inability of pRAC1 to induce dimorphic transition in *mhy1Δ* cells (Fig. 4-1, panels D and G); the presence of three copies of the pentanucleotide STRE sequence CCCCT in the promoter region of *YlRAC1* (Fig. 4-2), one of which had been shown to be specifically bound by *in vitro*-synthesized Mhy1p (Chapter 3); and the finding that *rac1Δ* mutant cells can form pseudohyphae while *mhy1Δ* mutants are unable to grow as either the hyphal or pseudohyphal form (Fig. 4-7 and Fig. 4-8) suggested that Mhy1p might act to promote hyphal growth through these regulatory elements via *YlRAC1*.

In order to investigate the role of these putative STRE sequences in the induction of hyphal growth, mutagenesis of these elements in pRAC1 was performed. Three-base substitutions were introduced in the putative STREs found in the promoter region of the *YlRAC1* gene (CCCCT to *ATT*CT in STRE1; CCCCT to *AGCT*T in STRE2; and CCCCT to *GAT*CT in STRE3) (Fig. 4-2) by PCR using the oligonucleotides SE1 and SE2, EH1 and EH2, HB1 and HB2, and BS1 and BS2 (Table 2-1). The four PCR products (369-bp *Spe*I-*Eco*RI, 100-bp *Eco*RI-*Hin*dIII, 197-bp *Hin*dIII-*Bgl*II, and 122-bp *Bgl*II-*Sal*I) were then ligated to the 396-bp *Sal*I-*Sac*II fragment obtained by PCR using the oligonucleotides NT1 and NT2 (Table 2-1), and the resulting fragment (~1.2-kbp *Spe*I-*Sac*II) was used to replace its equivalent in the plasmid pRAC1.

No defect was observed in the ability to induce dimorphic transition upon introduction of the plasmid pRAC1-Mut (which contains mutations in all three STREs) into strain *rac1KO30*, suggesting that these elements are not necessary for the induction

of hyphal growth via *YlRAC1*.

4.9 Genomic DNA analysis of *RAC* genes in *Y. lipolytica*

As most organisms have multiple Rac and Rho homologues, genomic DNA from the *E122* strain was digested with various combinations of restriction endonucleases and analyzed by Southern blotting under low-stringency conditions with a labeled 240-bp *Sac*II-*Nde*I fragment of the *YlRAC1* gene, to look for evidence of other *RAC* genes in *Y. lipolytica*. A complex pattern of bands was observed, suggestive of the presence of several *RAC*-related superfamily members in this yeast species (Fig. 4-11).

4.10 Discussion

This chapter describes the isolation and initial characterization of the *Y. lipolytica* *RAC1* gene, which encodes the first fungal Rac homolog to be identified, and provides evidence that its protein product, *Yl*Rac1p, plays an important role in the regulation of hyphal growth in *Y. lipolytica*.

YlRAC1 is not an essential gene, and its deletion does not abolish the ability of cells to polarize actin at the site of growth. These findings might be explained by the presence of other genes in *Y. lipolytica* that are closely related to *YlRAC1*, as suggested by the complex banding pattern revealed by Southern analysis of *Y. lipolytica* genomic DNA under conditions of low stringency. Nevertheless, alterations in the cell morphology of *rac1Δ* mutants and the inability of these strains to grow as the hyphal form suggest that *YlRAC1* functions in some aspect of the polarization of cell growth.

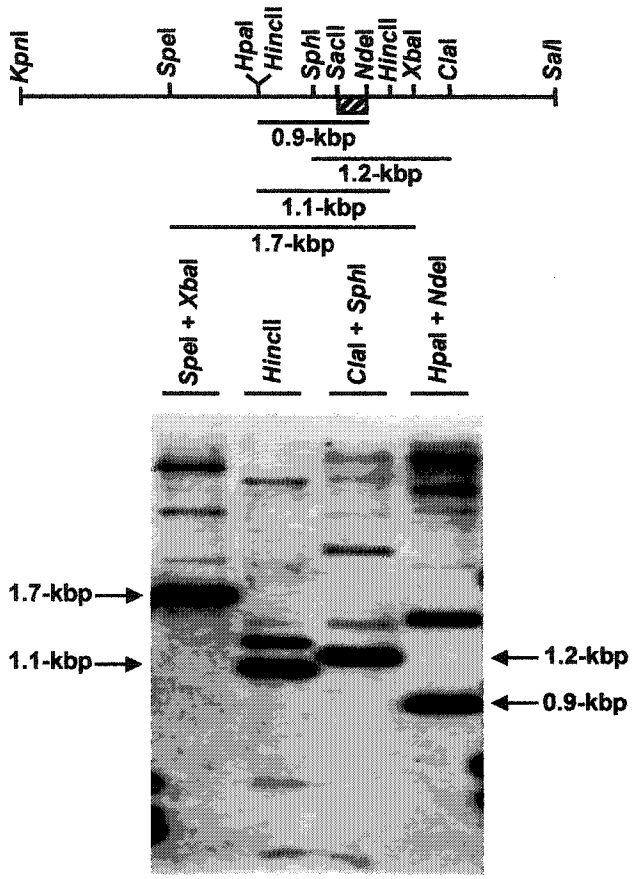

Figure 4-11. Southern blot analysis of *E122* genomic DNA. 10 μg of DNA per lane was digested with the indicated restriction enzymes, separated by electrophoresis, transferred to nitrocllulose, and probed with a 240-bp *Sac*II-*Nde*I-labeled fragment from *YlRAC1* (boxed), as described in Materials and Methods (Section 2.6.4).

Here it is also shown that while deletion of *MHY1* completely abolishes the ability of *Y. lipolytica* to grow as both the hyphal and pseudohyphal forms on solid minimal medium containing either glucose or acetate as the sole cabon source, strains lacking a functional *YlRAC1* gene are still able to form pseudohyphae and invade agar on glucose-based minimal medium, suggesting, as has been suggested for *C. albicans* (Lo *et al.*, 1997), that these two morphologies in *Y. lipolytica* are controlled, at least in part, by two parallel signaling pathways, each with a different and additive input, or that they represent a sequence of events in a single pathway of filamentous growth requiring a quantitatively stronger regulatory input to produce hyphae rather than pseudohyphae. Likewise, the analysis of a Ras homologue in *A. nidulans* has suggested a scenario in which several thresholds of Ras concentration exist, each of which allows development to proceed to a certain point, producing the proper cell type while inhibiting further development (Som and Kolaparthi, 1994). The observations that disruption of *YlRAC1* affects only hyphal growth while disruption of *MHY1* blocks both hyphal and pseudohyphal growth, and that pseudohyphal cells can give rise to hyphae (Fig. 4-7, bottom right panel, inset) support such a scenario and suggest that *MHY1* acts upstream of *YlRAC1* in the filamentous pathway(s).

It is important to point out that regardless of the fact that mutagenesis of all three STREs in the promoter of *YlRAC1* did not affect its ability to induce hyphal growth in *Y. lipolytica*, a role for these elements in the induction of dimorphism cannot be ruled out. The activity of other unidentified regulatory elements in the *YlRAC1* gene or compensation for the loss of transcriptional induction of *YlRAC1* by the activation of other related

GTPases may explain this negative result.

The isolation and initial characterization of the *YlCDC42* gene are also described in this chapter. In *C. albicans*, a transient increase in the *CaCDC42* mRNA levels was observed during the switch to hyphal growth (Mirbod *et al.*, 1997), and the *CaCDC42* gene is essential for proper polarized growth in both yeast and hyphal cells (Ushinsky *et al.*, 2002). Although no variation in the abundance of Cdc42p has been observed during the cell cycle of *S. cerevisiae* (Ziman *et al.*, 1993), *CDC42* has been shown to be a potent regulator of filamentous growth in this yeast, acting downstream of *RAS2* and activating pseudohyphal growth of diploid cells and invasive growth of haploid cells in response to nitrogen starvation via *STE20* (Leberer *et al.*, 1997; Mösch *et al.*, 1996; Peter *et al.*, 1996). The involvement of *YlCDC42* in the induction of filamentous growth in *Y. lipolytica* remains to be elucidated.

CHAPTER 5

ISOLATION AND CHARACTERIZATION OF *YlBEM1*, A GENE REQUIRED FOR CELL POLARIZATION AND DIFFERENTIATION IN *Y. lipolytica*

A version of this chapter has been accepted for publication in the journal *Eukaryotic Cell* as "Isolation and Characterization of *YlBEM1*, a Gene Required for Cell Polarization and Differentiation in the Dimorphic Yeast *Yarrowia lipolytica*" (Cleofe A.R. Hurtado and Richard A. Rachubinski).

5.1 Overview

This chapter describes the isolation and characterization of *YlBEM1*, a gene encoding a protein of 639 amino acids that is essential for the yeast-to-hypha transition in the yeast *Y. lipolytica* and whose transcription is significantly increased during this event. Deletion of *YlBEM1* is viable but results in substantial alterations in cell morphology, disorganization of the actin cytoskeleton, delocalization of cortical actin and chitin deposition, multinucleation, and loss of mating ability, thus pointing to a major role for *YlBEM1* in the regulation of cell polarity and morphogenesis in this fungus. This role is further supported by the localization of *Yl*Bem1p, which, like cortical actin, appears to be particularly abundant at sites of growth of yeast, hyphal and pseudohyphal cells. In addition, the potential involvement of *Yl*Bem1p in septum formation and/or cytokinesis is suggested by the concentration of a GFP-tagged version of this protein at the mother-bud neck during the last stages of cell division. Moreover, the involvement of proteins other than *Yl*Bem1p in cell polarity in *Y. lipolytica* is suggested by the partial induction of hyphal growth when the genes *MHY1*, *YlRAC1* and *YlSEC31* are present in multiple copies in *bem1* null mutant cells.

5.2 Isolation and characterization of the *YlBEM1* gene

The *Y. lipolytica* mutant strain *CHY33169* was initially isolated by its inability to form wild-type rough-surfaced colonies on YEPD-agar plates after 3 days of incubation at 28°C (Fig. 5-1B), an attribute that was stably maintained through multiple generations.

The *YlBEM1* gene was isolated from a *Y. lipolytica* genomic DNA library

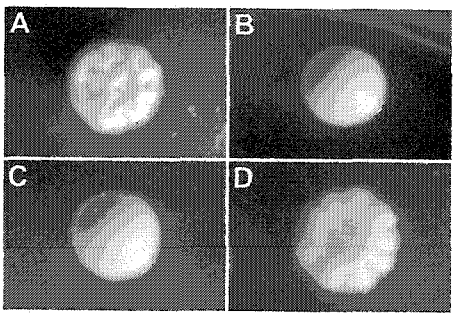

Figure 5-1. Colony morphology of *Y. lipolytica* strains. (A) Filamentous phenotype of a colony of wild-type *E122* cells. (B) Smooth phenotype of a colony of *CHY33169* cells. (C) Smooth phenotype of a colony of *bem1KO157* cells obtained by integrative disruption of the *YlBEM1* gene. (D) Enhanced filamentous phenotype of a colony of *bem1KO157* cells transformed with the plasmid pBEM1. Colonies were photographed at ×100 magnification after 3 days of incubation at 28°C on YNA-agar plates.

contained in the replicative *E. coli* shuttle vector pINA445 (Nuttley *et al.*, 1993) by its ability to induce the formation of rough-surfaced colonies when introduced into *CHY33169* cells. Of approximately 7,000 transformants screened, 3 showed a moderately enhanced filamentous phenotype (Fig. 5-1D). Restriction enzyme analysis revealed that all complementing plasmids shared a 4.7-kbp *Bam*HI-*Bam*HI fragment capable of restoring filamentous growth to *CHY33169*. Sequencing of this fragment revealed an ORF of 2577 bp interrupted by one intron, which is found between codons 3 and 4 (nucleotides +10 to +666 from the A residue of the potential initiating codon). The putative 5'-splice donor (GTGAGTPu) and 3'-splice acceptor (TACTAACNCAG) sequences are identical to the motifs found in other *Y. lipolytica* genes (Lopez *et al.*, 1994; Strick *et al.*, 1992; Teem *et al.*, 1984) (Fig. 5-2). Analysis of cDNA showed that transcription of the *YlBEM1* gene preferentially starts at position −3 from the A nucleotide of the potential initiating codon and that polyadenylation occurs following the guanosine at position +2829. A putative TATA box, TTATATAAA, is found between nucleotides −259 and −267 from the A nucleotide of the first ATG codon (Fig. 5-2).

The deduced protein product of *YlBEM1*, *Yl*Bem1p, is 639 amino acids in length and has a predicted molecular mass of 69,970 Da (Fig. 5-2). Analysis of the predicted amino acid sequence of *Yl*Bem1p suggests that its closest homologs are *S. pombe* Scd2p (*Sp*Scd2p) and *S. cerevisiae* Bem1p (*Sc*Bem1p) (Fig. 5-3). Notably, the regions of highest homology amongst the three proteins are segments corresponding to the *src* homology region 3 (SH3; residues 34−95 and 178−239 of *Yl*Bem1p) and the PhoX and Bem1 (PB1; residues 340−639 of *Yl*Bem1p) domains of those proteins (Fig. 5-3). In addition, three

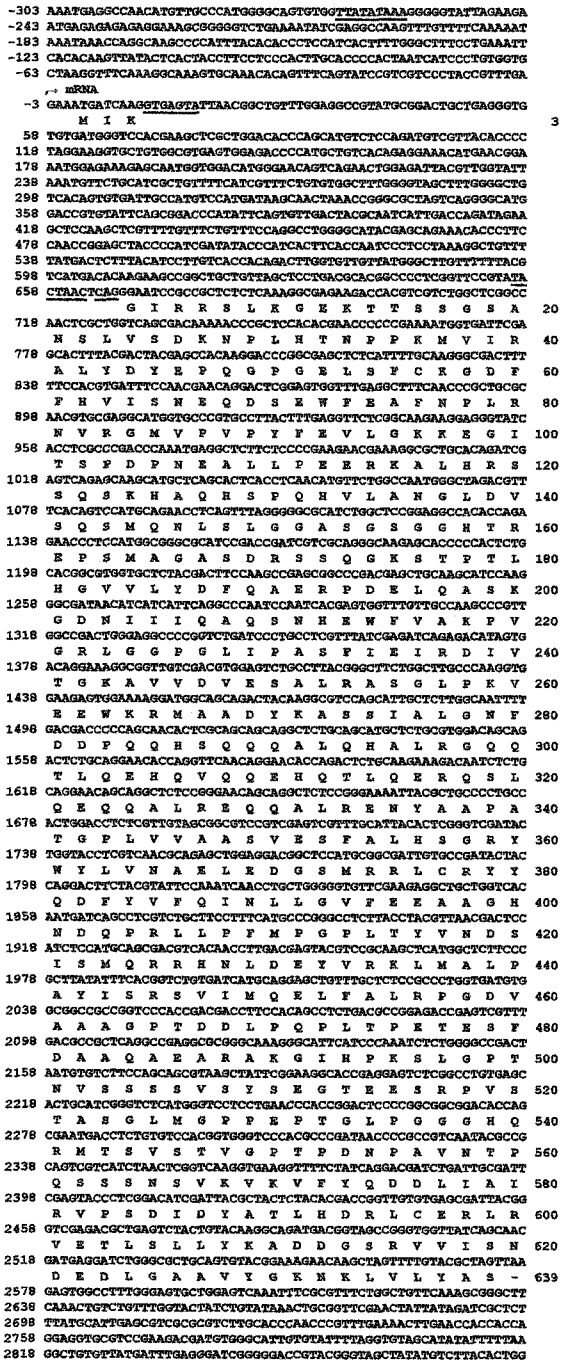

Figure 5-2. Nucleotide sequence of the *YlBEM1* gene and deduced amino acid sequence of *Yl*Bem1p. The transcriptional start site of the *YlBEM1* gene is indicated. The putative TATA box and consensus sequences for intron splicing are underlined.

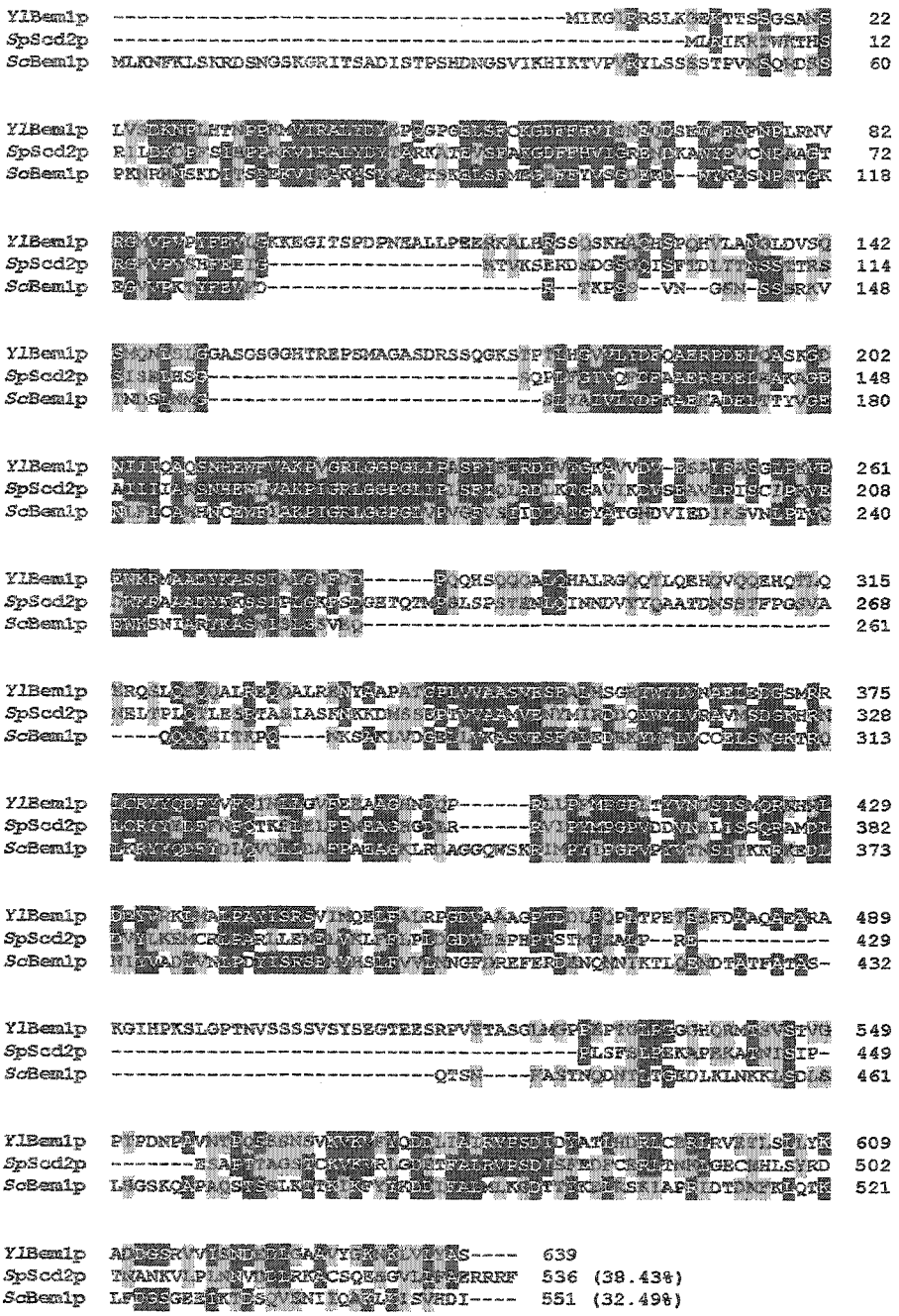

Figure 5-3. Amino acid sequence alignment of Bem1p of *Y. lipolytica* (*Yl*Bem1p) and its homologs from *S. pombe* (*Sp*Scd2p) and *S. cerevisiae* (*Sc*Bem1p). Amino acid sequences were aligned with the use of the ClustalW program (EMBL, Heidelberg, Germany). Identical residues (black) and similar residues (stippled) in at least two of the proteins are shaded. Similarity rules: G = A = S; V = I = L = M; I = L = M = F = Y = W; K = R = H; D = E = Q = N; and S = T = Q = N. GenBank accession numbers: AAA50557 (*Sp*Scd2p) and CAA45320 (*Sc*Bem1p).

putative PEST regions, which are commonly found in rapidly degraded proteins (Chevaillier, 1993; Rechsteiner and Rogers, 1996), are predicted at residues 98–113, 457–487, and 496–516 of *Yl*Bem1p.

5.3 Transcription of the *YlBEM1* gene is increased during the yeast-to-hypha transition

The dimorphic transition was induced in exponentially growing *E122* cells by a 15-min carbon source starvation period at 4°C, followed by transfer to YNBGlcNAc medium, as previously described (Guevara-Olvera *et al.*, 1993). Under these conditions, more than 80% of the cells produced germ tubes after 10 h of incubation at 28°C, while cells transferred to fresh glucose-containing (YNBGlc) medium grew almost exclusively as the yeast form. Northern blot experiments carried out with total RNA extracted from cells harvested following 3 and 10 h of incubation showed that *YlBEM1* mRNA was at levels undetectable by this approach. To circumvent this limitation, semiquantitative RT-PCR experiments were performed using *YlHIS1*, a gene whose expression is maintained constant during the yeast-to-hypha transition (Fig. 5-4), as an endogenous internal standard. RT-PCR analysis showed that the transcription of the *YlBEM1* gene is significantly augmented during dimorphic transition (4- to 5-fold), while only slightly increased during growth as the yeast form (Fig. 5-5).

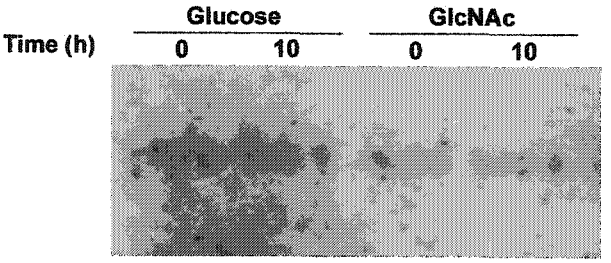

Figure 5-4. Transcription of the *YlHIS1* gene during the dimorphic transition. Total RNA was isolated from *E122* cells incubated at 28°C in YNBGlcNAc (induction of hyphal growth) or YNBGlc (control culture, growth as the yeast form) for the times indicated and subjected to Northern blot analysis. 10 μg of RNA from each time point was separated on a formaldehyde agarose gel and transferred to nitrocellulose. Blots were hybridized with a probe specific for the *YlHIS1* gene. Equal loading of RNA was ensured by ethidium bromide staining.

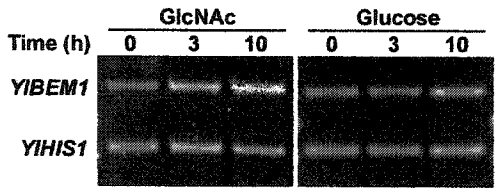

Figure 5-5. Transcription of the *YlBEM1* gene is increased during the dimorphic transition. Total RNA was isolated from *E122* cells incubated at 28°C in YNBGlcNAc (induction of hyphal growth) or YNBGlc (control culture, growth as the yeast form) for the times indicated and subjected to semiquantitative RT-PCR analysis. The 600-bp and 400-bp RT-PCR products were resolved by electrophoresis on 2% agarose and visualized by staining with ethidium bromide. *YlBEM1* mRNA expression was normalized to *YlHIS1* mRNA.

5.4 *Yl*Bem1p is concentrated at sites of growth and at the mother-bud neck in cells of *Y. lipolytica*

To determine the subcellular localization of *Yl*Bem1p, a plasmid expressing *Yl*Bem1p fused at its carboxyl terminus to the green fluorescent protein (GFP) was introduced into the *Y. lipolytica* strain *bem1KO157*. After incubation of these cells for 24 h in YNBGlc liquid medium at 28°C, the *Yl*Bem1p-GFP chimera was found to be localized in as yet unidentified vesicular structures dispersed throughout the cytosol, and particularly concentrated at sites of growth of yeast, hyphal and pseudohyphal cells (Fig. 5-6A, C and D). Interestingly, the chimeric protein was also found to be concentrated at the mother-bud neck in yeast cells in the late stages of cell division (Fig. 5-6B).

5.5 Disruption of the *YlBEM1* gene is viable but severely affects cell morphology of *Y. lipolytica*

A 2.7-kbp fragment of pBEM1, corresponding to nucleotides -3 to +2700 of *YlBEM1*, was replaced by a 1.6-kbp fragment containing the *Y. lipolytica URA3* gene (Fig. 5-7A). This construct was digested with *Bam*HI and *Cla*I to liberate a 3.2-kbp fragment containing the entire *YlURA3* gene flanked by 0.6-kbp and 1.0-kbp of the 5' and 3' regions of *YlBEM1*, respectively, and this linear fragment was used to transform the wild-type *Y. lipolytica* strain *E122* (Table 2-5 and Fig. 5-1A) to uracil prototrophy. Of 199 Ura^+ transformants obtained, five showed a fully smooth phenotype after 3 days on YEPD-agar. One of these five, *bem1KO157* (Table 2-5 and Fig. 5-1C), was selected for further studies

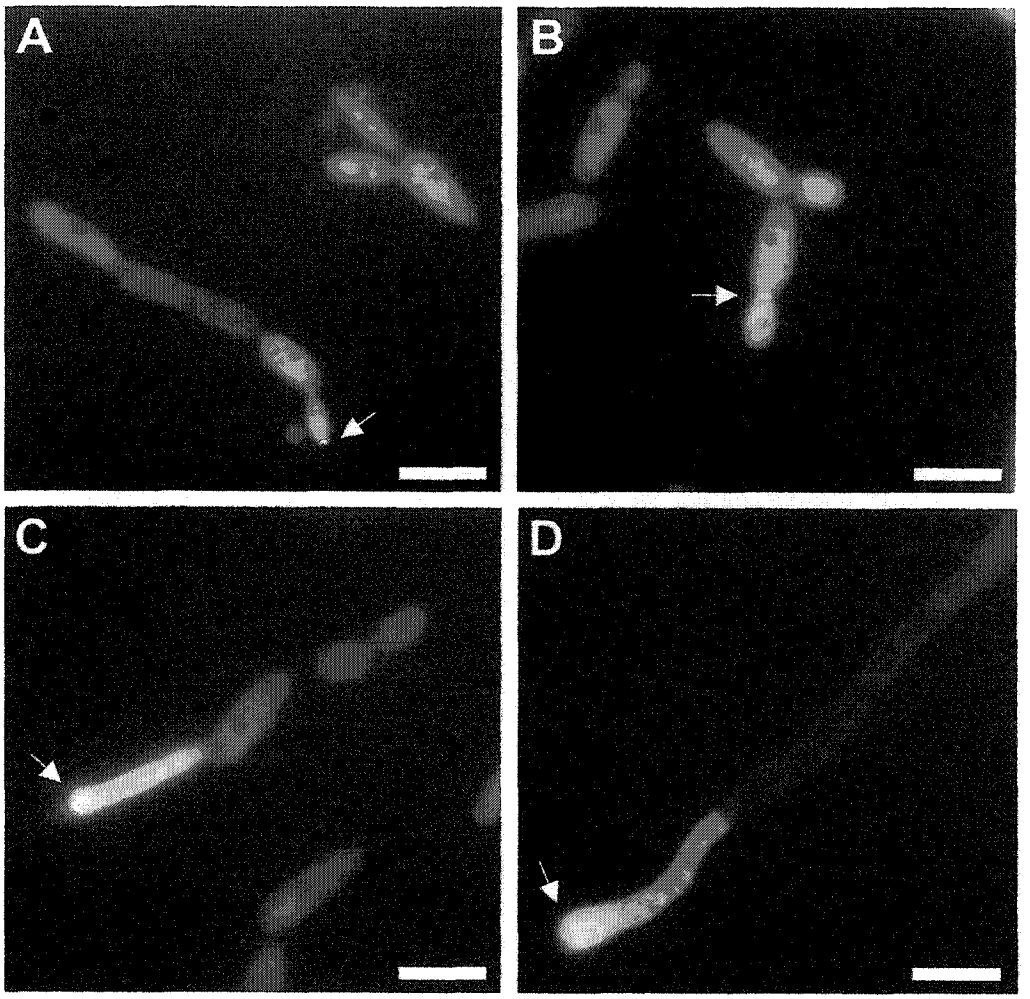

Figure 5-6. Localization of GFP-tagged *Yl*Bem1p in yeast (A and B), pseudohyphal (C) and hyphal (D) *bem1KO157* cells carrying plasmid pBEM1-GFP. Arrows indicate sites at which the *Yl*Bem1p-GFP chimera concentrates. Bars, 5 μm.

following Southern blot analysis confirming the correct replacement of the *YlBEM1* gene by *YlURA3* (Fig. 5-7B).

Because the products of the *S. pombe scd2* and *S. cerevisiae BEM1* genes are required for cell polarization and morphogenesis (Chang *et al.*, 1994; Fukui and Yamamoto, 1988), deletion of *YlBEM1* was expected to result in morphological defects in *Y. lipolytica*. *bem1Δ* cells grown in liquid media were indeed unable to form hyphae or pseudohyphae, even after prolonged periods of incubation (Fig. 5-8). Remarkably, *bem1Δ* cells were found to be spherical and considerably larger than their wild-type counterparts (Fig. 5-8). Furthermore, 30-40% of the cells were binucleate (Fig. 5-9). However, when cells were incubated on solid media, these defects were less severe, and a few pseudohyphal cells could be observed (Fig. 5-15B).

5.6 Disruption of the *YlBEM1* gene affects the localization of actin and chitin

Since the organization of the actin cytoskeleton is involved directly in the definition of cell morphology, and as Bem1p is believed to be an actin cytoskeleton-associated protein that provides a cell surface scaffold for the localized concentration of signaling kinases in *S. cerevisiae*, the effects of disruption of the *YlBEM1* gene on actin localization in *Y. lipolytica* were investigated. As previously described (Chapter 4), actin-rich zones were observed at the apices of hyphal, pseudohyphal and yeast forms of wild-type cells, combined with a background of diffuse staining and punctate actin patches (Fig. 5-10, panels A to F). In the *bem1Δ* mutant strain, however, actin-rich zones were randomly distributed, and most of the actin was dispersed throughout the periphery of cells

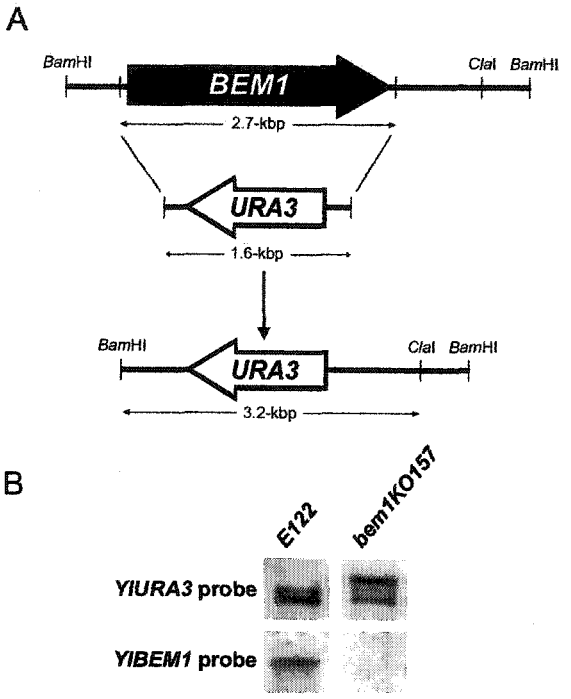

Figure 5-7. Integrative disruption of the *YlBEM1* gene. (A) Diagram illustrating the targeted gene replacement strategy for the *YlBEM1* gene. The ORFs and directionality of the *YlBEM1* and *YlURA3* genes are indicated by the arrows. (B) Southern blot analysis of *Bam*HI-digested genomic DNA from *Y. lipolytica* wild-type strain *E122* and mutant strain *bem1KO157*, confirming the replacement of the *YlBEM1* gene segment by the *YlURA3*-containing linear molecule.

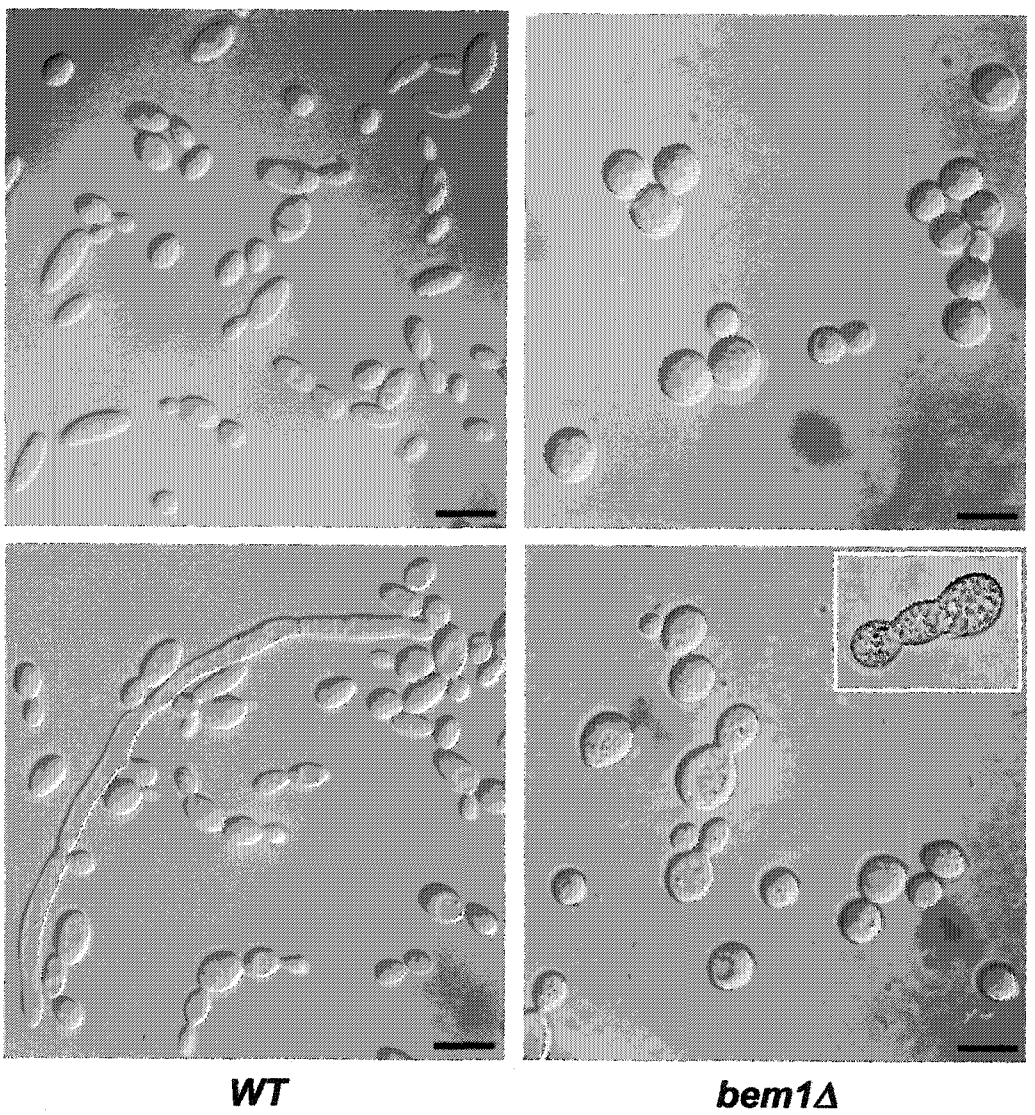

Figure 5-8. Disruption of the *YlBEM1* gene affects cell morphology and impairs hyphal and pseudohyphal growth of *Y. lipolytica* in YEPD liquid medium. Top panels, exponential growth phase (optical density at 600 nm [OD_{600}] = 1). Bottom panels, stationary phase (OD_{600} = 10). *WT*, wild-type strain *E122*. *bem1Δ*, strain *bem1KO157*. Bars, 5 μm.

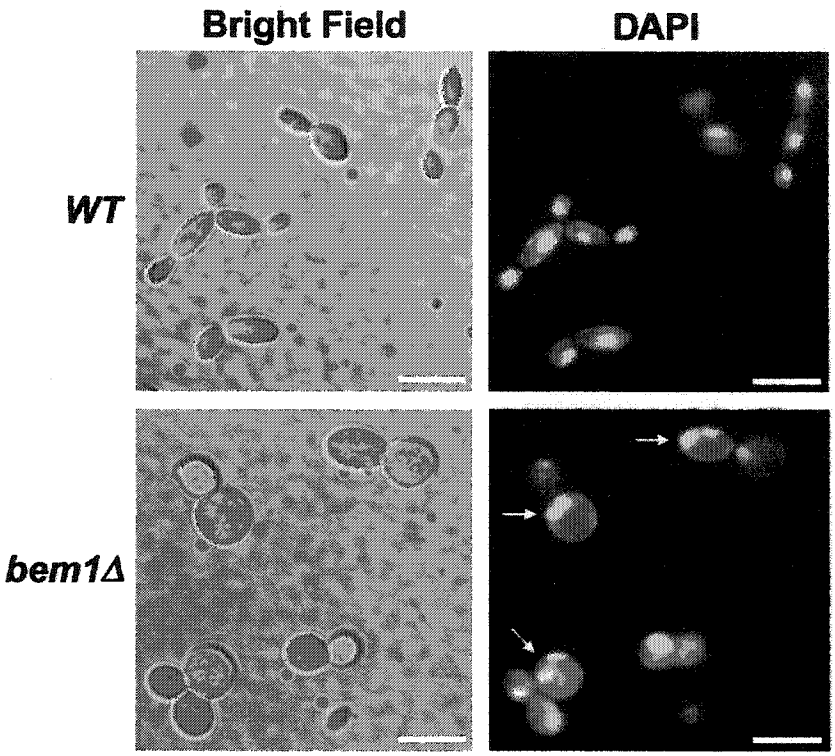

Figure 5-9. ***Y. lipolytica bem1*** **null mutants exhibit binucleation.** Bright field images of cells and DAPI staining of nuclei of cells from the wild-type strain *E122* (*WT*, upper panels) and mutant strain *bem1KO157* (*bem1Δ*, bottom panels), grown in YEPD liquid medium for 12 h at 28°C. Arrows indicate binucleate cells. Bars, 5 μm.

(Fig. 5-10, panels G to I). Furthermore, in contrast to what is observed in wild-type cells (Fig. 5-10E), *bem1Δ* cells appear to be unable to form organized actin cytoskeletal structures when cultivated in liquid media (Fig. 5-10, panels G to I).

In a similar way, deposition of cell wall material was affected in the *bem1Δ* strain. While chitin was concentrated primarily at the bud scars and septa of wild-type cells, it was found over the entire surface of *bem1Δ* cells. In addition, bud scars of *bem1Δ* cells were considerably larger than those of wild-type cells, and the random selection of budding sites appears to be prevalent in *bem1Δ* cells, whereas budding in wild-type cells is preferentially bipolar, with the rare occurrence of lateral budding events (Fig. 5-11).

5.7 *bem1* null mutants of *Y. lipolytica* are unable to mate

Because mating is a phenomenon that involves an extensive reorganization of the actin cytoskeleton and is closely connected to dimorphism in fungi (Madhani and Fink, 1998), we investigated whether disruption of the *YlBEM1* gene had an effect on the mating ability of *Y. lipolytica*. No diploid strains were obtained upon crossing strain *bem1KO157* with the isogenic wild-type strain *22301-3* (Table 2-5), thus concluding that *YlBEM1* is essential for mating in *Y. lipolytica*.

5.8 Isolation and characterization of the *YlSEC31* gene

The *YlSEC31* gene was isolated from a *Y. lipolytica* genomic DNA library contained in the replicative *E. coli* shuttle vector pINA445 (Nuttley *et al.*, 1993) by its

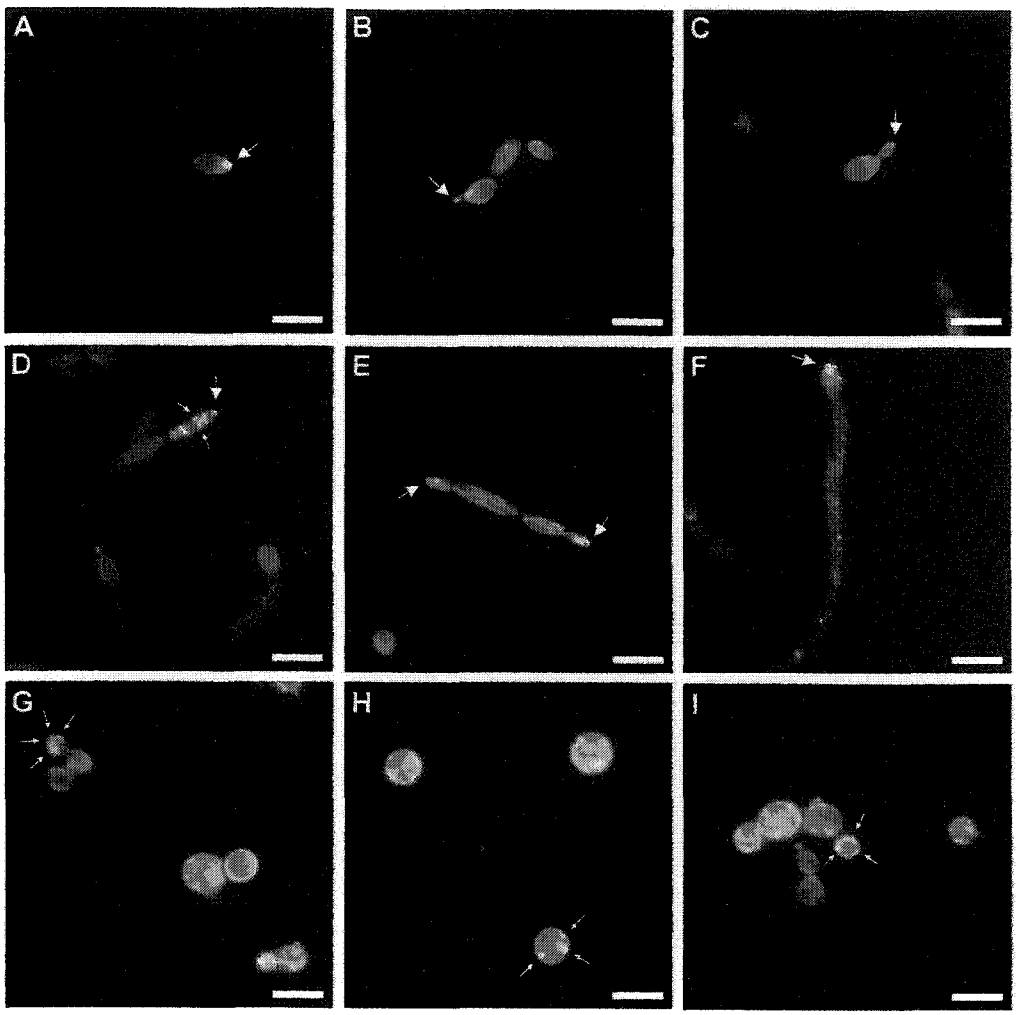

Figure 5-10. Distribution and organization of actin at different developmental stages of wild-type and *bem1Δ* cells. Actin was stained with Oregon Green 488 phalloidin and detected by fluorescence microscopy. (A to F) Wild-type strain *E122*. (G to I) *bem1Δ* strain *bem1KO157*. (A to C) Wild-type yeast cells; (D and E) wild-type pseudohyphal cells; (F) wild-type hyphal cells; (G to I) yeast-like *bem1Δ* cells. Arrows indicate actin-rich zones in *E122* and *bem1KO157* cells. Bars, 5 μm.

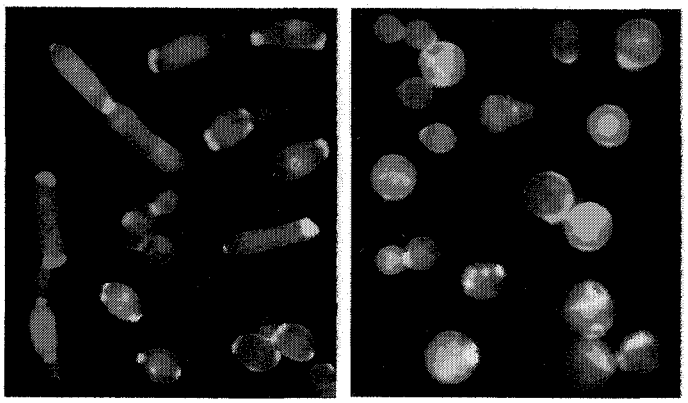

Figure 5-11. Disruption of the *YlBEM1* gene affects the budding pattern and chitin deposition in *Y. lipolytica*. Chitin was stained with Fluorescent Brightener 28 and detected by fluorescence microscopy. *WT*, wild-type strain *E122*. *bem1Δ*, strain *bem1KO157*.

ability to enhance filamentous growth upon introduction into *Y. lipolytica E122* cells (Table 2-5, Fig. 5-12A). Of approximately 3,000 transformants screened, one showed an enhanced filamentous phenotype (Fig. 5-12B). Restriction enzyme analysis of the plasmid recovered from this transformant demonstrated that it contained a 6.2-kbp *Bam*HI-*Sph*I fragment capable of enhancing hyphal growth upon introduction into the wild-type *E122* strain. Sequencing of this fragment revealed that the largest ORF, the *YlSEC31* gene, contained 3615 bp coding for a 1204-amino acid protein, *Yl*Sec31p, with a predicted molecular weight of 126,997 Da (Fig. 5-13).

Analysis of the predicted amino acid sequence of *Yl*Sec31p suggests that its closest homologs are Sec31p from *S. cerevisiae* (*Sc*Sec31p) and *S. pombe* (*Sp*Sec31p) (31.3% and 27.6% identity, respectively) (Fig. 5-14), two WD-proteins that are essential components of the COPII coat and are required for transport vesicle budding from the endoplasmic reticulum (Salama *et al.*, 1997; Tang *et al.*, 2000).

5.9 Overexpression of *MHY1, YlRAC1* or *YlSEC31* partially restores hyphal growth to *bem1* null mutants of *Y. lipolytica*

To gain some initial insight into the interactions among *YlBEM1*, *YlRAC1*, *YlSEC31* and *MHY1*, autonomously replicating plasmids carrying these genes (pBEM1, pRAC1, pSEC31, and pMHY1, respectively) were introduced into the null mutants *bem1KO157*, *rac1KO30* and *mhy1KO9* (Table 2-5). These plasmids were based on the shuttle vector pINA445, which is believed to be present in two to five copies per cell (Fournier *et al.*, 1993).

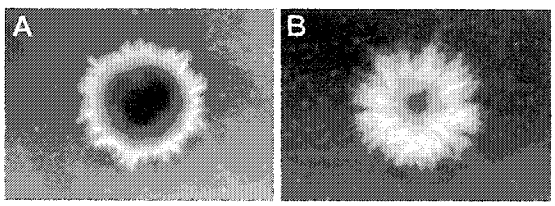

Figure 5-12. Overexpression of *YlSEC31* enhances filamentous growth in the wild-type strain *E122*. (A) Filamentous phenotype of a colony of wild-type *E122* cells. (B) Enhanced filamentous phenotype of a colony of *E122* cells transformed with the plasmid pSEC31. Colonies were photographed at ×100 magnification after 3 days of incubation at 28°C on YNA-agar plates.

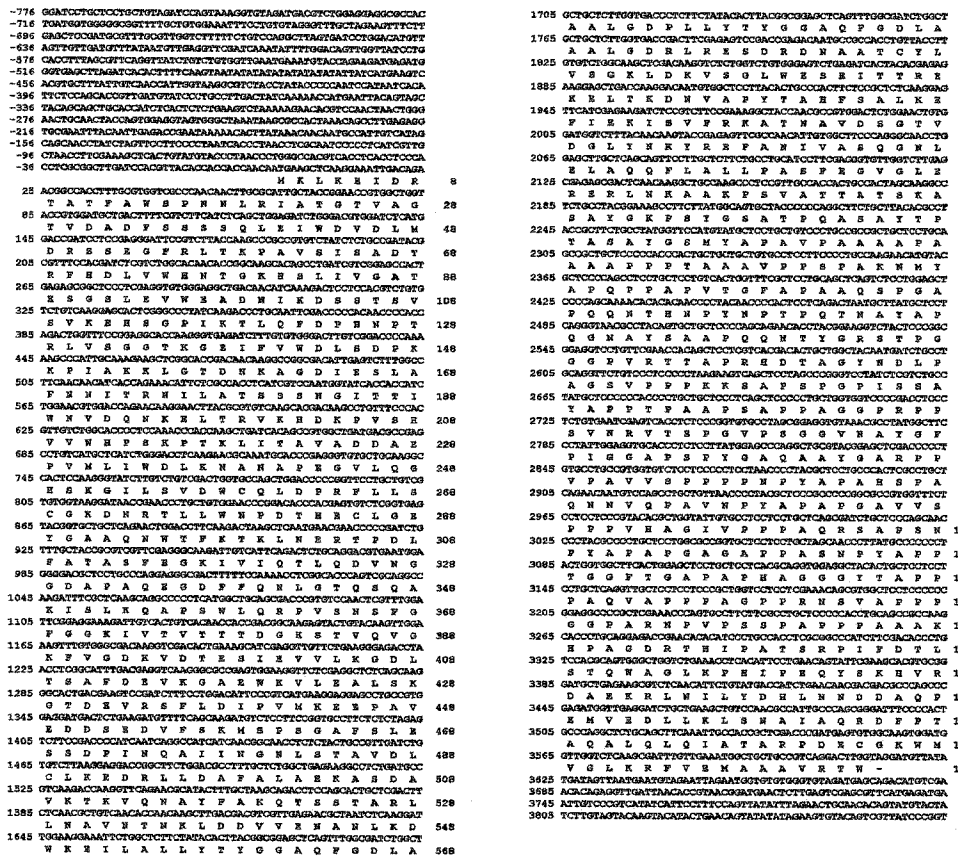

Figure 5-13. Nucleotide sequence of the *YlSEC31* gene and deduced amino acid sequence of *Yl*Sec31p. Putative TATA boxes are underlined. Putative transcription termination signals are doubly underlined.

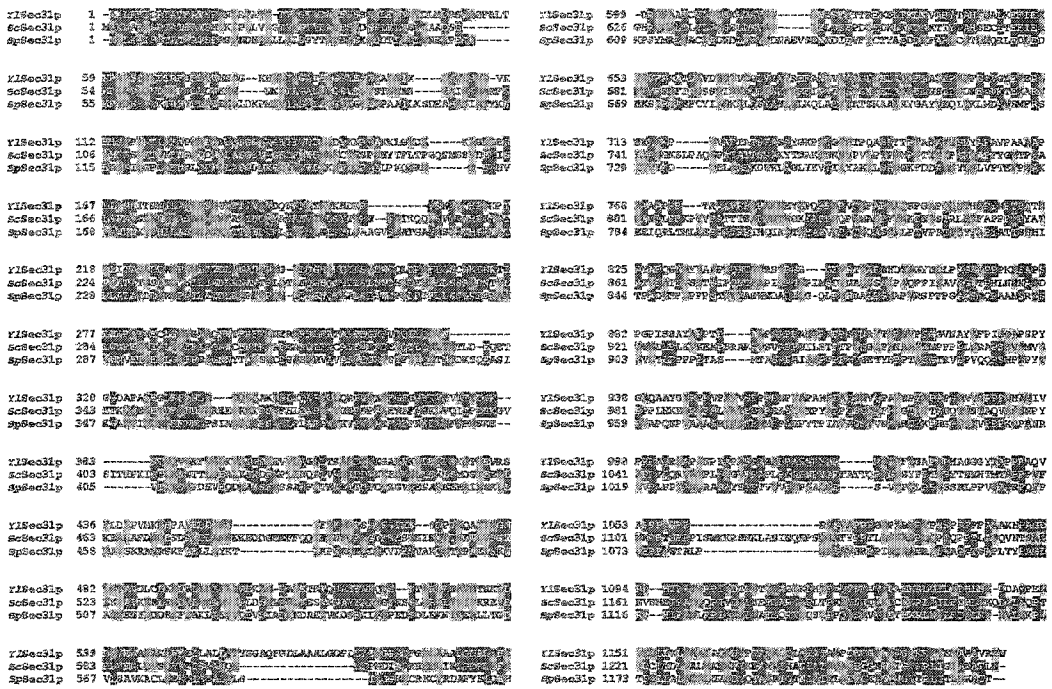

Figure 5-14. Amino acid sequence alignment of Sec31p of *Y. lipolytica* (*Yl*Sec31p) and its homologs from *S. cerevisiae* (*Sc*Sec31p) and *S. pombe* (*Sp*Sec31p). Amino acid sequences were aligned with the use of the ClustalW program (EMBL, Heidelberg, Germany). Identical residues (black) and similar residues (stippled) in at least two of the proteins are shaded. Similarity rules: G = A = S; V = I = L = M; I = L = M = F = Y = W; K = R = H; D = E = Q = N; and S = T = Q = N. GenBank accession numbers: S58782 (*Sc*Sec31p) and CAA17835 (*Sp*Sec31p).

After 3 days of incubation on YNA-agar plates at 28°C, overexpression of *MHY1*, *YlRAC1* and *YlSEC31* appeared to partially suppress the morphological defects of the *YlBEM1* gene disruption (Fig. 5-15, panels A to E). Notably, *MHY1* was the strongest inducer of filamentous growth in the *bem1Δ* background (Fig. 5-15C), and *YlRAC1* was a stronger inducer of filamentation than *YlSEC31* (Fig. 5-15, compare panel D to E). In addition, overexpression of *MHY1* or *YlRAC1* in *bem1Δ* cells resulted in hyphae with a higher degree of branching than those of the wild-type strain (Fig. 5-15, compare panels C and D to panel A)

Interestingly, *YlBEM1* induced hyphal growth when overexpressed in *rac1Δ* cells (Fig. 5-15, panels F and G), but to a much lesser degree than when *YlRAC1* was overexpressed in the *bem1Δ* background (Fig. 5-15, panels B and D; compare panels D and G). No apparent effect was observed when *YlBEM1* was overexpressed in *mhy1Δ* cells (Fig. 5-15, panels H and I).

5.10 Discussion

This chapter describes the isolation of the *Y. lipolytica BEM1* gene and the initial characterization of its protein product, *Yl*Bem1p. *Yl*Bem1p shares a number of structural features with Bem1p from *S. cerevisiae* and Scd2p from *S. pombe*, is involved in the regulation of cell polarization, and is necessary for the yeast-to-hypha transition in the dimorphic yeast *Y. lipolytica*. Like its two closest homologs, *Yl*Bem1p contains two potential SH3 domains at its amino terminus and a potential PB1 domain at its carboxyl

Figure 5-15. Colony (upper panels) and cell (bottom panels) morphology of *Y. lipolytica* strains transformed with autonomously replicating plasmids carrying the *MHY1*, *YlRAC1*, *YlSEC31* and *YlBEM1* genes. (A) Wild-type strain *E122*; (B) mutant strain *bem1KO157*; (C) strain *bem1KO157* transformed with plasmid pMHY1; (D) strain *bem1KO157* transformed with plasmid pRAC1; (E) strain *bem1KO157* transformed with plasmid pSEC31; (F) mutant strain *rac1KO30*; (G) strain *rac1KO30* transformed with plasmid pBEM1; (H) mutant strain *mhy1KO9*; (I) strain *mhy1KO9* transformed with plasmid pBEM1. Colonies and cells were photographed after 3 days of incubation at 28°C on YNA-agar plates. Colony magnification, ×100. Bars, 5 μm.

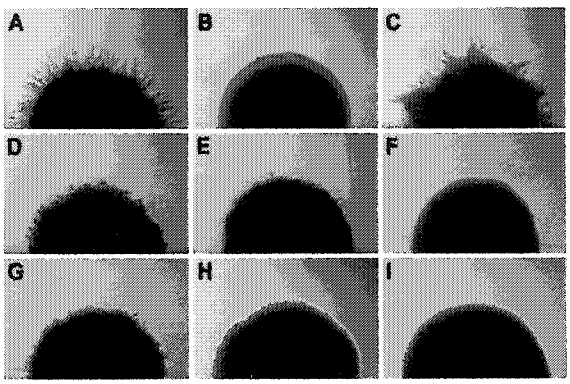

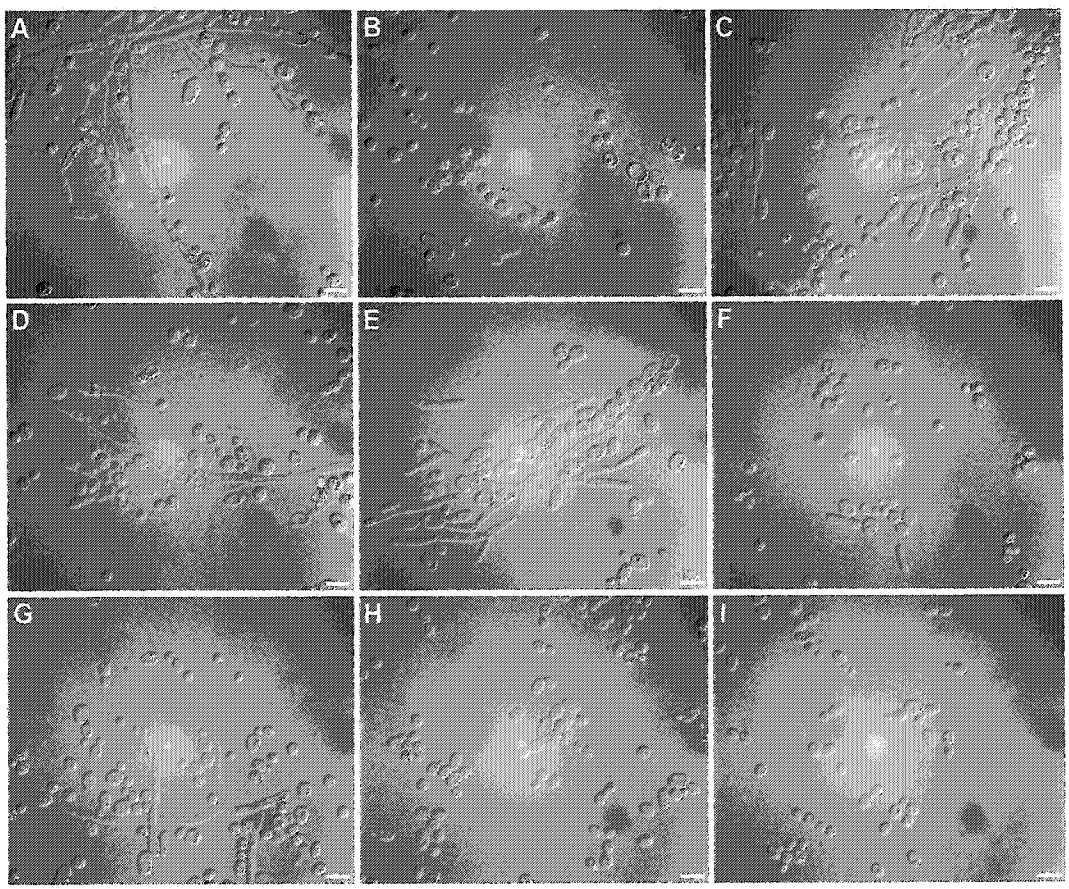

terminus. These domains are involved in the assembly of protein complexes via binding to proline-rich peptides (Morton and Campbell, 1994) and tyrosine kinase-mediated signal transduction (Ito *et al.*, 2001; Lock *et al.*, 1998), respectively.

The *Y. lipolytica BEM1* gene is not essential and its deletion results in a phenotype similar to that observed in *S. cerevisiae bem1* and *S. pombe scd2* null mutants, *i.e.* disorganized actin cytoskeleton, delocalized cortical actin and chitin deposition, multinucleation, round cell morphology, and inability to mate. In addition, *Y. lipolytica bem1* null mutants show obvious defects in bud site selection. These characteristics clearly point to a role for *Yl*Bem1p in cell cycle control and the establishment of cell polarity in *Y. lipolytica*. The latter role is further supported by the fact that, like actin, *Yl*Bem1p is concentrated at the growing tips of yeast, hyphal and pseudohyphal cells. However, it is remarkable that while *Yl*Bem1p levels are increased at the bud tip during early bud growth, *Yl*Bem1p appears to be concentrated at the mother-bud neck during the last stages of budding. Thus, although no role in cytokinesis or septum formation has been proposed for the homologs of *Yl*Bem1p, this hypothesis is compatible with the concept that localized deposition of cell wall material is required at the mother-bud neck during these events.

Interestingly, the expression levels of *YlBEM1* are significantly increased during the yeast-to-hypha transition and *Yl*Bem1p appears to be abundant during the entire cell cycle in actively growing hyphal and pseudohyphal cells. It is also noteworthy that although *Y. lipolytica bem1* null mutant cells are unable to form hyphae in both liquid and solid media, their ability to form pseudohyphae is partially restored upon cultivation on agar plates. The causes of this behavior are unknown, but it has been demonstrated that

filamentous growth in fungi is intimately linked to thigmotropism (directional growth response to physical contact) (Perera *et al.*, 1997; Sherwood *et al.*, 1992), and it is generally proposed that pseudohyphae represent an intermediate state of cell polarization between yeast and hyphal growth (Brown and Gow, 1999). Thus, one may hypothesize that other polarity proteins exist in *Y. lipolytica* that act in conjunction with *Yl*Bem1p to promote hyphal growth. In the absence of *Yl*Bem1p, these other factors would still be able to support pseudohyphal growth in response to thigmotropic stimuli, but this response would be insufficient to increase polarization to a level at which hyphal formation is possible.

In this chapter it is also shown that overexpression of *MHY1* partially suppresses the morphological defects of *Y. lipolytica bem1* null mutants, whereas *YlBEM1* has no apparent effect when overexpressed in cells lacking functional *MHY1*. More remarkably, overexpression of *YlRAC1* in *bem1Δ* cells was able to induce greater hyphal growth than overexpression of *YlBEM1* in cells lacking functional *YlRAC1*. These observations, coupled with the observations that overexpression of *MHY1* does not suppress the morphological defects of *rac1Δ* cells (Chapter 4) and *bem1Δ* and *rac1Δ* cells are still able to form pseudohyphae on solid medium, while *MHY1* is essential for both hyphal and pseudohyphal growth, suggest that *MHY1* acts upstream of *YlRAC1* and *YlBEM1*, and *YlRAC1* is a stronger regulator of hyphal growth than *YlBEM1*. Moreover, our results give further support to the proposition that these two morphologies in *Y. lipolytica* are controlled by at least two parallel signaling pathways, each with a different and additive input, and that filamentous growth comprises a sequence of events that requires a

quantitatively stronger regulatory input to produce hyphae rather than pseudohyphae. Thus, increased production of polarity factors other than *Yl*Bem1p would support hyphal growth when either *MHY1* or *YlRAC1* is overexpressed in *bem1Δ* cells, but the lack of functional *Yl*Bem1p would result in increased branching. Conversely, an increased production of *Yl*Bem1p would result in partial induction of hyphal growth in *rac1Δ* cells due to a partial increase in cell polarity, whereas in the absence of functional Mhy1p this increase would be insufficient to induce any filamentation.

In closing, the observation that *YlSEC31* partially restores hyphal growth when overexpressed in *bem1Δ* cells further supports the hypothesis that polarity proteins other than *Yl*Bem1p exist in *Y. lipolytica* and suggests that the secretory apparatus is a limiting factor in the transport of these proteins during filamentous growth.

CHAPTER 6

ISOLATION AND CHARACTERIZATION OF *YlBMH1* AND *YlBMH2*, TWO GENES ENCODING 14-3-3 PROTEINS OF *Y. lipolytica*

A version of this chapter has been submitted to the journal *Microbiology* as "*YlBMH1* encodes a 14-3-3 protein that promotes filamentous growth in the dimorphic yeast *Yarrowia lipolytica*" (Cleofe A.R. Hurtado and Richard A. Rachubinski).

6.1 Overview

In order to identify genes that are involved in the regulation of the yeast-to-hypha transition, morphological mutants that were unable to form hyphal cells were isolated after chemical mutagenesis of the dimorphic yeast *Y. lipolytica.* Screening of a *Y. lipolytica* genomic DNA library for genes able to complement this defect led to the isolation of *YlBMH1*, a gene encoding a 14-3-3 protein and whose transcription levels are increased during the yeast-to-hypha transition. Remarkably, overexpression of *YlBMH1* was able to enhance pseudohyphae formation in a strain lacking functional *YlRAC1* but caused no visible effects in *mhy1Δ* and *bem1Δ* cells, thus suggesting that *YlBMH1* is involved in the regulation of both hyphal and pseudohyphal growth in this organism. This chapter also describes the identification of *YlBMH2*, a gene encoding a second 14-3-3 protein, *Yl*Bmh2p, that contains a 19-amino acid insertion absent in all other members of this family. Differently from *YlBMH1*, the transcription levels of *YlBMH2* do not show any apparent variation during the induction of hyphal growth, and its overexpression has no effect on cells lacking functional *MHY1*, *YlRAC1*, or *YlBEM1*. Taken together, these observations suggest that, in spite of their high conservation, *Yl*Bmh1p and *Yl*Bmh2p have different cellular functions.

6.2 Isolation of the *Y. lipolytica CHY3350* mutant strain

The *Y. lipolytica* mutant strain *CHY3350* (Fig. 6-1B) was isolated after chemical mutagenesis of *Y. lipolytica E122* cells (Fig. 6-1A) with 1-methyl-3-nitro-1-nitrosoguanidine by its inability to form wild-type rough-surfaced colonies on YEPD-agar

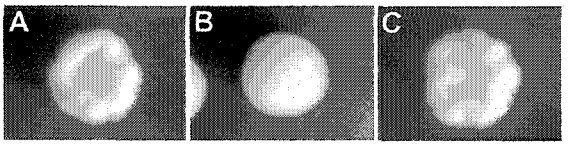

Figure 6-1. Colony morphology of *Y. lipolytica* strains. (A) Rough phenotype of a colony of wild-type *E122* cells. (B) Smooth phenotype of a colony of *CHY3350* cells. (C) Rough phenotype of a colony of *CHY3350* cells transformed with the plasmid pBMH1. Colonies were photographed at × 100 magnification after 3 days of incubation at 28°C on YNA-agar plates.

plates after 3 days of incubation at 28°C (Nuttley *et al.*, 1993). Subsequent analysis showed that this attribute was lost at a rate of 3-5 × 10^{-2} per generation and that the smooth phenotype was not due to mutations in the *YlBMH1* gene.

6.3 Isolation and characterization of the *YlBMH1* gene

The *YlBMH1* gene was isolated from a *Y. lipolytica* genomic DNA library contained in the replicative *E. coli* shuttle vector pINA445 (Nuttley *et al.*, 1993) by its ability to restore hyphal growth upon introduction into *CHY3350* cells. Of approximately 12,000 transformants screened, 12 showed a wild-type filamentous phenotype, but only one contained a plasmid, pBMH1, capable of inducing the formation of rough-surfaced colonies upon reintroduction into *CHY3350* cells (Fig. 6-1C). Restriction enzyme analysis revealed that this plasmid contained a 5.0-kbp *Bam*HI-*Bam*HI fragment capable of restoring filamentous growth to the *CHY3350* strain. Sequencing of both strands of this fragment revealed an ORF of 1482 bp interrupted by one intron located between codons 4 and 5 (nucleotides +13 to +663 from the A residue of the potential initiating codon). Interestingly, the A nucleotide at the fifth position of the putative 5'-splice donor sequence (GTAAATPu) diverges from the G nucleotide normally found in eukaryotic genes (Newman, 1998), and an unusual 3' intronic end (TAG, as opposed to the consensus sequence CAG) (Lopez *et al.*, 1994; Strick *et al.*, 1992; Teem *et al.*, 1984) is found three nucleotides downstream of the 3' internal consensus TACTAAC sequence.

The upstream regulatory region of the *YlBMH1* gene lacks a putative TATA box but contains a CT/CA-rich region, which is thought to play a role in transcriptional

regulation in *Y. lipolytica* (Nuttley *et al.*, 1994; Xuan *et al.*, 1990) (Fig. 6-2). Analysis of cDNA showed that transcription of the *YlBMH1* gene preferentially begins at position −23 from the A nucleotide of the initiating codon and that polyadenylation occurs following the A nucleotide at position +1524.

The deduced protein product of *YlBMH1*, *Yl*Bmh1p, is 276 amino acids in length (Fig. 6-2), has a predicted molecular mass of 31,166 Da, and a typical acidic pI of 4.91 (Fu *et al.*, 2000). Analysis of the predicted amino acid sequence revealed that *Yl*Bmh1p belongs to the 14-3-3 family of proteins and that it is most closely related to Ftt2p from the filamentous fungus *Trichoderma reesei* (72.1% identity, Fig. 6-4). Additionally, a putative PEST region, which is commonly found in rapidly degraded proteins (Chevaillier, 1993; Rechsteiner and Rogers, 1996), is predicted at residues 234−263 of *Yl*Bmh1p.

6.4 Isolation and characterization of the *YlBMH2* gene

Numerous unsuccessful attempts to disrupt *YlBMH1* suggested that this gene may be essential or that other 14-3-3 proteins might exist in *Y. lipolytica* that would be able to support hyphal growth in the absence of functional *Yl*Bmh1p. Indeed, a comprehensive database screening revealed the existence of a partial sequence (GenBank accession number: AL413320) encoding a potential 14-3-3 protein different from *Yl*Bmh1p. Based on this sequence, a 3.7-kbp *Bam*HI-*Bam*HI fragment was isolated by high fidelity PCR using a *Y. lipolytica* genomic DNA library as template. Sequencing of this fragment (*YlBMH2*) revealed an ORF of 1583 bp, interrupted by one intron within codon 1 (nucleotides +1 to +813 from the A residue of the potential initiating codon) and flanked

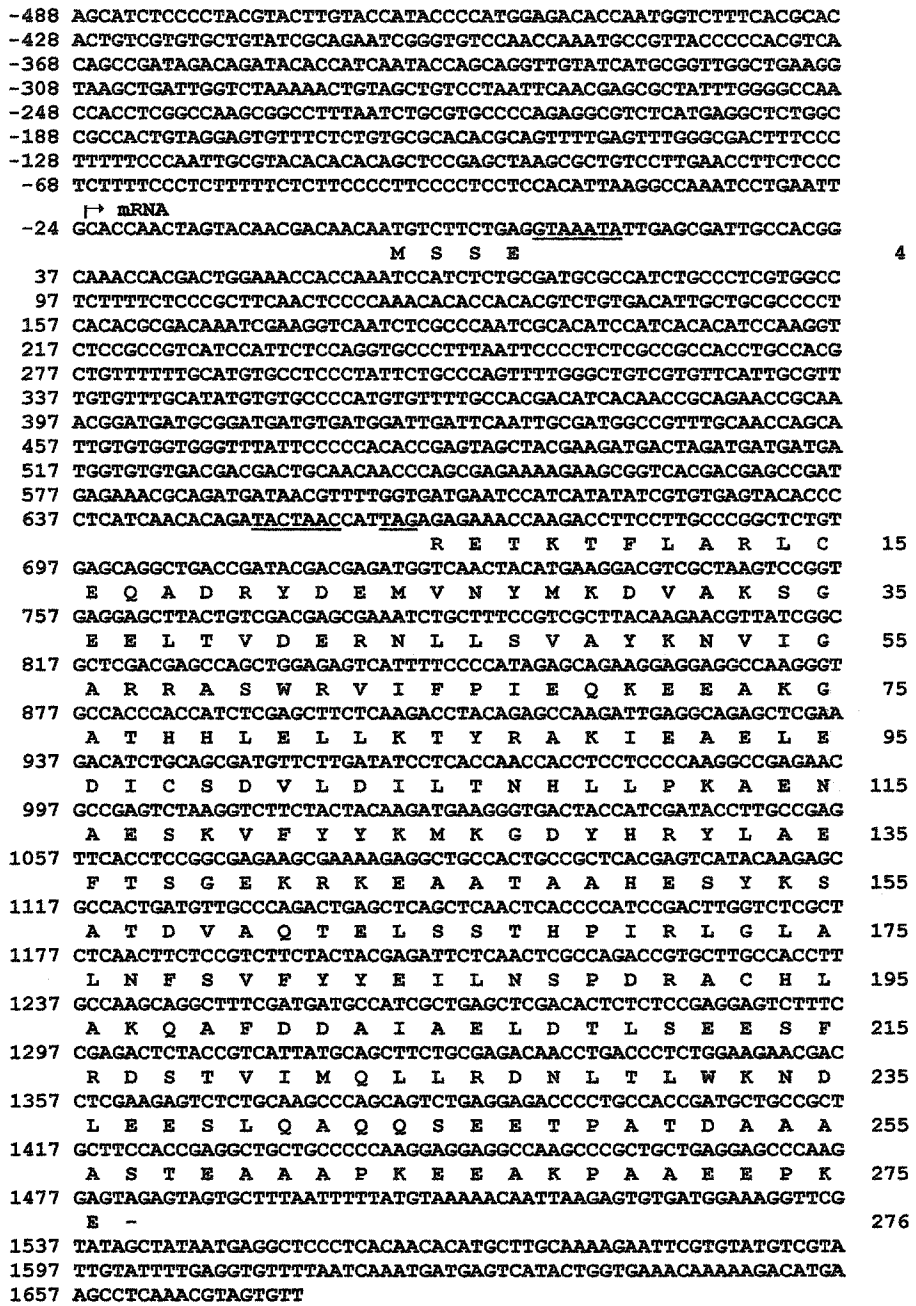

Figure 6-2. Nucleotide sequence of the *YlBMH1* gene and deduced amino acid sequence of *Yl*Bmh1p. The transcriptional start site of the *YlBMH1* gene is indicated. The consensus sequences for intron splicing are underlined.

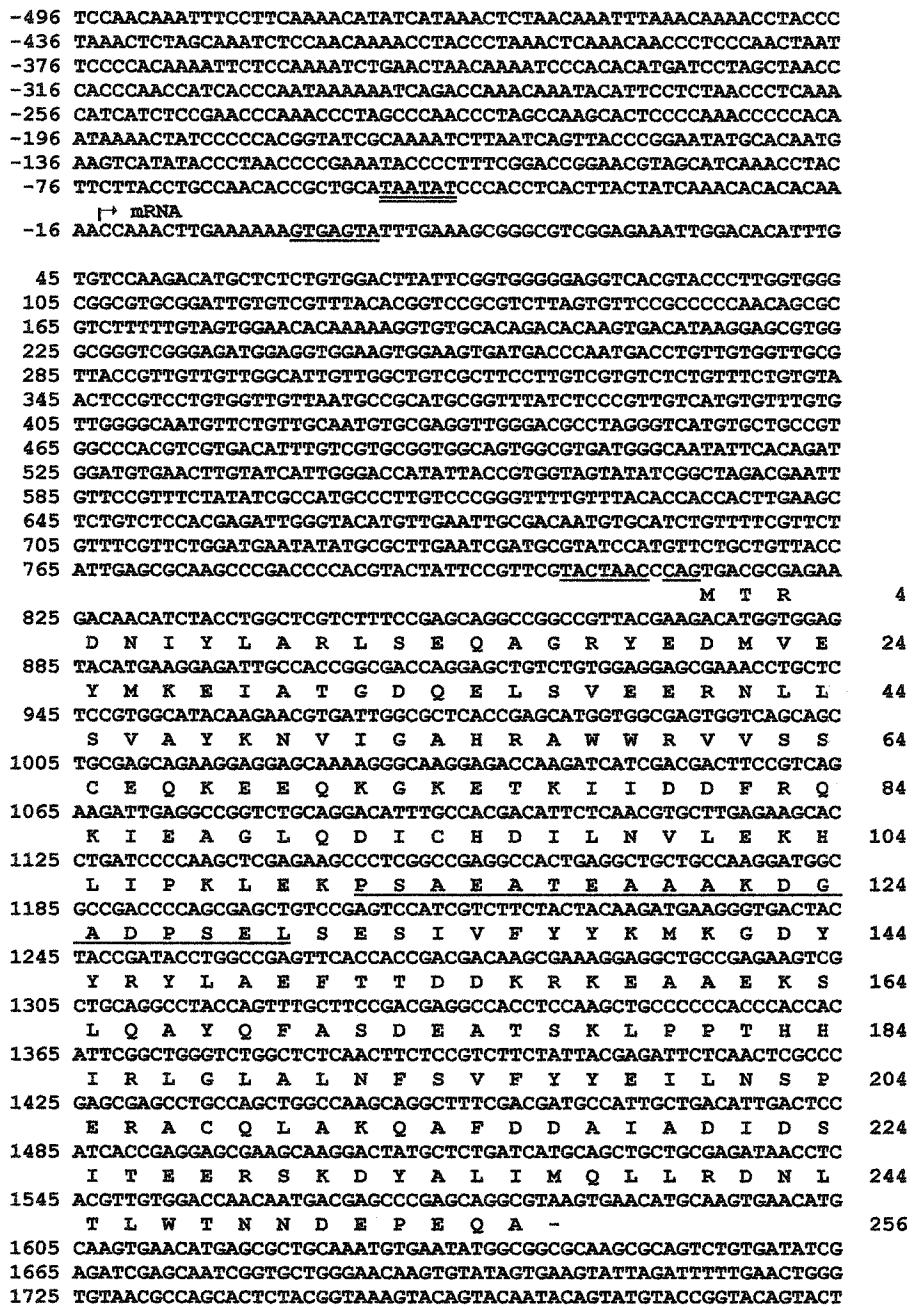

Figure 6-3. Nucleotide sequence of the *YlBMH2* gene and deduced amino acid sequence of *Yl*Bmh2p. The transcriptional start site of the *YlBMH2* gene is indicated. The putative consensus sequences for intron splicing and the 19-amino acid insertion are underlined. The putative TATA box is double underlined.

```
YlBmh1p    -MSSERETKTFLARLCEQADRYDEMVNYMKDVAKSGEELTVDERNLLSVAYKNVIGARRA  59
YlBmh2p    ---MTREDNIYLARLSEQAGRYEDMVEYMKEIATGDQELSVEERNLLSVAYKNVIGAHRA  57
TrFtt1p    ---MGHEDAVYLAKLAEQAERYEEMVENMKIVASEDRDLTVEERNLLSVAYKNVIGARRA  57
TrFtt2p    -MATERESKTFLARLCEQAERYDEMVTYMKEVAQLGGELSVDERNLLSVAYKNVVGTRRA  59
CaBmh1p    -MPASREDSVYLAKLAEQAERYEEMVENMKAVASSGQELSVEERNLLSVAYKNVIGARRA  59
SpRad24p   MSTTSREDAVYLAKLAEQAERYEGMVENMKSVASTDQELTVEERNLLSVAYKNVIGARRA  60
SpRad25p   -MSNSRENSVYLAKLAEQAERYEEMVENMKKVACSNDKLSVEERNLLSVAYKNIIGARRA  59
ScBmh1p    -MSTSREDSVYLAKLAEQAERYEEMVENMKTVASSGQELSVEERNLLSVAYKNVIGARRA  59
ScBmh2p    -MSQTREDSVYLAKLAEQAERYEEMVENMKAVASSGQELSVEERNLLSVAYKNVIGARRA  59
           .. ..*. ..**.*.***.**..**..** .*.....*.*.***********..*..**

YlBmh1p    SWRVIFPIEQKEEAKG-ATHHLELLKTYRAKIEAELEDICSDVLDILTNHLLPKAEN---- 115
YlBmh2p    WWRVVSSCEQKEEQKG--KE-TKIIDDFRQKIEAGLQDICHDILNVLEKHLIPKLEKPSA 114
TrFtt1p    SWRIVTSIEQKEESKG-NSSQVALIKEYRQKIEAELAKICDDILEVLDQHLIPSAKS---- 113
TrFtt2p    SWRIISSIEQKEESKG-SDKHVATIKEYRSKIELELEKVCEDVLNVLDTSLIPNAAT---- 115
CaBmh1p    SWRIVSSIEQKEEAKG-NESQVALIRDYRAKIEAELSKICEDILSVLSDHLITSAQT---- 115
SpRad24p   SWRIVSSIEQKEESKG-NTAQVELIKEYRQKIEQELDTICQDILTVLEKHLIPNAAS---- 116
SpRad25p   SWRIISSIEQKEESRG-NTRQAALIKEYRKKIEDELSDICHDVLSVLEKHLIPAATT---- 115
ScBmh1p    SWRIVSSIEQKEESKEKSEHQVELICSYRSKIETELTKISDDILSVLDSHLIPSATT---- 116
ScBmh2p    SWRIVSSIEQKEESKEKSEHQVELIRSYRSKIETELTKISDDILSVLDSHLIPSATT---- 116
           .**.....*****...   ... .....* *** .* ....*.*..*. .*.. . .

YlBmh1p    ----------------AESKVFYYKMKGDYHRYLAEFTSGEKRKEAATAAHESYKSATDV 159
YlBmh2p    EATEAAAKDGADPSELSESIVFYYKMKGDYYRYLAEFTTDDKRKEAAEKSLQAYQFASDE 174
TrFtt1p    ----------------GESKVFYHKMKGDYHRYLAEFAIGDRRKDSADKSLEAYKAATEV 157
TrFtt2p    ----------------GESKVFYHKMKGDYHRYLAEFASGEKRKVAATAAHEAYKNATDV 159
CaBmh1p    ----------------GESKVFYYKMKGDYHRYLAEFAIAVFRKEAADLSLEAYKAASDV 159
SpRad24p   ----------------AESKVFYYKMKGDYYRYLAEFAVGEKRQHSADQSLEGYKAASEI 160
SpRad25p   ----------------GESKVFYYKMKGDYYRYLAEFTVGEVCKEAADSSLEAYKAASDI 159
ScBmh1p    ----------------GESKVFYYKMKGDYHRYLAEFSSGDAREKATNASLEAYKTASEI 160
ScBmh2p    ----------------GECKVFYYKMKGDYHRYLAEFSSGDAREKATNSSLEAYKTASEI 160
                           .*..***.******.******.......... ....*. *...

YlBmh1p    AQTELSSTHPIRLGLALNFSVFYYEILNSPDRACHLAKQAFDDAIAELDTLSEESFRDST 219
YlBmh2p    ATSKLPPTHHIRLGLALNFSVFYYEILNSPERACQLAKQAFDDAIADIDSITEERSKDYA 234
TrFtt1p    AQTELPPTHPIRLGLALNFSVFYYEILNAPDQACHLAKQAFDDAIAELDTLSEESYKDST 217
TrFtt2p    AQTELTPTHPIRLGLALNFSVFYYEILNSPDRACHLAKQAFDDAIAELDSLSEESYRDST 219
CaBmh1p    AVTELPPTHPIRLGLALNFSVFYYEILNSPDRACHLAKQAFDDAVADLETLSEDSYKDST 219
SpRad24p   ATAELAPTHPIRLGLALNFSVFYYEILNSPDRACYLAKQAFDEAISELDSLSEESYKDFT 220
SpRad25p   AVAELPPTDPMRLGLALNFSVFYYEILDSPESACHLAKQVFDEAISELDSLSEESYKDST 219
ScBmh1p    ATTELPPTHPIRLGLALNFSVFYYEIQNSPDKACHLRKQAFDDAIAELDTLSEESYKDST 220
ScBmh2p    ATTELPPTHPIRLFLALNFSVFYYEIQNSPDKACHLAKQAFDDAIAELDTLSEESYKDST 220
           * ..*..*...**.************...*..**.*.**.**.*........*....*..

YlBmh1p    VIMQLLRDNLTLWKNDLEESLQAQQSEETPATDAAAASTEAAAPKEEAKPAAEEPKE 276
YlBmh2p    LIMQLLRDNLTLWTNNDEPEQA---------------------------------- 256 (58.2%)
TrFtt1p    LIMQLLRDNLTLWTSSEAETSAGQVEAPPKEDTPAEAAAPAEEPKAE---------- 264 (67.1%)
TrFtt2p    LIMQLLRDNLTLWTSSDSGEAEQAGEAKKDEGEAAKPAEEEPKAEEPAPEATS---- 272 (72.1%)
CaBmh1p    LIMQLLRDNLTLWTDLSEAPAATEEQQQSSQAPAAQ------P--TEG-KADQE---- 264 (66.3%)
SpRad24p   LIMQLLRDNLTLWTSDAEYSAAAAGGNTEGAQENAPSNAPEGEAEPKADA------- 270 (64.8%)
SpRad25p   LIMQLLRDNLTLWTSDAEYNQSAKEEAPAAAAASENEHPEPKESTTDTVKA------ 270 (63.3%)
ScBmh1p    LIMQLLRDNLTLWTSDMSESGQAEDQQQQQQHQQQQ------PPAAAEGEAPK---- 267 (65.5%)
ScBmh2p    LIMQLLRDNLTLWTSDISESGQEDQQQQQQQQQQQQQQQQQQAPAEQTQGEPTK---- 273 (62.2%)
           .************... . ... .           .                .
```

Figure 6-4. Amino acid sequence alignment of Bmh1p and Bmh2p of *Y. lipolytica* (*Yl*Bmh1p and *Yl*Bmh2p) and 14-3-3 proteins from *T. reesei* (*Tr*Ftt1p and *Tr*Ftt2p), *C. albicans* (*Ca*Bmh1p), *S. pombe* (*Sp*Rad24p and *Sp*Rad25p), and *S. cerevisiae* (*Sc*Bmh1p and *Sc*Bmh2p). Percentages refer to the percent identity of a given protein to *Yl*Bmh1p. GenBank accession numbers: CAC20377 (*Tr*Ftt1p), CAC20378 (*Tr*Ftt2p), AAB96910 (*Ca*Bmh1p), CAA55795 (*Sp*Rad24p), CAA55796 (*Sp*Rad25p), CAA46959 (*Sc*Bmh1p), and CAA59275 (*Sc*Bmh2p).

by 1.8 kbp and 340 bp of sequence upstream and downstream, respectively (Fig. 6-3). A potential TATA box, TAATAT, is found at nucleotides −52 to −47 from the A nucleotide of the first ATG codon (Fig. 6-3). Analysis of cDNA revealed that transcription of the *YlBMH2* gene preferentially starts at position −14 from the A nucleotide of the initiating codon and that polyadenylation occurs following the A nucleotide at position +1719. The putative 5'-splice donor and 3'-splice acceptor sequences of *YlBMH2* (GTGAGTPu and TACTAACNCAG, respectively) are identical to the motifs found in most *Y. lipolytica* genes (Lopez *et al.*, 1994; Strick *et al.*, 1992; Teem *et al.*, 1984).

The deduced protein product of *YlBMH2*, *Yl*Bmh2p, is 256 amino acids in length (Fig. 6-3), has a predicted molecular mass of 29,435 Da, and a typical acidic pI of 4.79 (Fu *et al.*, 2000). Analysis of the predicted amino acid sequence of *Yl*Bmh2p showed that it also belongs to the 14-3-3 family of proteins, does not contain any predicted PEST sequence, and is most closely related to Ftt1p from the filamentous fungus *Schizophyllum commune* (64.5% identity). Interestingly, *Yl*Bmh2p contains a 19-amino acid insertion (PSAEATEAAAKDGADPSEL, residues 112 −130) (Fig. 6-4) encompassing a putative *N*-myristoylation site not found in other known 14-3-3 proteins.

6.5 *YlBMH2* is unable to restore hyphal growth to the *Y. lipolytica CHY3350* mutant strain

Because no smooth *Δbmh1* colonies could be obtained after transformation of *Y. lipolytica E122* cells with a disruption cassette containing the *YlURA3* gene flanked by sequences from the *YlBMH1* gene, the *YlBMH2* gene was investigated as to its possible

role in the induction of hyphal growth in *Y. lipolytica* and to determine if its ability to induce hyphae could hinder the selection of *bmh1* null mutants by means of their colony morphology. Accordingly, a 3.7-kbp *Bam*HI-*Bam*HI fragment containing the entire *YlBMH2* gene was cloned into the *Bam*HI site of the shuttle vector pINA445 to obtain plasmid pBMH2, and the ability of this plasmid to induce hyphal growth in *Y. lipolytica* was evaluated. Interestingly, no effect on hyphal formation was observed upon introduction of pBMH2 into *CHY3350* mutant cells.

6.6 Transcription of *YlBMH1* and *YlBMH2* during the dimorphic transition

The yeast-to-hypha transition was induced in exponentially growing *E122* cells by a 15-min carbon source starvation at 4°C, followed by transfer to prewarmed YNBGlcNAc medium and incubation at 28°C (Guevara-Olvera *et al.*, 1993). Under these conditions, more than 80% of the cells produced germ tubes after 10 h of incubation, whereas cells transferred to fresh glucose-containing (YNBGlc) medium grew almost exclusively as the yeast form. Northern blot experiments performed with total RNA extracted from cells harvested at 3 h and 10 h of incubation showed that *YlBMH1* mRNA was at levels undetectable by this procedure. However, semiquantitative RT-PCR carried out with *YlHIS1* as an endogenous internal standard revealed that transcription of the *YlBMH1* gene increases during the formation of germ tubes (approximately 2-fold), while there is no apparent variation in the transcription levels of *YlBMH2* (Fig. 6-5).

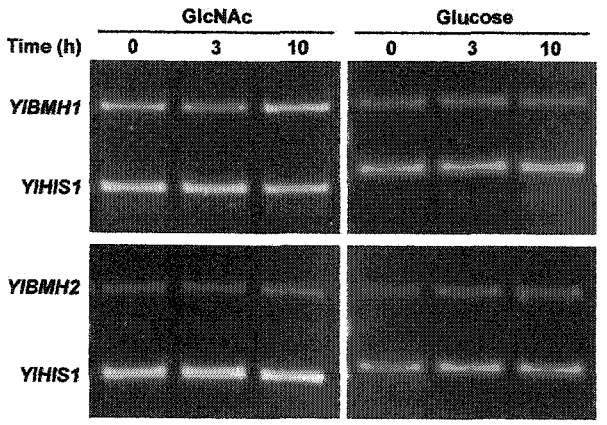

Figure 6-5. Transcription of the *YlBMH1* and *YlBMH2* genes during the dimorphic transition. Total RNA was isolated from *E122* cells incubated at 28°C in YNBGlcNAc (induction of hyphal growth) or YNBGlc (control culture, growth as the yeast form) for the times indicated and subjected to semiquantitative RT-PCR analysis. The 600-bp and 400-bp RT-PCR products were resolved by electrophoresis on 2% agarose and visualized by staining with ethidium bromide. *YlBMH1* and *YlBMH2* mRNA expression was normalized to *YlHIS1* mRNA.

6.7 Overexpression of *YlBMH1* enhances pseudohyphal growth in *rac1* null mutants of *Y. lipolytica*

To gain additional information regarding the involvement of *YlBMH1* and *YlBMH2* in filamentous growth in *Y. lipolytica*, the effects of introducing the multicopy plasmids pBMH1 and pBMH2 into the null mutant strains *mhy1KO9*, *rac1KO30* and *bem1KO157* (Table 2-5) were analyzed.

Following 3 days of incubation on YNA-agar plates at 28°C, overexpression of the *YlBMH1* gene induced the formation of peripheral extensions in *rac1KO30* colonies (Fig. 6-6, panels H and I), whereas no effect was observed when *YlBMH2* was overexpressed in the same strain (Fig. 6-6, panels H and J). Further analysis revealed that these extensions were produced by the enhancement of pseudohyphal growth by *YlBMH1* overexpression in *rac1Δ* cells (Fig. 6-7, panels H and I), and that no morphological alteration was induced by the overexpression of *YlBMH2* in these cells (Fig. 6-7, panels H and J). No effect on either colony morphology or cell morphology was observed when either *YlBMH1* or *YlBMH2* was overexpressed in the *mhy1Δ* or *bem1Δ* background (Fig. 6-6 and Fig. 6-7, panels B to G).

6.8 Discussion

This chapter describes the isolation of the *Y. lipolytica* genes *BMH1* and *BMH2* and shows that *YlBMH1* is involved in the regulation of filamentous growth in this organism. These genes encode two different 14-3-3 proteins showing 58.2% identity, and their primary transcripts are interrupted by one intron near their 5'-ends. Interestingly, the A

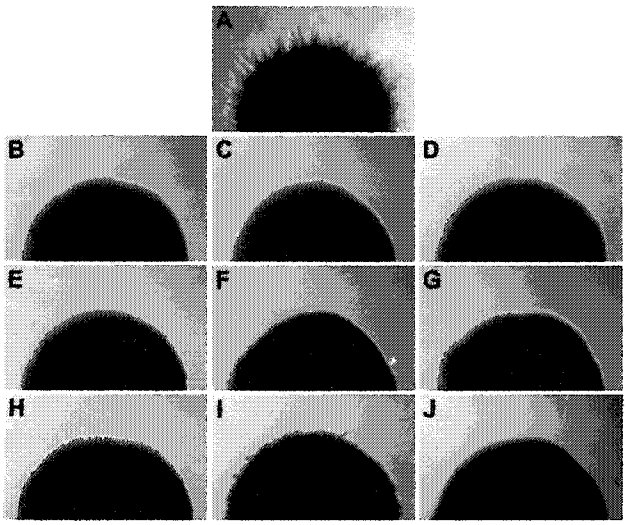

Figure 6-6. Colony morphology of *Y. lipolytica* strains transformed with autonomously replicating plasmids carrying the *YlBMH1* and *YlBMH2* genes. (A) Wild-type strain *E122*; (B) mutant strain *bem1KO157*; (C) strain *bem1KO157* transformed with plasmid pBMH1; (D) strain *bem1KO157* transformed with plasmid pBMH2; (E) mutant strain *mhy1KO9*; (F) strain *mhy1KO9* transformed with plasmid pBMH1; (G) strain *mhy1KO9* transformed with plasmid pBMH2; (H) mutant strain *rac1KO30*; (I) strain *rac1KO30* transformed with plasmid pBMH1; (J) strain *rac1KO30* transformed with plasmid pBMH2. Colonies were photographed after 3 days of incubation at 28°C on YNA-agar plates. Colony magnification, ×100.

Figure 6-7. Cell morphology of *Y. lipolytica* strains transformed with autonomously replicating plasmids carrying the *YlBMH1* and *YlBMH2* genes. (A) Wild-type strain *E122*; (B) mutant strain *bem1KO157*; (C) strain *bem1KO157* transformed with plasmid pBMH1; (D) strain *bem1KO157* transformed with plasmid pBMH2; (E) mutant strain *mhy1KO9*; (F) strain *mhy1KO9* transformed with plasmid pBMH1; (G) strain *mhy1KO9* transformed with plasmid pBMH2; (H) mutant strain *rac1KO30*; (I) strain *rac1KO30* transformed with plasmid pBMH1; (J) strain *rac1KO30* transformed with plasmid pBMH2. Cells were photographed after 3 days of incubation at 28°C on YNA-agar plates. Bars, 5 μm.

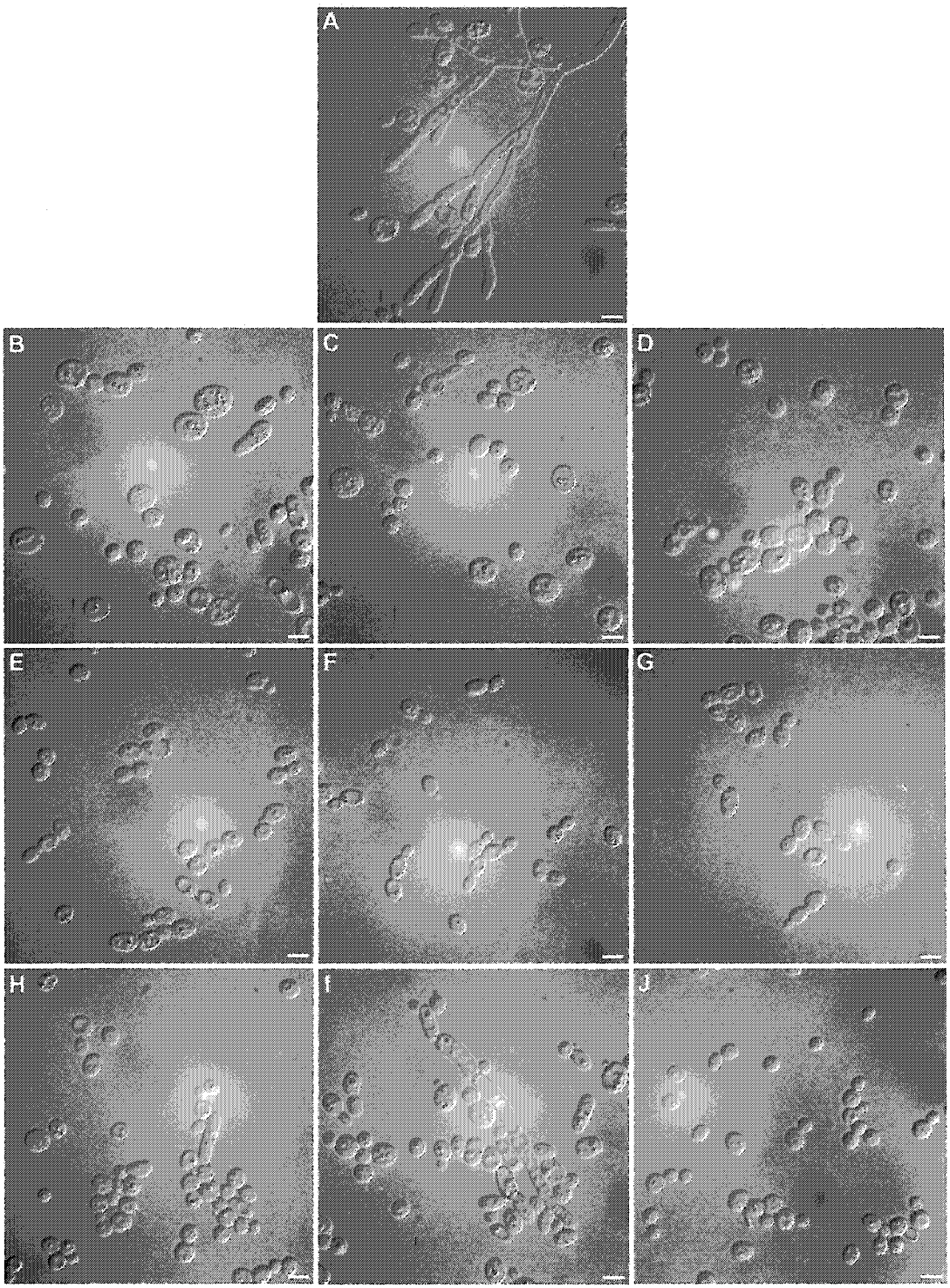

nucleotide at the fifth position of the putative 5'-splice donor sequence of *YlBMH1* (GTAAATPu) diverges from the G nucleotide normally found in *Y. lipolytica* genes, and an unusual 3' intronic end (TAG, as opposed to the consensus sequence CAG) is found three nucleotides downstream of the consensus sequence TACTAAC. These features, when compared to those previously found in *YlRAC1* (Chapter 4), *YlBEM1* (Chapter 5), and other *Y. lipolytica* genes (Lopez *et al.*, 1994; Smith *et al.*, 2000; Strick *et al.*, 1992), suggest that a higher degree of variation in the splice and branch sites is tolerated in *Y. lipolytica* than in *S. cerevisiae*. Thus, as in higher eukaryotes (Newman, 1998), only the GT and AG dinucleotides at the intron termini are invariant, but an abbreviated version of the *S. cerevisiae* consensus branchpoint sequence (CTAAC, as opposed to TACTAAC) (Kaufer and Potashkin, 2000; Teem *et al.*, 1984) is still required in *Y. lipolytica.*

In this chapter it is also shown that, in *Y. lipolytica*, the expression levels of *YlBMH1* are increased during the yeast-to-hypha transition, whereas no variation is observed in the transcription of *YlBMH2* during this event. Although no data on the variation of the expression levels of *ScBMH1* or *ScBMH2* during the dimorphic transition in *S. cerevisiae* are currently available, it is known that overexpression of these genes stimulates cell elongation and agar invasion in this organism (Roberts *et al.*, 1997). Similarly, disruption of one of the wild-type alleles of the *C. albicans* essential gene *CaBMH1* results in a significant reduction of filamentation (Cognetti *et al.*, 2002), thus suggesting the existence of a positive correlation between protein abundance and filamentous growth. This hypothesis is further supported by our observation that, in addition to enhanced pseudohyphae formation in cells lacking functional *YlRAC1*,

overexpression of *YlBMH1* is able to induce hyphal growth in *CHY3350* mutant cells. On the other hand, the absence of variation in the transcription levels of *YlBMH2*, its inability to induce hyphal or pseudohyphal growth when overexpressed in the *CHY3350*, *mhy1KO9*, *rac1KO30*, and *bem1KO157* mutant strains, and the presence of a 19-amino acid insertion that contains a potential *N*-myristoylation site in *Yl*Bmh2p, suggest that *YlBMH2* may have functions different from those of *YlBMH1* and thus not be involved in the regulation of filamentous growth in *Y. lipolytica*. This is not entirely surprising, because it has been observed that in *S. pombe*, for instance, disruption of the *rad24* gene results in serious morphological defects, while the absence of *rad25*, which encodes the other 14-3-3 protein of fission yeast, has little or no effect (Ford *et al.*, 1994). Nevertheless, a role for *YlBMH2* in the regulation of filamentous growth cannot be completely ruled out at this time.

Disruption of the genes *YlBMH1* and *YlBMH2* has so far remained elusive. The reasons for this are unknown, but one may speculate that either both genes are essential or other 14-3-3 proteins that perform the same functions as *Yl*Bmh1p and *Yl*Bmh2p exist in *Y. lipolytica*. It is interesting to note that disruption of one allele of *YlBMH1* in the *Y. lipolytica E122//22301-3* diploid strain results in a drastic reduction of sporulation, and a similar effect has been described in *S. cerevisiae*, where diploid strains lacking both *ScBMH1* and *ScBMH2* are unable to sporulate (Roberts *et al.*, 1997).

In conclusion, the results presented in this chapter demonstrate that *YlBMH1* is involved in the regulation of both hyphal and pseudohyphal growth in *Y. lipolytica*, while the participation of *YlBMH2* or other as yet unidentified genes encoding 14-3-3 proteins in these events remains unclear.

CHAPTER 7

GENERAL DISCUSSION AND FUTURE PERSPECTIVES

7.1 *MHY1* and the regulation of hyphal growth in *Y. lipolytica*

7.1.1 *MHY1*, stress response and dimorphism in *Y. lipolytica*

Msn2p and Msn4p are transcriptional activators of the multistress response in *S. cerevisiae*. They act via *cis*-acting DNA STREs and are able to mediate transcription induced by a broad range of environmental and physiological conditions, thereby enabling cells to develop tolerance to different forms of stress (cross protection) (Kobayashi and McEntee, 1993; Marchler *et al.*, 1993; Martinez-Pastor *et al.*, 1996; Ruis and Schüller, 1995; Schüller *et al.*, 1994; Treger *et al.*, 1998). In this study, it is shown that, like *S. cerevisiae* Msn2p and Msn4p, *Y. lipolytica* Mhy1p specifically recognizes and binds to sequences containing the AGGGG pentanucleotide, strongly suggesting a role in the transcriptional regulation of genes containing this sequence in their promoter regions. In addition, the transcriptional levels of *MHY1* are shown to be dramatically increased during the yeast-to-hypha transition in this organism.

Remarkably, transcription of *MHY1* appears to be significantly reduced during carbon-source starvation, osmotic shock and oxidative stress in *Y. lipolytica*. This is in evident contrast to the situation in *S. cerevisiae*, where *MSN2* and *MSN4* appear to be constitutively transcribed (DeRisi *et al.*, 1997), and their protein products, Msn2p and Msn4p, are activated by their translocation from the cytosol to the nucleus in response to stress conditions such as heat shock, carbon-source starvation, osmotic stress, and the presence of ethanol or sorbate (Görner *et al.*, 1998). Moreover, it has been shown that the Ras2/cAMP-dependent pathway induces invasive growth in *S. cerevisiae* by suppressing the cellular stress response, and that the strain normally used in dimorphism studies

(Σ1278b) is non-responsive to stress because this pathway is overactive (Stanhill *et al.*, 1999). Thus, based on these observations, and on the recent report that osmotic and oxidative stresses inhibit GlcNAc-induced hyphal growth in *Y. lipolytica* (Kim *et al.*, 2000), it is tempting to speculate that Mhy1p may function as a transcriptional repressor of stress-responsive genes, thereby inducing hyphal growth in this organism.

However, because putative STREs are also found in the promoter of *MHY1* and of other genes required for the induction of filamentous growth in *Y. lipolytica*, the possibility of a dual role for Mhy1p cannot be ruled out. In this model, Mhy1p would play a role in the repression of the general stress response and in the induction of filamentous growth, and the specificity of its function would be determined by its interactions with other proteins. An example of this situation is provided by the *S. cerevisiae* transcription factor Ste12p, which is a terminal component of two different signaling cascades. In this organism, Ste12p forms homodimers to bind to pheromone response elements (PREs) and promote mating, whereas it cooperates with Tec1p to bind to FREs and promote filamentous and invasive growth (Madhani and Fink, 1997).

Another possibility is that filamentation in *Y. lipolytica* constitutes a specialized form of response to particular conditions of environmental stress, and that this mechanism developed while preserving some of the components of the multistress response machinery present in *S. cerevisiae*. In agreement with this hypothesis, transcription of *MHY1* was unaffected by thermal stress (Fig. 3-10), and it has been suggested that heat shock acts synergistically with GlcNAc to fully induce hyphal growth in *Y. lipolytica* (Guevara-Olvera *et al.*, 1993).

The detection of weak specific AGGGG-binding activity in cell extracts from *mhy1Δ* cells grown in GlcNAc-containing medium (Fig. 3-5, white arrow) suggests that, like in *S. cerevisiae*, several proteins with the ability to bind putative STREs may exist in *Y. lipolytica*. Interestingly, no function has so far been attributed to the *S. cerevisiae* ORF YER130C. The predicted protein product of this ORF is believed to be also able to bind these transcriptional regulatory elements (Fig. 3-2) (Martinez-Pastor *et al.*, 1996), and it is therefore possible that Yer130cp regulates pseudohyphal growth in *S. cerevisiae* through mechanisms similar to those of Mhy1p in *Y. lipolytica*. Remarkably, it has been observed that nitrogen starvation, thermal stress, osmotic shock, and the addition of compounds that affect the lipid bilayer organization of the cell membrane are able to induce pseudohyphal growth in *S. cerevisiae*, likely through the coordinated action of the MAP kinase cascade and the cAMP-dependent pathway (Zaragoza and Gancedo, 2000). Furthermore, several putative STREs are found in the promoter regions of *STE12* and *PHD1*, two important regulators of pseudohyphal growth in *S. cerevisiae* (Gimeno and Fink, 1994; Liu *et al.*, 1993).

It is important to point out that the study of stress response in *Y. lipolytica* is still early, and no stress-responsive genes have been isolated to date from this organism. Consequently, future experiments aimed at the isolation of these genes, the functional characterization of the *Y. lipolytica* STREs and the elucidation of the conditions they regulate, as well as the determination of the nature of the weak AGGGG-binding activity observed for *Y. lipolytica mhy1Δ* cells, will be fundamental to a better understanding of the links between stress response and filamentous growth in dimorphic organisms, two

phenomena with large implications for the development of virulence by fungal pathogens (Banuett, 1995; Bruatto *et al.*, 1993; Maresca and Kobayashi, 1989; Odds, 1988; Shepherd, 1988).

7.1.2 Regulation of *MHY1* and its protein product, Mhy1p

The upstream regulatory region of the *MHY1* gene contains consensus sequences for the binding of several transcription factors implicated in the regulation of fungal development and in the response of cells to specific environmental conditions, including multiple copies of the pentanucleotide AGGGG (Fig. 3-3 and Table 7-1).

Analysis of the upstream region of *MHY1* suggests a rather complex pattern of regulation of expression, involving feedback regulatory loops with possible connections to nitrogen starvation and stationary phase maintenance. It will be interesting to investigate whether these putative regulatory elements are functional and to search for proteins that can recognize these sequences. If these regulatory elements do function, *MHY1* may represent a point of integration of several signaling pathways that control morphogenesis in *Y. lipolytica.*

Table 7-1 Potential Binding Sites for Transcription Factors in the Promoter of the *MHY1* Gene

Binding Site[a]	Organism	Function	Reference
abaA (*Ca*Tec1p, *Sc*Tec1p)	*A. nidulans*	Mediates a genetic switch controlling development	Boylan *et al.*, 1987; Bürglin, 1991; Schweizer *et al.*, 2000
StuA (*Ca*Efg1p, *Sc*Phd1p)	*A. nidulans*	Mediates regulation of developmental complexity	Dutton *et al.*, 1997; Gimeno and Fink, 1994; Stoldt *et al.*, 1997

PacC (*Ca*Rim101p, *Sc*Rim101p)	*A. nidulans*	Mediates regulation of gene expression by ambient pH	Davis *et al.*, 2000; Li and Mitchell, 1997; Tilburn *et al.*, 1995
NIT2	*N. crassa*	Mediates synergistic gene activation during conditions of nitrogen limitation	Fu and Marzluf, 1990
GCN4	*S. cerevisiae*	Mediates general amino acid control (response to starvation)	Arndt and Fink, 1986
STRE	*S. cerevisiae*	Mediates transcriptional activation by multiple stress conditions	Kobayashi and McEntee, 1993
SPRE	*S. cerevisiae*	Putative activator of stationary phase-expressed genes	Wang *et al.*, 1997

[a] The *S. cerevisiae* and *C. albicans* homologs of the transcription factors known to bind these sites are shown in parentheses.

Two remarkable differences between Mhy1p and the *S. cerevisiae* transcription factors Msn2p and Msn4p are its size (approximately 32 kDa, as compared to 78 and 70 kDa for Msn2p and Msn4p, respectively) and its lack of a putative nuclear localization signal (NLS). These characteristics, combined with the demonstration that proteins smaller than 45 kDa do not need an active nuclear protein import machinery (Jans and Hübner, 1996) and the finding that the 62-kDa fusion protein Mhy1p-GFP accumulates in the cytosol and is unable to induce hyphal growth (Section 3.7 and Fig. 3-9), suggest that Mhy1p freely diffuses into and out of the nucleus and that protein-protein interactions are essential for its subcellular localization.

Interestingly, analysis of the primary structure of Mhy1p suggests that this putative transcription factor has a strong potential to interact with other proteins. Thus, in addition to the C_2H_2-type zinc finger at its carboxyl terminus, a remarkable feature of Mhy1p is its

high content of glutamine, serine, proline, and acidic amino acid residues at its amino terminus (Fig. 3-2). This pattern is commonly found in the activation domains of eukaryotic transcription factors, and regions containing these residues have been implicated in the formation of homo- and heteromultimers, as well as in interactions with the basal transcriptional machinery (Ferré-D'Amaré *et al.*, 1993; Frankel and Kim, 1991; Hoey *et al.*, 1993; McEwan *et al.*, 1996; Pascal and Tjian, 1991; Remacle *et al.*, 1997; Xiao and Jeang, 1998). It will be interesting to identify proteins that interact with Mhy1p and to determine how they modulate Mhy1p function in the regulation of morphogenesis in *Y. lipolytica.*

7.1.3 The function of *MHY1* in filamentous growth

A hypothesis suggested for the function of *MHY1* in the induction of the dimorphic transition of *Y. lipolytica* is that high levels of active Mhy1p would be essential for both the repression of stress-responsive genes and the induction of genes whose products are necessary for the redirection of cell growth to a filamentous mode and the maintenance of this pattern. Under conditions that favor growth as the yeast form, Mhy1p would be constitutively synthesized at a basal level, and the protein would be retained in the cytosol by an anchor protein. However, under environmental conditions that promote filamentous growth, transcription factors acting through the various regulatory elements found in the promoter of *MHY1* would contribute to an increase of its levels of expression, and optimal intracellular concentrations would be achieved through a positive feedback loop via AGGGG sequences present in its upstream regulatory region. Concomitantly, Mhy1p

would be released from its cytoplasmic anchor, leading to its translocation into the nucleus and, consequently, to the inactivation of genes involved in the multistress response and to the induction of genes necessary for filamentous growth. Once the germ tube had achieved its maximum extension, the nucleus would divide, and Mhy1p would be equally distributed between the two nuclei. Mhy1p would then continue to promote filamentous growth at the growing tip, but it would be rapidly degraded in the mother cell through a process mediated by its PEST domains.

7.2 *YlRAC1* and *YlCDC42* in the regulation of hyphal growth in *Y. lipolytica*

Cdc42/Rac proteins have been implicated in the control of a diverse and extensive set of cellular processes (Zohn *et al*, 1998), including, notably, the regulation of assembly and organization of the actin cytoskeleton (Hall, 1994; 1998; Nobes and Hall, 1995; Ridley, 1994; 1995; Symons, 1995; Tapon and Hall, 1997; van Aelst and D'Souza-Schorey, 1997). As a consequence, changes in actin organization or in gene expression mediated by Cdc42/Rac are believed to play a pivotal role in the control of cell shape, cell attachment, cell motility and invasion, cell-cell interaction, and cell proliferation and differentiation (Zohn *et al.*, 1998).

In this work, the isolation and initial characterization of the first fungal Rac homolog are described, and evidence is provided indicating that *Yl*Rac1p plays an important role in the regulation of hyphal growth in *Y. lipolytica*. At this time, only two other genes encoding fungal Rac homologs have been identified: *RAC1* from the ectomycorrhiza-forming fungus *Suillus bovinus* (Gorfer *et al.*, 2001) and *RHO5* from *S.*

cerevisiae (Roumanie *et al.*, 2001). Interestingly, *Sc*Rho5p is at 331 amino acids considerably larger than all known Rac proteins, and its deletion has no detectable effects on cell growth or morphology (Roumanie *et al.*, 2001). The cellular roles of both *Sc*Rho5p and *Sb*Rac1p remain to be determined.

Rac GTPases are known to act, in conjunction with Cdc42, Ras and Rho GTPases, in rather complex cascades that integrate the signals received from a variety of surface receptors to a network of pathways with multiple overlaps, feedback loops, and uni- and bidirectional signals in higher eukaryotes (Scita *et al.*, 2000; Symons, 1996; van Aelst and D'Souza-Schorey, 1997; Zohn *et al.*, 1998). In plants, Rac homologs are thought to be involved in the regulation of growth of the pollen tube, a process that shares several characteristics with filamentous growth in fungi. Pollen tube elongation is based on a process known as tip growth, where polarized secretion is restricted to the apex, and cell membrane and cell wall material are delivered exclusively to this location (Kost *et al.*, 1999; Lin *et al.*, 1996; Steer and Steer, 1989; Taylor and Hepler, 1997). Significantly, plant Rac homologs have been shown to be localized to the plasma membrane of the pollen tube in the region of the tip (Lin *et al.*, 1996). The localization of *Yl*Rac1p in *Y. lipolytica* has so far remained elusive. Although an epitope-tagged *Yl*Rac1p could be detected at the growing tip of filamentous *Y. lipolytica* cells, this fusion protein was unable to induce hyphal growth in *rac1Δ* cells, making it impossible to ascertain whether the distribution of the tagged protein was truly representative of that of the natural protein. The availability of antibodies specific for *Yl*Rac1p will be extremely useful in addressing this question.

This work also describes the identification of the *CDC42* homolog of *Y. lipolytica* (Section 4.4). There is accumulating evidence that the Cdc42p GTPase plays an important role in the regulation of several aspects of the generation and/or maintenance of cell polarity in many, if not all, eukaryotic cells (Johnson, 1999). Future work will elucidate if, like in *C. albicans* (Mirbod *et al.*, 1997; Ushinsky *et al.*, 2002), *YlCDC42* is essential for proper polarized growth in yeast and hyphal *Y. lipolytica* cells, and if transcription levels of *YlCDC42* are also altered during the yeast-to-hypha transition in this organism. In addition, it will be interesting to investigate if the mutations *cdc42*^{G12V}, *cdc42*^{Q16L} and *cdc42*^{D118A} have the same morphological effects in *Y. lipolytica* as they do in *S. cerevisiae* (Johnson, 1999; Ziman *et al.*, 1993), and if they are suppressed by *rac1Δ*, *bem1Δ*, *mhy1Δ* and/or *cla4Δ*, a gene recently shown to regulate filamentous growth in *Y. lipolytica* (Szabo, 2001).

The results presented herein also suggest that *YlRAC1* controls some aspects of cell polarization and demonstrate that its function is essential for hyphal, but not for pseudohyphal, growth (Chapter 4). Accordingly, it will be interesting to investigate the genetic interactions among *YlRAC1*, *YlCDC42* and *YlRAS2*, a gene recently shown to be essential for both hyphal and pseudohyphal growth of *Y. lipolytica* (Richard *et al.*, 2001). These studies, combined with the isolation of genes encoding other Rho-like GTPases of *Y. lipolytica*, will be fundamental for an understanding of the mechanisms by which environmental conditions induce changes in the growth pattern of this organism and for the elucidation of the sequence of events regulated by Ras2p, Cdc42p, Rac1p, and other small GTPases in *Y. lipolytica*.

It should be pointed out that, as one of the mechanisms of Ras transformation relies on the signaling cascades controlled by Rac and Rho GTPases and evolutionary trees locate *Y. lipolytica* on an isolated branch clearly separated from *S. pombe* on one hand and from the bulk of other ascomycetous yeasts on the other (Barn *et al.*, 1991; Barth and Gaillardin, 1996; Okuma *et al.*, 1993), *Y. lipolytica* may represent a more suitable model for the understanding of complex morphogenesis events in mammalian cells, with important repercussions for the search for potential drug targets for Ras-mediated malignancies (Joneson and Bar-Sagi, 1999; Symons, 1995; Welch, 1993; Zohn *et al.*, 1998).

7.3 *YlBEM1* and polarization of cell growth in *Y. lipolytica*

In *S. cerevisiae* and *S. pombe*, the homologs of *Yl*Bem1p (*Sc*Bem1p and Scd2p, respectively) are known to interact with several proteins involved in the activation of the small GTPase, Cdc42p, and are assumed to function as scaffolds for proteins involved in the development of cell polarity, pheromone signaling and cytoskeletal organization (Bender *et al.*, 1996; Butty *et al.*, 1998; Chang *et al.*, 1994; 1999; Chant, 1999; Drees *et al.*, 2001; Ito *et al.*, 2001; Leew *et al.*, 1995; Lyons *et al.*, 1996; Matsui *et al.*, 1996; Moskow *et al.*, 2000; Park *et al.*, 1997; Peterson *et al.*, 1994; Zheng *et al.*, 1995). During vegetative growth of *S. cerevisiae*, cortical markers left by previous cell divisions result in recruitment and local activation of the *Sc*Rsr1p GTPase (Michelitch and Chant, 1996), which is subsequently linked to *Sc*Cdc42p via a *Sc*Bem1p-mediated interaction with the guanine-nucleotide-exchange factor, *Sc*Cdc24p (Chant, 1999; Park *et al.*, 1999; Zheng *et*

al., 1995). In addition, *Sc*Bem1p interacts with actin and *Sc*Ste20p (Leew *et al.*, 1995), suggesting that *Sc*Bem1p acts to concentrate active *Sc*Cdc42p at a specific site of the cell membrane, thus promoting both the local activation of the MAP kinase cascade and reorganization of the actin cytoskeleton by *Sc*Ste20p (Section 1.8.1) (Bose *et al.*, 2001; Lorenz *et al.*, 2000a; Moskow *et al.*, 2000). Deletion of *S. cerevisiae BEM1* and *S. pombe scd2* is viable, but the mutants display severe morphological defects and are unable to mate (Chang *et al.*, 1994; Chenevert *et al.*, 1992; Fukui and Yamamoto, 1988). Furthermore, *S. cerevisiae bem1* null mutants are defective in butanol-induced cell elongation and filamentous growth, diploid pseudohyphal growth and haploid invasive growth (Lorenz *et al.*, 2000a).

In this work it is shown that, like its homologs in *S. cerevisiae* and *S. pombe*, *YlBEM1* plays an important role in the establishment of cell polarity in *Y. lipolytica* (Chapter 5). In addition, the expression levels of *YlBEM1* are significantly increased during the dimorphic transition, and its deletion results in complete abolishment of the ability of cells to form hyphae. However, cells of *bem1* null mutants are still able to form pseudohyphae on solid media, suggesting that other polarity proteins are involved in the onset of filamentous growth in *Y. lipolytica* (Section 5.5).

Remarkably, the fusion protein *Yl*Bem1p-GFP was found to concentrate at the mother-bud neck during cytokinesis/septum formation (Section 5.4 and Fig. 5-6) and no role in this process has been reported for *Sc*Bem1p or *Sp*Scd2p to this time. This observation suggests that, in contrast to what is observed for *S. cerevisiae* and *S. pombe*, *Yl*Bem1p may play a role in the reorientation of the actin cytoskeleton towards the mother-

bud neck during cytokinesis/septum formation and, subsequently, in the localized deposition of cell wall material at this location (Section 1.7.5). In addition, although pINA445-based plasmids are believed to be present in two to five copies per cell (Fournier *et al.*, 1993), and this may have some effect on the localization of the chimeric *Yl*Bem1p-GFP, our finding that *bem1Δ* cells are binucleate, significantly larger than wild-type cells, and sometimes exhibit aberrant morphologies in which new buds are seen to emerge from daughter cells before formation of a septum at the mother-daughter neck (Section 5.5 and Fig. 5-8, inset), gives further support to a potential role for *Yl*Bem1p in cytokinesis/septum formation. The isolation of genes encoding septins of *Y. lipolytica* will be essential to determining the possible interactions of *Yl*Bem1p with these proteins and to elucidating the mechanisms of cytokinesis and septum formation in this organism. In addition, co-immunoprecipitation experiments with *Yl*Bem1p will be extremely useful for the identification of other proteins involved in the dimorphic transition of *Y. lipolytica* and septum formation in this organism.

7.4 14-3-3 proteins and the regulation of filamentous growth in *Y. lipolytica*

The results presented herein demonstrate that *Yl*Bmh1p is involved in the regulation of the dimorphic transition in *Y. lipolytica* and suggest that *Yl*Bmh2p may not be involved in this event. Although the exact role of *YlBMH1* and *YlBMH2* in the induction of filamentous growth remains to be elucidated, analysis of their predicted amino acid sequences revealed that *Yl*Bmh1p and *Yl*Bmh2p are closely related to the *S. cerevisiae* 14-3-3 proteins *Sc*Bmh1p and *Sc*Bmh2p, and thus may have similar functions to these two

proteins in *Y. lipolytica* (Fig. 6-4). In *S. cerevisiae*, *BMH1* and *BMH2* are required for Ras/MAPK signaling during pseudohyphal development (Roberts *et al.*, 1997). More precisely, *Sc*Bmh1p and *Sc*Bmh2p act downstream of *Sc*Ras2p and *Sc*Cdc42p, binding directly to *Sc*Ste20p and promoting cell elongation through activation of the transcription factors *Sc*Ste12p and *Sc*Tec1p via the MAP kinases *Sc*Ste11p, *Sc*Ste7p and Kss1p (Roberts *et al.*, 1997). It is noteworthy to mention, however, that 14-3-3 proteins from different species do not appear to have identical functions, and several other features of *Sc*Bmh1p and *Sc*Bmh2p suggest that the role of *Yl*Bmh1p in the regulation of filamentous growth may not be restricted to Ras/MAPK signaling. Thus, 14-3-3 proteins are known to bind to a wide variety of cellular proteins (more than 100 have been described so far), and it is currently believed that they function as direct regulators of enzyme activity and as localization anchors, adapters or scaffolds for numerous cellular processes (Fu *et al.*, 2000; van Hemert *et al.*, 2001a; 2001b). Moreover, *Sc*Bmh1p and *Sc*Bmh2p have been implicated in vesicular transport (Gelperin *et al.*, 1995), and the TOR and cAMP/PKA pathways have been found to negatively control Msn2p and Msn4p nuclear localization through the anchor protein *Sc*Bmh2p (Beck and Hall, 1999; Görner *et al.*, 1998; 2002).

Remarkably, overexpression of *YlBMH1* was observed to enhance pseudohyphal growth in *Y. lipolytica* cells lacking *YlRAC1*, while producing no visible effect in *mhy1Δ* and *bem1Δ* cells (Section 6.7 and Fig. 6-7). This suggests that, in the absence of functional *Yl*Rac1p and, consequently, of the activation of effectors required for hyphal growth, increasing amounts of *Yl*Bmh1p would amplify the output of the remaining signaling pathways (perhaps the Ras/MAP kinase pathway among them) and, hence, increase the

formation of pseudohyphae in the *rac1Δ* strain.

To further define the roles of the 14-3-3 proteins in the regulation of filamentous growth in *Y. lipolytica*, future experiments should be designed to isolate genes encoding other components of the 14-3-3 protein family, as well as to identify proteins that interact with *Yl*Bmh1p and/or *Yl*Bmh2p. It will also be important to determine whether *Yl*Bmh1p interacts with Mhy1p and to investigate if the cAMP/PKA pathway is involved in this interaction.

7.5 *YlSEC31* and hyphal growth in *Y. lipolytica*

In this work, the *YlSEC31* gene was isolated by its ability to enhance hyphal growth when overexpressed in wild-type *Y. lipolytica* cells, thus validating this procedure as a distinct approach to the isolation of genes involved in the regulation of the dimorphic transition in this organism. In addition to allowing for the identification of essential genes involved in the induction of the yeast-to-hypha transition, this method appears to be less time-consuming, because it obviates the need for microscopical analysis of individual colonies after transformation.

Although the exact role of *Yl*Sec31p in the yeast-to-hypha transition of *Y. lipolytica* remains undetermined, a pivotal role for this protein in this process is supported by recent evidence showing that, in *Plasmodium falciparum*, Sec31p is attached to the cytoskeleton (Adisa *et al.*, 2001) and by previous reports of the involvement of several components of the secretory pathway in the regulation of hyphal growth (Lopez *et al.*, 1994; Titorenko *et al.*, 1997). In addition, vectorial secretion in yeast is known to involve the delivery of

secretory vesicles along polarized actin cables (Pruyne and Bretscher, 2000b), and it is generally proposed that increased transport of cell wall material to the growing tip is required for hyphal formation in fungi (Gow, 1994b).

The generation of antibodies to *Yl*Sec31p will be crucial to investigating both the distribution of COPII vesicles and the dynamics of polarized secretion during the induction and maintenance of hyphal growth in *Y. lipolytica.*

7.6 Concluding remarks

During this work, we have uncovered several important regulators of morphogenesis in *Y. lipolytica.* Our results suggest that, as in *C. albicans*, hyphal and pseudohyphal growth are controlled by at least two parallel signaling pathways in *Y. lipolytica*, each with a different and additive input, and that filamentous growth comprises a sequence of events that requires a quantitatively stronger regulatory input to produce hyphae rather than pseudohyphae. However, the complexity of the morphological effects induced by the overexpression of *MHY1*, *YlBEM1*, *YlRAC1*, *YlBMH1* or *YlSEC31* in *mhy1Δ*, *rac1Δ* and *bem1Δ* cells (Table 7-2) indicates that further studies aimed at the identification of other molecular players will be necessary to determine the hierarchy of these regulators in the onset of the dimorphic transition in *Y. lipolytica.*

In closing, the data presented herein extend earlier reports that present *Y. lipolytica* as a suitable alternative model for the study of fungal dimorphism and give additional support to the idea that studies in different organismal systems are required to achieve a complete understanding of the molecular mechanisms that regulate morphogenesis in

fungi. Moreover, our results suggest that *Y. lipolytica* has tremendous potential as a model system for the study of the molecular aspects of stress response and differentiation, two cellular processes with strong implications for the etiology of cancer.

Table 7-2 Morphological Effects of Overexpression of *MHY1*, *YlRAC1*, *YlBEM1*, *YlBMH1* or *YlSEC31* in Various *Y. lipolytica* Strains

	Plasmid / Phenotype					
Strain	no plasmid	pMHY1	pRAC1	pBEM1	pBMH1	pSEC31
E122	Y, PH, H	Y, PH, H^+	Y, PH, H	Y, PH, H	Y, PH, H	Y, PH, H^+
mhy1KO9	Y	Y, PH, H^+	Y	Y	Y	Y
rac1KO30	Y, PH	Y, PH	Y, PH, H	Y, PH, H	Y, PH^+	Y, PH^+
bem1KO157	Y, PH[a]	Y, PH, H[b]	Y, PH, H	Y, PH, H	Y, PH	Y, PH, H

Y = yeast growth.
PH = pseudohyphal growth.
PH^+ = enhanced pseudohyphal growth.
H = hyphal growth.
H^+ = enhanced hyphal growth.
[a] On solid media only.
[b] Highly branched.

CHAPTER 8

BIBLIOGRAPHY

Adams, A.E.M., and J.R. Pringle. 1984. Relationship of actin and tubulin distribution to bud growth in wild-type and morphogenetic-mutant *Saccharomyces cerevisiae*. J. Cell Biol. **98:**934-945.

Adams, A.E.M., and J.R. Pringle. 1991. Staining of actin with fluorochrome-conjugated phalloidin. Methods Enzymol. **194:**729-731.

Adams, A.E.M., D. Johnson, R. Longnecker, B. Sloat, and J.R. Pringle. 1990. *CDC42* and *CDC42*, two additional genes involved in budding and the establishment of cell polarity in the yeast *Saccharomyces cerevisiae*. J. Cell Biol. **111:**131-142.

Adisa, A., F.R. Albano, J. Reeder, M. Foley, and L. Tilley. 2001. Evidence for a role for a *Plasmodium falciparum* homologue of Sec31p in the export of proteins to the surface of malaria parasite-infected erythrocytes. J. Cell Sci. **114:**3377-3386.

Ahn, S.H., A. Acurio, and S. Kron. 1999. Regulation of G2/M progression by the STE mitogen-activated protein kinase pathway in budding yeast filamentous growth. Mol. Biol. Cell **10:**3301-3316.

Akashi, T., T. Kanbe, and K. Tanaka. 1994. The role of the cytoskeleton in the polarized growth of the germ tube in *Candida albicans*. Microbiology. **140:**271-280.

Albertyn, J., S. Hohmann, J.M. Thevelein, and B.A. Prior. 1994. *GPD1*, which encodes glycerol-3-phosphate dehydrogenase, is essential for growth under osmotic stress in *Saccharomyces cerevisiae*, and its expression is regulated by the high-osmolarity glycerol response pathway. Mol. Cell. Biol. **14:**4135-4144.

Alex, L.A., C. Korch, C.P. Selitrennikoff, and M.I. Simon. 1998. *COS1*, a two-component histidine kinase that is involved in hyphal development in the opportunistic pathogen *Candida albicans*. Proc. Natl. Acad. Sci. USA **95:**7069-7073.

Alfa, C.E., and J.S. Hyams. 1990. Distribution of tubulin and actin through the cell division cycle of the fission yeast *Schizosaccharomyces japonicus* var. *versitalis*: comparison with *Schizosaccharomyces pombe*. J. Cell Sci. **96:**71-77.

Alspaugh, J.A., J.R. Perfect, and J. Heitman. 1998. Signal transduction pathways regulating differentiation and pathogenicity of *Cryptococcus neoformans*. Fungal Genet. Biol. **25:**1-14.

Altschul, S.F., W. Gish, W. Miller, E.W. Myers, and D.J. Lipman. 1990. Basic local alignment search tool. J. Mol. Biol. **215:**403-410.

Altschul, S.F., T.L. Madden, A.A. Schaffer, J. Zhang, Z. Zhang, W. Miller, and D.J. Lipman. 1997. Gapped BLAST and PSI-BLAST: a new generation of protein database search programs. Nucleic Acids Res. **25**:3389-3402.

Amberg, D. 1998. Three-dimensional imaging of the yeast actin cytoskeleton through the budding cell cycle. Mol. Biol. Cell **9**:3259-3262.

Amberg, D, J. Zahner, J. Mulholland, J.R. Pringle, and D. Botstein. 1997. Aip3p/Bud6p, a yeast actin-interacting protein that is involved in morphogenesis and the selection of bipolar budding sites. Mol. Biol. Cell **8**:729-753.

Anderson, J.M., and D.R. Soll. 1986. Differences in actin localization during bud and hypha formation in the yeast *Candida albicans*. J. Gen. Microbiol. **132**:2035-2047.

Ansari, K., S. Martin, M. Farkasovsky, I.-M. Ehbrecht, and H. Küntzel. 1999. Phospholipase C binds to the receptor-like *GPR1* protein and controls pseudohyphal differentiation in *Saccharomyces cerevisiae*. J. Biol. Chem. **274**:30052-30058.

Arndt, K., and G.R. Fink. 1986. GCN4 protein, a positive transcription factor in yeast, binds general control promoters at all 5' TGACTC 3' sequences. Proc. Natl. Acad. Sci. USA **83**:8516-8520.

Ausubel, F.J., R. Brent, R.E. Kingston, D.D. Moore, J.G. Seidman, J.A. Smith, and K. Struhl (ed). 1989. Current Protocols in Molecular Biology. Greene Publishing Associates, New York, NY.

Bahn, Y.S., and P. Sundstrom. 2001. *CAP1*, an adenylate cyclase-associated protein gene, regulates bud-hypha transitions, filamentous growth, and cyclic AMP levels and is required for virulence of *Candida albicans*. J. Bacteriol. **183**:3211-3223.

Banuett, F. 1995. Genetics of *Ustilago maydis*, a fungal pathogen that induces tumors in maize. Annu. Rev. Genet. **29**:179-208.

Barbet, N.C., U. Schneider, S.B. Heliwell, I. Stansfield, M.F. Tuite, and M.N. Hall. 1996. TOR controls translation initiation and early G_1 progression in yeast. Mol. Biol. Cell **7**:25-42.

Bardwell, L. J.G. Cook, D. Voora, D.M. Baggott, A.R. Martinez, and J. Thorner. 1998. Repression of yeast Ste12 transcription factor by direct binding of unphosphorylated Kss1 MAPK and its regulation by the Ste7 MEK. Genes Dev. **12**:2887-2898.

Barns, S.M., D.J. Lane, M.L. Sogin, C. Bibeau, and W.G. Weisburg. 1991. Evolutionary relationships among pathogenic *Candida* species and relatives. J. Bacteriol.

173:2250-2255.

Barth, G., and C. Gaillardin. 1996. *Yarrowia lipolytica*, pp. 313-388. *In* K. Wolf (ed.), Non-conventional Yeasts in Biotechnology. A Handbook. Springer-Verlag, New York, NY.

Barth, G., and H. Weber. 1984. Improved conditions for mating of the yeast *Saccharomycopsis lipolytica*. Z. Allg. Mikrobiol. **24:**403-405.

Barth, G., and H. Weber. 1986. Improvement of sporulation in the yeast *Yarrowia lipolytica*. Antonie Leewenhoek J. Microbiol. Serol. **51:**167-177.

Bassel, J., J. Warfel, and R. Mortimer. 1971. Complementation and genetic recombination in *Candida lipolytica*. J. Bacteriol. **108:**609-611.

Beck, T., and M.N. Hall. 1999. The TOR signalling pathway controls nuclear localization of nutrient-regulated transcription factors. Nature **402:**689-692.

Beck-Sague, C., and W.R. Jarvis. 1993. Secular trends in the epidemiology of nosocomial fungal infections in the United States, 1980-1990. National Nosocomial Infections Surveillance System. J. Infect. Dis. **167:**1247-1251.

Beckerich, J.-M., B.C. Cecealdi, M. Lambert, and M. Heslot. 1984. Evidence for the control of a mutation in lysine catabolism by the counting type in *Yarrowia lipolytica*. Curr. Genet. **8:**531-536.

Beckerich, J.-M., A. Boisramé-Baudevin, and C. Gaillardin. 1998. *Yarrowia lipolytica*: a model organism for protein secretion studies. Int. Microbiol. **1:**123-130.

Benachour, A., G. Sipos, I. Flury, F. Reggiori, E. Canivenc-Gansel, C. Vionnet, A. Conzelmann, and M. Benghezal. 1999. Deletion of *GPI7*, a yeast gene required for addition of a side chain to the glycosylphosphatidylinositol (GPI) core structure, affects GPI protein transport, remodeling, and cell wall integrity. J. Biol. Chem. **274:**15251-15261.

Bender, L., H.S. Lo, H. Lee, V. Kokojan, J. Peterson, and A. Bender. 1996. Associations among PH and SH3 domain-containing proteins and Rho-type GTPases in yeast. J. Cell Biol. **133:**879-894.

Benton, B., A. Tinkelenberg, I. Gonzalez, and F. Cross. 1997. Cla4p, a *Saccharomyces cerevisiae* Cdc42p-activated kinase involved in cytokinesis, is activated at mitosis. Mol. Cell. Biol. **17:**5067-5076.

Bi, E., and J.R. Pringle. 1996. *ZDS1* and *ZDS2*, genes whose products may regulate Cdc42p in *Saccharomyces cerevisiae*. Mol. Cell. Biol. **16:**5264-5275.

Bockmuhl, D.P., and J.F. Ernst. 2001. A potential phosphorylation site for an A-type kinase in the Efg1 regulator protein contributes to hyphal morphogenesis of *Candida albicans*. Genetics **157:**1523-1530.

Bockmuhl, D.P., S. Krishnamurthy, M. Gerads, A. Sonneborn, and J.F. Ernst. 2001. Distinct and redundant roles of the two protein kinase A isoforms Tpk1p and Tpk2p in morphogenesis and growth of *Candida albicans*. Mol. Microbiol. **42:**1243-1257.

Bonner, W.M., and R.A. Laskey. 1974. A film detection method for tritium-labelled proteins and nucleic acids in polyacrylamide gels. Eur. J. Biochem. **46:**83-88.

Boone, C.M., A.-M. Sdicu, M. Laroche, and H. Bussey. 1991. Isolation from *Candida albicans* of a functional homolog of the *Saccharomyces cerevisiae KRE1* gene, which is involved in cell wall β-glucan synthesis. J. Bacteriol. **173:**6859-6864.

Bose, I., J.E. Irazoqui, J.J. Moskow, E.S. Bardes, T.R. Zyla, and D.J. Lew. 2001. Assembly of scaffold-mediated complexes containing Cdc42p, the exchange factor Cdc24p, and the effector Cla4p required for cell cycle-regulated phosphorylation of Cdc24p. J. Biol. Chem. **276:**7176-7186.

Boylan, M.T., P.M. Mirabito, C.E. Willett, C.R. Zimmerman, and W.E. Timberlake. 1987. Isolation and physical characterization of three essential conidiation genes from *Aspergillus nidulans*. Mol. Cell. Biol. **7:**3113-3118.

Brade, A.M. 1992. Peroxisome assembly in *Yarrowia lipolytica*. M.Sc. Thesis, McMaster University, Hamilton, Ontario, Canada.

Bradford, M.M. 1976. A rapid and sensitive method for the quantitation of microgram quantities of protein using the principle of protein-dye binding. Ana. Biochem. **72:**248-254.

Braun, B.R., and A.D. Johnson. 1997. Control of filament formation in *Candida albicans* by the transcriptional repressor *TUP1*. Science **277:**105-109.

Braun, B.R., and A.D. Johnson. 1997. *TUP1*, *CPH1* and *EFG1* make independent contributions to filamentation in *Candida albicans*. Genetics **155:**57-67.

Braun, B.R., W.S. Head, M.X. Wang, and A.D. Johnson. 2000. Identification and characterization of *TUP1*-regulated genes in *Candida albicans*. Genetics **156:**31-44.

Brewster, J.L., T. de Valoir, N.D. Dwyer, E. Winter, and M.C. Gustin. 1993. An osmosensing signal transduction pathway in yeast. Science **259:**1760-1763.

Brown, A.J.P., and N.A.R. Gow. 1999. Regulatory networks controlling *Candida albicans* morphogenesis. Trends Microbiol. **7:**333-338.

Brown, J., M. Jaquenoud, M.P. Gulli, J. Chant, and M. Peter. 1997. Novel Cdc42-binding proteins Gic1 and Gic2 control cell polarity in yeast. Genes Dev. **11:**2972-2982.

Brown, Jr., D.H., A.D. Giusani, X. Chen, and C.A. Kumamoto. 1999. Filamentous growth of *Candida albicans* in response to physical environmental cues and its regulation by the unique *CZF1* gene. Mol. Microbiol. **34:**651-662.

Bruatto, M., M. Gremmi, A. Nardacchione, and M. Amerio. 1993. Effect of glucose starvation on germ-tube production by *Candida albicans*. Mycopathologia **123:**105-110.

Brummer, E., E. Castaneda, and A. Restrepo. 1993. Paracoccidioidomycosis: an update. Microbiol. Rev. **6:**89-117.

Buckholz, R.H., and M.A. Gleeson. 1991. Yeast systems for the commercial production of heterologous proteins. Biotechnology **9:**1067-1072.

Buffo, J., M.A. Herman, and D.R. Soll. 1984. A characterization of pH-regulated dimorphism in *Candida albicans*. Mycopathologia **85:**21-30.

Bürglin, T.R. 1991. The TEA domain: a novel, highly conserved DNA-binding motif. Cell **66:**11-12.

Butty, A.-C., P.M. Pryciak, L.S. Huang, I. Herkowitz, and M. Peter. 1998. The role of Far1p in linking the heterotrimeric G protein to polarity establishment proteins during yeast mating. Science **282:**1511-1516.

Byers, B. 1981. Cytology of the yeast life cycle, pp. 59-96. *In* Strathern, J., E. Jones, and J. Broach (ed.), The Molecular Biology of the Yeast *Saccharomyces*: Life Cycle and Inheritance. Cold Spring Harbor Laboratory, Cold Spring Harbor, NY.

Cabib, E., and M.S. Kang. 1987. Fungal 1,3-β-glucan synthase. Methods Enzymol. **138:**637-642.

Cabib, E., R. Ulane, and B. Bowers. 1974. A molecular model for morphogenesis: the primary septum of yeast. Curr. Top. Cell Regul. **8:**1-32.

Calderone, R.A. 1993. Recognition between *Candida albicans* and host cells. Trends Microbiol. **1**:55-58.

Casaregola, S., C. Neuvéglise, A. Lépingle, E. Bon, C. Feynerol, F. Artiguenave, P. Wincker, and C. Gaillardin. 2000. Genomic exploration of the hemiascomycetous yeasts: 17. *Yarrowia lipolytica*. FEBS Lett. **487**:95-100.

Chaffin, W.L. 1984. Site selection for bud and germ tube emergence in *Candida albicans*. J. Gen. Microbiol. **130**:431-440.

Chandarlapaty, S., and B. Errede. 1998. Ash1, a daughter-specific protein, is required for pseudohyphal growth of *Saccharomyces cerevisiae*. Mol. Cell. Biol. **18**:2884-2891.

Chang, E.C., M. Barr, Y. Wang, V. Jung, H.P. Xu, and M.H. Wigler. 1994. Cooperative interaction of *Schizosaccharomyces pombe* proteins required for mating and morphogenesis. Cell **79**:131-141.

Chang, E.C., G. Bartholomeusz, R. Pimental, J. Chen, H. Lai, L.L. Wang, P. Yang, and S. Marcus. 1999. Direct binding and in vivo regulation of the fission yeast p21-activated kinase Shk1 by the SH3 domain protein Scd2. Mol. Cell. Biol. **19**:8066-8074.

Chant, J. 1999. Cell polarity in yeast. Annu. Rev. Cell Dev. Biol. **15**:365-391.

Chant, J., and J.R. Pringle. 1991. Budding and cell polarity in *Saccharomyces cerevisiae*. Curr. Opin. Genet. Dev. **1**:342-350.

Chant, J., M. Mischke, E. Mitchell, I. Herkowitz, and J.R. Pringle. 1995. Role of Bud3p in producing the axial bud pattern of yeast. J. Cell Biol. **129**:767-778.

Chant, J., and J.R. Pringle. 1995. Patterns of bud-site selection in the yeast *Saccharomyces cerevisiae*. J. Cell Biol. **129**:751-765.

Chen, G.C., Y.J. Kim, and C. Chan. 1997. The Cdc42 GTPase-associated proteins Gic1 and Gic2 are required for polarized cell growth in *Saccharomyces cerevisiae*. Genes Dev. **11**:2958-2971.

Chen, J., S. Zhou, Q. Wang, X. Chen, T. Pan, and H. Liu. 2000. Crk1, a novel Cdc2-related protein kinase, is required for hyphal development and virulence in *Candida albicans*. Mol. Cell. Biol. **20**:8696-8708.

Chen, W., H.H. Lim, and L. Lim. 1993. The *CDC42* homologue from *Caenorhabditis elegans*. J. Biol. Chem. **268**:13280-13285.

Chenevert, J., K. Corrado, A. Bender, J. Pringle, and I. Herskowitz. 1992. A yeast gene (*BEM1*) necessary for cell polarization whose product contains two SH3 domains. Nature **356:** 77-79.

Chevaillier, P. 1993. PEST sequences in nuclear proteins. Int. J. Biochem. **25:**479-482.

Cid, V.J., A. Duran, F. del Rey, M.P. Snyder, C. Nombela, and M. Sanchez. 1995. Molecular basis of cell integrity and morphogenesis in *Saccharomyces cerevisiae*. Microbiol. Rev. **59:**345-386.

Cognetti, D., D. Davis, and J. Sturtevant. 2002. The *Candida albicans* 14-3-3 gene, *BMH1*, is essential for growth. Yeast **19:**55-67.

Colombo, S., P. Ma, L. Cauwenberg, J. Winderickx, M. Crauwels, A. Teunissen, D. Nauwelaers, J.H. de Winde, M.-F. Gorwa, D. Colavizza, and J.M. Thevelein. 1998. Involvement of distinct G-proteins, Gpa2 and Ras, in glucose- and intracellular acidification-induced cAMP signaling in the yeast *Saccharomyces cerevisiae*. EMBO J. **17:**3326-3341.

Cook, J.G., L. Bardwell, S.J. Kron, and J. Thorner. 1996. Two novel targets of the MAP kinase Kss1 are negative regulators of invasive growth in the yeast *Saccharomyces cerevisiae*. Genes Dev. **10:**2831-2848.

Cook, J.G., L. Bardwell, and J. Thorner. 1997. Inhibitory and activating functions for MAPK Kss1 in the *Saccharomyces cerevisiae* filamentous-growth signaling pathway. Nature **390:**85-88.

Csank, C., K. Schroppel, E. Leberer, D., Harcus, I.D., O Mohamed, S. Meloche, D.Y. Thomas, and M. Whiteway. 1998. Roles of the *Candida albicans* mitogen-activated protein kinase homolog, Cek1p, in hyphal development and systematic candidiasis. Infect. Immun. **66:**2713-2721.

Cutler, J.E. 1991. Putative virulence factors of *Candida albicans*. Annu. Rev. Microbiol. **45:**187-218.

Cutler, N.S., X. Pan, J. Heitman, and M.E. Cardenas. 2001. The TOR signal transduction cascade controls cellular differentiation in response to nutrients. Mol. Biol. Cell **12:**4103-4113.

Cvrckova, F., C. De Virgilio, E. Manser, J.R. Pringle, and K. Nasmyth. 1995. Ste20-like protein kinases are required for normal localization of cell growth and for cytokinesis in budding yeast. Genes Dev. **9:**1817-1830.

Dabrova, N., S.S. Taxer, and D.H. Howard. 1976. Germination of *Candida albicans* induced by proline. Infect. Immun. **13:**830-835.

Daly, S., A. Yacoub, W. Dundon, G. Mastromei, K. Islam, and R. Lorenzetti. 1997. Isolation and characterization of a gene encoding α-tubulin from *Candida albicans*. Gene **187:**151-158.

Davidow, L.S., D. Apostolakos, M.M. O'Donnell, A.R. Proctor, D.M. Ogrydziak, R.A. Wing, I. Stasko, and J.R. DeZeeuw. 1985. Integrative transformation of the yeast *Yarrowia lipolytica*. Curr. Genet. **10:**39-48.

Davis, D., R.B. Wilson, and A.P. Mitchell. 2000. *RIM101*-dependent and -independent pathways govern pH responses in *Candida albicans*. Mol. Cell. Biol. **20:**971-978.

Delmer, D.P., J.P. Pear, A. Andrawis, and D.M. Stalker. 1995. Genes encoding small GTP-binding proteins analogous to mammalian rac are preferentially expressed in developing cotton fibers. Mol. Gen. Genet. **248:**43-51.

De Marini, D., A. Adams, H. Fares, C. De Virgilio, G. Valle, J. Chuang, and J.R. Pringle. 1997. A septin-based hierarchy of proteins required for localized deposition of chitin in the *Saccharomyces cerevisiae* cell wall. J. Cell Biol. **139:**75-93.

de Nobel, J.G., and J.A. Barnett. 1991. Passage of molecules through yeast cell walls: a brief essay-review. Yeast **7:**313-323.

DeRisi, J. L., V. R. Iyer, and P. O. Brown. 1997. Exploring the metabolic and genetic control of gene expression on a genomic scale. Science **278:**680-686.

de Sampaio, G., J.P. Bourdineaud, and G.J. Lauquin. 1999. A constitutive role for GPI anchors in *Saccharomyces cerevisiae*: cell wall targeting. Mol. Microbiol. **34:**247-256.

Dever, T.E., M.J. Glynias, and W.C. Merrick. 1987. GTP-binding domain: three consensus sequence elements with distinct spacing. Proc. Natl. Acad. Sci. USA **84:**1814-1818.

Di Como, C.J., and K.T. Arndt. 1996. Nutrients, via the Tor proteins, stimulate the association of Tap42 with 2A phosphatases. Genes Dev. **10:**1904-1916.

Dominguez, A., E. Fermiñán, and C. Gaillardin. 2000. *Yarrowia lipolytica*: an organism amenable to genetic manipulation as a model for dimorphism in fungi. Contrib. Microbiol. **5:**151-172.

Doolin, M.-T., A.L. Johnson, L.H. Johnston, and G. Butler. 2001. Overlaping and distinct roles of the duplicated yeast transcription factors Ace2p and Swi5p. Mol. Microbiol. **40:**422-432.

Drees, B.L., B. Sundin, E. Brazeau, J.P. Caviston, G.-C. Chen, W. Guo, K.G. Kozminski, M.W. Lau, J.J. Moskow, A. Tong, L.R. Schenkman, A. McKenzie III, P. Brennwald, M. Longtime, E. Bi, C. Chan, P. Novick, C. Boone, J.R. Pringle, T.N. Davis, S. Fields, and D.G. Dubrin. 2001. A protein interaction map for cell polarity development. J. Cell Biol. **154:**549-571.

Dutton, J.R., S. Johns, and B.L. Miller. 1997. StuAp is a sequence-specific transcription factor that regulates developmental complexity in *Aspergillus nidulans*. EMBO J. **16:**5710-5721.

Eby, J., S. Holly, F. van Drogan, A. Grishin, M. Peter, D. Drubin, and K. Blumer. 1998. Actin cytoskeleton organization regulated by the PAK family of protein kinases. Curr. Biol. **8:**967-970.

Edgington, N., M. Blacketer, T. Bierwagen, and A. Myers. 1999. Control of *Saccharomyces cerevisiae* filamentous growth by cyclin-dependent kinase Cdc28. Mol. Cell. Biol. **19:**1396-1380.

Edskes, H.K., J.A. Hanover, and R.B. Wickner. 1999. Mks1p is a regulator of nitrogen catabolism upstream of Ure2p in *Saccharomyces cerevisiae*. Genetics **153:**585-594.

Eitzen, G.A., J.A. Aitchison, R.K. Szilard, M. Veenhuis, W.M. Nuttley, and R.A. Rachubinski. 1995. The *Yarrowia lipolytica* gene *PAY2* encodes a 42-kDa peroxisomal integral membrane protein essential for matrix protein import and peroxisome enlargement but not for peroxisome membrane proliferation. J. Biol. Chem. **270:**1429-1436.

Eitzen, G.A., V.I. Titorenko, J.J. Smith, M. Veenhuis, R.K. Szilard, and R.A. Rachubinski. 1996. The *Yarrowia lipolytica* gene *PAY5* encodes a peroxisomal integral membrane protein homologous to the mammalian peroxisome assembly factor PAF-1. J. Biol. Chem. **271:**20300-20306.

Eitzen, G.A., R.K. Szilard, and R.A. Rachubinski. 1997. Enlarged peroxisomes are present in oleic-acid grown *Yarrowia lipolytica* overexpressing the *PEX16* gene encoding an intraperoxisomal peripheral membrane peroxin. J. Cell Biol. **137:**1265-1278.

Enderlin, C.S., and D.M. Ogrydziak. 1994. Cloning, nucleotide sequence and functions of XPR6, which codes for a dibasic processing endoprotease from the yeast *Yarrowia lipolytica*. Yeast **10:**67-79.

Ernst, J.F. 2000. Transcription factors in *Candida albicans* - environmental control of morphogenesis. Microbiology **146:**1763-1774.

Estruch, F. 2000. Stress-controlled transcription factors, stress-induced genes and stress tolerance in budding yeast. FEMS Microbiol. Rev. **24:**469-486.

Evangelista, M., K. Blundell, M. Longtime, C. Chow, N. Adames, J.R. Pringle, M. Peter, and C. Boone. 1997. Bni1p, a yeast formin linking Cdc42p and the actin cytoskeleton during polarized morphogenesis. Science **276:**118-121.

Farbood, M.I., and B.J. Willis. 1985. Production of γ-decalactone. US patent 4,560,656.

Feng, Q., E. Summers, B. Guo, and G. Fink. 1999. Ras signaling is required for serum-induced hyphal differentiation in *Candida albicans*. J. Bacteriol. **181:**6339-6346.

Ferré-D'Amaré, A., G. C. Prendergast, E. B. Ziff, and S. K. Burley. 1993. Recognition by Max of its cognate DNA through a dimeric b/HLH/Z domain. Nature **363:**38-45.

Field, C., R. Li, and K. Oegema. 1999. Cytokinesis in eukaryotes: a mechanistic comparison. Curr. Opin. Cell Biol. **11:**68-80.

Fonzi, W.A. 1999. *PHR1* and *PHR2* of *Candida albicans* encode putative glycosidases required for proper cross-linking of β-1,3- and β-1,6-glucans. J. Bacteriol. **181:**7070-7079.

Ford, J.C., F. al-Khodairy, E. Fotou, K.S. Sheldrick, D.J. Griffiths, and A.M. Carr. 1994. 14-3-3 homologs required for the DNA damage checkpoint in fission yeast. Science **265:**533-535.

Forsberg, H., and P.O. Ljungdahl. 2001. Genetic and biochemical analysis of the yeast plasma membrane Ssy1p-Ptr3p-Ssy5p sensor of extracellular amino acids. Mol. Cell. Biol. **21:**814-826.

Fournier, P., A. Abbas, M. Chasles, B. Kudla, D.M. Ogrydziak, D. Yaver, J.-W. Xuan, A. Peito, A.-M. Ribet, C. Feynerol, F. He, and C. Gaillardin. 1993. Colocalization of centromeric and replicative functions on autonomously replicating sequences from the yeast *Yarrowia lipolytica*. Proc. Natl. Acad. Sci. USA **90:**4912-4916.

Frankel, A.D., and P.S. Kim. 1991. Modular structure of transcription factors: implications for gene regulation. Cell **65:**717-719.

Frost, D.J., K. Brandt, J. Capobianco, and R. Goldman. 1994. Characterization of

(1,3)-β-glucan synthase in *Candida albicans*: microsomal assay from the yeast or mycelial morphological forms and a permeabilized whole-cell assay. Microbiology **140:**2239-2246.

Fu, Y.-H., and G.A. Marzluf. 1990. nit-2, the major positive-acting nitrogen regulatory gene of *Neurospora crassa*, encodes a sequence-specific DNA-binding protein. Proc. Natl. Acad. Sci. USA **87:**5331-5335.

Fu, H., R.R. Subramanian, and S.C. Masters. 2000. 14-3-3 proteins: structure, function, and regulation. Annu. Rev. Pharmacol. Toxicol. **40:**617-647.

Fujita, A., A. Tonouchi, T. Hiroko, F. Inose, T. Nagashima, R. Satoh, and S. Tanaka. 1999. Hsl7p, a negative regulator of Ste20p protein kinase in the *Saccharomyces cerevisiae* filamentous growth-signaling pathway. Proc. Natl. Acad. Sci. USA **96:**8522-8527.

Fukui, Y., and M. Yamamoto. 1988. Isolation and characterization of *Schizosaccharomyces pombe* mutants phenotypically similar to *ras1*. Mol. Gen. Genet. **215:**26-31.

Gagiano, M., D. van Dyk, F.F. Bauer, M.G. Lambrechts, and I.S. Pretorius. 1999a. Divergent regulation of the evolutionarily closely related promoters of the *Saccharomyces cerevisiae STA2* and *MUC1* genes. J. Bacteriol. **181:**6497-6508.

Gagiano, M., D. Van Dyk, F.F. Bauer, M.G. Lambrechts, and I.S. Pretorius. 1999b. Msn1p/Mss10p, Mss11p and Muc1p/Flo11p are part of a signal transduction pathway downstream of Mep2p regulating invasive growth and pseudohyphal differentiation in *Saccharomyces cerevisiae*. Mol. Microbiol. **31:**103-116.

Gaillardin, C.M., and H. Heslot. 1988. Genetic engineering in *Yarrowia lipolytica*. J. Basic Microbiol. **28:**161-174.

Gaillardin, C.M., V. Charoy, and H. Heslot. 1973. A study of copulation, sporulation and meiotic segregation in *Candida lipolytica*. Arch. Mikrobiol. **92:**69-83.

Gale, C.A., C.M. Bendel, M. McClellan, M. Hauser, J.M. Becker, J. Berman, and M.K. Hostetter. 1998. Linkage of adhesion, filamentous growth, and virulence in *Candida albicans* to a single gene, *INT1*. Science **279:**1355-1358.

Gancedo, J.M. 2001. Control of pseudohyphae formation in *Saccharomyces cerevisiae*. FEMS Microbiol. Rev. **25:**107-123.

Garcia-Ranea, J.A., and A. Valencia. 1998. Distribution and functional diversification

of the ras superfamily in *Saccharomyces cerevisiae*. FEBS Lett. **434:**219-225.

Geli, M.I., and H. Riezman. 1996. Role of type I myosins in receptor-mediated endocytosis in yeast. Science **272:**533-535.

Gelperin, D., J. Weigle, K. Nelson, P. Roseboom, K. Irie, K. Matsumoto, and S. Lemmon. 1995. 14-3-3 proteins: potential roles in vesicular transport and Ras signaling in *Saccharomyces cerevisiae*. Proc. Natl. Acad. Sci. USA. **92:**11539-11543.

Georgopapadakou, N.H., and J.S. Tkacz. 1995. The fungal cell wall as a drug target. Trends Microbiol. **3:**98-104.

Gimeno, C.J., and G.R. Fink. 1994. Induction of pseudohyphal growth by overexpression of *PHD1*, a *Saccharomyces cerevisiae* gene related to transcriptional regulators of fungal development. Mol. Cell. Biol. **14:**2100-2112.

Gimeno, C.J., P.O. Ljungdahl, C.A. Styles, and G.R. Fink. 1992. Unipolar cell divisions in the yeast *S. cerevisiae* lead to filamentous growth: regulation by starvation and RAS. Cell **68:**1077-1090.

Gleeson, M.A., and P.E. Sudbery. 1988. Genetic analysis in the methylotrophic yeast *Hansenula polymorpha*. Yeast **4:**293-303.

Goldstein, A.L., C.A. Snay, C.V. Heath, and C.N. Cole. 1996. Pleiotropic nuclear defects associated with a conditional allele of the novel nucleoporin Rat9p/Nup85p. Mol. Biol. Cell **7:**917-934.

Goldstein, L.S.B. 1991. The kinesin superfamily: tails of functional redundancy. Trends Cell Biol. **1:**93-98.

Gonzalez-Lopez, C.I., R. Szabo, S. Blanchin-Roland, and C. Gaillardin. 2002. Genetic control of extracellular protease synthesis in the yeast *Yarrowia lipolytica*. Genetics **160:**417-427.

Gooday, G.W. 1994. Cell walls, pp. 43-62. *In* N.A.R. Gow and G.M. Gadd (ed.), The Growing Fungus. Chapman & Hall, London, United Kingdom.

Gorfer, M., M.T. Tarkka, M. Hanif, A.G. Pardo, E. Laitiainen, and M. Raudaskoski. 2001. Characterization of small GTPases Cdc42 and Rac and the relationship between Cdc42 and actin cytoskeleton in vegetative and ectomycorrhizal hyphae of *Suillus bovinus*. Mol. Plant Microbe Interact. **14:**135-144.

Görner, W., E. Durchschlag, M.T. Martinez-Pastor, F. Estruch, G. Ammerer, B. Hamilton, H. Ruis, and C. Schüller. 1998. Nuclear localization of the C_2H_2 zinc finger protein Msn2p is regulated by stress and protein kinase A activity. Genes Dev. **12:**586-597.

Görner, W., E. Durchschlag, J. Wolf, E.L. Brown, G. Ammerer, H. Ruis, and C. Schüller. 2002. Acute glucose starvation activates the nuclear localization signal of a stress-specific yeast transcription factor. EMBO J. **21:**135-144.

Gounalaki, N., and G. Thireos. 1994. Yap1p, a yeast transcriptional activator that mediates multidrug resistance, regulates the metabolic stress response. EMBO J. **13:**4036-4041.

Gow, N.A.R. 1994a. Growth and guidance of the fungal hypha. Microbiology **140:**3193-3205.

Gow, N.A.R. 1994b. Tip growth and polarity, pp. 277-299. *In* N.A.R. Gow and G.M. Gadd (ed.), The Growing Fungus. Chapman & Hall, London, United Kingdom.

Gow, N.A.R. 1994c. Yeast-hyphal dimorphism, pp. 403-422. *In* N.A.R. Gow and G.M. Gadd (ed.), The Growing Fungus. Chapman & Hall, London, United Kingdom.

Gow, N.A.R., and G.W. Gooday. 1984. A model for the germination and mycelial growth form of *Candida albicans*. Sabouraudia **22:**137-142.

Gow, N.A.R., G. Henderson, and G.W. Gooday. 1986. Cytological interrelationships between the cell cycle and the duplication cycle of *Candida albicans*. Microbios **47:**97-105.

Guevara-Olvera, L., C. Calvo-Mendez, and J. Ruiz-Herrera. 1993. The role of polyamine metabolism in dimorphism of *Yarrowia lipolytica*. J. Gen. Microbiol. **193:**485-493.

Gustin, M.C., J. Albertyn, M. Alexander, and K. Davenport. 1998. MAP kinase pathways in the yeast *Saccharomyces cerevisiae*. Microbiol. Mol. Biol. Rev. **62:**1264-1300.

Hackney, D.D. 1996. The kinetic cycles of myosin, kinesin and dynein. Ann. Rev. Physiol. **58:**731-750.

Hall, A. 1994. Small GTP-binding proteins and the regulation of the actin cytoskeleton. Annu. Rev. Cell. Biol. **10:**31-54.

Hall, A. 1998. Rho GTPases and the actin cytoskeleton. Science **279:**509-514.

Hancock, J.F., A.I. Magee, J.E. Childs, and C.J. Marshall. 1989. All ras proteins are polyisoprenylated but only some are palmitoylated. Cell **57:**1167-1177.

Hanish, J., and M. McClelland. 1988. Activity of DNA modification and restriction enzymes in KGB, a potassium glutamate buffer. Gene Anal. Tech. **5:**105-107.

Harold, F.M. 1990. To shape a cell: an inquiry into the causes of morphogenesis of microorganisms. Microbiol. Rev. **54:**381-431.

Harshman, K.D., W.S. Moye-Rowley, and C.S. Parker. 1988. Transcriptional activation by the SV40 AP-1 recognition element in yeast is mediated by a factor similar to AP-1 that is distinct from GCN4. Cell **53:**321-330.

Hauser, M., A.M. Donhardt, D. Barnes, F. Naider, and J.M. Becker. 2000. Enkephalins are transported by a novel eukaryotic peptide uptake system. J. Biol. Chem. **275:**3037-3041.

Heath, I.B. 1987. Preservation of a labile cortical array of actin microfilaments in growing hyphal tips of the fungus *Saprolegnia ferax*. Eur. J. Cell Biol. **44:**10-16.

Heath, I.B. 1994. The cytoskeleton, pp. 100-134. *In* N.A.R. Gow and G.M. Gadd (ed.), The Growing Fungus. Chapman & Hall, London, United Kingdom.

Helliwell, S.B., I. Howald, N. Barbet, and M.N. Hall. 1998. *TOR2* is part of two related signaling pathways coordinating cell growth in *Saccharomyces cerevisiae*. Genetics **148:**99-112.

Herrero, A.B., M.C. Lopez, L. Fernandez-Lago, and A. Dominguez. 1999. *Candida albicans* and *Yarrowia lipolytica* as alternative models for analyzing budding patterns and germ tube formation in dimorphic fungi. Microbiology **145:**2727-2737.

Herscovics, A., and P. Orlean. 1993. Glycoprotein biosynthesis in yeast. FASEB J. **52:**540-553.

Ho, J., and A. Bretscher. 2001. Ras regulates the polarity of the yeast actin cytoskeleton through the stress response pathway. Mol. Biol. Cell **12:**1541-1555.

Hoey, T., R. O. J. Weinzierl, G. Gill, J. -L. Chen, B. D. Dynlacht, and R. Tjian. 1993. Molecular cloning and functional analysis of *Drosophila* TAF110 reveal properties expected of coactivators. Cell **72:**247-260.

Hogan, L.H., B.S. Klein, and S.M. Levitz. 1996. Virulence factors of medically inportant fungi. Clin. Microbiol. Rev. **9:**469-488.

Holly, S., and K. Blumer. 1999. PAK-family kinases regulate cell and actin polarization throughout the cell cycle of *Saccharomyces cerevisiae*. J. Cell Biol. **147:**845-856.

Horisberger, M., and M. Vonlanthen. 1977. Localization of mannan and chitin on thin sections of budding yeasts with gold markers. Arch. Microbiol. **115:**1-7.

Huynh, T.V., R.A. Young, and R.W. Davis. 1988. DNA cloning, Vol. I, pp. 49-78. *In* D.M. Glover (ed.), DNA Cloning: A Practical Approach. IRL Press, Oxford, United Kingdom.

Imamura, H., K. Tanaka, T. Hihara, M. Umikawa, T. Kamei, K. Takahashi, T. Sasaki, and Y. Takai. 1997. Bni1p and Bnr1p: downstream targets of the Rho family small G-proteins which interact with profilin and regulate actin cytoskeleton in *Saccharomyces cerevisiae*. EMBO J. **15:**2745-2755.

Ishii, N., M. Yamamoto, F. Yoshihara, M. Arisawa, and Y. Aoki. 1997. Biochemical and genetic characterization of Rbf1p, a putative transcription factor of *Candida albicans*. Microbiology **143:**429-435.

Ito, T., Y. Matsui, T. Ago, K. Ota, and H. Sumimoto. 2001. Novel modular domain PB1 recognizes PC motif to mediate functional protein-protein interactions. EMBO J. **20:**3938-3946.

Jans, D. A., and S. Hübner. 1996. Regulation of protein transport to the nucleus: central role of phosphorylation. Physiol. Rev. **76:**651-685.

Johnson, D.I. 1999. Cdc42: an essential Rho-type GTPase controlling eukaryotic cell polarity. Microbiol. Mol. Biol. Rev. **63:**54-105.

Johnson, D.I. and J.R. Pringle. 1990. Molecular characterization of *CDC42*, a *Saccharomyces cerevisiae* gene involved in the development of cell polarity. J. Cell Biol. **111:**143-152.

Joneson, T., and D. Bar-Sagi. 1999. Suppression of Ras-induced apoptosis by the Rac GTPase. Mol. Cell. Biol. **19:**5892-5901.

Kang, P.J., A. Sanson, B. Lee, and H.O. Park. 2001. A GDP/GTP exchange factor involved in linking a spatial landmark to cell polarity. Science **292:**1376-1378.

Kaufer, N.F., and J. Potashkin. 2000. Analysis of the splicing machinery in fission yeast: a comparison with budding yeast and mammals. Nucleic Acids Res. **28:**3003-3010.

Khalaf, R.A., and R.S. Zitomer. 2001. The DNA binding protein Rfg1 is a repressor of filamentation in *Candida albicans*. Genetics **157:**1503-1512.

Kim, J., S.A. Cheon, S. Park, Y. Song, and J.-Y. Kim. 2000. Serum-induced hypha formation in the dimorphic yeast *Yarrowia lipolytica*. FEMS Microbiol. Lett. **190:**9-12.

Kimura, L.H., and N.N. Pearsall. 1980. Relationship between germination of *Candida albicans* and increased adherence to human bucal epithelial cells. Infect. Immun. **28:**464-468.

Kishi, T., and F. Yamao. 1998. An essential function of Grr1 for the degradation of Cln2 is to act as a binding core that links Cln2 to Skp1. J. Cell Sci. **111:**3655-3661.

Klis, F.M. 1994. Cell wall assembly in yeast. Yeast **10:**851-869.

Kobayashi, N., and K. McEntee. 1993. Identification of *cis* and *trans* components of a novel heat shock stress regulatory pathway in *Saccharomyces cerevisiae*. Mol. Cell. Biol. **13:**248-256.

Koch, G., K. Tanaka, T. Matsuda, W. Yamochi, H. Nonaka, and Y. Takai. 1997. Association of the Rho family small GTP-binding proteins with Rho GDP dissociation inhibitor (Rho GDI) in *Saccharomyces cerevisiae*. Oncogene **15:**417-422.

Kohno, H., K. Tanaka, A. Mino, M. Umikawa, H. Imamura, T. Fukiwara, Y. Fujita, K. Hotta, H. Qadota, T. Watanabe, Y. Ohya, and Y. Takai. 1996. Bni1p implicated in cytoskeletal control is a putative target of Rho1p small GTP binding protein in *Saccharomyces cerevisiae*. EMBO J. **15:**6060-6068.

Kolodziej, P.A., and R.A. Young. 1991. Epitope tagging and protein surveillance. Methods Enzymol. **194:**508-519.

Kopecka, M., H.J. Phaff, and G.H. Fleet. 1974. Demonstration of a fibrillar component in the cell wall of the yeast *Saccharomyces cerevisiae* and its chemical nature. J. Cell Biol. **62:**66-76.

Kost, B., E. Lemichez, P. Spielhofer, Y. Hong, K. Tolias, C. Carpenter, and N.-H. Chua. 1999. Rac homologues and compartmentalized phosphatidylinositol 4,5-bisphosphate act in a common pathway to regulate polar pollen tube growth. J. Cell. Biol. **145:**317-330.

Kraakman, L., K. Lemaire, P. Ma, A.W.R.H. Teunissen, M.C.V. Donaton, P. van Dijck, J. Winderickx, J.H. de Winde, and J.M. Thevelein. 1999. A *Saccharomyces cerevisiae* G-protein coupled receptor, Gpr1, is specifically required for glucose activation of the cAMP pathway during the transition to growth on glucose. Mol. Microbiol. **32:**1002-1012.

Kreger-van Rij, N.J.W., and M. Veenhuis. 1973. Electron microscopy of septa in ascomycetous yeasts. Antonie van Leeuwenhoek. **39:**481-490.

Kron, S.J., and N. Gow. 1995. Budding yeast morphogenesis: signaling, cytoskeleton and cell cycle. Curr. Opin. Cell Biol. **7:**845-855.

Kron, S.J., C.A. Styles, and G.R. Fink. 1994. Symmetric cell division in pseudohyphae of the yeast *Saccharomyces cerevisiae*. Mol. Biol. Cell **5:**1003-1022.

Kübler, H., H.U. Mösch, S. Rupp, and M.P. Lisanti. 1997. Gpa2p, a G-protein alpha-subunit, regulates growth and pseudohyphal development in *Saccharomyces cerevisiae* via a cAMP-dependent mechanism. J. Biol. Chem. **272:**20321-20323.

Kurischko, C., P. Fournier, M. Chasles, H. Weber, and C. Gaillardin. 1992. Cloning of the mating-type gene *MATA* of the yeast *Yarrowia lipolytica*. Mol. Gen. Genet. **232:**423-426.

Kwon, Y.H., H.C. Hoch, and R.C. Staples. 1991. Cytoskeletal organization in *Uromyces* urediospore germling apices during appressorium formation. Protoplasma **165:**37-50.

Lambrechts, M.G., F.F. Bauer, J. Marmur, and I.S. Pretorius. 1996. Muc1, a mucin-like protein that is regulated by Mss10, is critical for pseudohyphal differentiation in yeast. Proc. Natl. Acad. Sci. USA **93:**8419-8424.

Land, G.A., W.C. McDonald, R.L. Stjernholm, and L. Friedman. 1975. Factors affecting filamentation in *Candida albicans*: relationship of the uptake and distribution of proline to morphogenesis in *C. albicans*. Infect. Immun. **11:**1014-1023.

Lane, S., S. Zhou, T. Pan, Q. Dai, and H. Liu. 2001. The basic helix-loop-helix transcription factor Cph2 regulates hyphal development in *Candida albicans* partly via Tec1. Mol. Cell. Biol. **21:**6418-6428.

Laurent, B.C., M.A. Treitel, and M. Carlson. 1990. The SNF5 protein of *Saccharomyces cerevisiae* is a glutamine- and proline-rich transcriptional activator that affects expression of a broad spectrum of genes. Mol. Cell. Biol. **10:**5616-5625.

Leberer, E., D., Harcus, I.D. Broadbent, K.L. Clark, D. Dignard, K. Ziegelbauer, A. Schmidt, N.A. Gow, A.J. Brown, and D.Y. Thomas. 1996. Signal transduction through homologs of the Ste20p and Ste7p protein kinases can trigger hyphal formation in the pathogenic fungus *Candida albicans*. Proc. Natl. Acad. Sci. USA **93:**13217-13222.

Leberer, E., C. Wu, T. Leeuw, A. Fourest-Lieuvin, J.E. Segall, and D.Y. Thomas. 1997a. Functional characterization of the Cdc42p binding domain of yeast Ste20p protein kinase. EMBO J. **16:**83-97.

Leberer, E., K. Ziegelbauer, A. Schmidt, D. Harcus, D. Dignard, J. Ash, L. Johnson, and D.Y. Thomas. 1997b. Virulence and hyphal formation of *Candida albicans* require the Ste20p-like protein kinase Cla4p. Curr. Biol. 7:539-546.

Lee, I.H., and D.M. Ogrydziak. 1997. *Yarrowia lipolytica SRP54* homolog and translocation of Kar2p. Yeast **13:**499-513.

Leeuw, T., A. Fourest-Lieuvin, C. Wu, J. Chenevert, K. Clark, M. Whiteway, D. Thomas, and E. Leberer. 1995. Pheromone response in yeast: association of Bem1p with proteins of the MAP kinase cascade and actin. Science **270:**1210-1213.

Leeuw, T., C. Wu, J. Schrag, M. Whiteway, D. Thomas, and E. Leberer. 1998. Interaction of a G-protein β-subunit with a conserved sequence in Ste20/PAK family protein kinases. Nature **391:**191-195.

Leng, P., P.R. Lee, H. Wu, and A.J. Brown. 2001. Efg1, a morphogenetic regulator in *Candida albicans*, is a sequence-specific DNA binding protein. J. Bacteriol. **183:**4090-4093.

Leslie, D.M., B. Grill, M.P. Rout, R.W. Wozniak, and J.A. Aitchison. 2002. Kap121p-mediated nuclear import is required for mating and cellular differentiation in yeast. Mol. Cell. Biol. **22:**2544-2555.

Lew, D.J. 2000. Cell-cycle checkpoints that ensure coordination between nuclear and cytoplasmic events in *Saccharomyces cerevisiae*. Curr. Opin. Genet. Dev. **10:**47-53.

Lew, D.J., and S.I. Reed. 1993. Morphogenesis in the yeast cell cycle: regulation by Cdc28 and cyclins. J. Cell Biol. **120:**1305-1320.

Lew, D.J., and S.I. Reed. 1995. Cell cycle control of morphogenesis in budding yeast. Curr. Opin. Genet. Dev. **5:**17-23.

Li, W., and A.P. Mitchell. 1997. Proteolytic activation of Rim1p, a positive regulator of yeast sporulation and invasive growth. Genetics **145:**63-73.

Lin, F.C., and K.T. Arndt. 1995. The role of *Saccharomyces cerevisiae* type 2A phosphatase in the actin cytoskeleton and in entry into mitosis. EMBO J. **14:**2745-2759.

Lin, Y., Y. Wang, J.-K. Zhu, and Z. Yang. 1996. Localization of a Rho GTPase implies a role in tip growth and movement of the generative cell in pollen tubes. Plant Cell. **8:**293-303.

Liu, H. 2001. Transcriptional control of dimorphism in *Candida albicans*. Curr. Opin. Microbiol. **4:**728-735.

Liu, H., C.A. Styles, and G.R. Fink. 1993. Elements of the yeast pheromone response pathway required for filamentous growth of diploids. Science **262:**1741-1744.

Liu, H., J. Kohler, and G.R. Fink. 1994. Suppression of hyphal formation in *Candida albicans* by mutation of a *STE12* homolog. Science **266:**1723-1726.

Lo, H.-S., J.R. Köhler, B. DiDomenico, D. Loebenberg, A. Cacciapuoti, and G.R. Fink. 1997. Nonfilamentous *C. albicans* mutants are avirulent. Cell **90:**939-949.

Lo, W.S., and A.M. Dranginis. 1998. The cell surface flocculin Flo11 is required for pseudohyphae formation and invasion by *Saccharomyces cerevisiae*. Mol. Biol. Cell **9:**161-171.

Lock, P., C.L. Abram, T. Gibson, and S.A. Courtneidge. 1998. A new method for isolating tyrosine kinase substrates used to identify fish, and SH3 and PX domain-containing protein, and Src substrate. EMBO J. **17:**4346-4357.

Loeb, J.D.L., T.A. Kerentseva, T. Pan, M. Sepulveda-Becerra, and H. Liu. 1999. *Saccharomyces cerevisiae* G1 cyclins are differentially involved in invasive and pseudohyphal growth independent of the filamentation mitogen-activated protein kinase pathway. Genetics **153:**1535-1546.

Longtine, M. D. DeMarini, M. Valencik, Q. Al-Awar, H. Fares, C. DeVirgilio, and J.R. Pringle. 1996. The septins: roles in cytokinesis and other processes. Curr. Opin. Cell Biol. **8:**106-119.

Lopez, M.C., J.-M. Nicaud, H.B. Skinner, C. Vergnolle, J.C. Kader, V.A. Bankaitis, and C. Gaillardin. 1994. A phosphatidylinositol/phosphatidylcholine transfer protein is required for differentiation of the dimorphic yeast *Yarrowia lipolytica* from the yeast to the mycelial form. J. Cell Biol. **124:**113-117.

Lorch, Y., J. Beve, C.M. Gustafsson, L.C. Myers, and R.D. Kornberg. 2000. Mediator-nucleosome interaction. Mol. Cell **6:**197-201.

Lorenz, M.C., and J. Heitman. 1997. Yeast pseudohyphal growth is regulated by GPA2, a G protein α homolog. EMBO J. **16:**7008-7018.

Lorenz, M.C., and J. Heitman. 1998a. Regulators of pseudohyphal differentiation in *Saccharomyces cerevisiae* identified through multicopy suppressor analysis in ammonium permease mutant strains. Genetics **150:**1443-1457.

Lorenz, M.C., and J. Heitman. 1998b. The MEP2 ammonium permease regulates pseudohyphal differentiation in *Saccharomyces cerevisiae*. EMBO J. **17:**1236-1247.

Lorenz, M.C., N.S. Cutler, and J. Heitman. 2000a. Characterization of alcohol-induced filamentous growth in *Saccharomyces cerevisiae*. Mol. Biol. Cell **10:**183-199.

Lorenz, M.C., X. Pan, T. Harashima, M.E. Cardenas, Y. Xue, J.P. Hirsch, and J. Heitman. 2000b. The G protein-coupled receptor Gpr1 is a nutrient sensor that regulates pseudohyphal differentiation in *Saccharomyces cerevisiae*. Genetics **154:**609-622.

Losberger, C., and J.F. Ernst. 1989. Sequence of the *Candida albicans* gene encoding actin. Nucleic Acids Res. **17:**9488.

Lyons, D.M., S.K. Mahanty, K.-Y. Choi, M. Manandhar, and E.A. Elion. 1996. The SH3-domain protein Bem1 coordinates mitogen-activated protein kinase cascade activation with cell cycle control in *Saccharomyces cerevisiae*. Mol. Cell. Biol. **16:**4095-4106.

Ma, P., S. Wera, P.V. Dijck, and J.M. Thevelein. 1999. The *PDE1*-encoded low-affinity phosphodiesterase in the yeast *Saccharomyces cerevisiae* has a specific function in controlling agonist-induced cAMP signaling. Mol. Biol. Cell **10:**91-104.

Madden, K., C. Costigan, and M. Snyder. 1992. Cell polarity and morphogenesis in *Saccharomyces cerevisiae*. Trends Cell Biol. **2:**22-29.

Madhani, H.D., and G.R. Fink. 1997. Combinatorial control required for the specificity of yeast MAPK signaling. Science **275:**1314-1317.

Madhani, H.D., and G.R. Fink. 1998. The control of filamentous differentiation and virulence in fungi. Trends Cell Biol. **8:**348-353.

Madhani, H.D., C.A. Styles, and G.R. Fink. 1997. MAP kinases with distinct inhibitory functions impart signaling specificity during yeast differentiation. Cell **91:**673-684.

Madhani, H.D., T. Galitski, E. Lander, and G.R. Fink. 1999. Effectors of a developmental mitogen-activated protein kinase cascade revealed by overexpression signatures of signaling mutants. Proc. Natl. Acad. Sci. USA **96:**12530-12535.

Maeda, T., S.M. Wurgler-Murphy, and H. Saito. 1994. A two-component system that regulates an osmosensing MAP kinase cascade in yeast. Nature **369:**242-245.

Maeda, T., M. Takekawa, and H. Saito. 1995. Activation of yeast PBS2 MAPKK by MAPKKKs or by binding of an SH3-containing osmosensor. Science **269:**554-558.

Mallet, L. G. Renault, and M. Jacquet. 2000. Functional cloning of the adenylate cyclase gene of *Candida albicans* in *Saccharomyces cerevisiae* within a genomic fragment containing five other genes, including homologues of *CHS6* and *SAP185*. Yeast **16:**959-966.

Maniatis, T., E.F. Fritsch, and J. Sambrook. 1982. Molecular Cloning. A Laboratory Manual. Cold Spring Harbor Laboratory, Cold Spring Harbor, NY.

Manners, D.J., A.J. Masson, and J.C. Patterson. 1973a. The structure of a β-(1,3)-D-glucan from yeast cell walls. Biochem. J. **135:**19-30.

Manners, D.J., A.J. Masson, and J.C. Patterson. 1973b. The structure of a β-(1,6)-D-glucan from yeast cell walls. Biochem. J. **135:**31-36.

Marchler, G., C. Schüller, G. Adam, and H. Ruis. 1993. A *Saccharomyces cerevisiae* UAS element controlled by protein kinase A activates transcription in response to a variety of stress conditions. EMBO J. **12:**1997-2003.

Maresca, B., and G. S. Kobayashi. 1989. Dimorphism in *Histoplasma capsulatum*: a model for the study of cell differentiation in pathogenic fungi. Microbiol. Rev. **53:** 186-209.

Marks, J, and J.S. Hyams. 1985. Localization of F-actin through the cell division cycle of *Schizosaccharomyces pombe*. Eur. J. Cell Biol. **39:**27-32.

Marschall, L.G., R.L. Jeng, J. Mulholland, and T. Stearns. 1996. Analysis of Tub4p, a yeast γ-tubulin-like protein: implications for microtubule-organizing center function. J. Cell Biol. **134:**443-454.

Martinez-Pastor, M.T., G. Marchler, C. Schuller, A. Marchler-Bauer, H. Ruis, and F. Estruch. 1996. The *Saccharomyces cerevisiae* zinc finger proteins Msn2p and Msn4p are required for transcriptional induction through the stress-response element (STRE). EMBO J. **15:**2227-2235.

Matheos, D.P., T.J. Kingsbury, U.S. Ahsan, and K.W. Cunningham. 1997. Tcn1p/Crz1p, a calcineurin-dependent transcription factor that differentially regulates gene expression in *Saccharomyces cerevisiae*. Genes Dev. **11:**3445-3458.

Matsui, Y., R. Matsui, R. Akada, and A. Tohe. 1996. Yeast src homology region 3 domain-containing proteins involved in bud formation. J. Cell Biol. **133:**865-878.

Matsuura, A., and Y. Anraku. 1993. Characterization of the *MKS1* gene, a new negative regulator of the Ras-cyclic AMP pathway in *Saccharomyces cerevisiae*. Mol. Gen. Genet. **238:**6-16.

Mazur, P., and W. Baginsky. 1996. In vitro activity of 1,3-β-D-glucan synthase requires the GTP-binding protein Rho1. J. Biol. Chem. **271:**14604-14609.

Mbonyi, K., L.V. Aelst, J.C. Arguelles, A.W.H. Jans, and J.M. Thevelein. 1990. Glucose-induced hyperaccumulation of cyclic AMP and defective glucose repression in yeast strains with reduced activity of cyclic AMP-dependent protein kinase. Mol. Cell. Biol. **10:**4518-4523.

McEwan, I. J., K. Dahlman-Wright, J. Ford, and A. P. H. Wright. 1996. Functional interaction of the c-myc transactivation domain with the TATA binding protein: evidence for an induced fit model of transactivation domain folding. Biochemistry **35:**9584-9593.

McMillan, J., M. Longtine, R. Sia, C. Theesfeld, E. Bardes, J.R. Pringle, and D. Lew. 1999. The morphogenesis checkpoint in *Saccharomyces cervisiae*: cell cycle control of Swe1p degradation by Hsl1p and Hsl7p. Mol. Cell. Biol. **19:**6929-6939.

Michelitch, M., and J. Chant. 1996. A mechanism of Bud1p GTPase action suggested by mutational analysis and immunolocalization. Curr. Biol. **6:**446-454.

Mio, T., M. Adachi-Shimizu, Y. Tachibana, H. Tabuchi, S.B. Inoue, T. Yabe, T. Yamada-Okabe, M. Arisawa, T. Watanabe, and H. Yamada-Okabe. 1997a. Cloning of the *Candida albicans* homolog of *Saccharomyces cerevisiae GSC1/FKS1* and its involvement in β-1,3-glucan synthesis. J. Bacteriol. **179:**4096-4106.

Mio, T., T. Yamada-Okabe, T. Yabe, T. Nakajima, M. Arisawa, and H. Yamada-Okabe. 1997b. Isolation of the *Candida albicans* homologs of *Saccharomyces cerevisiae*

KRE6 and *SKN1*: expression and physiological function. J. Bacteriol. **179:**2363-2372.

Mirbod, F., S. Nakashima, Y. Kitajima, R.D. Cannon, and Y. Nozawa. 1997. Molecular cloning of a Rho family, *CDC42Ca* gene from *Candida albicans* and its mRNA expression changes during morphogenesis. J. Med. Vet. Mycol. **135:**173-179.

Mitchell, A.P. 1998. Dimorphism and virulence in *Candida albicans*. Curr. Opin. Microbiol. **1:**687-692.

Mockrin, S., and E. Korn. 1980. *Acanthamoeba* profilin interacts with G-actin to increase the rate of exchange of actin-bound adenosine 5'-triphosphate. Biochemistry **19:**5359-5362.

Morton, C.J., and I.D. Campbell. 1994. SH3 domains. Molecular "Velcro". Curr. Biol. **4:**615-617.

Mösch, H.-U., R.L. Roberts, and G.R. Fink. 1996. Ras2 signals via the Cdc42/Ste20/mitogen-activated protein kinase module to induce filamentous growth in *Saccharomyces cerevisiae*. Proc. Natl. Acad. Sci. USA **93:**5352-5356.

Moskow, J.J., A.S. Gladfelter, R.E. Lamson, P.M. Pryciak, and D.J. Lew. 2000. Role of Cdc42p in pheromone-stimulated signal transduction in *Saccharomyces cerevisiae*. Mol. Cell. Biol. **20:**7559-7571.

Murad, A.M., C. d'Enfert, C. Gaillardin, H. Tournu, F. Tekaia, D. Talibi, D. Marechal, V. Marchais, J. Cottin, and A.J. Brown. 2001. Transcript profiling in *Candida albicans* reveals new cellular functions for the transcriptional repressors *Ca*Tup1p, *Ca*Mig1p and *Ca*Ngr1p. Mol. Microbiol. **42:**981-993.

Murray, L.E., N. Rowley, I.W. Dawes, C.G. Johnston, and R.A. Singer. 1998. A yeast glutamine tRNA signals nitrogen status for regulation of dimorphic growth and sporulation. Proc. Natl. Acad. Sci. USA **95:**8619-8624.

Nakafuku, M., T. Obara, K. Kaibuchi, I. Miyajima, A. Miyajima, H. Itoh, S. Nakamura, K. Arai, K. Matsumoto, and Y. Kaziro. 1988. Isolation of a second yeast *Saccharomyces cerevisiae* gene (*GPA2*) coding for guanine nucleotide-binding regulatory protein: studies on its structure and possible functions. Proc. Natl. Acad. Sci. USA **85:**1374-1378.

Needleman, R.B., and A. Tzagoloff. 1975. Breakage of yeast: a simple method for processing multiple samples. Anal. Biochem. **64:**545-549.

Newman, A. 1998. RNA splicing. Curr. Biol. **8:**R903-R905.

Ni, L., and M. Snyder. 2001. A genomic study of the bipolar bud site selection pattern in *Saccharomyces cerevisiae*. Mol. Biol. Cell **12:**2147-2170.

Niimi, M., K. Niimi, J. Tokunaga, and H. Nakayama. 1980. Changes in cyclic nucleotide levels and dimorphic transition in *Candida albicans*. J. Bacteriol. **142:**1010-1014.

Nikawa, J., S. Cameron, T. Toda, K.M. Ferguson, and M. Wigler. 1987. Rigorous feedback control of cAMP levels in *Saccharomyces cerevisiae*. Genes Dev. **1:**931-937.

Nobes, C.D., and A. Hall. 1995. Rho, Rac and Cdc42 GTPases regulate the assembly of multimolecular focal complexes associated with actin stress fibers, lamellipodia, and filopodia. Cell **81:**53-62.

Novick, P., and D. Botstein. 1985. Phenotypic analysis of temperature-sensitive yeast actin mutants. Cell **40:**405-416.

Novotny, C., L. Dolezalova, and J. Lieblova. 1994. Dimorphic growth and lipase production in lipolytic yeasts. Folia Microbiol. **39:**71-73.

Nuttley, W.M., A.M. Brade, C. Gaillardin, G.A. Eitzen, J.R. Glover, J.D. Aitchison, and R.A. Rachubinski. 1993. Rapid identification and characterization of peroxisomal assembly mutants in *Yarrowia lipolytica*. Yeast **9:**507-517.

Nuttley, W.M., A.M. Brade, G.A. Eitzen, M. Veenhuis, J.D. Aitchison, J.R. Glover, and R.A. Rachubinski. 1994. *PAY4*, a gene required for peroxisome assembly in the yeast *Yarrowia lipolytica*, encodes a novel member of a family of putative ATPases. J. Biol. Chem. **269:**556-566.

Oda, Y., K. Huang, F. Cross, D. Cowburn, and B. Chait. 1999. Accurate quantitation of protein expression and site-specific phosphorylation. Proc. Natl. Acad. Sci. USA **96:**6591-6596.

Odds, F.C. 1988. *Candida* and Candidosis. A Review and Bibliography. Bailliere Tindal, London, United Kingdom.

Odds, F.C. 1994. Pathogenesis of *Candida* infections. J. Am. Acad. Dermatol. **31:**S2-S5.

O'Donnell, A.G., M. Goodfellow, and D.L. Hawksworth. 1994. Theoretical and practical aspects of the quantification of biodiversity among microorganisms. Phil. Trans. R. Soc. Lond. **345:**65-73.

Ogrydziak, D.M., and S.J. Scharf. 1982. Alkaline extracellular protease produced by *Saccharomycopsis lipolytica*. J. Gen. Microbiol. **128:**1225-1234.

Ogrydziak, D.M., S. Cheng, and S.J. Scharf. 1982. Characterization of *Saccharomycopsis lipolytica* mutants producing lowered levels of alkaline extracellular proteases. J. Gen. Microbiol. **128:**2271-2280.

Okuma, M., C.W. Hwang, Y. Masuda, H. Nishida, J. Sugiyama, A. Ohta, and M. Takagi. 1993. Evolutionary position of *n*-alkane-assimilating yeast *Candida maltosa* shown by nucleotide sequence of small-subunit ribosomal RNA gene. Biosci. Biotech. Biochem. **57:**1793-1794.

O'Rourke, S.M., and I. Herskowitz. 1998. The Hog1 MAPK prevents cross talk between the HOG and pheromone response MAPK pathways in *Saccharomyces cerevisiae*. Genes Dev. **12:**2874-2886.

Ota, Y., S. Oikawa, Y. Morimoto, and Y. Minoda. 1984. Nutritional factors causing mycelial development of *Saccharomycopsis lipolytica*. Agric. Biol. Chem. **48:**1933-1939.

Palecek, S.P., A.S. Parikh, and S.J. Kron. 2000. Genetic analysis reveals that *FLO11* upregulation and cell polarization independently regulate invasive growth in *Saccharomyces cerevisiae*. Genetics **156:**1005-1023.

Pan, X., and J. Heitman. 1999. Cyclic AMP-dependent protein kinase regulates pseudohyphal differentiation in *Saccharomyces cerevisiae*. Mol. Cell. Biol. **19:**4874-4887.

Pan, X., and J. Heitman. 2000. Sok2 regulates yeast pseudohyphal differentiation via a transcription factor cascade that regulates cell-cell adhesion. Mol. Cell. Biol. **22:**8364-8372.

Park, H.O., J. Chant, and I. Herskowitz. 1993. *BUD2* encodes a GTPase-activating protein for Bud1/Rsr1 necessary for proper bud-site selection in yeast. Nature **365:**269-274.

Park, H.O., E. Bi, J.R. Pringle, and I. Herskowitz. 1997. Two active states of the Ras-related Bud1/Rsr1 protein bind to different effectors to determine yeast cell polarity. Proc. Natl. Acad. Sci. USA. **94:**4463-4468.

Park, H.O., A. Sanson, and I. Herskowitz. 1999. Localization of Bud2p, a GTPase-activating protein necessary for programming cell polarity in yeast to the presumptive bud site. Genes Dev. **13:**1912-1917.

Pascal, E., and R. Tjian. 1991. Different activation domains of Sp1 govern formation of multistress and mediate transcriptional synergism. Genes Dev. **5:**1646-1656.

Pazin, M.J., and J.T. Kadonaga. 1997. What's up and down with histone deacetylation and transcription? Cell **89:**325-328.

Perera, T.H., D.W. Gregory, D. Marshall, and N.A. Gow. 1997. Contact-sensing by hyphae of dermatophytic and saprophytic fungi. J. Med. Vet. Mycol. **35:**289-293.

Perez-Campo, F.M., and A. Dominguez. 2001. Factors affecting the morphogenetic switch in *Yarrowia lipolytica*. Curr. Microbiol. **43:**429-433.

Pertuiset, B., J.-M. Beckerich, and C. Gaillardin. 1995. Molecular cloning of Rab-related genes in the yeast *Yarrowia lipolytica*. Analysis of *RYL1*, an essential gene encoding a SEC4 homologue. Curr. Genet. **27:**123-130.

Peter, M., A.M. Neiman, H.O. Park, M. van Lohuizen, and I. Herskowitz. 1996. Functional analysis of the interaction between the small GTP binding protein Cdc42 and the Ste20 protein kinase in yeast. EMBO J. **15:**7046-7059.

Peters, I.I., and F.E. Nelson. 1948. Factors influencing the production of lipase by *Mycotorula lipolytica*. J. Bacteriol. **55:**581-591.

Peterson, J., Y. Zheng, L. Bender, A. Myers, R. Cerione, and A. Bender. 1994. Interactions between the bud emergence proteins Bem1p and Bem2p and Rho-type GTPases in yeast. J. Cell Biol. **127:**1395-1406.

Pfaller, M.A., R.N. Jones, S.A. Messer, M.B. Edmond, and R.P. Wenzel. 1998a. National surveillance of nosocomial blood stream infection due to species of *Candida* other than *Candida albicans*: frequency of occurrence and antifungal susceptibility in the SCOPE Program. SCOPE Participant Group. Surveillance and Control of Pathogens of Epidemiologic Interest. Diagn. Microbiol. Infect. Dis. **30:**121-129.

Pfaller, M.A., R.N. Jones, S.A. Messer, M.B. Edmond, R.P. Wenzel. 1998b. National surveillance of nosocomial blood stream infection due to *Candida albicans*: frequency of occurrence and antifungal susceptibility in the SCOPE Program. Diagn. Microbiol. Infect. Dis. **31:**327-332.

Popolo, L., D. Gilardelli, P. Bonfante, and M. Vai. 1997. Increase in chitin as an essential response to defects in assembly of cell wall polymers in the *ggp1Δ* mutant of *Saccharomyces cerevisiae*. J. Bacteriol. **179:**463-469.

Popolo, L., and M. Vai. 1999. The Gas1 protein, a putative wall polymer cross-linker. Biochim. Biophys. Acta **1426**:385-400.

Posas, F., and H. Saito. 1997. Osmotic activation of the HOG MAPK pathway via Ste11p MAPKKK: scaffold role of Pbs2p MAPKK. Science **276**:1702-1705.

Posas, F., and H. Saito. 1998. Activation of the yeast SSK2 MAP kinase kinase kinase by the SSK1 two-component response regulator. EMBO J. **17**:1385-1394.

Posas, F., M. Takekawa, and H. Saito. 1998. Signal transduction by MAP kinase cascades in budding yeast. Curr. Opin. Microbiol. **1**:175-182.

Pringle, J.R. 1991. Staining of bud scars and other cell wall chitin with calcofluor. Methods Enzymol. **194**:732-735.

Pringle, J.R., A.E.M. Adams, D.G. Drubin, and B.K. Haarer. 1991. Immunofluorescence methods for yeast. Methods Enzymol. **194**:565-602.

Pruyne, D., and A. Bretscher. 2000a. Polarization of cell growth in yeast. II. Establishment and maintenance of polarity states. J. Cell Sci. **113**:365-375.

Pruyne, D., and A. Bretscher. 2000b. Polarization of cell growth in yeast. II. The role of the cortical actin cytoskelton. J. Cell Sci. **113**:571-585.

Pruyne, D., D. Schott, and A. Bretscher. 1998. Tropomyosin-containing actin cables direct the Myo2p-dependent delivery of secretory vesicles in budding yeast. J. Cell Biol. **143**:1931-1945.

Ram, S.P., P.A. Sullivan, and M.G. Shepherd. 1983. The *in situ* assay of *Candida albicans* enzymes during yeast growth and germ-tube formation. J. Gen. Microbiol. **129**:2367-2378.

Ramon, A.M., R. Gil, M. Burgal, R. Sentandreu, and E. Valentin. 1996. A novel cell wall protein specific to the mycelial form of *Yarrowia lipolytica*. Yeast **12**:1535-1548.

Rechsteiner, M., and S.W. Rogers. 1996. PEST sequences and regulation by proteolysis. Trends Biochem. Sci. **21**:267-271.

Remacle, J. E., G. Albrecht, R. Brys, G. H. Braus, and D. Huylebroeck. 1997. Three classes of mammalian trascription activation domains stimulate transcription in *Schizosaccharomyces pombe*. EMBO J. **16**:5722-5729.

Reyna-Lopez, G.E., J. Simpson, and J. Ruiz-Herrera. 1997. Differences in DNA methylation patterns are detectable during the dimorphic transition of fungi by amplification of restriction polymorphisms. Mol. Gen. Genet. **253:**703-710.

Richard, M., R. R. Quijano, S. Bezzate, F. Bordon-Pallier, and C. Gaillardin. 2001. Tagging morphogenetic genes by insertional mutagenesis in the yeast *Yarrowia lipolytica*. J. Bacteriol **183:**3098-3107.

Ridley, A.J. 1994. Membrane ruffling and signal transduction. BioEssays. **16:**321-327.

Ridley, A.J. 1995. Rho-related proteins: actin cytoskeleton and cell cycle. Curr. Opin. Genet. Dev. **5:**24-30.

Rieder, S.E., L.M. Banta, K. Kohrer, J.M. McCaffrey, and SD. Emr. 1996. Multilamellar endosome-like compartment accumulates in the yeast *vps28* vacuolar protein sorting mutant. Mol. Biol. Cell **7:**985-999.

Roberson, R.W. 1992. The actin cytoskeleton in hyphal cells of *Sclerotium rolfsii*. Mycologia. **84:**41-51.

Roberts, R.L., and G.R. Fink. 1994. Elements of a single MAP kinase cascade in *Saccharomyces cerevisiae* mediate two developmental programs in the same cell type: mating and invasive growth. Genes Dev. **8:**2974-2985.

Roberts, R.L., H.U. Mosch, and G.R. Fink. 1997. 14-3-3 proteins are essential for RAS/MAPK cascade signaling during pseudohyphal development in *Saccharomyces cerevisiae*. Cell **89:**1055-1065.

Robertson, L.S., and G.R. Fink. 1998. The three yeast A kinases have specific signaling functions in pseudohyphal growth. Proc. Natl. Acad. Sci. USA **95:**13783-1378.

Rodriguez, C., and A. Dominguez. 1984. The growth characteristics of *Saccharomycopsis lipolytica*: morphology and induction of mycelium formation. Can. J. Microbiol. **30:**605-612.

Roemer, T., and H. Bussey. 1995. Yeast Kre1p is a cell surface *O*-glycoprotein. Mol. Gen. Genet. **249:**209-216.

Roemer, T., K. Madden, J. Chang, and M. Snyder. 1996a. Selection of axial growth sites in yeast requires Axl2p, a novel plasma membrane glycoprotein. Genes Dev. **10:**777-793.

Roemer, T., L.G. Vallier, and M. Snyder. 1996b. Selection of polarized growth sites in yeast. Trends Cell Biol. **6:**434-441.

Roemer, T., L. Vallier, Y.J. Sheu, and M. Snyder. 1998. The Spa2p-related protein, Sph1p, is important for polarized growth in yeast. J. Cell Sci. **111:**479-494.

Roemer, T., S. Delaney, and H. Bussey. 1993. *SKN1* and *KRE6* define a pair of functional homologs encoding putative membrane proteins involved in β-glucan synthesis. Mol. Cell. Biol. **13:**4039-4048.

Roncero, C., M.H. Valdivieso, J.C. Ribas, and A. Duran. 1988. Effect of Calcofluor white on chitin synthases from *Saccharomyces cerevisiae*. J. Bacteriol. **170:**1945-1949.

Rose, M.D., F. Winston, and P. Hieter. 1988. Laboratory Course Manual for Methods in Yeast Genetics. Cold Spring Harbor Laboratory, Cold Spring Harbor, NY.

Roumanie, O., C. Weinachter, I. Larrieu, M. Crouzet, and F. Doignon. 2001. Functional characterization of the Bag7, Lrg1 and Rgd2 RhoGAP proteins from *Saccharomyces cerevisiae*. FEBS Lett. **506:**149-156.

Ruis, H., and C. Schüller. 1995. Stress signaling in yeast. BioEssays **17:**959-965.

Rupp, S., E. Summers, H.J. Lo, H. Madhani, and G. Fink. 1999. MAP kinase and cAMP filamentation signaling pathways converge on the unusually large promoter of the yeast *FLO11* gene. EMBO J. **18:**1257-1269.

Sabie, F.T., and G.M. Gadd. 1989. Involvement of a Ca^{2+}-calmodulin interaction in the yeast-mycelial transition of *Candida albicans*. Mycopathologia **108:**47-54.

Sabie, F.T., and G.M. Gadd. 1992. Effect of nucleosides and nucleotides and the relationship between cellular adenosine 3':5'-cyclic monophosphate (cyclic AMP) and germ tube formation in *Candida albicans*. Mycopathologia **119:**147-156.

Salama, N.R., J.S. Chuang, and R.W. Schekman. 1997. *SEC31* encodes en essential component of the COPII coat required for transport vesicle budding from the endoplasmic reticulum. Mol. Biol. Cell **8:**205-217.

San-Blas, G., and F. San-Blas. 1984. Molecular aspects of fungal dimorphism. CRC Crit. Rev. Microbiol. **11:**101-127.

Sanger, F., S. Niklen, and A.R. Coulson. 1977. DNA sequencing with chain-terminating inhibitors. Proc. Natl. Acad. Sci. USA **74:**5463-5467.

Schatz, P.J., L. Pillus, P. Grisafi, F. Solomon, and D. Botstein. 1986. Two functional α-tubulin genes of the yeast *Saccharomyces cerevisiae* encode divergent proteins. Mol. Cell. Biol. **6**:3711-3721.

Schekman, R. 1985. Protein localization and membrane traffic in yeast. Annu. Rev. Cell Biol. **1**:115-143.

Schroppel, K., K. Sprosser, M. Whiteway, D.Y. Thomas, M. Rollinghoff, and C. Csank. 2000. Repression of hyphal proteinase expression by the mitogen-activated protein (MAP) kinase phosphatase Cpp1p of *Candida albicans* is independent of the MAP kinase Cek1p. Infect. Immun. **68**:7159-7161.

Schüller, C., J. L. Brewster, M. R. Alexander, M. C. Gustin, and H. Ruis. 1994. The HOG pathway controls osmotic regulation of transcription via the stress response element (STRE) of the *Saccharomyces cerevisiae CTT1* gene. EMBO J. **13**:4382-4389.

Schweizer, A., S. Rupp, B.N. Taylor, M. Rollinghoff, and K. Schroppel. 2000. The TEA/ATTS transcription factor CaTec1p regulates hyphal development and virulence in *Candida albicans*. Mol. Microbiol. **38**:435-445.

Scita, G., P. Tenca, E. Frittoli, A. Tocchetti, M. Innocenti, G. Giardina, and P.P. Di Fiore. 2000. Signaling from Ras to Rac and beyond: not just a matter of GEFs. EMBO J. **19**:2393-2398.

Sekine, A., M. Fujiwara, and S. Narumiya. 1989. Asparagine residue in the Rho gene product is the modification site for botulinum ADP-ribosyltransferase. J. Biol. Chem. **264**:8602-8605.

Shepherd, M.G, R.T.M. Poulter, and P.A. Sullivan. 1985. *Candida albicans*: biology, genetics, and pathogenicity. Ann. Rev. Microbiol. **39**:579-614.

Shepherd, M.G. 1988. Morphogenetic transformation in fungi. Curr. Top. Med. Mycol. **2**:278-304.

Sherwood, J., N.A.R. Gow, G.W. Goodway, D.W. Gregory, and D. Marshall. 1992. Contact sensing in *Candida albicans*: a possible aid to epithelial penetration. J. Med. Vet. Mycol. **30**:461-469.

Sheu, Y.J., B. Santos, N. Fortin, C. Costigan, and M. Snyder. 1998. Spa2p interacts with cell polarity proteins and signaling components involved in yeast cell morphogenesis. Mol. Cell. Biol. **18**:4035-4069.

Smith, H.A., H.S. Allaudeen, M.H. Whitman, Y. Koltin, and J.A. Gorman. 1988. Isolation and characterization of a β-tubulin gene from *Candida albicans*. Gene **63:**53-63.

Smith, J.J., R.K. Szilard, M. Marelli, and R.A. Rachubinski. 1997. The peroxin Pex17p of the yeast *Yarrowia lipolytica* is associated peripherally with the peroxisomal membrane and is required for the import of a subset of matrix proteins. Mol. Cell. Biol. **17:**2511-2520.

Smith, J.J., T.W. Brown, G.A. Eitzen, and R.A. Rachubinski. 2000. Regulation of peroxisome size and number by fatty acid β-oxidation in the yeast *Yarrowia lipolytica*. J. Biol. Chem. **275:**20168-20178.

Smith, R.F., B.A. Wiese, M.K. Wojzynski, D.B. Davison, and K.C. Worley. 1996. BCM Search Launcher--An Integrated Interface to Molecular Biology Data Base Search and Analysis Services Available on the World Wide Web. Genome Res. **6**:454-462.

Soll, D.R., M. Stasi, and G. Bedell. 1978. The regulation of nuclear migration and division during pseudomycelium outgrowth in the dimorphic yeast *Candida albicans*. Exp. Cell Res. **116:**207-215.

Som, T., and V.S. Kolaparthi. 1994. Developmental decisions in *Aspergillus nidulans* are modulated by Ras activity. Mol. Cell. Biol. **14:**5333-5348.

Sonneborn, A., D. Bockmühl, and J.F. Ernst. 1999. Chlamydospore formation in *Candida albicans* requires the Efg1p morphogenetic regulator. Infect. Immun. **67:**4655-4660.

Staab, J.F., S.D. Bradway, P.L. Fidel, and P. Sundstrom. 1999. Adhesive and mammalian transglutaminase substrate properties of *Candida albicans* Hwp1. Science **283:**1535-1538.

Stanhill, A., N. Schick, and D. Engelberg. 1999. The yeast ras/cyclic AMP pathway induces invasive growth by suppressing the cellular stress response. Mol. Cell. Biol. **19:**7529-7538.

Stathopoulos, A.M., and M.S. Cyert. 1997. Calcineurin acts through the *CRZ1/TCN1*-encoded transcription factor to regulate gene expression in yeast. Genes Dev. **11:**3432-3444.

Steer, M.W., and J.M. Steer. 1989. Pollen tube tip growth. New Phytol. **111:**323-358.

Stevenson, B., B. Ferguson, C. De Virgilio, E. Bi, J.R. Pringle, J. Ammerer, and G. Sprague Jr. 1995. Mutation of RGA1, which encodes a putative GTPase-activating

protein for the polarity establishment protein Cdc42p, activates the pheromone-response pathway in the yeast *Saccharomyces cerevisiae*. Genes Dev. **9**:2949-2963.

Stoldt, V.R., A. Sonneborn, C.E. Leuker, and J.F. Ernst. 1997. Efg1p, an essential regulator of morphogenesis of the human pathogen *Candida albicans*, is a member of a conserved class pf bHLH proteins regulating morphogenetic processes in fungi. EMBO J. **16**:1982-1991.

Stratford, M. 1994. Another brick in the wall? Recent developments concerning the yeast envelope. Yeast **10**:1741-1752.

Strick, C.A., L.C. James, M.M. O'Donnell, M.G. Gollaher, and A.E. Franke. 1992. The isolation and characterization of the pyruvate kinase-encoding gene from the yeast *Yarrowia lipolytica*. Gene **118**:65-72.

Sullivan, P.A., C.Y. Yin, C. Molloy, M.D. Templeton, and M.G. Shepherd. 1983. An analysis of the metabolism and cell wall composition of *Candida albicans* during germ-tube formation. Can. J. Microbiol. **29**:1514-1525.

Symons, M. 1995. The Rac and Rho pathways as a source of drug targets for Ras-mediated malignancies. Curr. Opin. Biotechnol. **6**:668-674.

Symons, M. 1996. Rho family GTPases: the cytoskeleton and beyond. Trends Biochem. Sci. **21**:178-181.

Szabo, R. 1999. Dimorphism in *Yarrowia lipolytica*: filament formation is suppressed by nitrogen starvation and inhibition of respiration. Folia Microbiol. **44**:19-24.

Szabo, R. 2001. Cla4 protein is essential for filament formation and invasive growth of *Yarrowia lipolytica*. Mol. Gent. Genomics **265**:172-179.

Szabo, R., and V. Štofaníková. 2002. Presence of organic sources of nitrogen is critical for filament formation and pH-dependent morphogenesis in *Yarrowia lipolytica*. FEMS Microbiol. Lett. **206**:45-50.

Szilard, R.K., V.I. Titorenko, M. Veenhuis, and R.A. Rachubinski. 1995. Pay32p of the yeast *Yarrowia lipolytica* is an intraperoxisomal component of the matrix protein translocation machinery. J. Cell Biol. **131**:1453-1469.

Taheri, N., T. Kohler, G.H. Braus, and H.U. Mosch. 2000. Asymetrically localized Bud8p and Bud9p proteins control yeast cell polarity and development. EMBO J. **19**:6686-6696.

Tang, B.L., T. Zhang, D.Y. Low, E.T. Wong, H. Horstmann, and W. Hong. 2000. Mammalian homologues of yeast Sec31p. An ubiquitously expressed form is localized to endoplasmic reticulum (ER) exit sites and is essential for ER-Golgi transport. J. Biol. Chem. **275:**13597-13604.

Tapon, N., and A. Hall. 1997. Rho, Rac and Cdc42 GTPases regulate the organization of the actin cytoskeleton. Curr. Opin. Cell. Biol. **9:**86-92.

Taylor, L.P., and P.K. Hepler. 1997. Pollen germination and tube growth. Annu. Rev. Plant Physiol. **48:**461-491.

Teem, J.L., N. Abovich, N.F. Kaufer, W.F. Schwindinger, J.R. Warner, A. Levy, J. Woolford, R.J. Leer, M.M.C. van Raamsdonk-Duin, W.H. Mager, R.J. Planta, L. Schultz, J.D. Friesen, H. Fried, and M. Rosbach. 1984. A comparison of yeast ribosomal protein gene DNA sequences. Nucleic Acids Res. **12:**8295-8312.

Thomas, J.H., N.F. Neff, and D. Botstein. 1985. Isolation and characterization of mutations in the β-tubulin gene of *Saccharomyces cerevisiae*. Genetics **111:**715-734.

Tilburn, J., S. Sarkar, D.A. Widdick, E.A. Espeso, M. Orejas, J. Mungroo, M.A. Penalva, and H.N. Arst Jr. 1995. The *Aspergillus nidulans* PacC zinc finger transcription factor mediates regulation of both acid- and alkaline-expressed genes by ambient pH. EMBO J. **14:**779-790.

Titorenko, V.I., D.M. Ogrydziak, and R.A. Rachubinski. 1997. Four distinct secretory pathways serve protein secretion, cell surface growth, and peroxisome biogenesis in the yeast *Yarrowia lipolytica*. Mol. Cell. Biol. **17:**5210-5226.

Titorenko, V.I., J.J. Smith, R.K. Szilard, and R.A. Rachubinski. 2000. Peroxisome biogenesis in the yeast *Yarrowia lipolytica*. Cell. Biochem. Biophys. **32:**21-26.

Tjandra, H., J. Compton, and D. Kellogg. 1998. Control of mitotic events by the Cdc42 GTPase, the Clb2 cyclin and a member of the PAK kinase family. Curr. Biol. **8:**991-1000.

Tobe, S., T. Takami, and S. Ikeda. 1976. Production and some enzymatic properties of alkaline proteinase of *Candida lipolytica*. Agric. Biol. Chem. **40:**1087-1092.

Tokunaga, M., Niimi, M., M. Kusamichi, and H. Koike. 1990. Initial attachment of *Candida albicans* cells to buccal epithelial cells. Demonstration of ultrastructure with the rapid-freezing technique. Mycopathol. **111:**61-66.

Tolliday, N., N. Bouquin, and R. Li. 2001. Assembly and regulation of the cytokinetic apparatus in budding yeast. Curr. Opin. Microbiol. **4:**690-695.

Torres-Guzman, J.C., and A. Dominguez. 1997. *HOY1*, a homeo gene required for hyphal formation in *Yarrowia lipolytica*. Mol. Cell. Biol. **17:**6283-6293.

Treger, J.M., T.R. Magee, and K. McEntee. 1998. Functional analysis of the stress response element and its role in the multistress response of *Saccharomyces cerevisiae*. Biochem. Biophys. Res. Commun. **243:**13-19.

Treton, B., S. Blanchin-Roland, M. Lambert, A. Lepingle, and C. Gaillardin. 2000. Ambient pH signaling in ascomycetous yeasts involves homologues of the *Aspergillus nidulans palF* and *palH*. Mol. Gen. Genet. **263:**505-513.

Tzschoppe, K., A. Augstein, R. Bauer, S.D. Kohlwein, and G. Barth. 1999. *trans*-Dominant mutations in the *GPR1* gene cause high sensitivity to acetic acid and ethanol in the yeast *Yarrowia lipolytica*. Yeast **15:**1645-1656.

Umikawa, M., K. Tanaka, K. Shimizu, H. Imamura, T. Sasaki, and Y. Takai. 1998. Interaction of Rho1p target Bni1p with F-actin-binding elongation factor 1α: implication in Rho1p-regulated reorganization of the actin cytoskeleton in *Saccharomyces cerevisiae*. Oncogene **16:**2011-2016.

Ushinsky, S. C., D. Harcus, J. Ash, D. Dignard, A. Marcil, J. Morchhauser, D.Y. Thomas, M. Whiteway, and E. Leberer. 2002. *CDC42* is required for polarized growth in human pathogen *Candida albicans*. Eukaryotic Cell **1:**95-104.

Valentin, E., E. Herrero, H. Rico, F. Miragall, and R. Sentandreu. 1987. Cell wall mannoproteins during the population growth phases in *Saccharomyces cerevisiae*. Arch. Microbiol. **148:**88-94.

Vallee, R. 1991. Cytoplasmic dynein: advances in microtubule-based motility. Trends Cell Biol. **1:**25-29.

van Aelst,, L., and C. D'Souza-Schorey. 1997. Rho GTPases and signaling networks. Genes Dev. **11:**2295-2322.

van der Walt, J.P., and J.A. von Arx. 1980. The yeast genus *Yarrowia gen. nov.* Antonie van Leeuwenhoek **46:**517-521.

van Hemert, M.J., H. Y. de Steensma, and G.P.H. van Heusden. 2001a. 14-3-3 proteins: key regulators of cell division, signalling and apoptosis. BioEssays **23:**936-946.

van Hemert, M.J., G.P.H. van Heusden, and H.Y. Steensma. 2001b. Yeast 14-3-3 proteins. Yeast **18:**889-895.

Wang, A.M., Doyle, M.V., and D.F. Mark. 1989. Quantitation of mRNA by the polymerase chain reaction. Proc. Natl. Acad. Sci. USA. **86:**9717-9721.

Wang, W., T. Nishikawa, and K. Isono. 1997. Isolation and characterization of *Saccharomyces cerevisiae* genes differentially expressed under different growth conditions. J. Gen. Appl. Microbiol. **43:**217-224.

Welch, W. J. 1993. How cells respond to stress. Scientific American **268:** 34-41.

Whiteway, M. 2000. Transcriptional control of cell type and morphogenesis in *Candida albicans*. Curr. Opin. Microbiol. **3:**582-588.

Wimmer, E.A., H. Jackle, C. Pfeifle, and S.M. Cohen. 1993. A *Drosophila* homologue of human Sp1 is a head-specific segmentation gene. Nature **366:**690-694.

Wu, C., V. Lytvyn, D.Y. Thomas, and E. Leberer. 1997. The phosphorylation site for Ste20p-like protein kinases is essential for the function of myosin I in yeast. J. Biol. Chem. **272:**30623-30626.

Wu, C., E. Leberer, D.Y. Thomas, and M. Whiteway. 1999. Functional characterization of the interaction of Ste50p with Ste11p MAPKKK in *Saccharomyces cerevisiae*. Mol. Biol. Cell **10:**2425-2440.

Xiao, H. and K.-T. Jeang. 1998. Glutamine-rich domains activate transcription in yeast *Saccharomyces cerevisiae*. J. Biol. Chem. **273:**22873-22876.

Xuan, J.-W., P. Fournier, N. de Clerck, M. Chasles, and C. Gaillardin. 1990. Overlapping reading frames at the *LYS5* locus in the yeast *Yarrowia lipolytica*. Mol. Cell. Biol. **10:**4795-4806.

Yamada, T., and D. Ogrydziak. 1983. Extracellular acid proteases produced by *Saccharomycopsis lipolytica*. J. Bacteriol. **154:**23-31.

Yamashita, R.A., and G.S. May. 1998. Motoring along the hyphae: molecular motors and the fungal cytoskeleton. Curr. Opin. Cell Biol. **10:**74-79.

Yang, X., H.T. Matern, and D. Gallwitz. 1998. Specific binding to a novel and essential Golgi membrane protein (Yip1p) functionally links the transport GTPases Ypt1p and Ypt31p. EMBO J. **17:**4954-4963.

Yokoyama, K., H. Kaji, K. Nishimura, and M. Miyaji. 1990. The role of microfilaments and microtubules in apical growth and dimorphism of *Candida albicans*. J. Gen. Microbiol. **136:**1067-1075.

Zaragoza, O., and J.M. Gancedo. 2000. Pseudohyphal growth is induced in *Saccharomyces cerevisiae* by a combination of stress and cAMP signaling. Antonie van Leeuwenhoek **78:**187-194.

Zhang, Z., M.M. Smith, and J.S. Mymryk. 2001. Interaction of the E1A oncoprotein with Yak1p, a novel regulator of yeast pseudohyphal differentiation, and related mammalian kinases. Mol. Biol. Cell **12:**699-710.

Zheng, Y., A. Bender, and R. Cerione. 1995. Interactions among proteins involved in bud-site selection and bud-site assembly in *Saccharomyces cerevisiae*. J. Biol. Chem. **270:**626-630.

Ziman, M., J. O'Brien, L. Ouellette, W. Church, and D. Johnson. 1991. Mutational analysis of *CDC42Sc*, a *Saccharomyces cerevisiae* gene that encodes a putative GTP-binding protein involved in the control of cell polarity. Mol. Cell. Biol. **11:**3537-3544.

Ziman, M., D. Preuss, J. Mulholland, J.M. O'Brien, D. Botstein, and D.I. Johnson. 1993. Subcellular localization of Cdc42p, a *Saccharomyces cerevisiae* GTP-binding protein involved in the control of cell polarity. Mol. Biol. Cell. **4:**1307-1316.

Zohn, I.M., S.L. Campbell, R. Khosravi-Far, K.L. Rossman, and C.J. Der. 1998. Rho family proteins and Ras transformation: the RHOad less traveled gets congested. Oncogene **17:**1415-1438.